Helsinki University of Technology, Signal Processing Laboratory
Teknillinen korkeakoulu, Signaalinkäsittelytekniikan laboratorio
Espoo 2005 Report 53

ADAPTIVE POWER CONTROL IN CDMA CELLULAR COMMUNICATION SYSTEMS

Matti Rintamäki

Dissertation for the degree of Doctor of Science in Technology to be presented with due permission of the Department of Electrical and Communications Engineering for public examination and debate in Auditorium S4 at Helsinki University of Technology (Espoo, Finland) on the 18th of November, 2005, at 12 o'clock noon.

Helsinki University of Technology
Department of Electrical and Communications Engineering
Signal Processing Laboratory

Teknillinen korkeakoulu
Sähkö- ja tietoliikennetekniikan osasto
Signaalinkäsittelytekniikan laboratorio

Distribution:
Helsinki University of Technology
Signal Processing Laboratory
P.O. Box 3000
FIN-02015 HUT
Tel. +358-9-451 3211
Fax. +358-9-452 3614
E-mail: Mirja.Lemetyinen@hut.fi

ISBN 951-22-7897-9 (Printed)
ISBN 951-22-7898-7 (Electronic)
ISSN 1458-6401

Otamedia Oy
Espoo 2005

Abstract

Power control is an essential radio resource management method in CDMA cellular communication systems, where co-channel interference is the primary capacity-limiting factor. Power control aims to control the transmission power levels in such a way that acceptable quality of service for the users is guaranteed with lowest possible transmission powers. All users benefit from the minimized interference and the preserved signal qualities.

In this thesis new closed loop power control algorithms for CDMA cellular communication systems are proposed. To cope with the random changes of the radio channel and interference, adaptive algorithms are considered that utilize ideas from self-tuning control systems. The inherent loop delay associated with closed loop power control can be included in the design process, and thus alleviated with the proposed methods. Another problem in closed-loop power control is that extensive control signaling consumes radio resources, and thus the control feedback bandwidth must be limited. A new approach to enhance the performance of closed-loop power control in limited-feedback-case is presented, and power control algorithms based on the new approach are proposed.

The performances of the proposed algorithms are evaluated through both analysis and computer simulations, and compared with well-known algorithms from the literature. The results indicate that significant performance improvements are achievable with the proposed algorithms.

Keywords: CDMA, power control, adaptive control, self-tuning control, radio resource management

Preface

I joined the Signal Processing Laboratory in August 1998. After completing my Master's degree in June 2000, I received a position in the Graduate School in Electronics, Telecommunications and Automation (GETA) and decided to stay in the Signal Processing Laboratory as a postgraduate student. This choice turned out to be a very good one for me.

I wish to thank my supervisor and GETA director Prof. Iiro Hartimo for his encouragement and support throughout this project. It has truly been a privilege to work in his laboratory. I would also like to thank Prof. Heikki Koivo for enlightening discussions and his invaluable guidance. I greatly appreciate the support from Professors Visa Koivunen, Jorma Skyttä, Timo Laakso, and Risto Wichman.

Many people have helped me in my research. I would like to thank especially Lic.Sc. Boris Makarevitch for his constructive comments, D.Sc. Michael Hall for his instructions related to computer simulations, and D.Sc. Mohammed Elmusrati for the delightful and fruitful conversations we have had. I also appreciate the discussions with Prof. Riku Jäntti and Lic.Sc. Vesa Hasu. I am grateful to everyone at GETA for providing me with the possibility of doing my research and sharing ideas.

The reviewers, D.Sc. Kari Kalliojärvi and Prof. Fredrik Gustafsson, deserve a praise for their efforts and valuable comments on a draft version of this thesis.

I would like to thank all my friends and colleagues at the Signal Processing Laboratory for creating an outstanding working atmosphere. In particular I want to thank D.Sc. Jarno Tanskanen for recruiting me to the laboratory in the first place and for his forbearing guidance, D.Sc. Matti Tommiska with whom I had the privilege to share a workroom for some very enlightening time in terms of discussions on matters including – but definitely not limited to – research, Prof. Jarkko Vuori, M.Sc. Juha Forsten, Mr. Petri Jehkonen, M.Sc. Jarno Martikainen, M.Sc. Esa Korpela, M.Sc. Kimmo Järvinen, M.Sc. Antti Hämäläinen, M.Sc. Kati Tenhonen, M.Sc Sampo Ojala and Mr. Jaakko Kairus. Special thanks goes to the secretaries in the lab, Anne Jääskeläinen and Mirja Lemetyinen, as well as Marja Leppäharju from GETA, the work and cheerful attitudes of yours are greatly appreciated.

This work was funded by the Graduate School in Electronics, Telecommunications and Automation (GETA) and partially by the SYTE and BROCOM projects of the National Technology Agency (TEKES). Also the financial support of Jenny and Antti Wihuri's foundation, Walter Ahlström's foundation, and the Finnish Society of Electronics Engineers is gratefully acknowledged.

I would like to thank my current employer, Texas Instruments, for their flexibility in the final

stages of preparing this thesis.

All my friends deserve my gratitude for supporting me throughout this project. Special thanks to Janna for her support and understanding at difficult times.

I dedicate this thesis to my parents Pirjo and Jorma, and my sisters Hanna and Leena, whose sincere love and support have carried me through all times in life.

Finally, I would like to express my sincere gratitude to my dear Hanne. In the final phases of this work, you inspired me to keep my mind in the essentials.

Espoo, October 2005

Matti Rintamäki

Contents

List of abbreviations and symbols

Abbreviations

1G, 2G, 3G	1st, 2nd, 3rd Generation
3GPP	3rd Generation Partnership Project
3GPP2	3rd Generation Partnership Project 2
ALP	Active Link Protection
AML	Approximate Maximum Likelihood
AMPS	Advanced Mobile Phone Service
AR	Auto-Regressive Process
ARIX	Auto-Regressive Integrated Process with Exogenous Input
ARIMAX	Auto-Regressive Integrated Moving Average Process with Exogenous Input
ARX	Auto-Regressive Process with Exogenous Input
ARMA	Auto-Regressive Moving Average Process
ARMAX	Auto-Regressive Moving Average Process with Exogenous Input
AS	Adaptive Step
AS-A	Asymmetric Adaptive Step
AS-G	Gradual Adaptive Step
AS-VG	Variable Gain Adaptive Step
ASPC	Adaptive Step Power Control
ASPC-A	Asymmetric Adaptive Step Power Control

ASPC-G	Gradual Adaptive Step Power Control
ASPC-VG	Variable Gain Adaptive Step Power Control
AWGN	Additive White Gaussian Noise
BEP	Bit Error Probability
BER	Bit Error Rate
BPSK	Binary Phase Shift Keying
BS	Base Station
CDF	Cumulative Distribution Function
CDMA	Code Division Multiple Access
CDPD	Cellular Digital Packet Data
CIR	Carrier-to-Interference ratio
CSOPC	Constrained Second-Order Power Control
DB	Distributed Balancing
DCPC	Distributed Constrained Power Control
DCS	Digital Cellular System
DDPC	Distributed Discrete Power Control
DF	Describing Function
DFB	Decision Feedback
DFM1, DFM2	Decision Feedback Method 1, 2
DPC	Distributed Power Control
DPCCH	Dedicated Physical Control Channel
DS	Direct Sequence
EDGE	Enhanced Data Rates for GSM Evolution
FDD	Frequency Division Duplex
FDMA	Frequency Division Multiple Access

FDPC	Fully Distributed Power Control
FER	Frame Error Rate
FH	Frequency Hopping
FSPC	Fixed-Step Power Control
GDCPC	Generalized Distributed Constrained Power Control
GMV	Generalized Minimum Variance
GMV-PC	Generalized Minimum Variance Power Control
GMVD-PC	Generalized Minimum Variance Decision Feedback Power Control
GMVI-PC	Generalized Minimum Variance Incremental Power Control
GMVID-PC	Generalized Minimum Variance Incremental Decision Feedback Power Control
GPC	Generalized Predictive Control
GPC-PC	Generalized Predictive Power Control
GPCD-PC	Generalized Predictive Decision Feedback Power Control
GPCI-PC	Generalized Predictive Incremental Power Control
GPCID-PC	Generalized Predictive Incremental Decision Feedback Power Control
GPRS	General Packet Radio Service
GSM	Global System of Mobile Communications (originally named as Groupe Spécial Mobile)
HSCSD	High Speed Circuit Switched Data
HSD	High Speed Data
HSDPA	High Speed Downlink Packet Access
IFB	Information Feedback
IFM1, IFM2	Information Feedback Method 1, 2
IS-xx	Interim Standard - xx
IMT-2000	International Mobile Communications for the year 2000

JTACS	Japanese Total Access Communications System
LMS	Least Mean Squares
LOS	Line of Sight
MA	Moving Average Process
M-DB	Modified Distributed Balancing
MMSE	Minimum-Mean-Square-Error
MODPC	Multi-Objective Distributed Power Control
MOTDPC	Multi-Objective Totally Distributed Power Control
MRC	Maximal Ratio Combining
MS	Mobile Station
MTP	Minimum Transmission Power
MUD	Multiuser Detection
MV	Minimum Variance
MV-PC	Minimum Variance Power Control
MVD-PC	Minimum Variance Decision Feedback Power Control
MVI-PC	Minimum Variance Incremental Power Control
MVID-PC	Minimum Variance Incremental Decision Feedback Power Control
NLOS	No Line of Sight
NMT	Nordic Mobile Telephone
NTT	The Nippon Telephone and Telegraph
ODFM	Optimal Decision Feedback Method
PC	Power Control
PCA	Power Control Algorithm
PDC	Personal Digital Cellular
PDF	Probability Density Function

PL	Path loss
PRBS	Pseudo-Random Binary Sequence
QoS	Quality of Service
RELS	Recursive Extended Least Squares
RLS	Recursive Least Squares
RRM	Radio Resource Management
SAS	Soft and Safe Admission Control
SIR	Signal-to-Interference Ratio
SMS	Short Message Service
TACS	Total Access Communications System
TDD	Time Division Duplex
TDMA	Time Division Multiple Access
TPC	Transmission Power Control
UMTS	Universal Mobile Telecommunication System
UTRA	Universal Terrestial Radio Access
WCDMA	Wideband Code Division Multiple Access

Symbols

Symbols in Chapter 1

$()^*$	complex conjugate
$()^T$	matrix transpose
$\hat{x}$	estimate of variable x
a	correlation coefficient of shadow fading
$\boldsymbol{A}$	normalized channel attenuation matrix
A_f	fast fading component
A_p	path loss constant
$A(q^{-1})$	process model denominator polynomial
b/s	bits per second
b_i	base station assignment variable
$B(q^{-1})$	process model numerator polynomial
chip/s	chips per second
C	Capacity
$C(q^{-1})$	noise filter numerator polynomial
d	path loss exponent
E_b/I_o	bit-energy-to-interference-spectral-density ratio
$(E_b/I_o)_i$	bit-energy-to-interference-spectral-density ratio of user i
$E\{\cdot\}$	expectation operator
$e(t)$	power control misadjustment (error between measured SIR and SIR target) at time instant t
$e_{\mathrm{d}}(t)$	process disturbance at time instant t
$\hat{F}_n(a)$	estimator of a probability distribution function $F(a)$ based on n samples
g	link attenuation

g_m	multipath fading power attenuation
g_p	path loss power attenuation
g_s	shadowing power attenuation
g_{ij}	link attenuation between receiver i and transmitter j
$g(t)$	link attenuation at time instant t
G_p	processing gain
$\boldsymbol{H}$	normalized channel attenuation and link quality requirement matrix
$\boldsymbol{I}$	identity matrix
I_o	interference power spectral density
$I(t)$	interference power in decibels at time instant t
$I(\boldsymbol{p})$	interference function
k	total loop delay
n	additional loop delay ($n = k - 1$)
$n_a, n_b, n_c, \ldots$	order of polynomial A, B, C, $\ldots$
N	number of users
N_1	minimum output horizon
N_2	maximum output horizon
N_o	noise power spectral density
N_u	control horizon
$p_i(t)$	transmission power of user i at iteration t
p_r	received power
$\boldsymbol{p}$	normalized transmission power vector
$\boldsymbol{p}^*$	optimal transmission power vector
P_b	bit error probability
$P_{\text{PCE}}(t)$	probability of bit error in the power control command transmission at time instant t

$\boldsymbol{P}(t)$	covariance matrix at time instant t
q^{-1}	backward time shift operator
r	distance in meters
$r(t)$	reference signal at time instant t
R	source information rate
$R_a(k)$	shadow fading correlation sequence
R_b	data rate in bits/second
$R_{b,i}$	data rate of user i
$\boldsymbol{R}_b(\boldsymbol{p})$	rate vector with power vector $\boldsymbol{p}$
T	sampling period
T_{PC}	power control period
$u(t)$	process input at time instant t
$u_{\text{rx}}(t)$	received power control command at time instant t
$u_{\text{tx}}(t)$	transmitted power control command at time instant t
v	speed
Var$\{\cdot\}$	Variance operator
$w(t)$	future reference trajectory
W	transmission bandwidth
$\boldsymbol{x}(t)$	regression vector at time instant t (RLS algorithm)
$y(t)$	process output at time instant t
$Y_f(E, N, \delta_e)$	describing function
z_u	u-percentile of the standard normal density function
α_f	forgetting factor
β	PC algorithm parameter
γ	Signal-to-interference ratio (SIR)

γ_i	SIR of user i
$\gamma_i(\boldsymbol{p})$	SIR of user i with power vector $\boldsymbol{p}$
$\gamma_i^t(t)$	SIR target of user i at time t
γ^*	maximum achievable SIR
δ	power control step size
δ_{down}	downwards step size in outer-loop PC algorithm
δ_e	error signal threshold for switching to backup controller / power control update parameter
δ_e^{down}	power control update parameter downwards
δ_e^{up}	power control update parameter upwards
δ_{up}	upwards step size in outer-loop PC algorithm
δ_{VG}	variable gain update parameter
δ_u	control signal threshold for switching to backup controller
$\delta(j)$	weighting sequence
Δ	time difference operator
ϵ_D	correlation between two points separated by distance D
$\epsilon(t)$	prediction error at time instant t
$\epsilon_{\text{E}}(t)$	prediction error at time instant t (RELS and AML algorithms)
ζ	normally distributed shadowing component
ζ_i	fraction of desired signal power that receiver i is able to utilize
$\eta(t)$	additive disturbance signal of a linear process model
η_i	noise power at the receiver of user i
$\boldsymbol{\eta}$	normalized noise power vector
$\boldsymbol{\theta}(t)$	parameter vector at time instant t
$\boldsymbol{\theta}_{\text{E}}(t)$	parameter vector at time instant t (RELS and AML algorithms)

λ	weighting parameter
$\lambda(j)$	weighting sequence
$\xi(t)$	Gaussian distributed white noise sample at time instant t
$\rho(\boldsymbol{H})$	spectral radius of matrix $\boldsymbol{H}$
σ_s^2	shadow fading variance
τ_p	propagation delay
$\phi(t)$	residual at time instant t
$\phi_{\mathrm{E}}(t)$	residual at time instant t (RELS and AML algorithms)
$\phi_{\mathrm{O}}(t)$	process pseudo-output at time instant t
$\boldsymbol{\Phi}(t)$	regression vector at time instant t (RELS algorithm)
$\boldsymbol{\Psi}(t)$	regression vector at time instant t (AML algorithm)
$\omega(t)$	relaxation factor

Chapter 1

Introduction

Wireless cellular communication systems have experienced a rapid growth during the last two decades. The first-generation (1G) systems were analog and provided wireless speech service. The major improvement in the transition to second-generation (2G) systems was the digital transmission technology, which enabled the use of error correction coding and increased service quality and capacity. The 2G systems have evolved further to provide also packet-switched data service in addition to the conventional circuit-switched services like the familiar speech service. Today, data rates of the order of tens or even hundreds of kilobits per second are provided. Still, the 2G systems were designed mainly for wireless speech service.

As the markets have emerged for high-speed wireless multimedia, the old speech-optimized infrastructures are no longer enough. 2G systems, like the Global System for Mobile Communications (GSM), will continue to evolve to provide data services with data rates up to 384 kb/s. To go beyond this, new infrastructures that are suitable for the transmission of high-speed wireless data are being built all over the world. These infrastructures, called third-generation (3G) systems, are specified to provide data rates up to 2 Mb/s, which enables many new services, including streaming video, web browsing and file transfer.[1] To be of interest to the customers, the new services should be cheap and of high quality. An important step for achieving these goals is the selection of the multiple access method. Wideband Code Division Multiple Access (Wideband CDMA or WCDMA) has been selected as the air interface for these networks. The reasons for this choice are discussed in section 1.1. The 3G system in Europe is called the Universal Mobile Telecommunication System (UMTS) [2, 3, 4].

In CDMA systems the users transmit their signals simultaneously in the same frequency band. Each user is given a dedicated *spreading code*, which is used to identify the users in the

[1] With the aid of High Speed Downlink Packet Access (HSDPA), even 10 Mb/s peak data rates can be supported in hotspot areas [1]

receivers by correlating the received signal with a replica of the desired user's code.[2] The cross-correlation of different spreading codes is ideally zero, but due to multipath propagation and non-ideal spreading codes this is not the case in practice. The receiver therefore sees the other users' signals as interference and the more users in the system the more interference is generated.

CDMA is interference-limited, which means that it is the interference from other users that limits the capacity of the system. To increase capacity, some methods are needed for interference management.

Power control (PC) aims to control the transmission powers in such a way that the co-channel interference is minimized, while at the same time achieving sufficient *quality of service* (QoS). Since in CDMA the users interfere with one another, the co-channel interference is minimized if minimum possible transmission powers are used. The problem is then to find the minimum transmission powers such that the QoS requirements of the users are fulfilled. Minimizing the transmission powers has the additional desirable effect of prolonging the battery lives of the mobile terminals. The power control problem is discussed in detail in Chapter 3.

Other means to co-channel interference management are *spatial filtering* and *multiuser detection* (MUD). Spatial filtering involves the use of smart antennas (or adaptive antennas), which consist of multi-antenna arrays with adaptive weights in the antennas. By varying the weights of the antennas, the antenna gain towards the users can be adjusted so that the desired user's signal is amplified and the interfering users' signals are attenuated. Multiuser detection takes advantage of the known spreading code structure, and aims to cancel the interfering users' signals with known spreading codes from the received signal [5].

In this thesis the focus is on power control.

1.1 Multiple access methods

The basis for the design of the air interface in a communication system is how the common transmission medium is shared between users, that is, the multiple access method. Different methods have been developed to distinguish users from each other. Various aspects of different multiple access methods are discussed, e.g., in [6, 7, 8, 9, 10].

In *frequency division multiple access* (FDMA), the total bandwidth of the system is divided into narrow frequency channels using bandpass filters. These channels are then allocated to the users. FDMA was mainly used in first generation analog cellular networks. An example of an FDMA based system is the *Nordic Mobile Telephone* (NMT).

In *time division multiple access* (TDMA) each frequency channel is divided into time slots

[2] This applies to direct sequence CDMA (DS-CDMA). In frequency hopping CDMA (FH-CDMA) the code is utilized in a different way (see section 1.1)

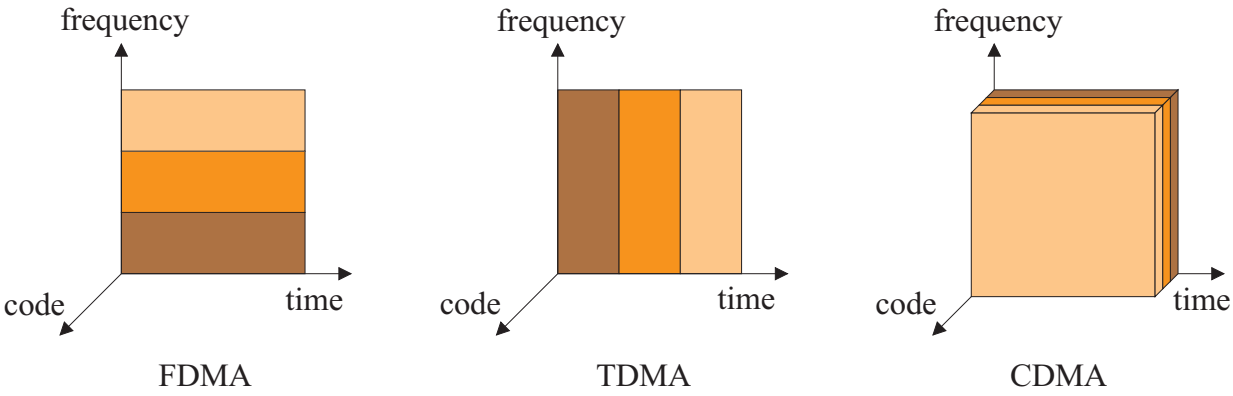

Figure 1.1: Multiple access methods.

that are allocated to the users. An example of a TDMA based system is the *Global System of Mobile Communications* (GSM), where eight users are time-multiplexed to a common 200 kHz band. Also FDMA is employed to separate each group of eight users into separate frequency bands [7].

Code division multiple access (CDMA) is a spread spectrum technology, in which each user is assigned a pseudo-random spreading code. Using this code, the narrowband data signal of the user is spread in frequency so that the transmitted signal's bandwidth is much larger than the original signal's bandwidth. There are two approaches to the spreading: *direct sequence* (DS) and *frequency hopping* (FH). In FH-CDMA the transmission frequency is rapidly changed according to the spreading code. The rapid changes of the transmission frequency makes the signals appear as wideband signals. The DS method is employed in most commercial CDMA systems, including UMTS. In DS-CDMA the data bits are directly multiplied by the spreading code bits (called *chips*). Since the chip rate is much higher than the bit rate, the resulting signal has accordingly higher bandwidth than the raw data signal. All users transmit their signals simultaneously in the same frequency band. The users can be identified in the receivers by correlating the received signal with a replica of the desired user's code. In the thesis only DS-CDMA is considered, and the term CDMA refers to DS-CDMA unless otherwise noted.

The multiple access methods are illustrated in Figure 1.1.

CDMA offers many benefits that make it more bandwidth efficient than plain FDMA or TDMA [9, 11, 12]. These benefits are obtained by incorporating certain features that are possible due to the noise-like characteristics of the signal waveform. One of the most important of these is *universal frequency reuse*, that is, all users occupy a common frequency spectrum allocation. This increases the spectrum usage, and eliminates the need for planning for different frequency allocation for neighboring users or cells. Another benefit is the use of the *RAKE receiver*, which can constructively combine multipath components, thus mitigating channel fading [13]. CDMA

also enables soft handoffs among base stations, which improves cell boundary performance and prevents dropped calls. Yet another benefit is the use of voice activity (reducing the transmission rate during silent periods in a conversation), which reduces interference and thus has a direct impact on capacity.

There is no single well-defined definition for *wideband CDMA* (WCDMA) [14]. One proposed definition is based on the *coherence bandwidth* of the channel, i.e., the minimum distance between two frequencies such that the channel fading at those frequencies is essentially uncorrelated. The CDMA system is called wideband CDMA if the transmission bandwidth exceeds the coherence bandwidth. Some definitions are based on the chip rate or bandwidth as a fraction of center frequency. Anyway, there is no distinct threshold separating narrowband CDMA from WCDMA.

1.2 Problems and goals of this thesis

Three different power control modes can be identified in typical CDMA systems: *open loop PC*, *closed loop PC* (or *inner loop PC*) and *outer loop PC*. Open loop PC is used in the beginning of a radio link connection establishment to set the transmission power according to measurements of the return channel link gain. Outer loop PC sets the target signal-to-interference ratio (SIR) to such a level that sufficient quality of service is guaranteed, and closed loop PC aims to keep the receiver SIR at this target value using feedback signals from the receiver. Figure 1.2 shows a model of uplink (transmission from mobile unit to base station) power control in CDMA.

The purpose in this thesis is to study the power control problem and algorithms in CDMA cellular communication systems, identifying various real-world limitations and aspects, that may limit the use of some power control methods proposed in the literature. Various new closed-loop power control algorithms are developed for improving the performance of closed-loop power control under the said limitations. The proposed algorithms are evaluated by analytical methods and extensive computer simulations. In the following, the problems addressed in the thesis are discussed in slightly more detail.

1.2.1 Power control loop delay

The SIR measurement, processing and the transmission of the power control commands over the air interface constitute a delay between the time the power update command is calculated and the time it is applied in the transmitter. During this time the radio channel and interference conditions might have changed considerably, which deteriorates the performance of power control. Many of the power control algorithms proposed in the literature are studied without taking the loop

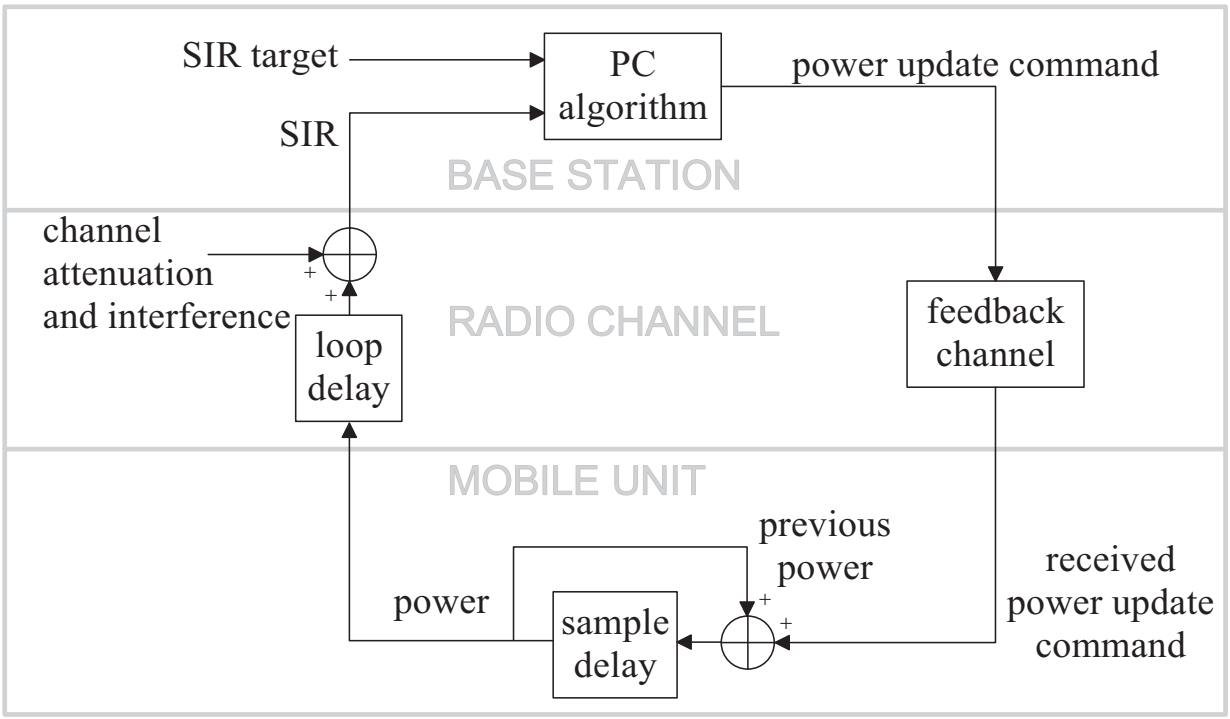

Figure 1.2: General model of uplink power control in CDMA.

delay into account. However, the loop delay can cause increased oscillations of the SIR around the setpoint, and even make the power control algorithm unstable if it is ignored in the design of the algorithm. In this thesis several adaptive closed-loop algorithms are proposed that are able to mitigate the effects of the loop delay.

1.2.2 Limited signaling bandwidth

In closed-loop power control the power update command must be transmitted through a feedback channel to the transmitter, which then adjusts its transmission power based on the received command. This signaling obviously consumes radio resources from the feedback channel, which is undesirable. In the thesis, two feedback methods are considered: *information feedback (IFB)* and *decision feedback (DFB)*. In IFB real-valued commands are fed back, while in DFB only the sign of the command is fed back. Thus, for a given period of transmission of the feedback signal, the IFB method consumes much more radio resources than the DFB method, which requires only one bit for the transmission of a single command. All the proposed algorithms in the thesis are given in both IFB and DFB forms, except the *adaptive step-size* PC algorithms in Chapter 6, which are inherently DFB-type algorithms.

1.2.3 Dynamic radio environment

A common way to study power control algorithms has been the so-called *snapshot* method, where the link gains of the radio channel are assumed to be fixed, or change very slowly compared to the dynamics of the power control algorithm. This is not very realistic, because in practice the transmitted signals experience various kinds of fading, noise and interference. In the thesis the main focus is on this kind of dynamical radio environment, and these dynamics are also taken into account in the design of the proposed improved closed-loop power control algorithms.

1.2.4 Ways to achieve the goals in the thesis

In this thesis adaptive self-tuning controllers are used to reduce the undesirable effects of the loop delay. The idea is to model the power control system from the input to the feedback channel (the power control command) to the received SIR as a linear process and then design a controller to make the process output, in this case the SIR at the receiver, to follow a desired reference signal, which is the SIR target provided by the outer loop power control. An adaptation mechanism is utilized for online identification of the model parameters. Practical versions of the proposed algorithms are provided that achieve performance improvements without any increase in power control signaling. Three controller approaches are considered, namely Minimum Variance (MV), Generalized Minimum Variance (GMV) and Generalized Predictive Control (GPC). The reasons for these choices are discussed in Chapter 4. An analytical study based on *describing functions* is presented for one of the minimum-variance-based algorithms. However, due to the complexity of the adaptation mechanisms in the proposed algorithms, their detailed analytical study becomes prohibitively complex. Therefore, the performances of the methods are investigated using extensive computer simulations. The results are compared with well-known algorithms from the literature. The simulations indicate that the proposed algorithms can improve the performance of closed-loop power control significantly compared to reference algorithms in the sense that the average SIR at a given outage probability level is higher. Outage probability is defined in Chapter 3.

Another approach proposed in the thesis is the *Adaptive Step Size (AS)* method. This method addresses the PC signaling bandwidth limitation in the DFB case, and aims at improving the performance of DFB-type PC algorithms by adaptation of the PC step size based on the ON-OFF PC commands. *Adaptive Step Power Control (ASPC)* algorithms based on the AS method are proposed. It is shown by simulations that for slowly moving mobiles, the proposed method improves the PC performance without violating the DFB limitation. The proposed step-size adaptation methods are independent from the actual power control algorithm, and can be combined also with other power control algorithms. Examples of the combinations of the AS method and

its variations with the adaptive PC algorithms proposed in Chapter 4 are given in the simulations in Chapter 7.

While the power control methods described in this thesis can be applied to CDMA systems in general, the main focus in this thesis is on WCDMA, and all the simulations presented are made for WCDMA systems.

1.3 Thesis Outline

The thesis is organized as follows. After the introduction in Chapter 1, an overview on cellular radio systems is given. This chapter is mainly for those unfamiliar with such systems, and introduces briefly the key aspects, problems and design challenges in these systems.

Power control in CDMA cellular communication systems is discussed in detail in Chapter 3, which gives the necessary background to understand the contributions made in the thesis. A literature survey of previous work in this area is also provided.

In Chapter 4 new adaptive closed-loop power control algorithms are proposed. The Chapter gives an introduction to adaptive self-tuning control and recursive system identification methods, as well as complete descriptions of the self-tuning control methods that form the basis of the proposed algorithms. New approaches to modify the controllers for DFB are also proposed.

An analysis of the MVD-PC algorithm from Chapter 4 is provided in Chapter 5. The analysis is based on the well-known *Describing Function (DF)* method. Although many simplifications had to be made to complete the analysis, the results give valuable insight to the behavior of the proposed algorithms.

Chapter 6 introduces the *Adaptive Step (AS)* method and the corresponding *Adaptive Step Power Control (ASPC)* algorithm. Various modifications to improve the properties of the algorithm are given, and some simulation examples demonstrating these properties are provided.

In Chapter 7 some special cases are studied, such as combinations of the AS methods of Chapter 6 with the algorithms proposed in Chapter 4, performance in the case of measurement errors, and performance in soft handovers.

Finally, summary and conclusions are given in Chapter 8 with comments about open issues.

1.4 Original contributions

The following original contributions are made in the thesis:

– Modeling of the closed-loop power control in WCDMA with a linear model in Chapter 4, section 4.5.

– Development of new closed-loop power control algorithms based on self-tuning controllers and the linear model of the closed-loop power control in Chapter 4. The considered control strategies are Minimum Variance (MV) in section 4.7, Generalized Minimum Variance (GMV) in section 4.8, and Generalized Predictive Control (GPC) in section 4.9. The algorithms are capable of alleviating the undesirable effects of the loop delay inherent in the closed-loop power control process.

– Decision feedback formulations of the considered control strategies in the case of hard-quantized control output signals in Chapter 4, Sections 4.7, 4.8 and 4.9.

– Both information feedback (unlimited signaling bandwidth) and decision feedback (limited signaling bandwidth) versions of the proposed closed-loop power control algorithms, where the proposed decision feedback formulations of the considered control strategies are employed in the proposed power control algorithms.

– Describing function analysis of the MVD-PC algorithm in Chapter 5.

– The new Adaptive Step method and its modifications, as well as new PC algorithms that are based on these methods. The ASPC algorithm was proposed in [15, 16]. The first idea of the ASPC algorithm and the mathematics of the ASPC algorithm were contributed by the first author in these papers. The author of this thesis refined the idea by proposing the PC misadjustment to be reconstructed instead of SIR. All the modifications and their related mathematics and all the simulations, including those presented in [17] are done by the author of this thesis.

– Extensive simulations of the proposed algorithms and reference algorithms taken from the literature.

1.5 Publications

Some of the material in the thesis has been, or will be, published elsewhere. The following is a list of publications by the author that relate to the material in this thesis. Publication P1 is the basis for Chapter 3. The material in Chapter 4 is for the most part covered in publications P2-P8. The ASPC algorithm and some of its modifications are presented in publications P9-P10.

[P1] M. Rintamäki, "Power Control in CDMA Cellular Communication Systems," in *Wiley Encyclopedia of Telecommunications*, J. G. Proakis, Ed. John Wiley & Sons, 2002.

[P2] I. Virtej, M. Rintamäki and H. Koivo, "Enhanced fast power control for WCDMA systems," in *Proc. IEEE Int. Symp. on Personal, Indoor and Mobile Radio Commun. (PIMRC)*, London, UK, Sept. 2000, pp. 1435-1439.

[P3] M. Rintamäki, I. Virtej and H. Koivo, "Two-mode fast power control for WCDMA systems," in *Proc. IEEE Veh. Tech. Conf. (VTC)*, vol. 4, Rhodos, Greece, May 2001, pp. 2893-2897.

[P4] M. Rintamäki and H. Koivo, "Adaptive robust power control for WCDMA systems," in *Proc. IEEE Veh. Tech. Conf. (VTC)*, vol. 1, Atlantic City, NJ, USA, Oct. 2001, pp. 62-66.

[P5] M. Rintamäki, K. Zenger and H. Koivo, "Self-tuning adaptive algorithms in the power control of WCDMA systems," in *Proc. Nordic Signal Processing Symp. (NORSIG)*, boat Hurtigruten, Norway, Oct. 2002.

[P6] M. Rintamäki, H. Koivo, and I. Hartimo, "Adaptive closed-loop power control algorithms for CDMA cellular communication systems," *IEEE Trans. Veh. Technol.*, to be published.

[P7] M. Rintamäki, H. Koivo, and I. Hartimo, "Adaptive closed-loop power control algorithms for CDMA cellular communication systems – part II," *IEEE Trans. Veh. Technol.*, submitted for publication.

[P8] M. Rintamäki, H. Koivo, and I. Hartimo, "Application of the generalized predictive control method in closed-loop power control of CDMA cellular communication systems," in *Proc. Nordic Signal Processing Symp. (NORSIG)*, Espoo, Finland, June 2004.

[P9] M. S. Elmusrati, M. Rintamäki, I. Hartimo, and H. Koivo, "Estimated step power control algorithm for wireless communication systems," in *Proc. Finnish Signal Processing Symp.*, Tampere, Finland, May 2003.

[P10] M. S. Elmusrati, M. Rintamäki, I. Hartimo, and H. Koivo, "Fully distributed power control algorithm with one bit signaling and nonlinear error estimation," in *Proc. IEEE Veh. Tech. Conf. (VTC)*, Orlando, FL, USA, Oct. 2003, pp. 727-731.

Chapter 2

Cellular radio communication systems

This Chapter explains the basic characteristics of cellular radio communication systems. The aim is not to give a detailed review of this enormous field, but to introduce the essential aspects necessary to understand the problems and design challenges in such systems. The subjects that are relevant to the thesis are presented in slightly more detail.

2.1 The development of wireless mobile communication systems

2.1.1 Historical events

The development of wireless mobile communication systems is covered in many sources, e.g., [18, 19, 20, 21, 7, 22, 23, 24].

The basic theory of electromagnetic fields was created by J. C. Maxwell after the middle of the 19th century. This theory was experimentally proved by H. G. Hertz in the late 19th century. Still before the 20th century, in 1898, the first successful use of mobile radio was done by M. G. Marconi, who was able to establish a ship-to-shore wireless radio link over a path of 18 miles. This event is considered to be the origin of mobile radio.

In the beginning of the 20th century, the mobile radio communication systems were used for simple Morse-coded on-off keying-based message transmission. It was not before 1928 that the first land mobile radio systems for broadcasting messages to police vehicles was deployed. Since then, the mobile radio communication concept was deployed by the military, as well as vital mobile services such as those of ambulance, fire, marine, aviation, etc. However, the quality of the communication was poor, because at that time the technology was not mature enough to successfully cope with the characteristics of radio wave propagation. Also, the equipment was bulky, heavy, and consumed lots of power. Therefore, the general commercial use of mobile

radio communications had to wait for the development of technology.

The mathematical foundations of information transmission were established by Shannon [25, 26, 27]. In his work he demonstrated that the effect of a transmission power constraint, a bandwidth constraint, and additive noise can be associated with the channel and incorporated into a single parameter, called the *channel capacity*. In case of Additive White Gaussian Noise (AWGN) channel, an ideal bandlimited channel of bandwidth W has a capacity C given by

$$C = W \log_2 \left(1 + \frac{p_r}{W N_0}\right) b/s, \tag{2.1}$$

where p_r is the average received power and N_0 is the power spectral density of the additive noise. Thus, if the source information rate R is less than C ($R < C$), then it is theoretically possible to have error-free transmission of the information through the channel with appropriate coding. If $R > C$, reliable transmission is not possible regardless of any signal processing at the transmitter or receiver [13]. Shannon's establishments gave birth to a new field called *information theory*.

2.1.2 The first generation (1G) cellular systems

The cellular radio concept was developed in Bell Laboratories in 1947. Instead of transmitting signals from one location with high power, the system capacity could be dramatically increased by limiting the range of the transmission, which enables the same frequencies to be reused at much shorter distances. However, the concept was not implemented until 1979. It was not until that time that the technological developments such as integrated circuits, microprocessors, frequency synthesizers, etc., had made it possible. Soon after this came the first generation of commercial cellular radio systems, such as The Nippon Telephone and Telegraph (NTT) system in 1979, the Nordic Mobile Telephone (NMT) system in 1981, the Advanced Mobile Phone Service (AMPS) in 1983 and the British Total Access Communications System (TACS) in 1985 (a modified version of AMPS). TACS is also used in Japan, where the system is called JTACS. These systems are/were analog, and were designed for wireless speech service.

2.1.3 The second generation (2G) cellular systems

The developments of digital signal processing methods along with the rapid development of integrated circuits and microprocessors led to the replacement of the analog 1G cellular systems by the digital 2G cellular systems. The first of these, the Global System for Mobile Communications (GSM)[1], was realized in 1992 in Europe. It operates in the 900 MHz band, and is based on

[1] Originally GSM was an acronym for Groupe Spècial Mobile, which was the group that was established in 1982 to define the future cellular radio standards in Europe.

FDMA/TDMA. Variants of GSM have been developed for higher frequency bands, such as the Digital Cellular System 1800 (DCS 1800) in Europe and PCS 1900 in North America. The GSM system became a huge success. As of December 2004, there were 626 GSM networks on air in 198 countries or territories around the world [28].

In North America, the AMPS system suffered from capacity limits, and it was decided that any second-generation system must be backwards compatible with AMPS. As a result, two systems were designed and deployed: the TDMA-based D-AMPS (Digital AMPS, also known as IS-54, and later IS-136) and the CDMA-based IS-95.

The first 2G system in Japan is called the Personal Digital Cellular (PDC) system. It is similar to the IS-54/136 system.

The major improvements offered by the digital transmission of the 2G systems over 1G systems were better speech quality, increased capacity, global roaming, and data services like the Short Message Service (SMS), which gained tremendous popularity in the 1990's. Major improvements in the data services were also the introduction of packet switched services such as the General Packet Radio Service (GPRS, [29, 30]), and higher-data-rate circuit switched services such as the High Speed Circuit Switched Data service (HSCSD, [31, 32]).

2.1.4 The third generation (3G) cellular systems

Although the 2G systems could already provide some basic data services, the possible data rates were still relatively low, and could not satisfy the needs of future mobile services like mobile web browsing, file transfer, real-time video, digital TV, etc. The 3G cellular systems are known with the name International Mobile Communications for the year 2000 (IMT-2000) [33], and are being implemented in many countries around the world. The 3G systems introduce wireless wideband packet-switched data services for wireless access to the Internet with speeds up to 2 Mb/s. The 2G systems have been (and still are) evolving towards the next generation with the introduction of new technology enhancements, such as GPRS and HSCSD in GSM, Cellular Digital Packet Data (CDPD, [34, 35]) that operates over AMPS, and High Speed Data (HSD, [36]) in IS-95. A step further towards the 3G networks is the Enhanced Data rates for GSM Evolution (EDGE, [37]) technology, which enables three times higher data rates than those possible with the ordinary GSM/GPRS network [38].

Several standardization bodies joined their forces in 1998 in the 3rd Generation Partnership Project (3GPP) agreement [4] with the joint goal of producing globally applicable technical specifications and technical reports for a 3rd generation mobile system. It has a sister project, the 3rd Generation Partnership Project 2 (3GPP2) [39], which comprises North American and Asian interests developing the 3G mobile systems. The 3GPP project produces the radio interface stan-

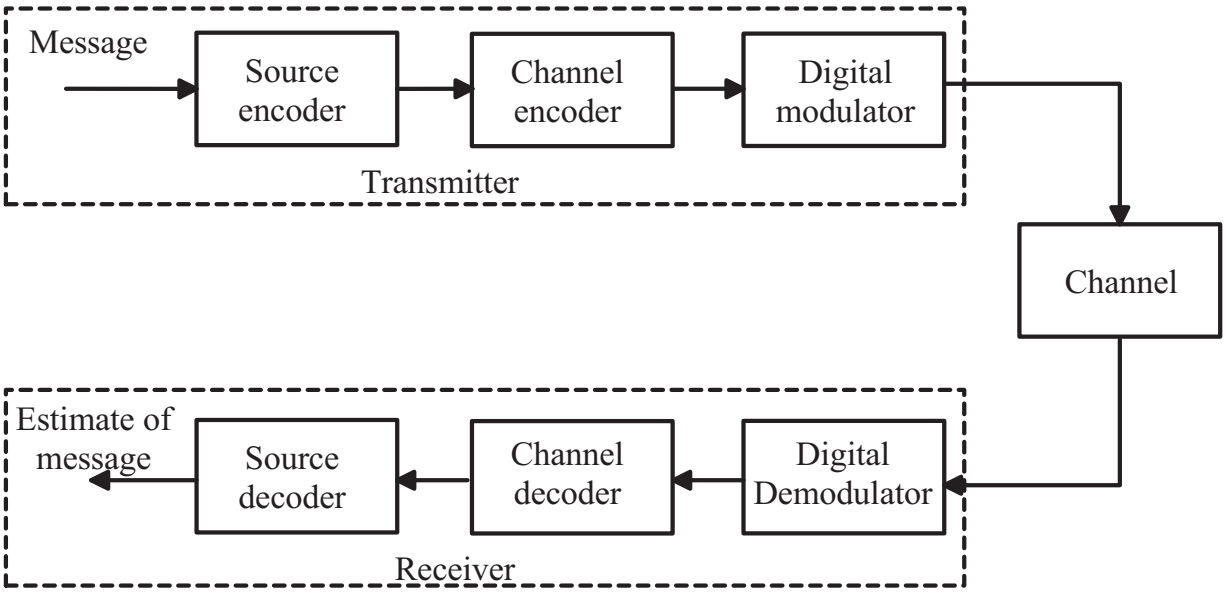

Figure 2.1: A digital communication link.

dard for the 3G networks, wideband CDMA (WCDMA), which is the main 3rd generation air interface in the world and will be deployed in Europe and Asia, including Japan and Korea. The 3G systems within the scope of 3GPP are generally known with the name *Universal Mobile Telecommunication Services* (UMTS), and WCDMA is called *Universal Terrestrial Radio Access* (UTRA) Frequency Division Duplex (FDD) and Time Division Duplex (TDD), the name WCDMA being used to cover both FDD and TDD operation [3].

The air interface to be developed by 3GPP2 is referred to as cdma2000, which is based partly on IS-95 principles. It is further divided to two standards, namely cdma2000 1x and cdma2000 3x. cdma2000 1x is considered a 2.5G system, and it has the same bandwidth (1.25 MHz) as IS-95. cdma2000 3x is the 3G variant of cdma2000. It is a wideband version with three times the bandwidth of IS-95 [40].

2.2 Wireless digital radio communication

Fig. 2.1 shows a simplified block diagram of a digital communication link [13]. In the source encoder of the transmitter, the message to be transmitted is transformed into a sequence of bits, that represents the original message. These bits are fed to the channel encoder, which introduces redundancy in the binary bit sequence in a controlled manner. This redundancy can be exploited in the channel decoder of the receiver by detection and/or correction of errors introduced by the channel. The binary information sequence output from the channel encoder is mapped into

signal waveforms in the digital modulator, and fed to the channel. In the case of wireless radio communication, the waveforms are transmitted as electromagnetic waves through transmission antenna(s).

The channel introduces various forms of corruption to the transmitted signal, like noise, interference from other transmitters, and fading (fluctuations in the channel gain). The task of the receiver is to capture the transmitted signal, and remove the effects of the channel as well as the processing in the transmitter. Firstly, the demodulator converts the received waveforms into a binary sequence, which is fed to the channel decoder. The channel decoder removes the redundancy introduced by the channel encoder in the transmitter, and attempts to detect and/or correct possible bit errors using the knowledge of the code used by the channel encoder and the redundancy contained in the received data. The frequency at which bit errors occur at the output of the channel decoder is a measure of the demodulator-decoder performance. Typically the *Bit Error Rate* (BER) at this point is kept at a desired level so as to have acceptable quality of communication with minimum resource usage. Finally, the source decoder tries to reconstruct the original message from the decoded binary sequence. This will be an estimation of the original message due to the possible corruption introduced to the data along its way through the communication link.

2.2.1 Properties of a radio communications channel

A radio communications link includes everything from the information source, through all the encoding and modulation steps, through the transmitter and channel, up to and including the receiver and all its signal processing steps, as well as the information sink [41]. The term *channel* can be defined in many ways, depending on the context that it is used in. Generally one can view a channel as the link between two points along a path of communications [7]. For example, a *digital channel* is the link between the input to the modulator and the output of the demodulator (see Fig. 2.1), while a *radio propagation channel* is the physical medium in which the radio waves propagate from the transmitter antenna to the receiver antenna. A *radio channel* is the combination of the transmitter and receiver antennas and the radio propagation channel. Radio channel is comprehensively discussed in, e.g., [41, 7, 10, 21]. The discussion here is limited to the radio channel.

The attenuation of a radio signal can be modeled as a product of three effects, namely *path loss* (g_p), *shadowing* (g_s) and *multipath fading* (g_m) [18, 19] as

$$g = g_p g_s g_m. \tag{2.2}$$

Path loss is the large-scale distance-dependent attenuation in the average signal power. *Shadowing* is the medium-scale attenuation, which is caused by diffraction and shielding phenomena

caused by terrain variations. *Multipath fading* is the rapid fluctuation in the received signal power that is caused by the constructive and destructive addition of the signals that propagate through different paths with different delays from the transmitter to the receiver. These effects are explained in more detail in the following.

2.2.1.1 Path loss

Path loss is the large-scale distance-dependent attenuation in the average signal power. Early studies by Okumura [42] and Hata [43] yielded path loss models for urban, suburban and rural areas. Based on their ideas, a widely accepted model for path loss (or path gain) g_p is described as

$$g_p = \frac{A_p}{r^d}, \tag{2.3}$$

where A_p is a constant depending on the antenna properties, transmission wavelength, and the environment (rural, suburban, urban), r is the distance between the transmitter and receiver in meters at time t and d is the path loss exponent with typical values ranging from 2 (free space propagation) to 5 (dense urban areas).

2.2.1.2 Shadowing

Shadowing, also known as slow fading, is the medium-scale attenuation, which is caused by diffraction and shielding phenomena caused by terrain variations. This results in relatively slow variations in the mean signal power over a distance of a few tens of wavelengths. It is caused by reflections, refractions and diffractions of the signal from buildings, trees, rocks, etc. It is commonly modeled as a log-normally distributed random variable with zero dB mean and a standard deviation of typically 3 to 10 dB. A simple model for the spatial correlation of shadowing was proposed in [44]. In this model, the shadowing is a log-normally distributed random variable with an exponential correlation function. The correlation function was fitted to experimental data from a 900 MHz measurement in suburban environment and from a 1700 MHz measurement in urban areas. Formally, the shadowing correlation is given by

$$R_a(k) = \sigma_s^2 a^{|k|}, \tag{2.4}$$

$$a = \epsilon_D^{vT/D}, \tag{2.5}$$

where σ_s^2 is the variance of the shadowing, a is the correlation coefficient, ϵ_D is the correlation between two points separated by distance D, v is the speed of the mobile station moving in the terrain, and T is the sampling period. This model can be easily implemented by filtering a white Gaussian noise process through a first-order filter with a pole at a.

2.2.1.3 Multipath fading

Multipath fading, or fast fading, is the rapid fluctuation in the received signal power that is caused by the constructive and destructive addition of the signals that propagate through different paths with different delays from the transmitter to the receiver. In urban environment the number of significant signal paths is typically much larger than in rural areas. This affects the *multipath spread*, which is the roughly the time between the first occurrence of the transmitted signal at the receiver and the last significant reflection of the same signal at the receiver. If the multipath spread is longer than the inverse of the bandwidth of the information-bearing signal, i.e., longer than the duration of a transmitted symbol, then the fading is said to be frequency-selective. Otherwise it is frequency-non-selective, or flat. In spread-spectrum systems, typically, the fading is frequency-selective, and this can be exploited with the use of a RAKE receiver, which coherently combines the signals received from different paths.

The multipath fading is usually modeled as a filtered complex Gaussian process, resulting in a Rayleigh-distributed envelope, and a classical Doppler spectrum. This model is applicable in no-line-of-sight (NLOS) situations. If a line-of-sight (LOS) signal is present, then the fading envelope can be modeled with a Rice distribution. Also Nakagami distribution has been widely used to model multipath fading [21]. Jakes [18] proposed a model for a Rayleigh fading simulator with the required spectral properties based on a sum of sinusoids. This model is still widely used.

2.2.1.4 Example: simulated channel gain

All the above three effects included, the power gain g of the channel in linear scale can be modeled as:

$$g = g_p g_s g_m = A_p r^{-d} 10^{\frac{\zeta}{10}} A_f \tag{2.6}$$

where ζ is a Gaussian random variable with zero mean, standard deviation between 3 to 10, and exponential correlation function. A_f is a random variable such that $\sqrt{A_f}$ is either Rayleigh-, Rice- or Nakagami distributed with a classical Doppler spectrum. An example of a simulated channel gain is shown in Fig. 2.2.

2.2.1.5 Wideband radio transmission

In spread spectrum systems such as DS-CDMA the transmission bandwidth is much greater than what is needed to represent the information signal. Wideband transmission has some appealing features over narrowband transmission. Since the transmission bandwidth in such systems is

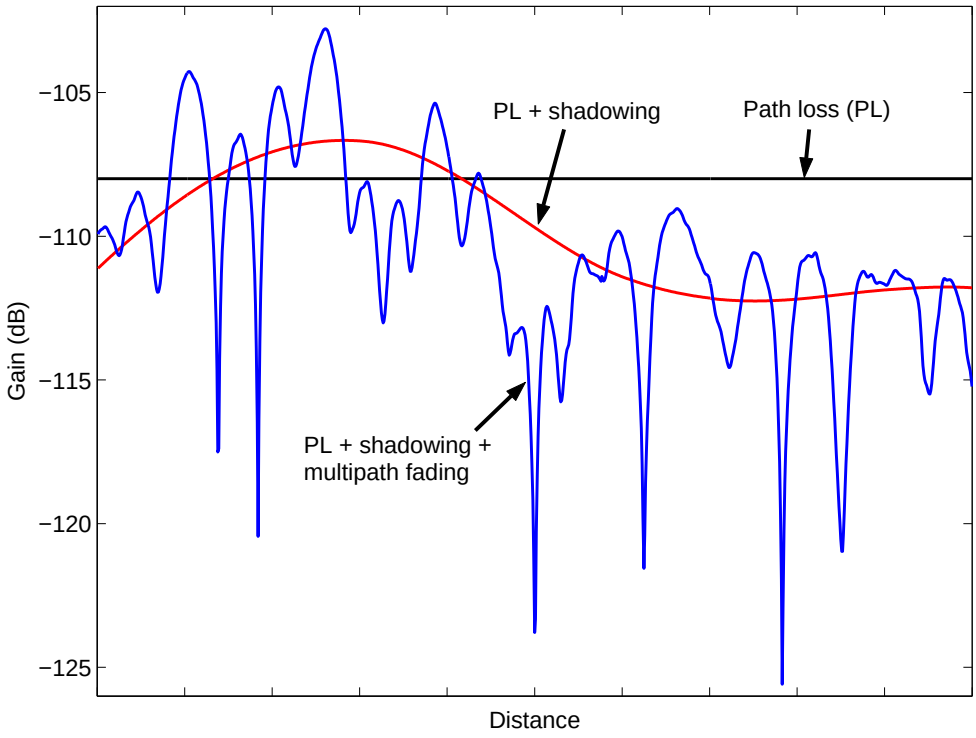

Figure 2.2: An example of a simulated channel gain.

typically much greater than the channel *coherence bandwidth*[2], the resultant power fades in a wideband channel are not as deep as in a narrowband channel [45, 19, 13]. Thus, a wideband channel affects the fading of signals as if a multi-branch diversity receiver were used at the receiving end of the channel. Fig. 2.3 shows examples of fading processes with different numbers of diversity branches.

2.3 Cellular Radio Systems

To cover a large area with mobile communication services, the area is divided into small subareas, called cells, each of which is served by a base station. The sizes of the cells can vary depending on the type of the area that they serve. For example, in a rural area with low density of users, the cells can be quite large (say, several kilometers in radius). These cells are referred to as *macro cells*. The cell sizes diminish when the number of potential users grows, like in cities and their central parts. There the cell radiuses can range from a few hundred meters to tens of meters (*micro cells*) or even meters (*pico cells*) covering, for example, a single room in a building.

[2]Channel coherence bandwidth is defined such that two sinusoids with frequency separation greater than the coherence bandwidth are affected differently by the channel, i.e., experience uncorrelated fading. The coherence bandwidth is roughly equal to the inverse of the delay spread of the channel.

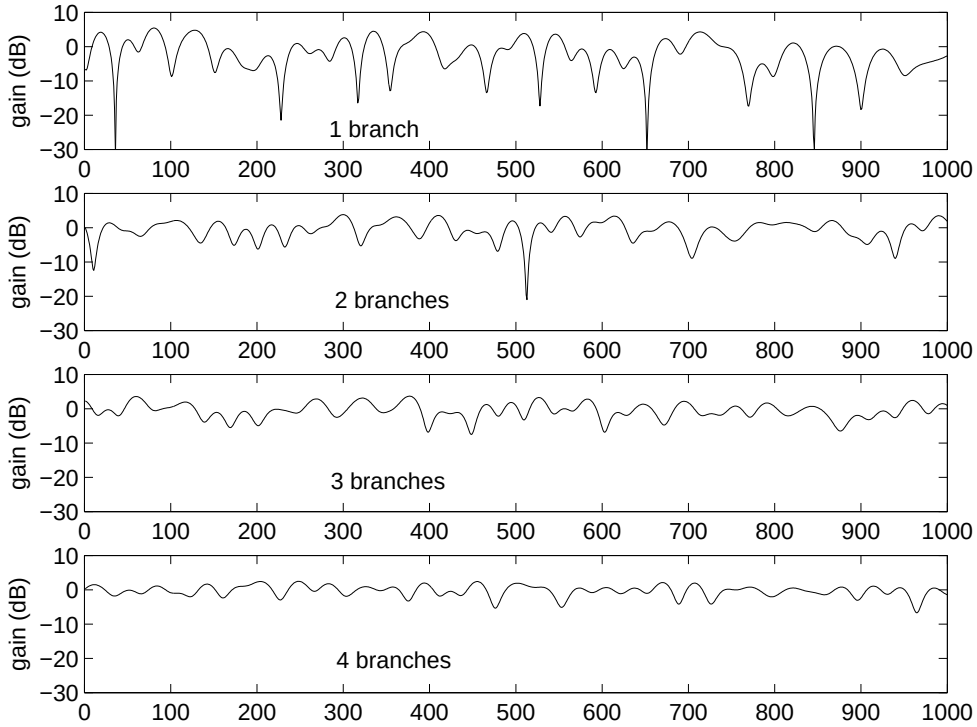

Figure 2.3: Channel fading processes with different numbers of diversity branches, assuming equal-mean-strength branches with independent Rayleigh fading.

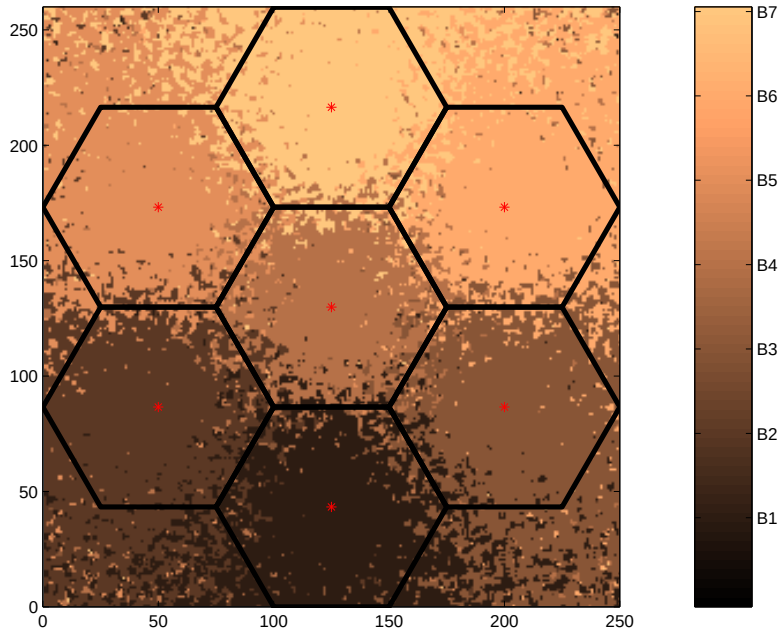

Figure 2.4: A seven-cell hexagonal pattern and cell coverage areas. The effect of shadowing makes the cell borders fragmented.

If omnidirectional antennas are used in the base stations, the cell shape is ideally a circle. In practice, however, a cell takes a rather irregular shape due to the random effects in the radio channel gain, as depicted in Fig. 2.4 (see also previous Sections). Moreover, for modeling and planning purposes, the circular form is not the most convenient one, since a plane filled up with circles can exhibit overlapped areas or gaps. Therefore, the shape of a cell is typically modeled as a regular polygon, such as an equilateral triangle, square, or hexagon, the hexagon being the most widely used shape. Of these shapes, the hexagonal array requires fewer cells for a given coverage area than a triangular or square array [20].

The beauty in the use of cells instead of a single base station is that the transmission power of the cells can be kept small, and, most importantly, the transmission frequency of a particular cell can be reused in another cell, which increases the capacity of the system tremendously. The cells using the same frequency must be located sufficiently apart so that the *co-channel interference* is kept in tolerable limits. Fig. 2.5 shows an example of a hexagonal cellular layout with reuse factor 7.

It is also possible to use directional instead of omnidirectional antennas at the base stations. Typically, the base station is equipped with three directional antennas, each covering a 120-degree sector. This can further increase network capacity, and decrease the cost of the system,

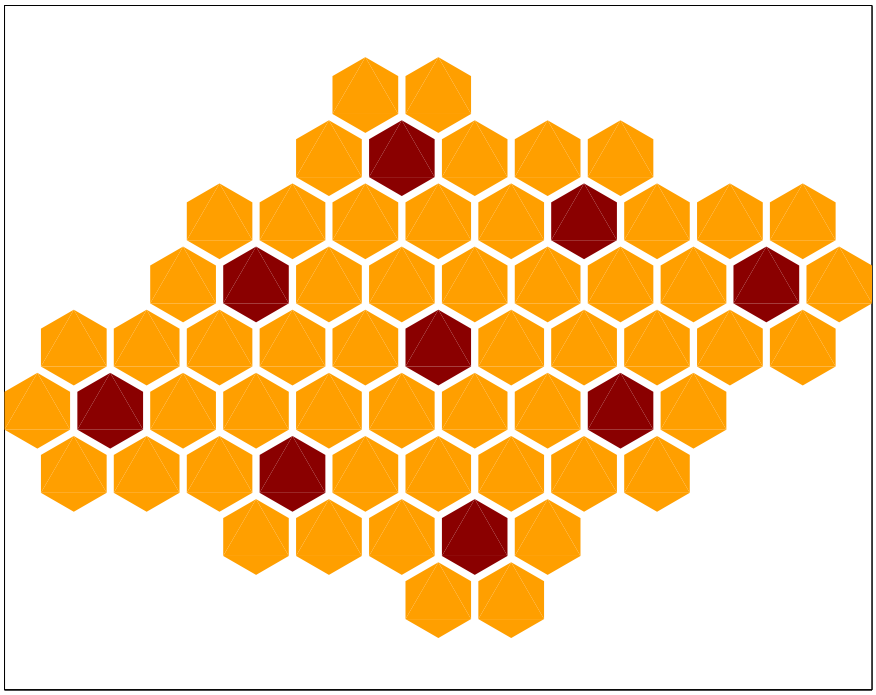

Figure 2.5: A hexagonal cell layout with frequency reuse factor 7. A group of co-channel cells is highlighted.

since the base station equipment is utilized more efficiently.

2.3.1 Co-channel interference

Co-channel interference is the interference received by a base station (uplink) or mobile station (downlink) that originates from other users transmitting simultaneously on the same frequency band as the desired user. This simultaneous transmission on the same channel is the result of frequency reuse, and is unavoidable in modern cellular communication systems.

The DS-CDMA systems are remarkable in that all users simultaneously share the same frequency band. This enables the same frequency to be used in adjacent cells, which means that the frequency reuse factor is equal to one (universal frequency reuse). However, since in practice the signals used in DS-CDMA systems are not completely orthogonal, all users in the system experience co-channel interference from all other users in the system. Thus, co-channel interference is a dominating factor in CDMA systems, and it must be efficiently controlled. Power control is an efficient technique for co-channel interference control in CDMA systems, as will be discussed in Chapter 3.

Chapter 3

Power control in CDMA cellular communication systems

The aim in this Chapter is to give a somewhat detailed overview of power control in CDMA cellular communication systems and to present the relevant problems within the scope of the thesis. A literature survey of power control algorithms is given. Although this thesis focuses mainly on power control, a survey of joint power control and other radio resource management methods is given for completeness. Some of the material in this chapter has been published in [46].

3.1 Introduction

Transmission power control (TPC) is vital for capacity and performance in cellular communication systems, where high interference is always present due to frequency reuse. The basic intent is to control the transmission powers in such a way that the interference power from each transmitter to other co-channel users (users that share the same radio resource simultaneously) is minimized while preserving sufficient quality of service (QoS) among all users. Co-channel interference management is important in any system employing frequency reuse. However, in CDMA there are interfering users both inside and outside a cell, which makes CDMA interference limited. Thus efficient TPC is essential in CDMA[1], especially in the uplink (from mobile to base station communication).

Consider the situation depicted in Figure 3.1. Mobile stations MS1 and MS2 share the same frequency band and their signals are separable at the base station BS by their unique spreading

[1]This applies to direct-sequence CDMA (DS-CDMA). In frequency-hopping CDMA (FH-CDMA) the intra-cell interference can be made very small. In this thesis the focus is on DS-CDMA, where transmission power control is more critical. Thus throughout the rest of the text, DS-CDMA is referred to simply as CDMA.

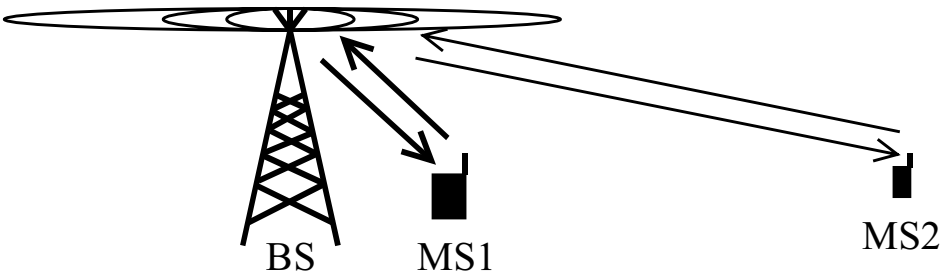

Figure 3.1: Near-far effect.

codes. The link attenuation of MS2 at a particular time instant might be much greater than that from MS1 to BS. If power control is not applied, the signal of MS1 will overpower the signal of MS2 at the base station. This is the so-called *near-far effect* [9]. To alleviate this effect, power control aims to set the transmission powers of MS1 and MS2 so that both signals are received at the same mean power level at the base station.

As can be understood from the discussion in Section 2.2.1, the received signal power attenuation is a random variable. Thus when power control is applied, it must adapt to the changing attenuation of the desired signals, as well as the changing interference conditions, since the attenuations of the co-channel users' signals are also changing, and those signals are power-controlled as well.

3.1.1 Uplink versus downlink power control

In CDMA the uplink transmission creates a near-far situation if power control is not used. This occurs because the signals of the different mobile stations propagate through different radio channels before reaching their serving base station. The task of power control is thus to vary the transmission powers in order to compensate for the varying channel attenuations, so that the signals from the different mobile stations are received with equal powers at the base station. Uplink power control is critical for the capacity of CDMA systems [9]. The requirement of the dynamic range of uplink power control can be of the order of 80 dB.

In downlink the situation is different, since all signals transmitted by a base station propagate through the same radio channel before reaching a mobile station. Therefore, since they undergo the same attenuation, power control is not needed for near-far problem. Instead, power control is used to provide more power to users located near the cell borders, suffering from high interference from nearby cells and, on the other hand, to use only sufficient transmission powers in order to minimize the interference procuded to nearby cells [47]. In principle, the downlink signals

to different users could be made orthogonal by using proper spreading codes. Unfortunately, the orthogonality of the downlink signals is lost in practice due to multipath propagation. Thus, allocating different powers for different users in downlink could cause a near-far situation at the mobile stations. For this reason, the dynamic range of downlink power control is usually much smaller than in uplink, typically of the order of 20-30 dB.

The focus in this thesis is on uplink power control, although the proposed algorithms could also be applied to downlink power control.

3.1.2 Quality measures for power control

A great deal of the work on power control in CDMA cellular systems has focused on how to set the transmission powers so that all users in the system have acceptable *bit-energy-to-interference-spectral-density ratios* (E_b/I_o).[2] This approach is based on the fairly reasonable assumption that the *bit error probability* (BEP) at a receiver is a strictly monotonically decreasing function of E_b/I_o. For instance, BEP P_b of binary phase shift keying (BPSK) modulation in an *additive white Gaussian noise* (AWGN) channel is given by [13]

$$P_b = Q\left(\sqrt{\frac{2E_b}{I_o}}\right), \tag{3.1}$$

where $Q(x)$ is defined by

$$Q(x) = \frac{1}{\sqrt{2\pi}} \int_x^\infty e^{-t^2/2} dt, \qquad x \geq 0. \tag{3.2}$$

A more relevant case for CDMA cellular systems is the BEP performance of RAKE receiver in fading channels. Assuming binary modulation, Rayleigh fading channel, and that the RAKE receiver can coherently combine L paths using maximal ratio combining (MRC) [13], the BEP performance is [48]

$$P_b = \frac{1}{\pi} \int_0^{\pi/2} \prod_{l=1}^{L} I_l(\bar{\Gamma}_l, g, \theta) d\theta, \tag{3.3}$$

where

$$I_l(\bar{\Gamma}_l, g, \theta) = \left(1 + \frac{g\bar{\Gamma}_l}{\sin^2\theta}\right)^{-1}, \tag{3.4}$$

and

$$\bar{\Gamma}_l \triangleq \frac{\Omega_l E_b}{I_o} \tag{3.5}$$

[2] Usually the term *bit-energy-to-noise-spectral-density ratio* (E_b/N_o) is used. However, since the CDMA cellular systems are in practice interference-limited, we prefer to speak about E_b/I_o, where I_o contains both the interference and background noise.

is the average signal-to-noise ratio per bit, corresponding to the lth channel (or resolvable path), and Ω_l is the mean strength of that channel (path). In (3.3), $g = 1$ for antipodal signals (like in BPSK) and $g = 0.5$ for orthogonal signals. Fig. 3.2 shows plots of (3.1) and (3.3) for BPSK with different numbers of resolvable paths with equal mean strength (flat multipath intensity profile) and with exponentially decaying multipath intensity profile, where the first path has mean strength normalized to one, and the mean strengths of the remaining paths decay in steps of 3 dB.

E_b/I_o is closely related with another measure, namely the *signal-to-interference ratio* (SIR), denoted by γ, such that

$$E_b/I_o = \gamma \frac{W}{R_b} \tag{3.6}$$

where W is the transmission bandwidth in Hz and R_b is the data rate in bits/s. The quantity W/R_b is called the *processing gain* [11]. When the data rate is fixed, the SIR differs from E_b/I_o by merely a scaling factor.

In digital cellular communication systems, typically, the information to be transmitted is arranged in strings of bits called *frames* [49], and error correction coding is applied to each frame to further decrease the *bit error rate* (BER) after decoding. A frame is useless if there are still bit errors in the frame after decoding, and it must be discarded. Hence, depending on the service, a sufficiently low *frame error rate* (FER) must be guaranteed. However, long time delays are needed to obtain reliable estimates of BER or FER. Since the channel conditions can change very rapidly, these delays might be unacceptably long in practice. Hence most of the attention in the power control field has been on SIR-based algorithms. Early work concentrated on algorithms based on received signal strength ([50, 51, 52]). These algorithms typically adjust the transmission powers inversely proportional to the link gain. In [53] it was shown that partial compensation of the link gain can give better results than full compensation. In [54, 55] it has been shown that SIR-based power control offers better performance than signal-strength-based algorithms. A both SIR-based and signal-strength-based power control algorithm was proposed in [56] and reported to perform better than plain SIR-based power control.

The frame error information can be used to adjust the target SIR, which a fast TPC algorithm is trying to achieve. This increases system capacity, since a worst-case setting of the SIR target is not required.

In addition to the SIR and FER requirements, the delay or *latency* requirements must be taken into account. For instance, a voice service tolerates a certain amount of data loss but is delay-critical, whereas file downloads do not tolerate bit errors at all (erroneous frames must be retransmitted), but the transmission need not be continuous and must only satisfy some delay limit on the average. The delay tolerances can be utilized in the design of power control algorithms for nonreal-time services, see e.g. [57].

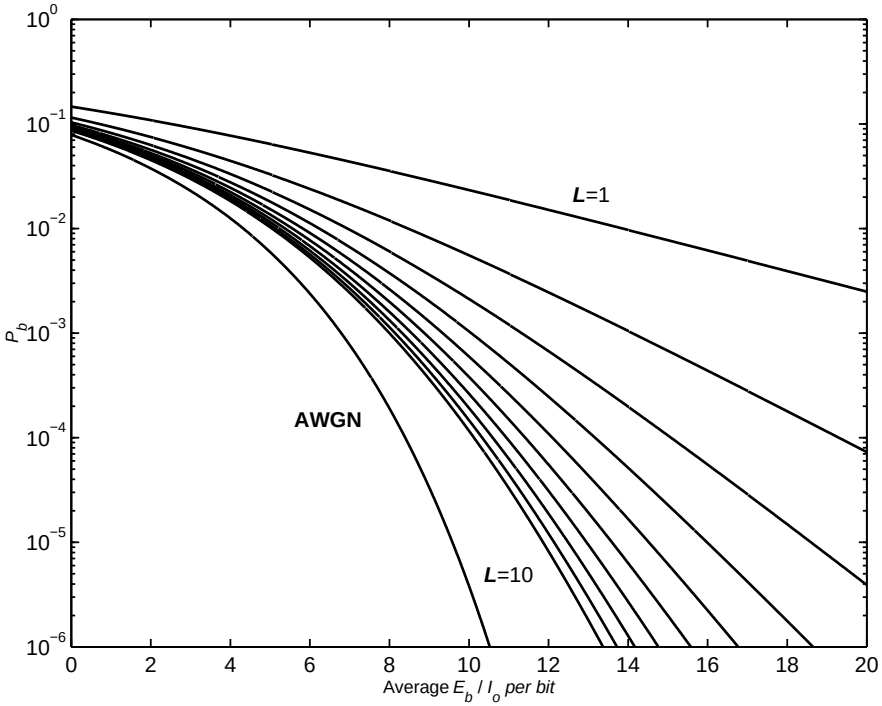

(a) Flat multipath intensity profile

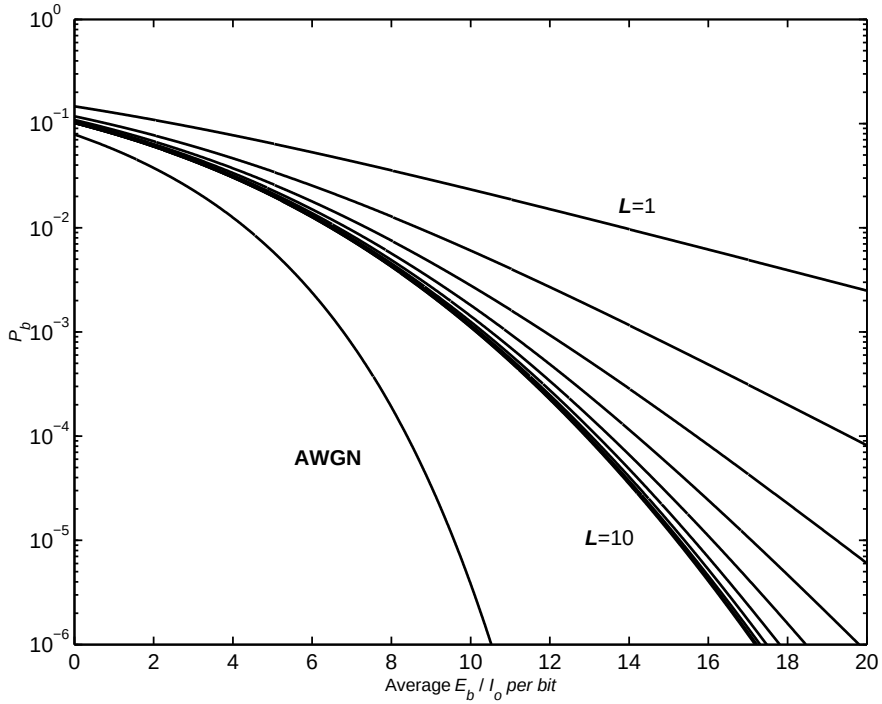

(b) Exponentially decaying multipath intensity profile (decay step -3dB).

Figure 3.2: Bit-error probability versus average E_b/I_o per bit of BPSK modulation in an AWGN channel and fading channels with RAKE receiver and maximal ratio combining.

3.1.3 Open loop, closed loop and outer loop power control

An intuitive way to compensate for the channel attenuation in the uplink would be to measure the strength of a pilot signal from the downlink, and adjust the transmission power proportionally to the inverse of this measurement. Since the pilot signal is transmitted at constant power, the variation of its strength gives information of the downlink link attenuation. This is called *open loop power control*. Unfortunately the center frequencies allocated to up- and downlink transmissions are usually widely separated, and thus the correlation between up- and downlink attenuations is generally weak. Therefore, the transmission power update of a mobile must be based on feedback information of the received SIR at the base station, forming a closed loop between them. This *closed loop power control* (or *inner loop power control*) aims to keep the received uplink signal power level at a specified target. Moreover, the target must also be varied, because the SIR requirement for a given BER is not constant, but depends on the radio propagation conditions. This is the task of the *outer loop power control*.

Open loop PC is usually used for initial power setting, when the two-way communication link is not yet established and closed loop is not possible.

Closed loop PC aims to keep the received SIR at a target value. This is what is happening in the DPC algorithm given in equation (3.19) as discussed later. However, in practice only one bit is used to signal the received SIR information at a fast rate to track the channel variations. The transmitter is commanded to increase its power by a fixed step if the received SIR is below the target, and decrease it otherwise. This kind of algorithm is used in the IS-95 system [58]. In WCDMA [59, 3] there are some more degrees of freedom, for instance, the possibility to signal a "no change" command when the received SIR is reasonably close to the target, thus reducing the "ping-pong"-effect around the target. This idea was exploited in the dynamic step size power control scheme proposed in [60, 61].

The outer loop control adjusts the SIR target so that a desired FER is guaranteed. A typical way to do this in practice is to raise the target by a larger step δ_{up} when a frame is discarded, and to decrease the target with a smaller step δ_{down} when a frame is correctly received. This kind of algorithm was proposed in [62], where they used step sizes $\delta_{\text{up}} = K\delta$ and $\delta_{\text{down}} = \delta$, where K is a positive integer. This relation between the step sizes gives the resulting average FER as $\text{FER} = \frac{1}{K+1}$. Another algorithm for SIR target adjustment was proposed in [63] for turbo-coded WCDMA systems. The scheme utilizes the fact that in turbo-decoding, the BER and FER decrease as the number of decoding iterations increases. Thus, the time required to achieve reliable BER or FER estimates can be decreased. In [64] another outer-loop PC algorithm was proposed that is able to detect changes in the multipath channel profile and compensate for errors in the mapping between FER and SIR target, yielding faster tracking of the channel changes.

3.1.4 Power control in soft handover

Handover in wireless cellular systems is needed when a mobile user moves from the coverage area from one cell into that of another cell. In the FDMA and TDMA systems, the handovers are typically *hard handovers*, meaning that the connection to the original cell is terminated before the connection to the new cell is established. In CDMA systems, due to the universal frequency reuse, a mobile user can be simultaneously connected to several cells. Thus, when a mobile moves from one cell to another, it can establish connection to the new cell *before* the connection to the old cell is terminated. In this case, the mobile is said to be in *soft handover* [3]. This is beneficial, since the mobile user can at each time instant use only enough transmission power to be able to reach one of the base stations to which it is connected. This way the average transmission power is lower than without soft handover, and less interference is produced to the other users. However, soft handover increases the radio resource usage in the downlink.

Power control has special implications during soft handover. In UMTS, PC in soft handover works as follows [59]. In uplink closed-loop PC, the mobile station receives power control commands from all the base stations in the *active set* (the set of base stations involved in the soft handover at a given time). It then combines these commands, and based on the combined command, it adjusts its transmission power. The basic principle is that if any of the base stations sends a power-down-command, the mobile station decreases its transmission power. The transmission power is increased only if the mobile station receives a power-up-command from all the base stations in the active set. However, the mobile station can also discard a command in the case that the reception of that command is poor.

In downlink closed-loop PC, the same PC command sent from a mobile station is received by all base stations in the active set. Due to errors in the reception of the PC command, the base station powers can start drifting apart. This is very undesirable, as it destroys the balance between up- and downlink power levels. A typical way to deal with the power drifting problem is a scheme called *power balancing*, where each base station in the active set periodically correct their transmission powers towards a reference level set by the network [3].

Soft handover has also special implications to the power control algorithms proposed in this thesis. These are discussed in Chapter 7 with some simulation examples.

3.1.5 Practical aspects on power control considered in this thesis

Many solutions to power control in CDMA systems have been proposed in the literature, as reviewed later in this Chapter. A lot of work has been devoted to finding optimal (in some sense) algorithms that may be unpractical to implement, but can be used to derive theoretical bounds to the performance of the system. Also, a great deal of work has been done to seek distributed

iterative algorithms that approach the optimal solutions, and are more practical to implement. To move closer to real implementation of the TPC algorithms, one must take into account a number of practical issues that limit the capacity gains achievable by TPC:

- *Loop delay*. The loop delay refers to the overall loop delay in closed loop power control. It greatly affects the performance of a power control algorithm. This delay is a combination of delays due to the SIR measurement process, the transmission of the SIR information over the radio channel, the processing of the SIR information to calculate and adjust the transmission power, and the propagation time after which the new transmission power affects the next SIR measurement. Therefore the power update is based on outdated information of the received SIR. This may cause instability in the power control algorithms, leading to large variations in the interference powers at the receivers and diminished capacity.

- *SIR estimation*. The received SIR is not known exactly at a receiver, but it must be estimated, and thus there will always be some estimation error. The estimation error can be made smaller by increasing the averaging time of the measurement, but this might lead to a longer loop delay, which is undesirable.

- *Feedback information accuracy*. The information of the SIR at the receiver should somehow be communicated to the transmitter. An accurate representation of the SIR measurement requires several bits, but this requires more signaling overhead. This form of feedback is referred to as *information feedback (IFB)*.

  A usual case in practice is that only one bit is used to inform the transmitter to either increase or decrease its transmission power by a fixed amount, typically by 1 dB (e.g. in WCDMA [59]). This form of feedback is referred to as *decision feedback (DFB)*.

  In [65] it was shown that in the case of quantized IFB (the information is represented with a finite number of bits) the performance gain of adding more bits for the TPC command becomes less and less when the number of bits is increased and, typically, this saturation of performance occurs already with a few number of bits. This phenomenon was also observed in [66], where a differential pulse-code modulation (DPCM) scheme was used to reduce the required number of bits for the TPC signaling.

- *TPC update rate*. In CDMA one has to deal with the near-far situation, and thus the update rate of the power control algorithm must be sufficiently high so that the variations in the link attenuation can be tracked. Typical update rates are from 800 Hz (used in the IS-95 system [58]) to 1500 Hz (used in WCDMA [59, 3]). Note that the update rate cannot be arbitrarily high because of the inherent delay imposed by the SIR measurement process.

Since the available feedback channel bandwidth for power control signaling is limited in practice, there is a tradeoff between feedback information accuracy and TPC update rate. Studies have shown that it is generally more beneficial to use high update rate and less information accuracy than vice versa [67], which supports the choice of 1-bit TPC commands in UMTS and IS-95.

- *Errors in the transmission of feedback information*. To minimize the loop delay, the TPC command bits are sent without error correction coding. Hence the probability of receiving an erroneous command can be relatively high, e.g. up to 10 %.

- *Soft handovers*. As discussed in the previous Section, soft handovers have special implications to the algorithms proposed in this thesis, which is discussed in Chapter 7.

More of these will be discussed in Chapter 4, where new adaptive closed-loop PC algorithms are proposed for enhancing the power control performance.

3.1.6 The power control model employed in this thesis

The algorithms proposed in this thesis are targeted to improve the TPC performance in the presence of the practical limitations. The assumption behind the new proposed algorithms is that the implementation of TPC is done using the combination of open loop, closed loop and outer loop PC.

The closed loop PC algorithm employed in UMTS and IS-95 systems is a fixed-step power control (FSPC) algorithm. This type of algorithm has been presented in [68]. It is given by

$$p_i(t+1) = p_i(t) + \delta \text{sign}\left(\gamma_i^t(t) - \gamma_i(t)\right) \tag{3.7}$$

where all the variables are in decibels, $p_i(t)$, $\gamma_i^t(t)$ and $\gamma_i(t)$ are the transmission power, SIR target and measured SIR, respectively, of user i at time t, δ is the fixed step size, and

$$\text{sign}(x) = \begin{cases} 1 & \text{if } x \geq 0 \\ -1 & \text{if } x < 0 \end{cases} \tag{3.8}$$

The power control system model is illustrated in Figure 3.3 for uplink. The n-sample delay block models the power control loop delay (see Section 3.1.5). Note that the integrator in the mobile unit inherently includes a delay of one sample. Hence the total loop delay is $k = n + 1$. At time t the base station measures the uplink SIR. This measurement can be written as

$$\gamma(t) = p(t-n) + g(t) - I(t) \tag{3.9}$$

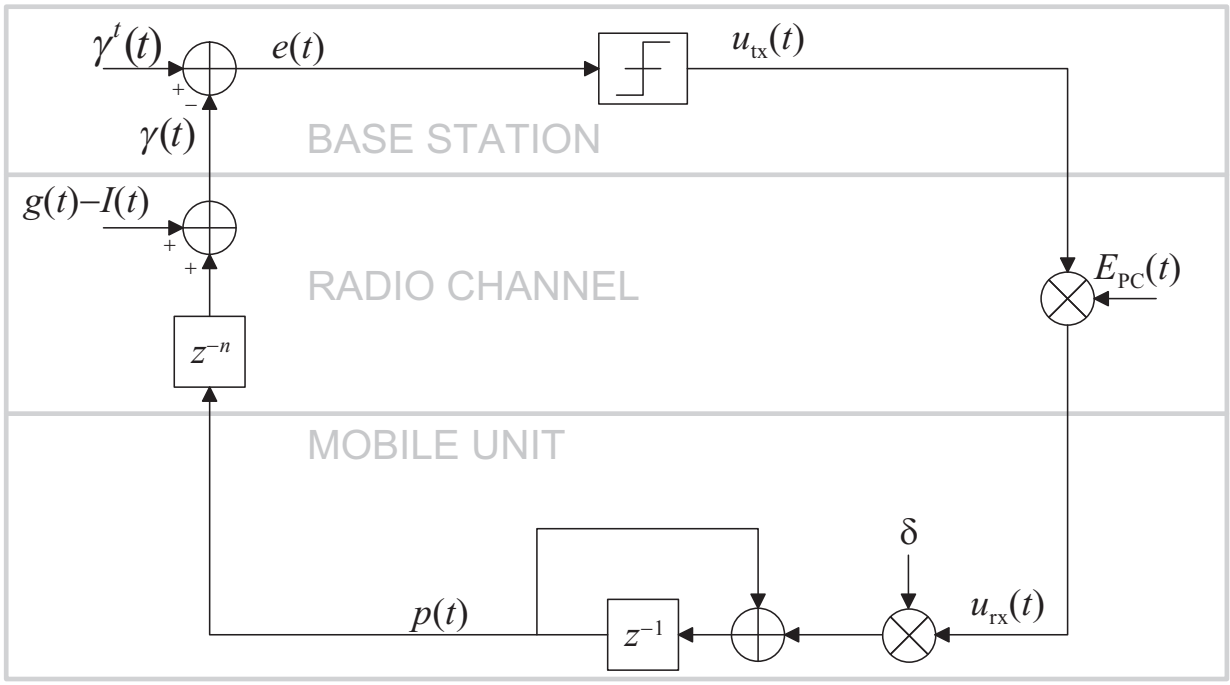

Figure 3.3: Closed-loop power control with conventional fixed-step controller.

where $g(t)$ and $I(t)$ are the channel attenuation and the total interference power at time t, all in decibels. The measurement is compared to the uplink SIR target set by the outer loop control. Based on this comparison, the base station sends a command $u_{\text{tx}}(t)$ to the mobile unit to either increase or decrease its power by a fixed step, typically 1 dB. The command is transmitted to the mobile unit uncoded to reduce processing delays, for which reason the command bit error probability can be relatively high, e.g., up to 10 percent. In Figure 3.3 the bit errors caused by the transmission channel are modeled with multiplication of the transmitted commands with the signal $E_{\text{PC}}(t)$, which has the value 1 with probability $P_{\text{PCE}}(t)$ and -1 with probability $1-P_{\text{PCE}}(t)$. $P_{\text{PCE}}(t)$ is the probability of bit error in power control command transmission at time t. The mobile receives the command $u_{\text{rx}}(t)$ and adds this value to its previous transmission power setting (in decibels).

In closed-loop power control the power control command is fed back to the transmitter. Thus it consumes the radio resources in the feedback channel. The following feedback cases are considered in this thesis:

Information Feedback (IFB):

The feedback signal is the exact power control command $u_i(t)$. Thus, real numbers are fed back.

Decision Feedback (DFB):

The feedback signal is the sign of the power control command $u_i(t)$. In this case only one bit is needed for the feedback signaling.

In the IFB case, the relay block is removed from the model, and TPC command errors are not taken into account.

3.2 The SIR balancing problem

A widely studied approach to transmission power control is the SIR balancing problem, i.e., how to set the transmission powers so that all users in the system have equal SIRs. This method is applicable for circuit-switched real-time services like voice, where the data rate is fixed. The *SIR balancing* concept was proposed in [69] for satellite communications systems. The problem was identified as an eigenvalue problem. These results were improved in [70, 71, 72], where it was shown that SIR balancing can improve the capacity of spread spectrum cellular mobile radio systems. Further refinement was done in [73]. However, SIR balancing may result in the catastrophic case, where the balanced SIR is too low for satisfactory reception for all users in the system. This problem was studied in [74], and a power control strategy was proposed that is optimal in the sense that it minimizes the *outage probability*[3] [75], i.e., the probability that a randomly chosen user has a SIR less than a given threshold, called the *system protection ratio*. Formally, the outage probability is defined as follows.

Definition 3.1 (Outage Probability)
Given the distribution $F(x) = Pr\{\gamma \leq x\}$ of the SIR γ, the outage probability *is defined by*

$$F(\gamma_0) = Pr\{\gamma \leq \gamma_0\}, \tag{3.10}$$

where γ_0 is the system protection ratio*, i.e., the lowest allowed SIR with which the link is still considered useful.*

In the following, the SIR balancing problem is discussed in detail.

Figure 3.4 illustrates a simple two-cell CDMA system. Only uplink is considered here, but the same analysis applies in downlink. The mobile stations MS1. . .MS3 share a common frequency band and their signals are separable at the base stations by their unique spreading codes. The link attenuation from mobile j to base station i is denoted by g_{ij} and is assumed to be fixed in the analysis. In this *snapshot approach* [74, 73], it is assumed that the link attenuations change slowly enough compared to the power control dynamics, and can thus be assumed constant. This assumption is rather optimistic in practice. Nevertheless, the snapshot approach gives valuable

[3] Also known as *co-channel interference probability*.

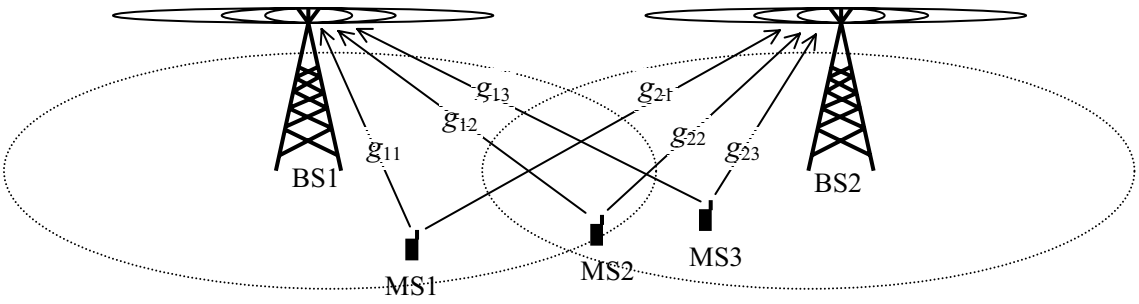

Figure 3.4: Illustration of a two-cell CDMA system with three mobile stations.

insight to the power control problem and the results of the analysis serve as upper bounds for the performance of various power control algorithms.

Define a base station assignment variable b_i so that $k = b_i$ if mobile i is served by base station k. Then the uplink SIR requirement for user i can be expressed as

$$\gamma_i = \frac{g_{b_i i} p_i}{\sum_{\substack{j=1 \\ j \neq i}}^{N} g_{b_i j} p_j + \eta_i} = \frac{p_i}{\sum_{\substack{j=1 \\ j \neq i}}^{N} \frac{g_{b_i j}}{g_{b_i i}} p_j + \frac{\eta_i}{g_{b_i i}}} \geq \gamma_i^t \tag{3.11}$$

where γ_i is the SIR at the receiver of the base station that is serving mobile station i, p_i is the transmission power of mobile i, N is the number of mobile stations using the same channel including the intra-cell and inter-cell users, η_i is the receiver noise power and γ_i^t is the uplink SIR target for user i. Define the vectors $\boldsymbol{p} = \{p_i\}$ and $\boldsymbol{\eta} = \{\gamma_i^t \eta_i / g_{b_i i}\}$ and matrix $\boldsymbol{H} = \{H_{ij}\}$ with elements $H_{ij} = \gamma_i^t g_{b_i j} / g_{b_i i}$ when $i \neq j$ and $H_{ii} = 0$. Now (3.11) can be put in matrix form:

$$(\boldsymbol{I} - \boldsymbol{H})\boldsymbol{p} \geq \boldsymbol{\eta} \tag{3.12}$$

where $\boldsymbol{I}$ denotes the identity matrix and the inequality holds component-wise. A minimum-power solution corresponds to the case where (3.12) is satisfied with equality. This is desirable, as it saves energy and thus prolongs the mobile station battery life.

Definition 3.2 *The problem is said to be feasible if there exists a non-negative power vector* $\boldsymbol{p}$ *such that the condition in* (3.12) *is satisfied.*

It has been shown that balancing the SIRs and making the balanced SIR as high as possible maximizes the minimum SIR in all links [74]. Consider the power control problem in (3.12) with $\gamma_i^t = \gamma^t$ for all i. Define matrix $\boldsymbol{A}$ so that $\boldsymbol{H} = \gamma^t \boldsymbol{A}$. If the interference in the receiver is

sufficiently high so that the receiver noise can be neglected, the problem can be identified as an eigenvalue problem:

$$\boldsymbol{p} = \boldsymbol{H}\boldsymbol{p} \Leftrightarrow \frac{1}{\gamma^t}\boldsymbol{p} = \boldsymbol{A}\boldsymbol{p} \tag{3.13}$$

The maximum possible value for γ^t (denoted by γ^*) is equal to the inverse of the maximum (real) eigenvalue of $\boldsymbol{A}$. The corresponding positive eigenvector $\boldsymbol{p}^*$ is the power vector achieving this maximum.

If receiver noise cannot be neglected, the optimal power vector is a solution to a set of linear equations [76]:

$$\boldsymbol{p}^* = \boldsymbol{H}\boldsymbol{p}^* + \boldsymbol{\eta} \tag{3.14}$$

Proposition 3.3 *The power control problem in* (3.14) *is feasible if the largest eigenvalue of the matrix* $\boldsymbol{H}$*, denoted by* $\rho(\boldsymbol{H})$*, is less than or equal to one.*

$\rho(\boldsymbol{H})$ is called the *spectral radius* of the matrix $\boldsymbol{H}$. The case $\rho(\boldsymbol{H}) = 1$ can only be met if the receiver noise is zero, otherwise infinite transmission power would be required. Naturally, in practice there always exists an upper limit for the transmission power.

Note that $\rho(\boldsymbol{H})$ can be considered as a measure of the relative system load (see [77]). For example, a heavily loaded system that is still feasible corresponds to a $\boldsymbol{H}$ matrix with $\rho(\boldsymbol{H})$ close to, but less than, unity.

The use of the optimal power vector $\boldsymbol{p}^*$ results to all users in the system having the same SIR. If the power control problem is not feasible, this results in the disastrous case that none of the users achieve the SIR requirement. To prevent this, a removal strategy must be employed, which removes transmitters from the channel until the power control problem becomes infeasible. The problem is to select which transmitters to remove. An intuitive approach is to remove those transmitters that produce the largest interference, i.e., transmitters having the worst link quality. Several removal strategies have been investigated in the literature ([74, 78, 79, 80]). Note that a removal of a transmitter from a channel does not necessarily mean that the connection is broken, but it can be handed over to another channel.

The SIR balancing problem treated here is based on the assumption of constant link attenuations. However, power control must in practice be applied in dynamically changing environment, where the assumption of constant link attenuations does not hold. In this case the eigenvalue problem (3.13) corresponds to open-loop control and suffers from poor robustness and high sensitivity. This motivates us to find solutions to power control that are more suitable for application in a dynamical environment, as is done in Chapter 4.

3.2.1 Auto-interference

In equation (3.11) the SIR is calculated assuming that all the received power from the desired user can be considered useful to the receiver. However, due to imperfections in channel equalization, multipath, transmission nonlinearities, etc., part of this power cannot be used for decoding, and can be considered interference from the receiver's viewpoint. This interference is called *auto-interference* [81]. In this case the uplink SIR of user i can be expressed as

$$\gamma_i = \frac{\zeta_i g_{b_i i} p_i}{\sum\limits_{\substack{j=1 \\ j \neq i}}^{N} g_{b_i j} p_j + (1 - \zeta_i)\, g_{b_i i} p_i + \eta_i} \tag{3.15}$$

where ζ_i is the fraction of the received power that the receiver can utilize for signal decoding.

The effect of auto-interference has been studied in [81], where it was shown that it lowers the maximum achievable SIR (γ^*). In [77] it was shown that the auto-interference does not violate the stability of linear power control algorithms.

The effect of auto-interference is not considered in this thesis. A study on its effect on the power control algorithms proposed in this thesis is left for future work.

3.2.2 A two-user example

Consider a system with only two mobile stations MS1 and MS2 and two base stations BS1 and BS2. Assume that MS1 is connected to BS1 and MS2 is connected to BS2. In this case the power control problem is the following:

$$\begin{cases} \gamma_1 = \dfrac{g_{11} p_1}{g_{12} p_2 + \eta_1} \geq \gamma_1^t \\ \gamma_2 = \dfrac{g_{22} p_2}{g_{21} p_1 + \eta_2} \geq \gamma_2^t \end{cases} \quad \Rightarrow \quad \begin{cases} p_1 \geq \gamma_1^t \left(\dfrac{g_{12}}{g_{11}} p_2 + \dfrac{\eta_1}{g_{11}} \right) \\ p_2 \geq \gamma_2^t \left(\dfrac{g_{21}}{g_{22}} p_1 + \dfrac{\eta_2}{g_{22}} \right) \end{cases} \tag{3.16}$$

This situation is depicted in Figure 3.5. The feasible region is shaded in the figure, and the optimal (minimum power) solution $\boldsymbol{p}^*$ is in the intersection of the two lines. Since $\boldsymbol{p}^*$ is within the maximum power limits, the problem is feasible. Consider that user 1 raises its target SIR γ_1^t while the link attenuations stay unchanged. It is then necessary for it to also raise its transmission power as seen from (3.16). This in turn forces user 2 to raise its transmission power. Thus it can happen that the optimal point $\boldsymbol{p}^*$ moves outside the maximum power limits, thereby making the problem unfeasible.

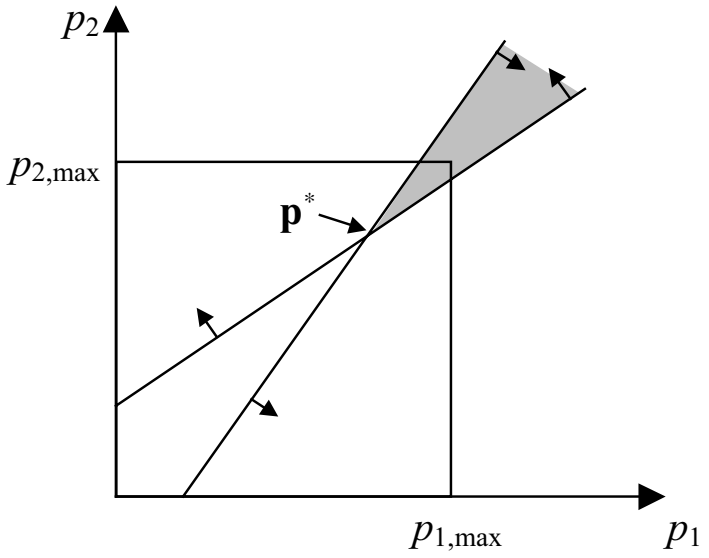

Figure 3.5: Power control problem for two-user case.

3.3 Distributed power control

Solving (3.14) directly is a centralized method, since it requires the information of all the link attenuations in the system. This is generally not suitable in real implementations, since it would require extensive signaling overhead. However, it is valuable in determining upper bounds for the performance of distributed algorithms that can be implemented in practice.

A distributed algorithm uses only local measurements to update the transmission powers. Hence it is more suitable for practical implementation than a centralized algorithm. Since in this case a user does not know all the link attenuations, the problem must be iteratively solved. It is thus necessary to find an iteration that depends only on local measurements, and converges to the optimal solution reasonably fast (faster than the link gains change). Fast convergence can be achieved in two ways: by making the iteration time-step smaller, and by designing an iteration with faster convergence property.

3.3.1 General iterative algorithm

A general iterative algorithm to solve the problem in (3.14) can be found from numerical linear algebra [82], and is given by

$$\boldsymbol{p}(t+1) = \boldsymbol{M}^{-1}\boldsymbol{N}\boldsymbol{p}(t) + \boldsymbol{M}^{-1}\boldsymbol{\eta}, \qquad t = 0, 1, \ldots \tag{3.17}$$

where $\boldsymbol{M}$ and $\boldsymbol{N}$ are matrices such that $\boldsymbol{p}^* = \boldsymbol{M}^{-1}\boldsymbol{N}\boldsymbol{p}^* + \boldsymbol{M}^{-1}\boldsymbol{\eta}$. By selecting $\boldsymbol{M}$ and $\boldsymbol{N}$ properly, the iteration in (3.17) will converge so that $\lim_{t\to\infty} \boldsymbol{p}(t) = \boldsymbol{p}^*$. For example, the selection $\boldsymbol{M} = \boldsymbol{I}$ and $\boldsymbol{N} = \boldsymbol{H}$ results to

$$\boldsymbol{p}(t+1) = \boldsymbol{H}\boldsymbol{p}(t) + \boldsymbol{\eta}, \qquad t = 0, 1, \ldots \tag{3.18}$$

Writing equation (3.18) component-wise gives

$$p_i(t+1) = \gamma_i^t \left(\sum_{\substack{j=1 \\ j\neq i}}^{N} \frac{g_{b_i j}}{g_{b_i i}} p_j(t) + \frac{\eta_i}{g_{b_i i}} \right) = \frac{\gamma_i^t}{\gamma_i(t)} p_i(t), \qquad t = 0, 1, \ldots \tag{3.19}$$

which is the DPC algorithm proposed in [83] (see equation (3.25)).

3.3.2 Convergence of the iterative algorithm

A necessary and sufficient condition for the iteration in (3.17) to converge is the following [82, 84]. Let $\alpha_1, \alpha_2, \ldots$ be the eigenvalues of the matrix $\boldsymbol{M}^{-1}\boldsymbol{N}$. Then the iteration converges if and only if $\max_i |\alpha_i| < 1$. Consider the DPC algorithm in (3.18). In this case $\boldsymbol{M}^{-1}\boldsymbol{N} = \boldsymbol{H}$. Hence the dominant eigenvalue of $\boldsymbol{H}$, $\rho(\boldsymbol{H})$, should be less than one. By Proposition 3.3, this ensures that the SIR requirements can be satisfied for all users. Hence DPC converges to $\boldsymbol{p}^*$ whenever the SIR requirements can be satisfied.

The speed of the convergence is very important, since the link attenuations are changing all the time. For the iteration in (3.17), it can be shown that the smaller the $\rho(\boldsymbol{M}^{-1}\boldsymbol{N})$, the faster the convergence. Hence the task is to find $\boldsymbol{M}$ and $\boldsymbol{N}$ such that $\rho(\boldsymbol{M}^{-1}\boldsymbol{N}) < 1$ and as small as possible.

3.3.3 Convergence using standard interference functions

A different way of proving convergence of iterative algorithms was developed in [85] and extended in [86]. There the iteration is formulated by defining an *interference function* $I(\boldsymbol{p})$ such that

$$\boldsymbol{p}(t+1) = I\left(\boldsymbol{p}(t)\right) \tag{3.20}$$

The standard interference function framework gives a *sufficient* but not *necessary* condition for convergence of the iteration in (3.17). The following definition and proposition summarize this framework.

Definition 3.4 ([85]) *An interference function $I(\boldsymbol{p})$ is called standard if for all non-negative power vectors the following properties are satisfied:*

$$\begin{aligned} &\bullet\ I(\boldsymbol{p}) > 0 \quad (\textit{positivity}) \\ &\bullet\ \boldsymbol{p} \geq \boldsymbol{p}' \Rightarrow I(\boldsymbol{p}) \geq I(\boldsymbol{p}') \quad (\textit{monotonicity}) \\ &\bullet\ \forall \alpha > 1, \quad \alpha I(\boldsymbol{p}) > I(\alpha \boldsymbol{p}) \quad (\textit{scalability}) \end{aligned} \tag{3.21}$$

Proposition 3.5 ([85]) *If the power control problem is feasible and $I(\boldsymbol{p})$ is a standard interference function, then for any initial non-negative power vector $\boldsymbol{p}$ the iteration in* (3.20) *converges to the unique non-negative fixed point $\boldsymbol{p}^*$.*

Recently, a generalization of the standard interference function method has been presented in [87, 88]. They identified a key condition for convergence of an iterative function:

Definition 3.6 ([87, 88]) *Two-sided scalability:*
For all $\alpha > 1$, $\frac{1}{\alpha}\boldsymbol{p} \leq \boldsymbol{p'} \leq \alpha \boldsymbol{p}$ implies $\frac{1}{\alpha} I(\boldsymbol{p}) < I(\boldsymbol{p'}) < \alpha I(\boldsymbol{p})$.

Proposition 3.7 (Theorem 1 in [87]) *Given a two-sided scalable iterative function $I(\boldsymbol{p})$, if a fixed point $\boldsymbol{p}^* = I(\boldsymbol{p}^*)$ exists, then that fixed point is unique and the iteration $\boldsymbol{p}(t+1) = I(\boldsymbol{p}(t))$ converges to $\boldsymbol{p}^*$ under both synchronous and totally asynchronous update model.*

3.4 A survey of power control algorithms and state of the art

Here the goal is to give an overview of the research efforts made on power control algorithms in the past and to present the state of the art of this widely studied field. The presentation is divided into fours parts and gives a somewhat – although not entirely – chronological view on how the research has evolved from the past to the present.

3.4.1 Distributed SIR balancing algorithms

Distributed versions of the SIR balancing problem draw a lot of attention in the 1990's. The starting point was to find iterative algorithms that would be suitable for distributed operation, and would solve the eigenvalue problem (3.13) in the noiseless case, or the set of linear equations (3.14) in the noisy case. The underlying assumption was that the channel power gains would change slowly compared to the dynamics of the power control iterations, and thus the convergence was mainly studied in a static "snapshot" scenario.

The first proposal was the *Distributed Balancing* (DB) algorithm proposed in [89]. It is described in the following.

The Distributed Balancing (DB) Algorithm:

$$p_i(t+1) = \beta p_i(t)\left(1 + \frac{1}{\gamma_i(t)}\right), \quad \beta > 0, \quad t = 0, 1, \ldots, \tag{3.22}$$

$\diamondsuit$

For a feasible system, the DB algorithm converges to the optimal power vector $\boldsymbol{p}^*$ with probability one[4] (see [89]). However, it suffers from poor convergence speed. Moreover, an improper selection of parameter β may result in ever-increasing (or decreasing) powers. The correct selection of β requires a normalization procedure, which is not possible to do in a completely distributed manner.

An improvement to the DB algorithm in terms of convergence speed was proposed in [90]. They proposed a modified version of the DB algorithm and called it the *Distributed Power Control* (DPC) algorithm. However, since the term DPC is used for another algorithm (described later), the algorithm of [90] is called the *Modified DB (M-DB) Algorithm*. It is described as follows.

The Modified DB (M-DB) Algorithm:

$$p_i(t+1) = \beta \frac{p_i(t)}{\gamma_i(t)}, \quad \beta > 0, \quad t = 0, 1, \ldots \tag{3.23}$$

$\diamondsuit$

The convergence of the M-DB algorithm to the optimal power vector and SIR balance has been proven in the noiseless case ([90]). Also, the convergence speed was shown to be faster than with the DB algorithm. This was also analytically shown in [76]. However, the problem of cleverly choosing β still remained.

The problem with the normalization procedure was avoided in the algorithm proposed in [91], the *Fully Distributed Power Control (FDPC) Algorithm*. It is given in the following.

The Fully Distributed Power Control (FDPC) Algorithm:

$$p_i(t+1) = p_i(t)\frac{\min\left(\gamma_i(t), \beta\right)}{\gamma_i(t)}, \quad t = 0, 1, \ldots \tag{3.24}$$

$\diamondsuit$

Clearly, $\beta \to \infty$ corresponds to constant power case (no power control). For very small values of β the FDPC algorithm approaches the M-DB algorithm. The FDPC algorithm can achieve

[4]Convergence with probability one here is based on the assumption that the link gains in matrix $\boldsymbol{H}$ are stochastic variables, and the matrix has therefore full rank. This assumption is feasible since the link gain in a wireless communication channel is inherently a stochastic variable.

SIR balance with probability one in the noiseless case, if $\beta \leq \gamma^*$, where γ^* is the maximum achievable SIR in the system (see Section 3.2). A drawback of the algorithm is that if $\beta < \bar{\gamma}$, where $\bar{\gamma}$ is the system protection ratio, the powers are ever-decreasing, which is a problem in the noisy case.

The algorithm proposed in [83] finally solved the problem of choosing β of the M-DB algorithm in the noisy case. They identified β in the noisy case to be the target SIR which the algorithm is trying to achieve. This algorithm is called the *Distributed Power Control (DPC) Algorithm* in this thesis. It is described as follows.

The Distributed Power Control (DPC) Algorithm:

$$p_i(t+1) = p_i(t)\frac{\gamma^t}{\gamma_i(t)}, \quad t = 0, 1, \ldots \tag{3.25}$$

$\diamondsuit$

From control theory viewpoint, the DPC algorithm is an integrating P-controller. The convergence of the DPC algorithm in the case where the power updates occur asynchronously was proven in [92]. The DPC algorithm has received wide attention in the research community since it was published.

In all practical systems the transmission powers are limited so that

$$\mathbf{0} \leq \boldsymbol{p} \leq \boldsymbol{p}_{\max} \tag{3.26}$$

where $\mathbf{0}$ is a vector with all-zero elements and $\boldsymbol{p}_{\max} = [p_1^{\max}, p_2^{\max}, \ldots, p_N^{\max}]^T$ denotes the maximum transmission power of each transmitter. To take these limitations into account, the distributed constrained power control (DCPC) algorithm was suggested in [93]. The algorithm converges in a geometric rate [86]. It is defined in the following.

The Distributed Constrained Power Control (DCPC) Algorithm:

$$p_i(t+1) = \min\left(p_i^{\max}, p_i(t)\frac{\gamma_i^t}{\gamma_i(t)}\right), \quad t = 0, 1, \ldots \tag{3.27}$$

where $p_i^{\max}$ is the maximum allowed transmission power of transmitter i.

$\diamondsuit$

With DCPC it can happen that some transmitters are transmitting with the maximum power, thus producing maximum interference to other users, but still do not achieve their SIR target. Therefore it might be beneficial to lower the transmission power when link quality is bad. With this in mind, the following more general algorithm has been proposed in [94] that has DCPC as a special case:

The Generalized Distributed Constrained Power Control (GDCPC) Algorithm:

$$p_i(t+1) = \begin{cases} \frac{\gamma_i^t}{\gamma_i(t)} p_i(t) & \text{if } \frac{\gamma_i^t}{\gamma_i(t)} p_i(t) \leq p_i^{\max} \\ p_i' & \text{if } \frac{\gamma_i^t}{\gamma_i(t)} p_i(t) > p_i^{\max} \end{cases}, \quad t = 0, 1, \ldots \tag{3.28}$$

where $0 \leq p_i' \leq p_i^{\max}$.

$\diamondsuit$

It was shown in [94] that this algorithm converges to the optimal power vector $\boldsymbol{p}^*$ provided that the system in (3.14) has the optimal solution $\boldsymbol{p}^*$ in the power range given by (3.26).

3.4.1.1 Discrete transmission powers

All the above algorithms assume that the transmission power can be selected from a continuous range. Systems with quantized transmission powers are considered in [95, 96]. They proposed the *Distributed Discrete Power Control (DDPC) Algorithm*, which is based on simple quantizations of the transmission powers calculated by the DCPC algorithm. The same problem was addressed also in [97], where the problem is generalized to an integer programming problem with certain constraints. In [98] a distributed discrete power control method based on stochastic learning was proposed in a game theory framework for wireless data networks.

3.4.2 Aiming for faster convergence

The DPC algorithm was the first practical one to solve the problem of SIR balancing in a fully distributed manner. After that many efforts have been devoted for finding algorithms with faster convergence. For algorithms based on the general iterative algorithm (see Section 3.3.1), faster *asymptotic average rate of convergence* [99] is achieved by finding an iteration matrix $\boldsymbol{M}^{-1}\boldsymbol{N}$ with smaller spectral radius $\rho(\boldsymbol{M}^{-1}\boldsymbol{N})$.[5] I has been shown [99, 17] that $\rho(\boldsymbol{M}^{-1}\boldsymbol{N})$ for the DPC algorithm is smaller than for the DB algorithm, thus the DPC algorithm has faster convergence. For some algorithms it is difficult or even impossible to find the rate of convergence analytically, and one must resort to simulations to study the convergence. Fast convergence is important, since the power control algorithms are in practice operating in a dynamical system with random variations. However, the convergence of the algorithms has been mainly studied in a static environment, assuming that the variations in the radio channel power gains are slow in comparison with the power control dynamics and can thus be neglected.

[5] Of course the iteration matrix must be selected so that it enables a distributed implementation of the algorithm, see the discussion in [99] page 32.

In [100] a power control algorithm is proposed with faster convergence properties than the DPC algorithm. The algorithm differs from the first-order algorithms described above in the sense that it requires the current and the previous power levels to calculate the next one. The scheme is called the *Constrained Second-Order Power Control (CSOPC) Algorithm*. It is described as follows.

The Constrained Second-Order Power Control (CSOPC) Algorithm:

$$p_i(t+1) = \min\left(p_i^{\max}, \max\left(0, p_i(t)\omega(t)\frac{\gamma_i^t}{\gamma_i(t)} + (1-\omega(t))p_i(t-1)\right)\right), \quad t = 1, 2, \ldots \tag{3.29}$$

where $\omega(t)$ is called the *relaxation factor*, and is a decreasing sequence such that $1 < \omega(1) < 2$ and $\lim_{t\to\infty}\omega(t) = 1$.

$\diamondsuit$

From control theory viewpoint, the CSOPC algorithm is an integrating PD-controller with vanishing D-part. In the simulations of [100] the authors have used $\omega(t) = 1 + \frac{1}{1.5^t}, t = 1, 2, \ldots$.

Another algorithm with faster convergence properties is proposed in [101, 17]. The algorithm is called the *Multi-Objective Distributed Power Control (MODPC) Algorithm*, and is based on multi-objective optimization framework. Its convergence was shown to be faster than that of the DCPC. The MODPC algorithm is described as follows.

The Multi-Objective Distributed Power Control (MODPC) Algorithm:

$$p_i(t+1) = \min\left(p_i^{\max}, p_i(t)\frac{\lambda p_i^{\min} + (1-\lambda)\gamma_i^t}{\lambda p_i(t) + (1-\lambda)\gamma_i(t)}\right), \quad t = 0, 1, \ldots \tag{3.30}$$

where $p_i^{\min}$ is the minimum allowed transmission power of transmitter i, and $\lambda \in [0, 1]$ is a weighting parameter.

$\diamondsuit$

Note that selecting $\lambda = 0$ yields the DCPC algorithm. The MODPC algorithm was extended to jointly control power and data rate in [102]. A drawback of the MODPC algorithm is that for $\lambda > 0$ the algorithm converges to a smaller SIR balance than the DCPC algorithm (here it is assumed that the power control problem is feasible within the power limits). To see this, rewrite (3.30) in steady-state case, resulting in:

$$p_i = p_i\frac{\lambda p_i^{\min} + (1-\lambda)\gamma_i^t}{\lambda p_i + (1-\lambda)\gamma_i} \tag{3.31}$$

$$\Rightarrow \gamma_i = \gamma^t + \frac{\lambda}{1-\lambda}(p_i^{\min} - p_i) \leq \gamma^t. \tag{3.32}$$

Therefore, unless $p_i = p_i^{\min}$ or $\lambda = 0$, then $\gamma_i < \gamma^t$.

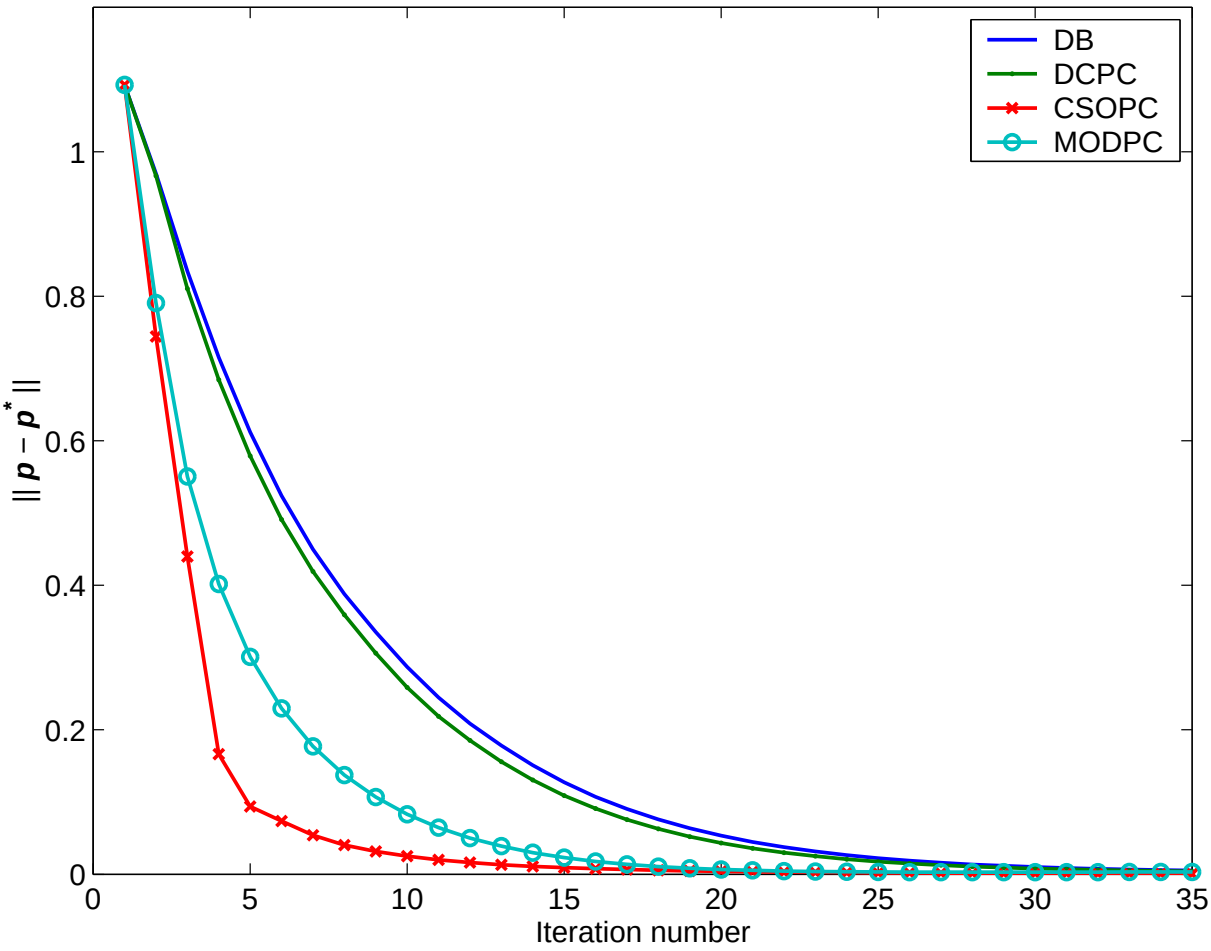

Figure 3.6: Convergence of the norm of the difference between the power vector and the optimal power vector $\boldsymbol{p}^*$ (equation (3.14)) in multiuser snapshot simulation (80 users).

3.4.2.1 Convergence example

Fig. 3.6 shows the simulated convergence of the DB, DCPC, CSOPC and MODPC algorithms in a multiuser case with 80 users, averaged over 100 realizations. The CSOPC clearly outperforms the other algorithms in terms of convergence speed. The MODPC has also fast convergence, but it converges to a slightly different power vector than the other algorithms, as discussed in the previous Section. The DCPC has only slightly faster convergence than the DB algorithm.

3.4.3 Power control for dynamical environment

The methods presented above are mostly based on finding the solution to the eigenvalue problem (3.13) or the set of linear equations (3.14) in a distributed manner. Later on, more efforts were put to the problem of controlling the powers in dynamic channel conditions and in the presence

of non-idealities such as loop delays and feedback bandwidth restrictions.

Adaptive fuzzy control -based power control algorithms are proposed in [103, 104]. The fuzzy rule base in the algorithms is based on assumptions on the channel fading characteristics. Specifically, it is assumed that the channel fading process can be modeled as a piecewise second-order system. Based on the rule base, they use a fuzzy *proportional integral* (PI) controller for power control. The system can be designed to take the loop delay into account to enhance the robustness of the algorithms. The main drawback of these algorithms is that the channel behavior must be estimated in advance to construct the fuzzy rule base (see also [105]). Also the limited feedback bandwidth is not taken into account.

The problem of compensating the loop delay in closed-loop power control has been addressed in [106, 107, 77]. There the authors identified the problems that the loop delay may cause with various power control algorithms, including the DCPC and FSPC algorithms (this is elaborated in Chapter 4). They proposed a time delay compensation (TDC) scheme to remove the effect of delays in the output powers from the measurements in the closed-loop power control. The TDC scheme is based on the fact that after issuing a power control command, the resulting output powers are known to the algorithm, and can be precalculated and used in the measurements. To elaborate, let $\gamma_i(t)$ be the SIR at the receiver of user i in decibels. Then

$$\gamma_i(t) = p_i(t-n) + g_{ii}(t) - I_i(t), \tag{3.33}$$

where $p_i(t)$ is the transmit power of user i at time t, $g_{ii}(t)$ is the link gain between the transmitter and receiver of user i at time t, $I_i(t)$ is the interference power at the receiver of user i at time t, and n is the additional loop delay in samples.[6] Consider the following general power control algorithm:

$$p_i(t+1) = p_i(t) + R_i\{\gamma_i^t(t), \gamma_i(t)\} \tag{3.34}$$

where $R_i\{\gamma_i^t(t), \gamma_i(t)\}$ is some arbitrary power control mechanism. With TDC the algorithm gets the following form:

$$\begin{aligned} &i) \quad \text{Adjust measurements: } \check{\gamma}_i(t) = \gamma_i(t) + \check{p}_i(t) - \check{p}_i(t-n). \\ &ii) \quad \text{Issue PC command: } s_i(t) = R_i\{\gamma_i^t(t), \check{\gamma}_i(t)\}. \\ &iii) \quad \text{Monitor output powers: } \check{p}_i(t+1) = \check{p}_i(t) + s_i(t). \end{aligned} \tag{3.35}$$

Time delay compensation is a simple scheme, which can effectively cancel the loop delay. It has, however, two drawbacks. One is that the loop delay must be known. This is in principle a problem in cellular CDMA systems, where the loop delay is usually known due to the known

[6] A general iterative power control algorithm as in (3.17) itself has a delay of one sample, since measurements at time t are used to update powers at time $t+1$. We use k to refer to the total loop delay including this internal delay. Thus, $n = k - 1$.

frame structure of the system. However, there are cases when there are uncertainties in the loop delay. The other drawback is that since the TDC method relies on the knowledge of the PC actions taken by the transmitter after receiving the PC commands, it cannot be used when the mobile station is in soft-handover [77]. The loop delay issue is discussed more thoroughly in Chapter 4, where algorithms are designed to take the loop delay into account in cases where it is known, and also in cases when it cannot be guaranteed to be known.

In [108] the closed-loop PC is considered with feedback bandwidth constraints as an instance of the classical quantization problem. In this scheme, the receiver estimates the variance of the PC misadjustment, which is used to optimally quantize the power control command. The scheme relies on the assumption that the PC misadjustment is log-normally distributed, which is also the assumption used in the algorithms proposed in this thesis in Chapter 4. Thus, the minimum-mean-square-error (MMSE) optimization criterion is used for the quantizer. The estimated variance must be communicated to the transmitter for the reconstruction, which is a drawback of the scheme. The authors also propose a loop filter to be used in the transmitter for exploiting the time-correlation of the PC misadjustment. Thus, in the presence of loop delays, the loop filter should be designed so that the loop remains stable. In Chapter 6 of this thesis, new methods are proposed to enhance the closed-loop PC performance at the transmitter side. These methods utilize only the received 1-bit TPC commands and do not require any other information.

3.4.4 Predictive power control

Various forms of predictive power control have been proposed in the literature to exploit the time correlation of the channel states, and to tackle the loop delay problem. The usual approach in predictive power control has been to predict the received signal power or SIR [109, 110, 111], channel state [112, 113, 114, 115, 116], or the next transmission power that should be used by the transmitter [117, 118], using linear K-step-ahead predictors based on current and previous values of the predicted signal, or neural networks.

In [109, 110, 111] prediction in the received signal power with polynomial predictors is proposed. The methods are based on the assumption that the channel power gain follows polynomial curves. Recall that this was also the assumption used in the fuzzy control schemes proposed in [103, 104]. As in those schemes, the predictive schemes of [109, 110, 111] need to estimate the channel behavior beforehand to select the polynomial predictors.

The channel state predictors utilized in [112, 113, 114, 115] are of the form

$$g(t+1) = \sum_{i=0}^{N} w(i)g(t-i), \tag{3.36}$$

where $g(t)$ is the channel power gain at time t, $w(i), i = 0 \ldots N$ are the weights of the prediction

filter and N is the order of the filter. The weights are updated using some adaptive algorithm such as the *Recursive Least Squares* (RLS, [113]), *Least Mean Squares* (LMS, [114, 115]) or *Normalized Least Mean Squares* (LMS, [112]) algorithm.[7] In [116] a K-step-ahead prediction algorithm is proposed, where the samples are iteratively predicted one sample ahead, each time utilizing the already predicted values to predict the next sample ahead, until the required number of predicted samples is reached. These algorithms require that the channel state (power gain) can be measured. In particular, the channel power gain is equal to the received power divided by the transmission power. Thus, it is assumed that the channel power gain can be calculated from the received power measurements and the transmission power commands sent to the transmitter in the feedback channel [112]. However, as already discussed, the feedback channel for the power control command is typically a relatively unreliable channel, and thus the estimated channel gain can easily become biased.

In [117, 118], a centralized predictive power control algorithm based on achievable SIR is proposed. It is assumed that the link gains of the entire system can be estimated, and the optimal power vector (see (3.13)) is calculated based on the link gain matrix. A similar prediction as in (3.36) is applied to estimate the next optimal power vector based on previously calculated power vectors. Two schemes are presented, where one uses an individual predictor based on the RLS algorithm for each user, and the other uses a global predictor based on a neural network to predict the entire power vector. The main problem with these schemes is that they, require an enormous amount of signaling overhead, which makes them difficult to implement in practice.

3.4.5 Discussion

It is clear that the design of power control for CDMA systems is not a simple problem. Many different solutions have been proposed for enhancing various aspects of power control. However, there are still questions that have not been answered. This thesis concentrates on finding answers to the following questions:

- How to minimize PC misadjustment in closed-loop power control and simultaneously compensate for the loop delay to enhance the capacity of the system?
- How to do this without increasing power control signaling bandwidth requirements?
- How to deal with unknown or varying loop delay?

In Chapters 4–7, solutions to these problems are proposed.

[7] See [119, 120] for information about these adaptive algorithms.

3.5 Power control in real-time versus nonreal-time and multi-rate services

The SIR balancing concept has the goal of maximizing the number of users in the system. If the users are real-time users requiring constant bit rates, this is a good strategy for maximizing capacity. However, as the cellular systems evolve to the next generation, the variety of services will be considerably different than those of the previous systems. In addition to the familiar real-time voice, there will be both real-time and nonreal-time services with different data rates. Hence, maximizing the data throughput instead of the number of users might be more interesting from the operators' point of view. Of course the delay requirements must be fulfilled, as merely maximizing throughput would be achieved by just letting the user with the best instantaneous link quality to transmit [121, 122].

Since CDMA is interference limited, any decrease in the transmission power of one user is directly advantageous for other users due to decreased interference. If the link quality between a transmitter and a receiver is bad, high transmission power is needed to satisfy the SIR requirements. This produces high interference to other receivers, and their serving transmitters must also increase their powers in order to cope with the increased interference.

In nonreal-time services the data rate must only be satisfied on the average sense, and therefore the instantaneous data rate can be considerably varied. This allows the TPC algorithm even to cut off the transmission when the link quality is bad, and to transmit at a high data rate when the link quality is good [122]. Thus, the situation as compared to conventional TPC designed for real-time services is reversed: the transmission power should be small when link quality is low, and vice versa. Since the time dimension can be utilized in the optimization, there is potential for significant capacity gain by minimizing the total transmitted *energy* instead of power. This can be accomplished by scheduling the data transmissions properly [57].

To elaborate this, consider a set of users requiring individual data rates. Using (3.6) and (3.11) the effective data rate of user i is written as:

$$R_{b,i} = \frac{W}{(E_b/I_o)_i}\gamma_i(\boldsymbol{p}) \tag{3.37}$$

where $\gamma_i(\boldsymbol{p})$ is the received SIR of user i with the power vector $\boldsymbol{p}$ and $(E_b/I_o)_i$ is the E_b/I_o requirement for user i for achieving the data rate $R_{b,i}$. Let the maximum transmission power vector for the users be $\boldsymbol{p}_{\max} = (p_1^{\max}, p_2^{\max}, \ldots, p_N^{\max})$.

Definition 3.8 ([84, 57]) *A rate vector* $\boldsymbol{R}_b(\boldsymbol{p}_{\max}) = (R_{b,1}, R_{b,2}, \ldots, R_{b,N})$ *is instantaneously achievable if there exists a non-negative power vector* $\boldsymbol{p} \leq \boldsymbol{p}_{\max}$ *such that* $R_{b,i} \leq \frac{W}{(E_b/I_o)_i}\gamma_i(\boldsymbol{p})$ *for all* $1 \leq i \leq N$.

Definition 3.9 ([84, 57]) *A rate vector* $\boldsymbol{R}_b^*(\boldsymbol{p}_{\max}) = \left(R_{b,1}^*, R_{b,2}^*, \ldots, R_{b,N}^*\right)$ *is achievable in the average sense if it may be expressed as* $\boldsymbol{R}_b^* = \sum_i \lambda_i R_{b,i}$*, where* $\lambda_i \in [0,1]$*,* $\sum_i \lambda_i = 1$*, and all the* $R_{b,i}$ *are instantaneously achievable rate vectors.*

Thus, different rate vectors can be assigned a fraction of time (or frequency) yielding the required rate vector on the average. Assume that each link i requires a minimum data rate $R_{b,i}^{\min}$. Any excess data rate is potentially consumed, and thus paid for, by the user. It is the interest of the operators then to provide as much excess data rate as possible. For nonreal-time services, therefore, the following optimization problem is of interest:

$$\begin{aligned} &\max \sum_{i=1}^{N} R_{b,i}^*(\boldsymbol{p}_{\max}) \\ &\text{subject to } R_{b,i}^*(\boldsymbol{p}_{\max}) \geq R_{b,i}^{\min}, \forall i \end{aligned} \tag{3.38}$$

3.6 Power control and other radio resource management

Optimizing power control alone is not always the best way to enhance capacity. By understanding the relations between power control and other radio resource management (RRM) functions, one can design more efficient algorithms by combining them in an ingenious way. For instance, base station assignment is closely related to the power control problem. The integration of base station assignment and power control was studied in [123]. They considered the following *minimum transmission power* (MTP) problem:

The Minimum Transmission Power (MTP) Problem:

minimize $\sum_i p_i$

subject to

$g_{b_i i} p_i \geq \left(\sum_{j \neq i} g_{b_i j} p_j + \eta_i\right), \quad 1 \leq i \leq N$

$p_i \geq 0, \quad 1 \leq i \leq N$

$b_i \in \{1, \ldots, M\}, \quad 1 \leq i \leq N,$

where N and M are the number of users and the number of base stations in the system, respectively.

$\diamondsuit$

They showed that by optimizing over all base station assignments and power vectors, there exists a unique minimum power vector that solves the MTP problem. They also presented iterative algorithms that solve the MTP problem in a distributed manner.

The task of admitting new users in the system is called *admission control*. In [124] an active link protection scheme was proposed, in which a candidate user to be admitted to the system

starts up with small power, and gradually increases it by a fixed step, while the other users update their powers with the DPC algorithm, but increasing their SIR targets with the same fixed power-up step. This way the SIRs of the active links are protected from falling below their predefined targets. The scheme is called *Distributed Power Control with Active Link Protection (DPC-ALP) Algorithm*, and is formally given as follows.

The Distributed Power Control with Active Link Protection (DPC-ALP) Algorithm:

$$p_i(t+1) = \begin{cases} \frac{\delta\gamma_i^t}{\gamma_i(t)} p_i(t) & \text{if } \gamma_i(t) \geq \gamma_i^t \\ \delta p_i(t) & \text{if } \gamma_i(t) < \gamma_i^t \end{cases}, \quad t = 0, 1, \ldots \tag{3.39}$$

where $\delta > 1$ is the power-up step.

$\diamondsuit$

Power constraints with the DPC-ALP scheme are considered in [125]. During the admission of a new user it may happen that the transmission power of the active users may achieve the maximum power limit, causing their SIRs to fall below the target. As a remedy, a *distress signaling* is proposed, where an active user approaching the power limit sends a distress signal to the new users that are then blocked and cease their transmission.

A drawback of the DPC-ALP scheme is that the system capacity is diminished due to the increase in the SIR targets of the active links during admission of new users. Another algorithm is proposed in [126] that does not suffer from capacity loss. The algorithm is called the *Soft and Safe Admission Control (SAS) Algorithm*. A drawback of SAS is that while it is fast in admitting a new mobile, it is very slow to reject it.

Combined power and rate control is interesting for services with heterogeneous bit rates and quality requirements as discussed in the last section (see also [99, 127, 128]). Other methods that have been considered jointly with power control include smart antennas and beamforming, where there are more degrees of freedom in the optimization of the algorithms [129, 130, 131, 17]. Without going into details about beamforming (for information about beamforming, see [132]), typically the joining of power control and beamforming is done in two phases: in the first phase, the beamforming weights are updated to maximize SIR, and in the second phase, the maximized SIR is used in power control calculations. Hence, any SIR-based power control method could then be used in combination with beamforming.

Recently, the joining of power control with spreading code allocation has been an active research topic in the literature. In these schemes, the spreading codes are allocated so as to minimize the interference, and power control is used again to ensure that the specified target SIR is achieved [133, 134].

3.7 Views into the future

The ultimate goal of radio resource management is to maximize the network capacity without sacrificing the satisfaction of the users too much. Efficient transmission power control is essential in CDMA cellular systems for achieving these goals. The efficiency of TPC depends on its ability to control the interference inherent in wireless multiuser systems. However, there are other methods for combating the multiple access interference in CDMA. One of these methods is *multiuser detection* (MUD). An optimal MUD-based receiver would theoretically eliminate the need for power control completely! In practice, however, an optimal MUD-receiver would be too complex, and suboptimal solutions must be used that are not completely immune to interference, and TPC can still provide additional gain. Using only TPC provides a much cheaper way of controlling interference. This situation might change in the future, as the microtechnology evolves very fast and more efficient chips become available.

Chapter 4

Adaptive closed-loop power control

4.1 Introduction

In this chapter new algorithms for closed-loop power control in CDMA systems are proposed. As discussed in Chapter 3, the closed-loop PC aims to keep the received SIR in a target set by an outer-loop controller, by sending feedback signals to the transmitter. To minimize the power control signaling, practical CDMA systems typically employ a simple fixed-step (decision feedback) power control scheme that does not take advantage of the power control command and measurement histories. However, due to the time variation of the radio channel and interference seen by a receiver, and the loop delay (see Chapter 3), the command may already be outdated by the time it can be applied in the transmitter. Even if the feedback information signals are not quantized, the loop delay can cause serious problems to power control algorithms if it is not properly taken into account. The new approach is to model the power control process with a linear process model, and to design an adaptive self-tuning controller to minimize the variance of the process output, which is the SIR at the receiver or its distance to SIR target. Decision feedback versions of the algorithms are also provided. Those algorithms are able to mitigate the undesirable effects of the loop delay without any increase in power control signaling.

The proposed algorithms are evaluated via computer simulations using the simulator described in Appendix A. Examples of simulation results are given throughout the Chapter at appropriate points.

This chapter is related to publications [135, 136, 137, 138, 139, 140, 141].

4.2 Motivation for adaptive controller approach

As discussed in Chapter 3, many of the distributed iterative power control algorithms proposed in the literature can be put in the general form (3.17). These algorithms have been derived from a

rather theoretical viewpoint, where it is assumed that the iteration converges fast enough so that the channel attenuations can be assumed to be constant during this time. In practice, however, there are several factors that may render this assumption incorrect, as discussed in Section 3.1.5. The delays involved in the SIR measurement process, transmission and the processing of the algorithm itself can be long enough so that the channel as well as interference conditions might be considerably changed during the delay. As seen later in simulations, this might be disastrous for the performance of the PC algorithms that do not take the loop delay into account. The loop delay is tackled in this thesis through linear prediction, which has been shown also in the work by others to be an effective way to increase power control performance in the presence of loop delays, as discussed in Section 3.4.4. Typically, the prediction is applied to the received signal-to-interference power ratio (SIR) based on its previous measurements, and the predicted SIR value is compared to the SIR target, which is set by outer-loop power control. In the proposed algorithms of this Chapter, a different approach has been taken. A linear model of the power control process is first constructed, and a *self-tuning controller* is designed to control the model. The loop delay can be included in the model, and the controllers are designed to minimize a cost function that includes k-samples-ahead prediction of the process output (in this case, either the SIR or the difference of SIR and SIR target), where k equals the loop delay in samples. In this way the information of both the previous estimates of the SIR and the previous control commands can be utilized to achieve better performance. In Section 4.9 algorithms are proposed to take into account situations where the loop delay might not always be known.

Another issue is the feedback bandwidth needed in closed loop power control for the power control command transmission. In practical systems the power control command is typically one bit long, allowing only power up / power down -commands to be fed back to the transmitter. This one-bit feedback is also called *decision feedback* (DFB). In order to take this limitation into account with the proposed algorithms, some modifications are needed to the standard self-tuning control methods to make them work in a decision feedback manner.

Finally, in order to follow the changes of the dynamical radio environment, the parameters of the linear model are estimated in real time with an adaptive algorithm.

The assumption behind the new proposed algorithms is that the SIR target is provided via outer loop PC, and the task of closed-loop PC is thus to follow that target. Thus, from viewpoint of system capacity, the goal is to enhance the target tracking capability of the closed-loop PC, which enables the outer-loop PC to reduce the SIR target, which in turn increases capacity due to diminished interference. This goal is elaborated in Section 4.2.3 in more detail.

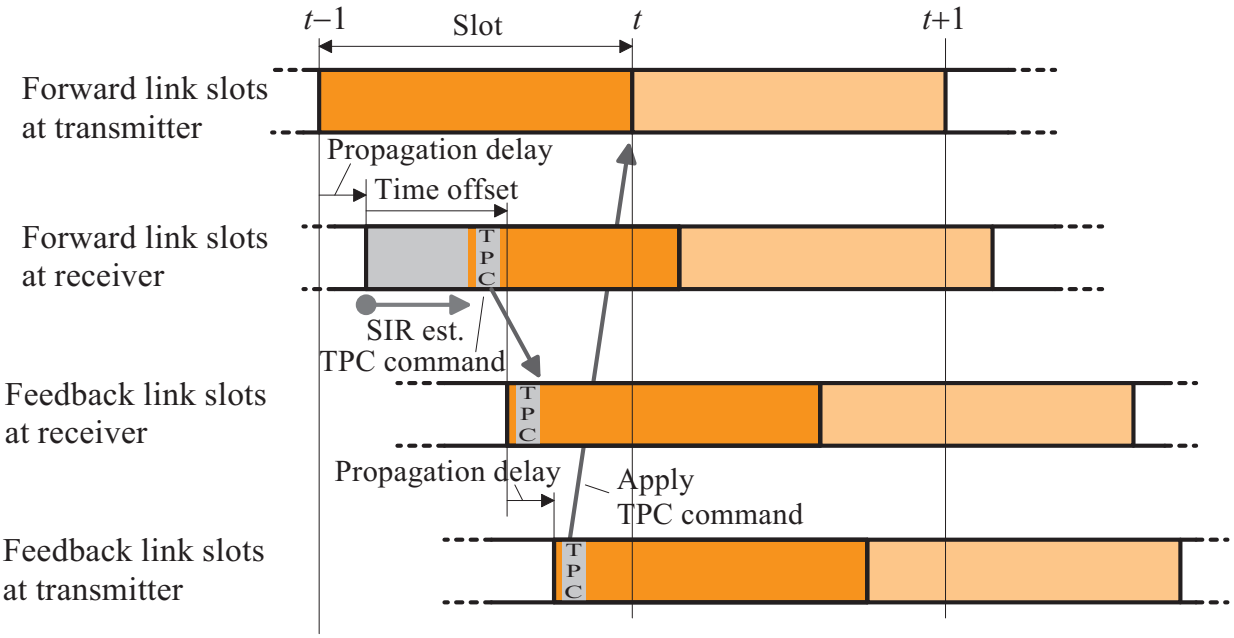

Figure 4.1: Example of power control timing in WCDMA [59]. To permit a short TPC delay, the frame timing of the feedback link is offset from that of the forward link. The receiver receives the slot that is transmitted at time $t-1$ after a propagation delay. The receiver then estimates the SIR from a number of pilot and/or data symbols, derives a TPC command, and transmits the command in the feedback link to the transmitter. The transmitter receives the command after a propagation delay and adjusts its transmission power for the next slot according to the command. Thus the loop delay is one PC period. If the delays due to SIR estimation and TPC command processing are longer, the command may not reach the transmitter within one-slot-time. In this case, the transmission power is changed for the slot that is transmitted at time $t+1$, resulting in a loop delay of two PC periods.

4.2.1 Loop delay example

A typical loop delay situation encountered in WCDMA is illustrated in Figure 4.1. Since the power control signaling is standardized, the loop delays are in principle known exactly. The slot at time $t-1$ is transmitted using power $p(t-1)$. The receiver measures the SIR $\gamma(t)$ over a number of pilot and/or data symbols and derives a TPC command. The command is transmitted to the transmitter in the feedback link and the transmitter adjusts its transmission power according to the command. If the SIR measurement window, processing delays and propagation delays are short enough, as in the example in Figure 4.1, the loop delay can be as short as one PC period. Otherwise, the TPC command cannot be applied at the transmitter within one-slot-time, resulting in longer loop delays. Note that the SIR estimation window affects the PC timing. If a short

window is used, the loop delay can be shorter, but the SIR estimation becomes more unreliable.

To elaborate, consider the uplink case. The number of pilot bits in WCDMA uplink *Dedicated Physical Control Channel* (DPCCH) slot can be from 3 to 8 [142]. The duration of one slot is 667 μs, and there are 10 bits in a DPCCH slot, so one pilot bit duration is 66.7 μs. Assuming that all available pilot bits are used for SIR estimation, the averaging time of the estimation ranges from 200 μs to 534 μs. The uplink frame is delayed from the downlink frame by 1024 chips (267 μs), measured at the mobile station antenna, so the time offset in Figure 4.1 is $667\ \mu\text{s} - 267\ \mu\text{s} - 2\tau_p = 400\ \mu\text{s} - 2\tau_p$, where τ_p is the propagation delay. Looking at Figure 4.1 it is seen that the one-slot loop delay requires that, starting from the beginning of the first pilot bit at the receiver, the TPC command must be ready within the time offset plus the offset of the TPC field from the beginning of the feedback slot. This limits the time available for SIR estimation and the available processing delay. Depending on the downlink slot format, the offset of the TPC command from the beginning of the slot can range from 0 to 130 μs [142]. Thus, from the beginning of the first pilot bit at the receiver, the time available for SIR measurement, TPC command generation and its placement into the downlink slot ranges from $400\ \mu\text{s} - 2\tau_p$ to $530\ \mu\text{s} - 2\tau_p$. The longest signal path in a typical WCDMA system can be 5 km, so the maximum propagation delay is about 17 μs. Thus, in the worst case, there will be $(400 - 34)\ \mu\text{s} = 366\ \mu\text{s}$ time for SIR measurement, TPC command generation and its placement into the downlink slot. If the TPC command is not ready within this time, it must be delayed to the next slot.

4.2.2 Problems caused by the loop delay

It has been shown that if not properly controlled, the loop delay can cause serious problems to the power control algorithms [106, 107, 77, 140]. Some IFB algorithms, like the widely known DCPC algorithm, can even become unstable in the precence of loop delays.

Since the maximum power adjustment is limited in the FSPC, the loop delay does not destroy the performance of the algorithm, but considerably increases the variance of the SIR at the receiver minus the SIR target. It has been shown [143, 77] that the FSPC algorithm converges to a bounded region

$$\left|\gamma_i^t - \gamma_i(t)\right| \leq 2\delta k \tag{4.1}$$

provided that the power control problem is feasible within this margin. Here δ is the step size of the algorithm and k is the total loop delay. Thus, longer loop delays lead to larger convergence bounds.

It can be shown [77] that with the FSPC algorithm time delay compensation (TDC, see Section 3.4.3) the PC misadjustment converges to

$$\left|\gamma_i^t - \gamma_i(t)\right| \leq \delta(k+1) \tag{4.2}$$

which should be compared to (4.1). However, the fact that the bound is tighter does not imply that the variance of the PC misadjustment is smaller.

Figure 4.2 shows how an additional loop delay of one sample, so that $k = 2$, affects various non-predictive PC algorithms without time delay compensation. In the simulation, only the randomly selected observed user is power controlled with different algorithms, while all other users use the FSPC algorithm. The speed of the selected user is 5 km/h. The total loop delay k is increased from one to two at sample number 300. It is seen that all the IFB-algorithms become unstable after this change. The FSPC algorithm remains stable, but the amplitude of the envelope of the SIR variation grows as predicted by (4.1).

4.2.3 Considered adaptive controllers

The disturbances in the power control process are stochastic in nature. Therefore it is natural to use stochastic measures to investigate the performances of various closed-loop power control methods. It is well established in the literature [55, 108] that for reasonable number of users in the system the SIR statistics at the receiver and the power control misadjustment (the difference between SIR target and SIR) are log-normally distributed. A natural optimization criterion is thus to minimize the variance of the power control misadjustment in decibels. Figure 4.3 shows two hypothetical PDFs of received SIR. Consider that the PDFs result from using power control algorithms (PCAs) 1 and 2 as shown in the figure. The SIR threshold is the lowest SIR required for acceptable reception of the signal at the receiver. The outer loop power control sets the SIR targets in such a way that the service quality is achieved up to a specified criterion, e.g., 1-% frame error rate. Since the variance of the received SIR is smaller with PCA 2, the SIR target with PCA 2 can be set smaller than with PCA 1 while achieving the same quality of service. Reducing the SIR target results in smaller transmission powers and thus less interference, leading to higher capacity.

The goals of closed-loop power control are thus to keep the mean received SIR at the target value, and to minimize the variance of the received SIR around the target. The *minimum variance* (MV) controller is a natural choice with this goal in mind. However, as discussed later in this chapter, MV control is not a robust technique, and is not suitable for nonminimum-phase processes. A modification of the MV controller, the *generalized minimum variance* (GMV) controller, can be designed also for nonminimum-phase processes, and is more robust than the standard MV method. Both the MV and GMV methods need accurate information of the delay of the process. If the delay is incorrectly estimated, the performances of these controllers become very poor. For these cases, a more recent method called *generalized predictive control* (GPC) is considered. The GPC method has been shown to possess some degree of robustness against

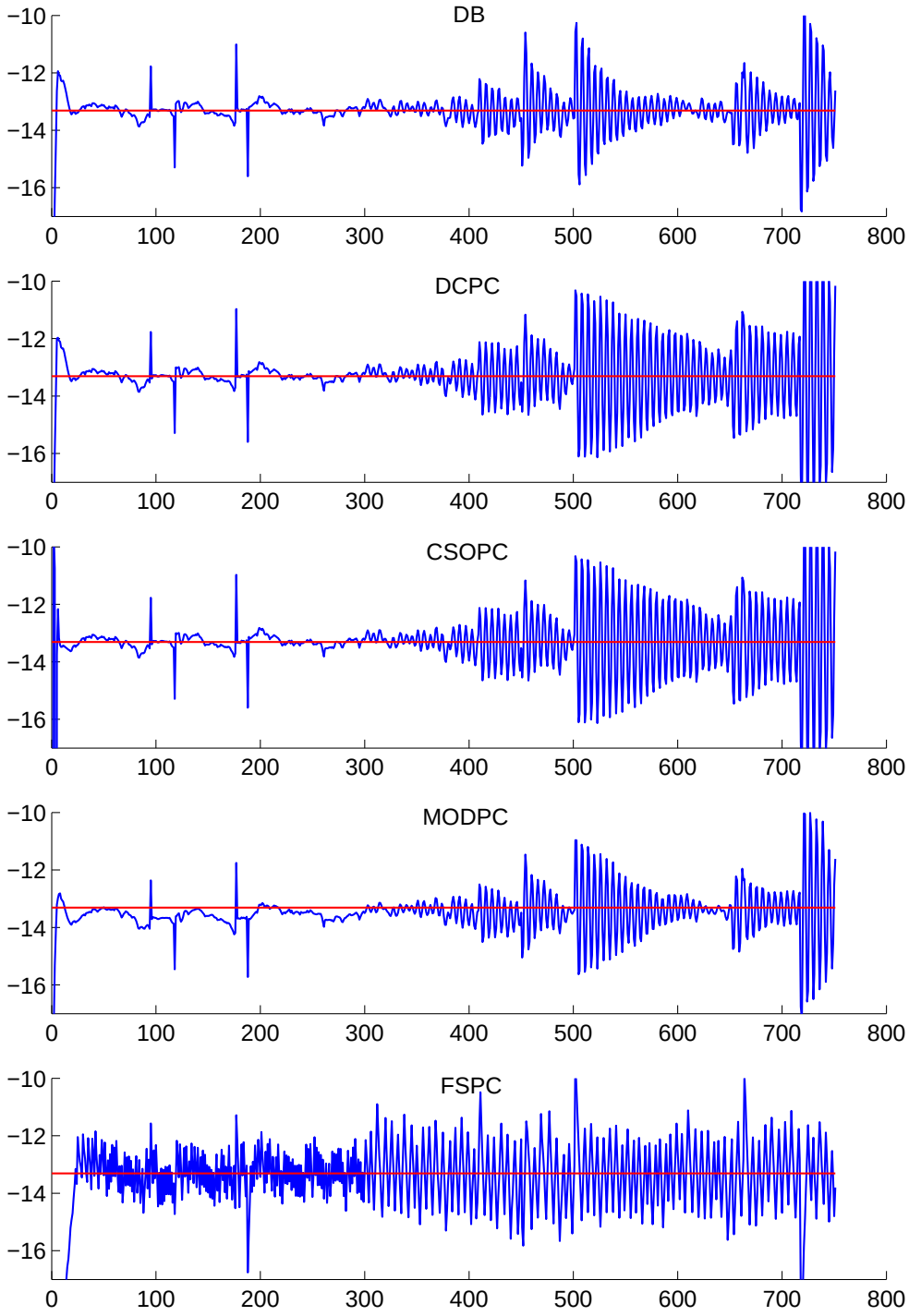

Figure 4.2: SIR variation around SIR target. Loop delay k changes from one to two at sample number 300. The speed of the observed user is 5 km/h.

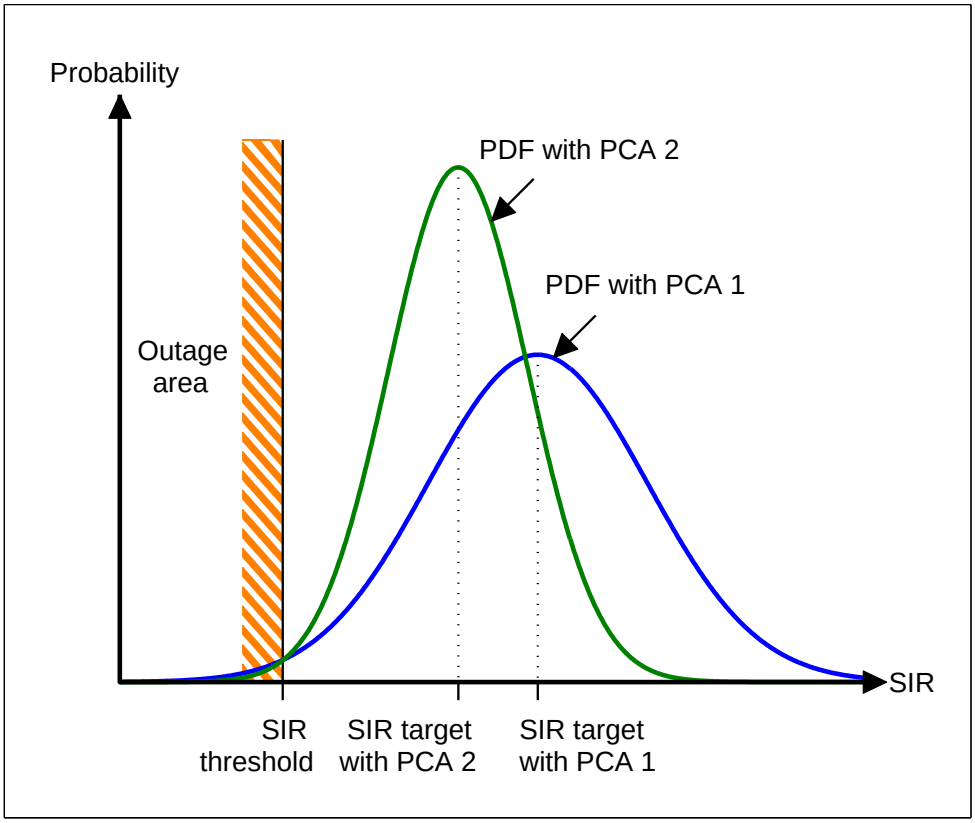

Figure 4.3: Illustration of the goals in the design of the proposed power control algorithms. The variance of received SIR with PCA 2 is smaller than with PCA 1. As a consequence, the SIR target required for the same outage probability can be reduced.

incorrect delay estimation and overparametrization of the process [144, 145, 146]. The drawback is the increased computational complexity.

4.2.3.1 Related work

The minimum variance power control approach was first proposed in [135] and refined in [140] by the author of this thesis (as joint work with the other authors in the papers). Minimum variance power control has also been proposed in [77], however, neither parameter estimation nor decision feedback is considered. The approach presented in [135, 140] (see Section 4.7 in this thesis) and the model identification presented in [138] (see Section 4.5 in this thesis) have also been recently partly re-invented in [147].

4.2.4 A note on the shift operator calculus used in this Chapter

In this Chapter a special kind of operator calculus called *shift operator calculus* is employed. It is widely used in control theory that is the origin of the methods on which the algorithms proposed in this Chapter are built. While the z-transform representation could also be used to represent the material, it is more natural to utilize similar representation as in the original related work. The shift operator calculus is described in Appendix B.

4.3 Overview of adaptive self-tuning control

4.3.1 History of adaptive control

Adaptive control is one type of a nonlinear control. The adaptive control theory originated in early 1950s, when sophisticated controllers were needed for aircraft autopilot systems. The problem was how to control a system having several operating points, which could also be time varying. Adaptive control combines closed-loop identification with control, which makes the problem nonlinear and extremely complex.

Basic concepts in adaptive control were introduced in the 1960s, namely, *model reference adaptive control* and *self-tuning regulator* or *pole-placement adaptive control*. As computers were gaining popularity in process control, the implementation of adaptive controllers became increasingly easy. The advent of microprocessors in 1971 and the first industrial digital controllers in 1975 motivated the development of adaptive digital control systems.

In 1970s and 1980s major stability results for adaptive control were found. However, adaptive control was regarded as difficult to apply in such a way that stability and performance specifications could be proven to hold. This has made researchers to find *robust adaptive* methods to overcome these difficulties, thus creating a field of *robust adaptive control*. This work is still going on [148, 149].

4.3.2 Characteristics of adaptive control systems

In adaptive control systems the controller parameters are adjusted all the time, so that they follow the changes of the controlled process. Because the convergence and stability properties of such systems are very difficult to analyze, it is assumed that the process has constant but unknown parameters. When the process is known, the design procedure specifies a set of desired controller parameters. An adaptive controller should converge to these parameter values even when the process is unknown. A controller with this property is called a *self-tuning controller*, since it automatically tunes itself to the desired performance [149]. There is a conceptual difference

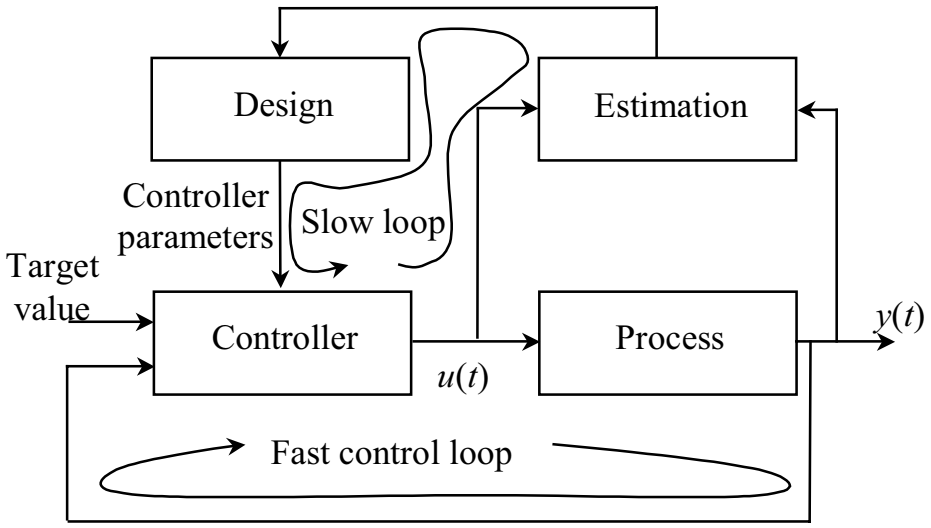

Figure 4.4: The self-tuning controller structure [149].

between *adaptive control* and *self-tuning control*. In self-tuning control the controller parameters are updated until the optimal parameter values are reached, after which the parameter updating mechanism can be turned off. If the updating mechanism is not turned off, the controller can respond to changes in the process characteristics by identifying the optimal parameters continuously. In this case the controller can be stated as adaptive. However, both of these terms convey the same idea, and the differences lie mainly in algorithmic details [150, 151, 149, 152].

The basic idea of self-tuning control is illustrated in Figure 4.4, where fast closed loop control is utilized to keep the output of the process at a given target value. In the block labeled "Estimation" the unknown process parameters are periodically identified in another loop, based on measured process input $u(t)$ and output $y(t)$ values. The update rate of this loop is usually slower than that of the fast feedback loop, since in many applications the update rate of the feedback loop may be relatively high in comparison with the dynamics of the process. However, if the dynamics of the process are comparable to the update rate of the fast feedback loop, the parameters can be estimated at the same rate. The block labeled "Design" in Figure 4.4 represents an on-line solution to the design problem for a system with known parameters. The most straightforward approach in self-tuning control is to estimate the parameters of the transfer function of the process and the disturbances. This gives an *indirect* or *explicit adaptive algorithm*, because the controller parameters are not updated directly, but rather indirectly via the estimation of the process model. Another approach is to re-parameterize the model in the controller parameters, such that the controller parameters can be estimated directly. This leads to a *direct* or

implicit adaptive algorithm. In this case the block "Design" in Figure 4.4 disappears (or rather is combined with the "Estimation" block). The parameter updating mechanism first identifies the parameters and then tracks the changes in the system by periodically adjusting the parameters. The parameters are identified using some adaptive algorithm such as the *least mean squares* (LMS) algorithm, or the *recursive least squares* (RLS) algorithm (see [119, 153, 120]). The LMS algorithm is computationally simpler than the RLS algorithm, but has slower convergence properties. Since the number of model parameters is relatively low in the algorithms considered in this thesis, the computational cost of the RLS algorithm is considered to be feasible. The LMS algorithm is not considered in the thesis.

4.4 System models

To construct the various self-tuning controllers considered in this thesis, a suitable linear model for the power control process is needed. In the following, the index identifying the user is omitted for notational clarity. A general model that covers all considered methods is given as:

$$Ay(t) = Bu(t-k) + e_{\mathrm{d}}(t) \tag{4.3}$$

where $y(t)$ is the output and $u(t)$ is the input of the process, $e_{\mathrm{d}}(t)$ is a disturbance signal, k is the delay of the process, A and B are polynomials in q^{-1}, given by[1]

$$A = 1 + a_1 q^{-1} + \ldots + a_{n_a} q^{-n_a} \tag{4.4}$$

$$B = b_0 + b_1 q^{-1} + \ldots + b_{n_b} q^{-n_b} \tag{4.5}$$

and q^{-1} is the backward shift operator. The disturbance signal $e_{\mathrm{d}}(t)$ is commonly modeled as a moving average (MA) process as:

$$e_{\mathrm{d}}(t) = C\xi(t) \tag{4.6}$$

where

$$C = 1 + c_1 q^{-1} + \ldots + c_{n_c} q^{-n_c} \tag{4.7}$$

and $\{\xi(t)\}$ is a white Gaussian sequence with variance σ_ξ^2. In many cases it is assumed that $C = 1$ so that the process disturbance model is purely autoregressive (AR).

It has been argued [145] that for many industrial processes with nonstationary disturbances this model is inappropriate, and an appropriate model for those cases is

$$e_{\mathrm{d}}(t) = \frac{C}{\Delta}\xi(t) \tag{4.8}$$

[1]The dependency of the polynomials on q^{-1} is often shown in the notation as, e.g., $A(q^{-1})$. However, the argument is dropped here in order to simplify notation.

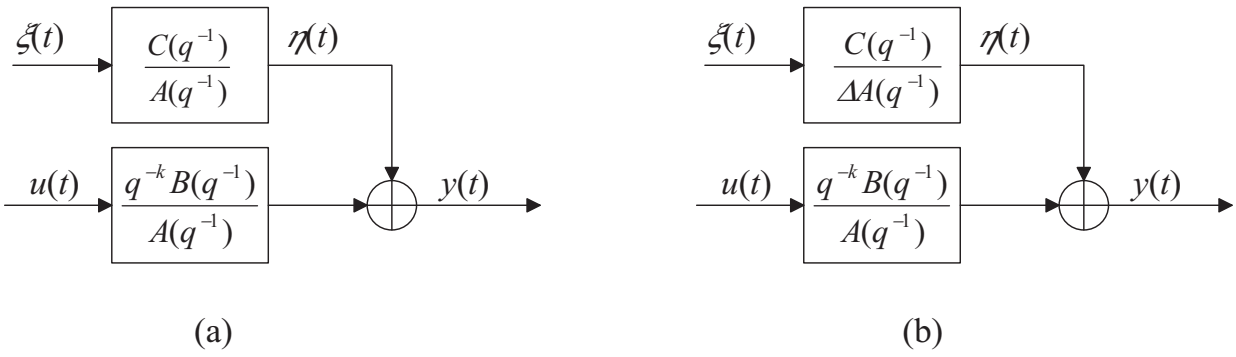

Figure 4.5: (a) ARMAX-model, (b) ARIMAX-model.

where $\Delta = 1 - q^{-1}$ is the differencing operator.

Depending on the selection of the disturbance signal $e_{\mathrm{d}}(t)$, four process models are obtained: the *autoregressive moving average process with exogenous input*, denoted by ARMAX(n_a, n_b, n_c, k), the *autoregressive process with exogenous input*, denoted by ARX(n_a, n_b, k), the *autoregressive integrated moving average process with exogenous input*, denoted by ARIMAX(n_a, n_b, n_c, k), and the *autoregressive integrated process with exogenous input*, denoted by ARIX(n_a, n_b, k). The model equations are:

$$\text{ARMAX}: \quad Ay(t) = Bu(t-k) + C\xi(t) \tag{4.9}$$

$$\text{ARX}: \quad Ay(t) = Bu(t-k) + \xi(t) \tag{4.10}$$

$$\text{ARIMAX}: \quad Ay(t) = Bu(t-k) + \frac{C}{\Delta}\xi(t) \tag{4.11}$$

$$\text{ARIX}: \quad Ay(t) = Bu(t-k) + \frac{\xi(t)}{\Delta} \tag{4.12}$$

The ARMAX and ARIMAX models are illustrated in Figure 4.5. The ARX and ARIX models can be obtained from these by setting $C = 1$. The models can be related to that in Figure 3.3 so that $y(t)$ corresponds to $\gamma(t)$, $u(t)$ corresponds to $u_{\mathrm{tx}}(t)$, and $(g(t) - I(t))$ corresponds to the disturbance term $\eta(t)$ (if the effects of PC command errors are ignored). Note that in all the models the process and the noise filter are assumed to have the same poles.

4.5 Model identification

The first step in the design of the adaptive controller is to find the best model from those in consideration to describe the process. This is done by collecting data from a radio network simulator and using the collected data to identify models with various structures and orders. The model with the best compromise between complexity and modeling accuracy is then selected.

4.5.1 Data collection

The simulation program described in Appendix A was used with the following parameters (other parameters are as described in the Appendix):

$$N = 200,$$
$$R_b = 12.9kb/s,$$
$$v_{\min} = 0km/h,$$
$$v_{\max} = 30km/h$$

In the beginning of the simulation, a randomly selected user, initially connected to the central cell, is selected for observation and its velocity is set to 5 km/h. Each user except the observed user is power controlled using the FSPC algorithm (3.7).

To collect the input-output data for the system identification, the power control loop of the observed user is opened at the line separating the base station and the radio channel in Figure 3.3. The power control commands for that user are then made to come from a pseudo-random binary signal (PRBS) generator, and the resulting SIR is measured at the base station. In other words, the selected mobile unit receives power control commands from the PRBS generator and adjusts its transmission power according to those commands. The generated PRBS sequence and the resulting SIR sequence (both in decibels) are then regarded as input and output, respectively, of an unknown system to be identified. Bit errors in the power control commands are not considered.

4.5.2 Model identification results

The input-output data collected from the radio network simulator according to the previous section is used to identify the model parameters, i.e., the coefficients of the polynomial operators A, B and C. The model is identified recursively using exponential forgetting to include the time variation of the system in the model. The identification methods are described in Appendix C.

The ARX and ARIX models have the desirable property that the linear regression equations (C.1) and (C.4) are unconditionally stable, and they are to be preferred over the ARMAX and ARIMAX models. To select the appropriate model and model order, i.e., the orders of the model polynomials, n_a, n_b and n_c, the recursive algorithms described in Appendix C with forgetting factor 0.99 are run with various values for n_a, n_b and n_c. Figure 4.6 shows an example of the variance of the prediction error signal $\epsilon(t)$ in various cases for non-integrated models. The "knee-point" in the figure occurs with the configuration $(n_a, n_b) = (2, 1)$, and there is practically no advantage in increasing the model order beyond this point. Moreover, the ARX model gives the best result at this point, so the best non-integrated model is concluded to be the ARX(2,1,k)

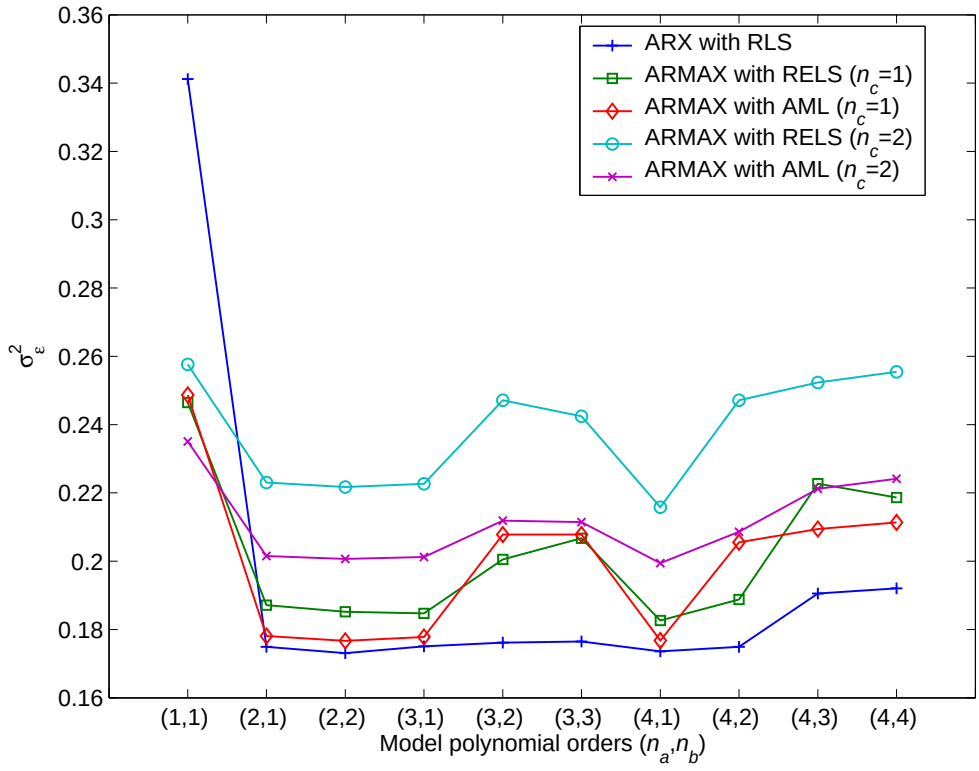

Figure 4.6: Variance of the prediction error $\epsilon(t)$ in the case of ARX and ARMAX models.

model. Based on several other experiments with the same method as well as with the aid of Matlab system identification toolbox, the conclusion is that although in some cases the ARMAX models could give similar or slightly better results, the difference was too small to justify using more parameters in the model.

Figure 4.7 shows the variance of the prediction error versus the model order for integrated models. Here the best results are achieved already with $(n_a, n_b) = (1, 1)$. In this case the ARIMAX(1,1,1,k) model is found to be the best. However, since the difference to the ARIX(1,1,k) model is quite small, the latter one is preferred. In numerical experiments, however, the slightly higher-order model ARIX(2,2,k) was seen to give slightly better results, and this model is therefore used in the simulations.

4.6 Controlled closed-loop model

Figure 4.8 shows a controlled closed-loop system model (cf. Figure 4.5). The model includes controllers G_C (in the direct path), G_{FR} (a prefilter) and G_{FY} (in the feedback path). The controllers are designed to output a control signal $u(t)$ so that the output of the system, $y(t)$, is made to follow the reference signal $r(t)$. If $r(t)$ is constant, the control problem is called a *regulator*

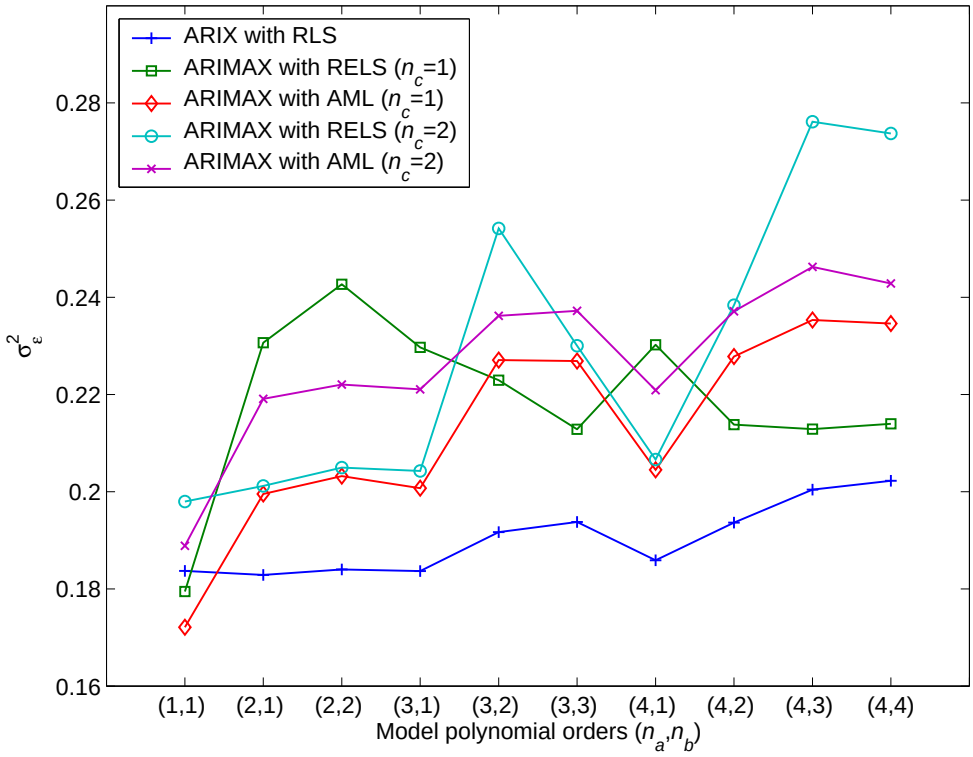

Figure 4.7: Variance of the prediction error $\epsilon(t)$ in the case of ARIX and ARIMAX models.

problem, otherwise it is called a *servo problem*.

4.7 Minimum variance (MV) control approach

Minimum variance control is the simplest approach in self-tuning control (see e.g. [151, 150, 149]). It's objective is to minimize the variance of the output of the controlled system, i.e.

$$J_{\text{MV}} = E\left\{y^2(t+k)\right\} \tag{4.13}$$

Note that k, the delay of the system, is included in the cost function, since the control signal can affect the system output only after k sample periods have passed. Originally the MV controller was developed for the *regulator problem*, i.e., $r(t)$ is constant (and usually zero).

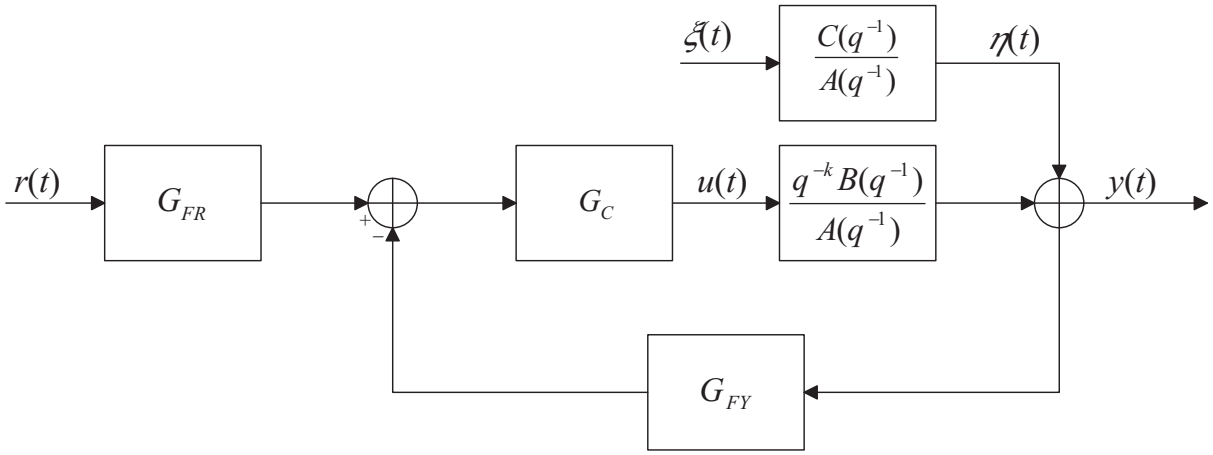

Figure 4.8: Controlled system model.

4.7.1 Control law

The minimum variance controller is now derived. The derivation follows that given in [151]. Define

$$\left.\begin{aligned} F &= 1 + f_1 q^{-1} + \ldots + f_{k-1} q^{-(k-1)} \\ G &= g_0 + g_1 q^{-1} + \ldots + g_{n_g} q^{-n_g} \\ n_g &= \max\left(n_a - 1, n_c - k\right) \end{aligned}\right\} \tag{4.14}$$

to satisfy the polynomial *Diophantine equation*

$$C = AF + q^{-k}G \tag{4.15}$$

Substituting (4.15) into (4.9) gives

$$y(t+k) = \left[\frac{B}{A}u(t) + \frac{G}{A}\xi(t)\right] + F\xi(t+k) \tag{4.16}$$

Substituting for $\xi(t)$ using (4.9) gives

$$y(t+k) = \left[\frac{B}{A}u(t) + \frac{G}{C}y(t) - q^{-k}\frac{BG}{AC}u(t)\right] + F\xi(t+k) \tag{4.17}$$

and, using (4.15),

$$y(t+k) = \left[\frac{BF}{C}u(t) + \frac{G}{C}y(t)\right] + F\xi(t+k) \tag{4.18}$$

This can be arranged as

$$y(t+k) = \hat{y}(t+k|\,t) + F\xi(t+k) \tag{4.19}$$

where

$$\hat{y}(t+k|\,t) = \left[\frac{BF}{C}u(t) + \frac{G}{C}y(t)\right] \tag{4.20}$$

is the best prediction of $y(t+k)$ based on data up to time t. The output prediction error is then

$$F\xi(t+k) = y(t+k) - \hat{y}(t+k|\, t) \tag{4.21}$$

This error arises from the noise sources $\xi(t), \xi(t-1), \ldots$, which cannot be eliminated by the control signal $u(t)$. The cost function (4.13) becomes

$$\begin{aligned} J_{\text{MV}} &= E\left\{y^2(t+k)\right\} = E\left\{\left[\hat{y}(t+k|\, t) + F\xi(t+k)\right]^2\right\} \\ &= E\left\{\hat{y}^2(t+k|\, t)\right\} + \left(1 + f_1^2 + \ldots + f_{k-1}^2\right)\sigma_\xi^2 \end{aligned} \tag{4.22}$$

which is minimized by setting the predicted output to zero:

$$\hat{y}(t+k|\, t) = 0 \tag{4.23}$$

This yields the control law

$$BFu(t) + Gy(t) = 0 \tag{4.24}$$

and the output signal

$$y(t) = F\xi(t) \tag{4.25}$$

so the minimum output variance is

$$J_{\text{MV,min}} = \left(1 + f_1^2 + \ldots + f_{k-1}^2\right)\sigma_\xi^2 \tag{4.26}$$

4.7.2 Properties of the MV controller

The minimum variance controller cost function (4.13) does not put any constraints for the control signal $u(t)$. This may cause the control signal to grow without limit. Indeed, the control law (4.24), rewritten as

$$u(t) = -\frac{G}{BF}y(t) \tag{4.27}$$

attempts to cancel the zeros of the process, i.e., the zeros of B. If these zeroes lie outside the unit circle (process is *nonminimum-phase*), the controller is clearly unstable. Consequently, the MV controller is only applicable to minimum phase processes. However, as explained later, in the current application the control signal is hard-quantized into two levels, and cannot thus grow unbounded. This makes the MV controller more applicable to the power control problem.

In the special case when $C = 1$ and $k = 1$ the control law becomes

$$u(t) = \frac{q\,[A-1]}{B}y(t) \tag{4.28}$$

which includes only the process polynomials. Thus a direct (or implicit) adaptive controller can be realized, since the controller parameters can be directly estimated (see section 4.3.2).

4.7.3 Self-tuning minimum variance based power control algorithms

Power control algorithms based on the MV controller are now described. Using the various methods described in the following sections for the addition of the reference signal (Method 1 or Method 2) and the quantization of the control signal (information feedback (IFB) or decision feedback (DFB)), four different power control algorithms are obtained:

- the *minimum variance power control* (MV-PC),
- the *minimum variance incremental power control* (MVI-PC),
- the *minimum variance decision feedback power control* (MVD-PC) and
- the *minimum variance incremental decision feedback power control* (MVID-PC).

The algorithms are presented in Appendix D. Certain aspects of the algorithms are described in the following.

4.7.3.1 Reference signal

Since in our case the reference signal $r(t)$ is the target SIR $\gamma^t(t)$, it cannot be assumed to be constant (it is changed by the outer loop power control as explained in section 3.1.5). To take this into account, two methods described in [151] are considered:

Method 1: Apply MV control directly to the signal $y(t) - r(t)$. Thus the variance of the difference between the reference signal and process output is minimized. Also the process model (4.9) is modified to include the reference signal as:

$$A\left[y(t) - r(t)\right] = Bu(t-k) + C\xi(t) \tag{4.29}$$

Method 2: Insert an integrator in the forward path of the control loop. In this case, the control law (4.27) is replaced with the incremental control law:

$$\Delta u(t) = \frac{G}{BF}\left(r(t) - y(t)\right) \tag{4.30}$$

where $\Delta = 1 - q^{-1}$ is the differencing operator, and the controller polynomials are obtained by solving the modified identity

$$C = \Delta AF + q^{-k}G \tag{4.31}$$

$$n_f = k - 1; \qquad n_g = \max\left(n_a, n_c - k\right) \tag{4.32}$$

Remark 1:

Method 2 is a modification of the standard minimum variance approach to force steady-state tracking error to zero. This will, however, compromise the goal of variance minimization [151]. Moreover, since the power control algorithm already has an integrator in the closed-loop, it is expected that Method 1 performs better in this application. This is also shown in the simulation results.

4.7.3.2 Information feedback and decision feedback

The calculated control signal $u(t)$ must be communicated over the radio connection to the transmitter, which then adjusts its transmit power according to the control signal. If the exact $u(t)$ is communicated, this is referred to as *information feedback* (IFB), as discussed in Section 3.1.6. In practical systems, however, the transmission of an exact signal would consume too much radio resources on the feedback channel. Usually only one information bit is allowed for the power control signaling. This means that the information is hard-quantized into two levels and the quantized signal is transmitted in the feedback channel. This is referred to as *decision feedback* (DFB). In this case the control laws (4.27) and (4.30) must be modified according to the following equations:

Case 1 (Method 1 is used for reference tracking):

$$\tilde{u}(t) = \frac{1}{b_0}\left[G\left(r(t) - y(t)\right) + \left(b_0 - BF\right)u(t)\right] \tag{4.33}$$

$$u(t) = \text{sign}\left(\tilde{u}(t)\right) \tag{4.34}$$

In the special case when $C = 1$ and $k = 1$ (4.33) becomes

$$\tilde{u}(t) = \frac{1}{b_0}\left[q(1-A)\left(r(t) - y(t)\right) + \left(b_0 - B\right)u(t)\right] \tag{4.35}$$

Case 2 (Method 2 is used for reference tracking):

$$\Delta\tilde{u}(t) = \frac{1}{b_0}\left[G\left(r(t) - y(t)\right) + \left(b_0 - BF\right)\Delta u(t)\right] \tag{4.36}$$

$$u(t) = \text{sign}\left(u(t-1) + \Delta\tilde{u}(t)\right) \tag{4.37}$$

$$\Delta u(t) = u(t) - u(t-1) \tag{4.38}$$

In the special case when $C = 1$ and $k = 1$ (4.36) becomes

$$\Delta\tilde{u}(t) = \frac{1}{b_0}\left[q(1-\Delta A)\left(r(t) - y(t)\right) + \left(b_0 - B\right)\Delta u(t)\right] \tag{4.39}$$

Figure 4.9 shows the MV controller with information feedback and decision feedback using either Method 1 or Method 2 for reference tracking.

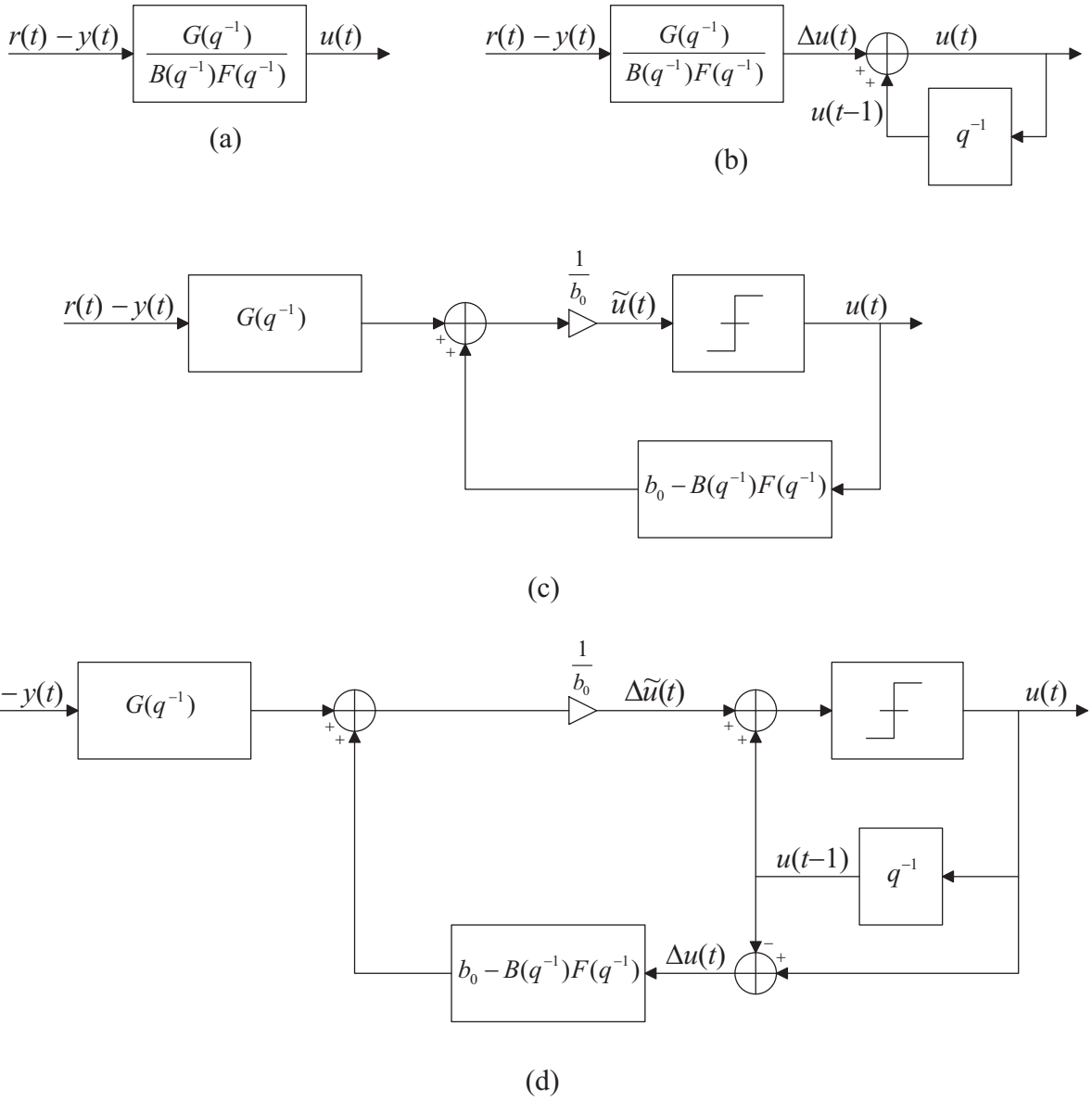

Figure 4.9: Minimum variance controllers. (a) IFB nonincremental, (b) IFB incremental, (c) DFB nonincremental, (d) DFB incremental.

4.7.3.3 Backup controller

In normal operating conditions the controller with the parameter estimation should perform adequately. However, the parameter estimation is a nonlinear process, and it might in some conditions start to lose its parameter tracking capabilities [151, 150]. Moreover, if the estimated process becomes nonminimum-phase, the minimum variance controller becomes unstable. In the case of decision feedback (section 4.7.3.2), the static nonlinearity (the sign-function) hard-limits the control signal $u(t)$, which alleviates the minimum phase requirement for the process. The internal control signal, however, can still grow very large, in which case the controller performance might degrade.

For these reasons, a backup-controller is included in the system. The algorithm switches to the backup controller if either the error signal $e(t) = \gamma^t(t) - \gamma(t)$ or the (internal) control signal becomes too high in absolute value, i.e., if $|e(t)| > \delta_e$, $|u(t)| > \delta_u$ or $|\tilde{u}(t)| > \delta_u$, where δ_e and δ_u are the corresponding deviation thresholds and $\tilde{u}(t)$ is the internal control signal (before quantization) in the case of decision feedback. Switching to the backup controller means that the control signal $u(t)$ is taken from the backup controller, while continuing the calculations of the adaptive controller. When $e(t)$ and $u(t)$ or $\tilde{u}(t)$ are again within specified limits, the algorithm switches back to the adaptive controller. The backup controller used here is a simple fixed-step controller:

$$u(t) = \delta \text{sign}\left(r(t) - y(t)\right) \tag{4.40}$$

where again δ is the step size.

4.7.4 Simulation results

The proposed algorithms were simulated using the radio network simulator described in Appendix A with $v_{\min} = 0$ km/h, $v_{\max} = 30$ km/h, $(n_a, n_b, n_c) = (2, 1, 0)$ and $(\delta_e, \delta_u) = (3, 3)$. The RLS algorithm was initialized using

$$\begin{aligned} &\hat{a}_1(0) = -1; \quad \hat{a}_m(0) = 0, \quad m = 2 \ldots n_a \\ &\hat{b}_0(0) = 0.1; \quad \hat{b}_m(0) = 0, \quad m = 1 \ldots n_b \\ &\boldsymbol{P}(0) = 10000\boldsymbol{I} \end{aligned} \tag{4.41}$$

The forgetting factor $\alpha_f = 0.99$.

Figure 4.10 shows the empirical cumulative distribution function (CDF) of E_b/I_o obtained from simulations with information feedback and a loop delay of one PC period (T_{PC}). It is seen that both proposed algorithms achieve smaller variance than the DCPC algorithm, but the tails of the distributions are heavier than with the DCPC algorithm. The MVI-PC gives the highest variance from the proposed algorithms.

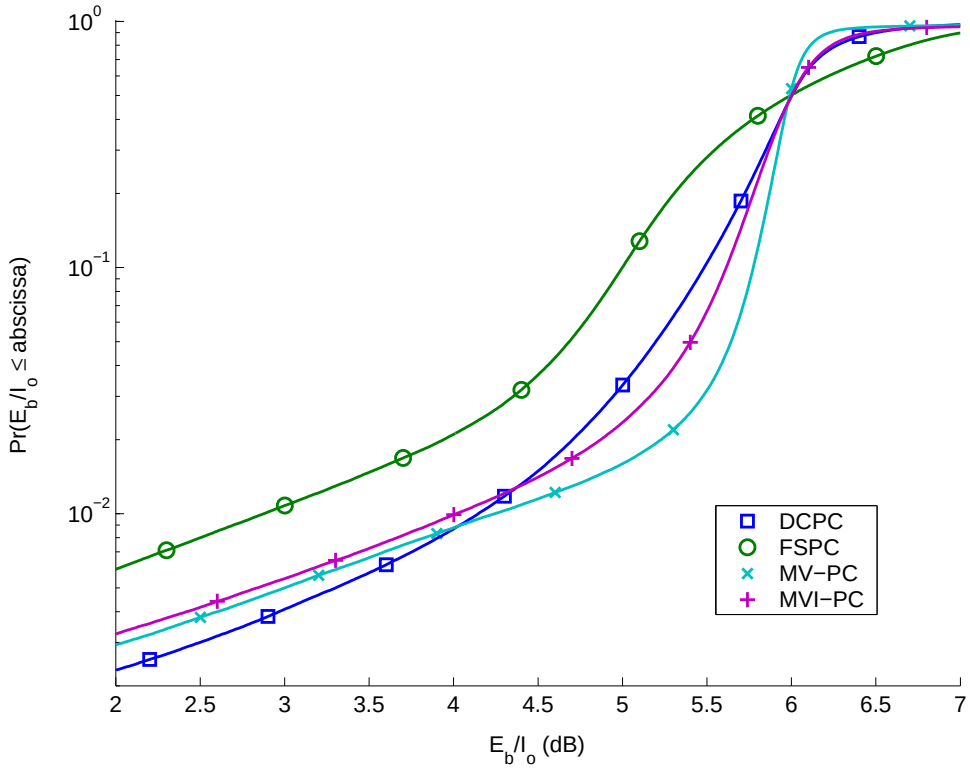

Figure 4.10: Empirical cumulative distribution function (CDF) of E_b/I_o, E_b/I_o target is 6 dB, loop delay 1 T_{PC}, unconstrained PC commands (information feedback).

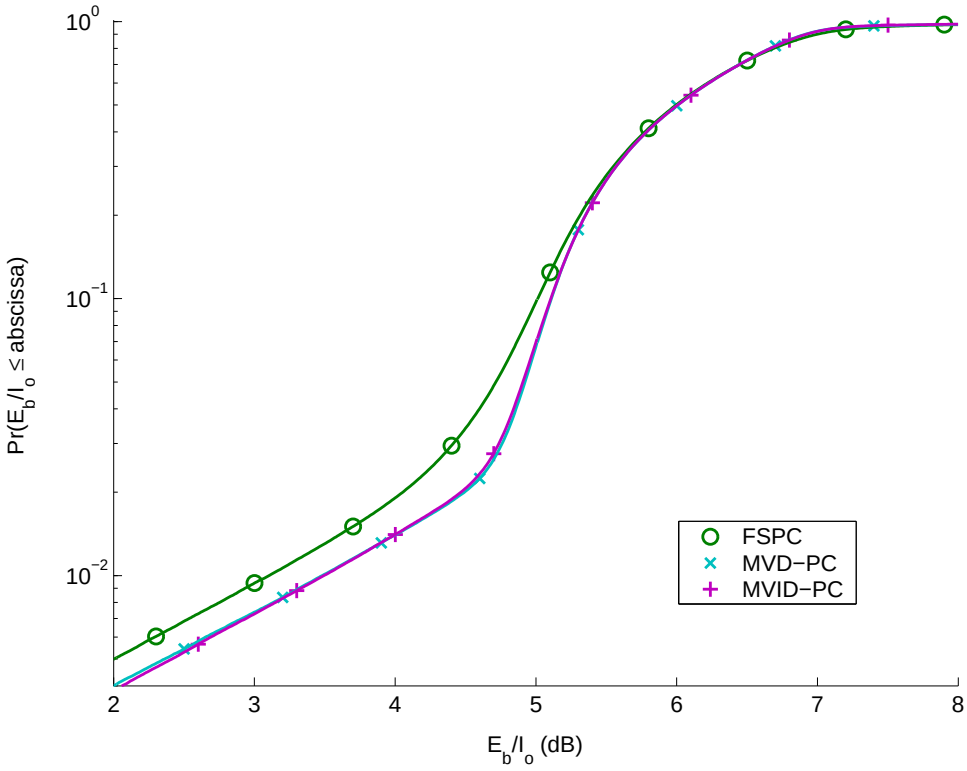

Figure 4.11: Empirical cumulative distribution function (CDF) of E_b/I_o, E_b/I_o target is 6 dB, loop delay 1 T_{PC}, 1-bit PC commands (decision feedback).

In Figure 4.11 the same simulation is done, this time using the decision feedback versions of the algorithms. The reference algorithm in this case is the FSPC algorithm. It is seen that in the DFB case, both the variances and the tails of the distributions are smaller with all the proposed algorithms in comparison with the FSPC algorithm. The performances of the MV- and MVI-PC algorithms are very similar. Note that the MVID-PC algorithm performs much better compared to the MVD-PC than it does in the IFB form.

Figure 4.12 shows the simulation results with a loop delay of two PC periods in the case of information feedback. As discussed in Section 4.2.1, the loop delay of one PC period can be achieved only if the mobile is relatively close to the base station, which makes the performance evaluation at longer loop delays very relevant.

It is seen that the DCPC algorithm is unstable with longer loop delays. This result is in accordance with those presented in [77]. However, the DCPC with time delay compensation (DPC) works well. The MV-PC achieves good performance, but the the performance of the MVI-PC suffers considerably from the increased loop delay.

Figure 4.13 shows the two-PC-period-loop-delay case with decision feedback. Similar results are observable in the figure as in the one-PC-period-loop-delay case, but the E_b/I_o gains are

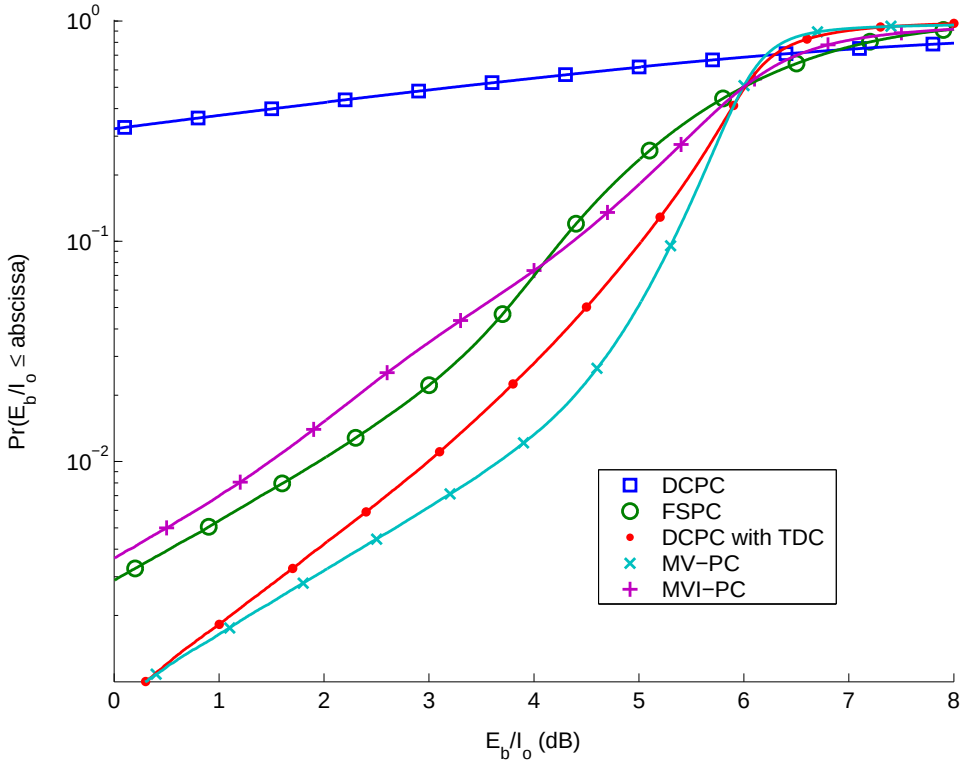

Figure 4.12: Empirical cumulative distribution function (CDF) of E_b/I_o, E_b/I_o target is 6 dB, loop delay 2 T_{PC}, unconstrained PC commands (information feedback).

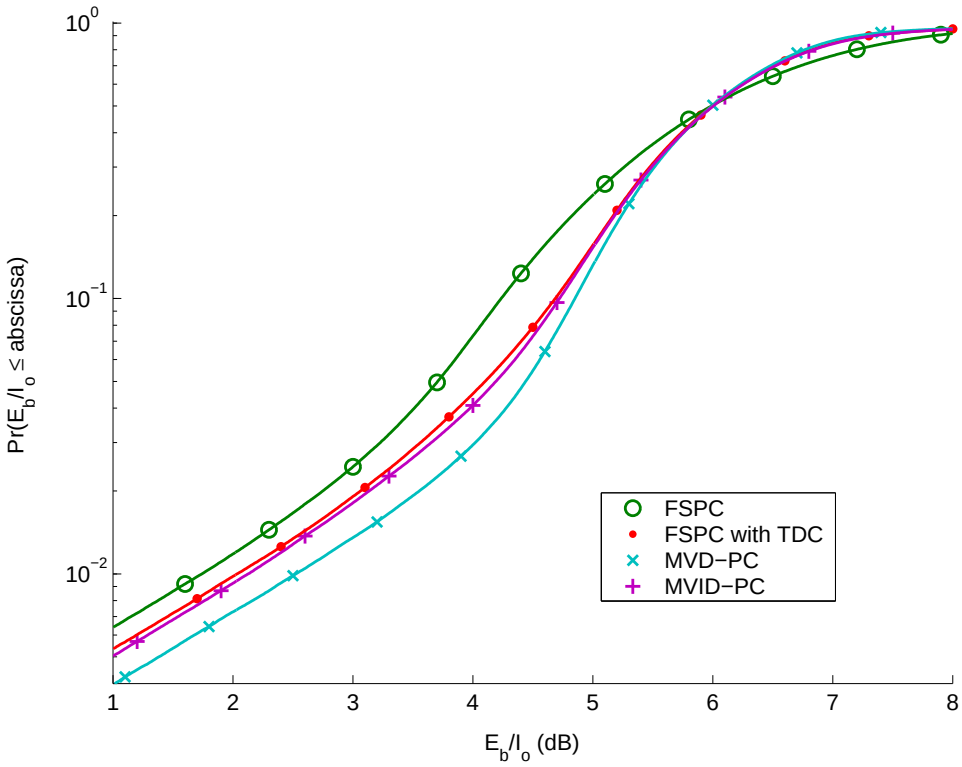

Figure 4.13: Empirical cumulative distribution function (CDF) of E_b/I_o, E_b/I_o target is 6 dB, loop delay 2 T_{PC}, 1-bit PC commands (decision feedback).

higher. The performance of the MVID-PC suffers also in this case from the increased loop delay, but gives still a gain of 0.38 dB 2-% probability level compared to the FSPC algorithm. All the proposed algorithms outperform the FSPC with TDC algorithm.

4.8 Generalized minimum variance (GMV) approach

One problem with the MV controller is that the cost function does not have a penalty for the control signal $u(t)$. In fact, if the process is nonminimum-phase, the control signal will grow unbounded, leading to numerical errors and overflows if implemented in a digital computer. The GMV controller is a modification of the MV controller, that allows also the control of nonminimum-phase processes and more sophisticated way of including a non-constant reference signal [151, 150]. The objective function is modified to include the reference signal and the control signal, which is thus penalized in the objective function. Define

$$\phi_{\text{O}}(t+k) = Py(t+k) + Qu(t) - Rr(t) \tag{4.42}$$

where P, Q and R are polynomials in q^{-1} with orders n_p, n_q and n_r, respectively. The GMV objective function is then

$$J_{\text{GMV}} = E\left\{\phi_{\text{O}}^2(t+k)\right\} \tag{4.43}$$

The polynomials in (4.42) can be selected to suit a particular application.

4.8.1 Control law

The GMV controller derivation is somewhat similar to the derivation of the MV controller, and is not described here in detail. A detailed derivation can be found from e.g. [151, 136]. The Diophantine equation for the GMV controller is

$$PC = LA + q^{-k}G \tag{4.44}$$

where

$$\left.\begin{aligned} L &= 1 + l_1 q^{-1} + \ldots + l_{k-1} q^{-(k-1)} \\ G &= g_0 + g_1 q^{-1} + \ldots + g_{n_g} q^{-n_g} \\ n_g &= \max\left(n_a - 1, n_p + n_c - k\right) \end{aligned}\right\} \tag{4.45}$$

The GMV controller that minimizes (4.43) is

$$Fu(t) + Gy(t) + Hr(t) = 0 \tag{4.46}$$

where

$$F = BL + QC \tag{4.47}$$

$$H = -CR \tag{4.48}$$

Substituting (4.46) into the process equation (4.9) yields the closed-loop equation

$$y(t) = \frac{q^{-k}BR}{PB + QA} r(t) + \frac{BL + QC}{PB + QA}\xi(t) \tag{4.49}$$

Thus the closed-loop poles are located at the zeroes of $PB + QA$. For zero steady-state tracking error the following condition must be satisfied:

$$\left.\frac{B(q^{-1})R(q^{-1})}{P(q^{-1})B(q^{-1}) + Q(q^{-1})A(q^{-1})}\right|_{q=1} = 1 \tag{4.50}$$

This is usually done by choosing

$$R = P(1) \quad \text{and} \quad Q(1) = 0 \tag{4.51}$$

Note that (4.51) requires that $(1 - q^{-1})$ is a factor of Q. In this case the GMV controller is referred to as *incremental GMV* or *GMVI*.

4.8.2 Properties of the GMV controller

The cost function (4.43) is the variance of a combination of the filtered output of the process, filtered reference signal, and filtered control signal. The role of Q is to penalize the control command so that it cannot grow without limit. However, the more the control signal is penalized, the greater will be the resulting output variance. Hence a compromise must be made between output variance minimization and the stability of the controller.

4.8.3 A direct form self-tuning GMV controller

It can easily be shown [151], that

$$\phi_{\mathrm{O}}(t+k) = \frac{1}{C}\left[Fu(t) + Gy(t) + Hr(t)\right] + L\xi(t+k) \tag{4.52}$$

and, under GMV control (4.46),

$$\phi_{\mathrm{O}}(t) = L\xi(t) \tag{4.53}$$

in the closed loop. A direct form adaptive controller can be then formed as follows.

1. Form the pseudo-output $\phi_{\mathrm{O}}(t) = Py(t) + Qu(t-k) - Rr(t-k)$.
2. Estimate $\hat{F}$, $\hat{G}$, $\hat{H}$ from

$$\phi_{\mathrm{O}}(t) = \hat{F}u(t-k) + \hat{G}y(t-k) + \hat{H}r(t-k) + \hat{\xi}(t) \tag{4.54}$$

3. Apply control $u(t)$ using

$$\hat{F}u(t) = -\hat{G}y(t) - \hat{H}r(t) \tag{4.55}$$

4. Set $t = t+1$ and go back to step 1.

This approach eliminates the need to estimate the C polynomial even if it is present. It is in fact estimated as a factor of $H(= -RC)$. However, there is no guarantee that the parameters converge to the correct values [151]. Also, in the simulation studies, it was shown that the performance of the direct form is similar or worse than that of the indirect form when employed in the proposed algorithms. Therefore, the direct form is not used in this thesis.

4.8.4 Self-tuning generalized minimum variance based power control algorithms

Four algorithms based on the GMV controller are considered that differ from each other by whether IFB or DFB is employed and whether incremental or nonincremental GMV controllers are used. The nonincremental algorithms are:

- the *generalized minimum variance power control* (GMV-PC),
- the *generalized minimum variance decision feedback power control* (GMVD-PC), and

The incremental algorithms are accordingly called GMVI-PC, and GMVID-PC. A backup controller is also included as with the minimum variance based algorithms.

As with the minimum variance controller approach, the command quantization into two levels (decision feedback) modifies the GMV control law. Thus the control law (4.46) is replaced by the following equations:

$$\tilde{u}(t) = \frac{1}{f_0}\left[-Gy(t) - Hr(t) + (f_0 - F)u(t)\right] \tag{4.56}$$

$$u(t) = \text{sign}\left(\tilde{u}(t)\right) \tag{4.57}$$

The algorithms are given in Appendix D.

4.8.5 Simulation results

Simulation results are again obtained using using the radio network simulator described in Appendix A with $v_{\min} = 0$ km/h, $v_{\max} = 30$ km/h, $(n_a, n_b, n_c) = (2, 1, 0)$ and $(\delta_e, \delta_u) = (3, 3)$. The polynomials of the GMV controller were selected as $P(q^{-1}) = R(q^{-1}) = 1$, and $Q(q^{-1}) = w_q$ for nonincremental algorithms and $Q(q^{-1}) = w_q\Delta$ for incremental algorithms, where w_q is a constant.

Figures 4.14 through 4.17 show the variances of the power control command (before the relay/quantizer for the DFB algorithms) and the power control misadjustment against the weight constant w_q of the command penalty polynomial $Q(q^{-1})$ for a selected user with 5 km/h speed. For comparison, the results are shown also for the MV-PC and MVD-PC algorithms. It is seen that the weighting helps to reduce the variance of the PC command before relay. Also the variance of the power control misadjustment is reduced, but the difference to the MV-based algorithms is quite small. Indeed, in the network performance simulations, no significant differences were observed between the MV and GMV based algorithms (see also Tables 4.2 and 4.3 in the end of this Chapter).

4.9 Generalized predictive control (GPC) approach

The MV and GMV controllers suffer from high sensitivity to the time delay estimation of the process. If the delay is known exactly, then the MV and GMV controllers perform well, as already seen. However, if the delay is not known, or incorrectly estimated, the performance of MV and GMV controllers becomes very poor.

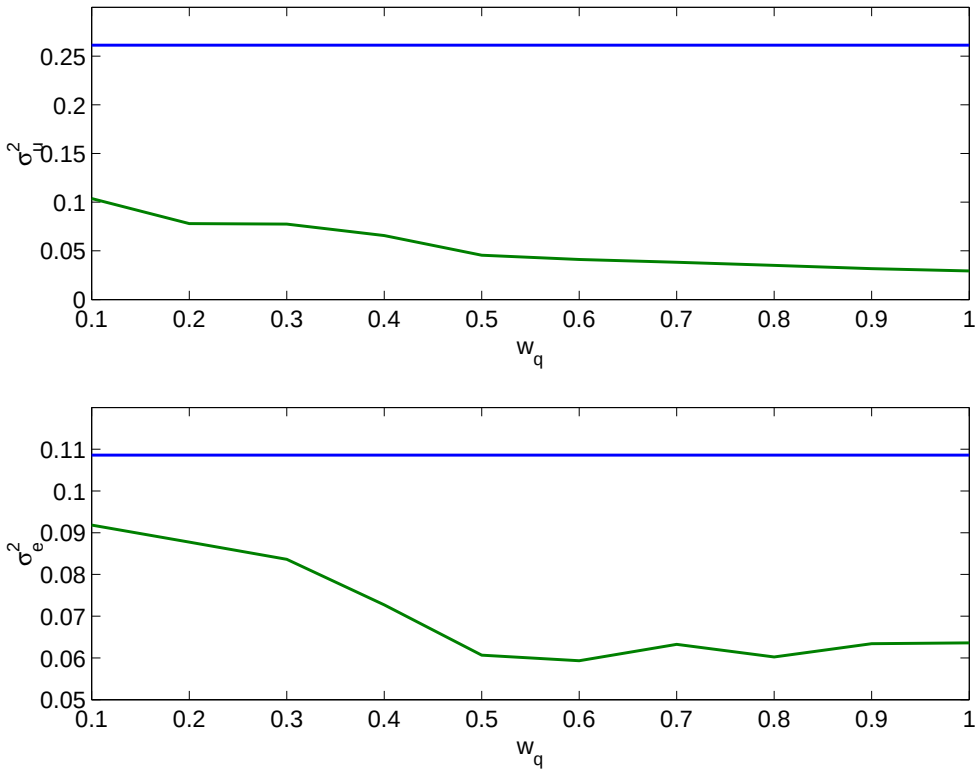

Figure 4.14: Variances of power control command $u(t)$ and power control misadjustment $e(t)$ with varying penalty factor, GMV-PC. Straight lines are for MV-PC for comparison.

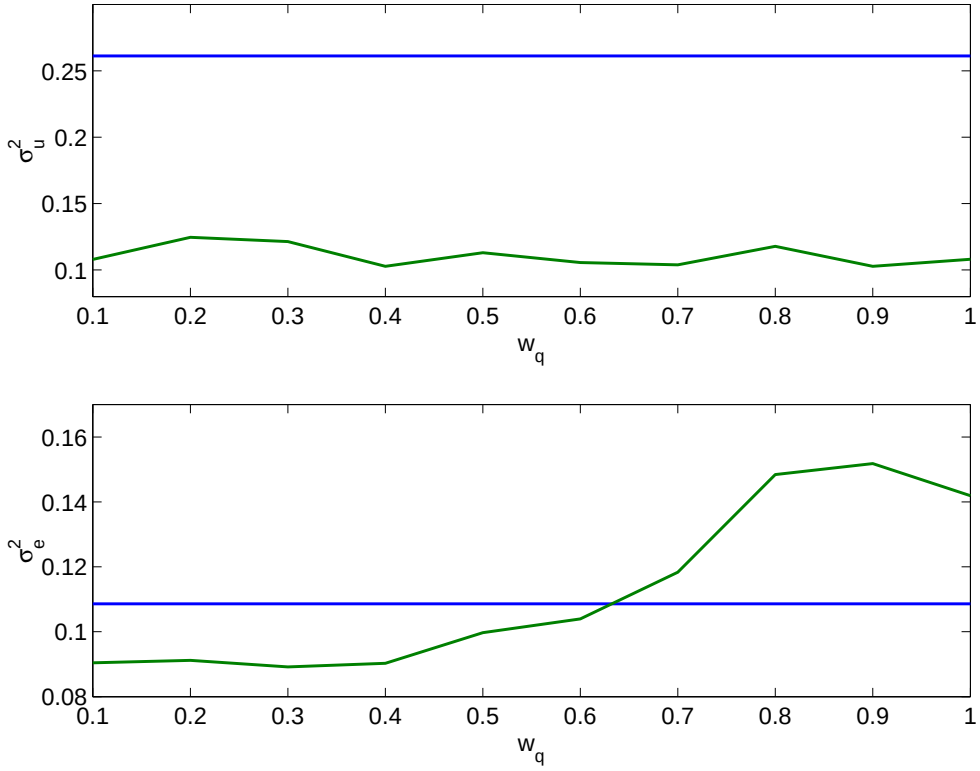

Figure 4.15: Variances of power control command $u(t)$ and power control misadjustment $e(t)$ with varying penalty factor, GMVI-PC. Straight lines are for MV-PC for comparison.

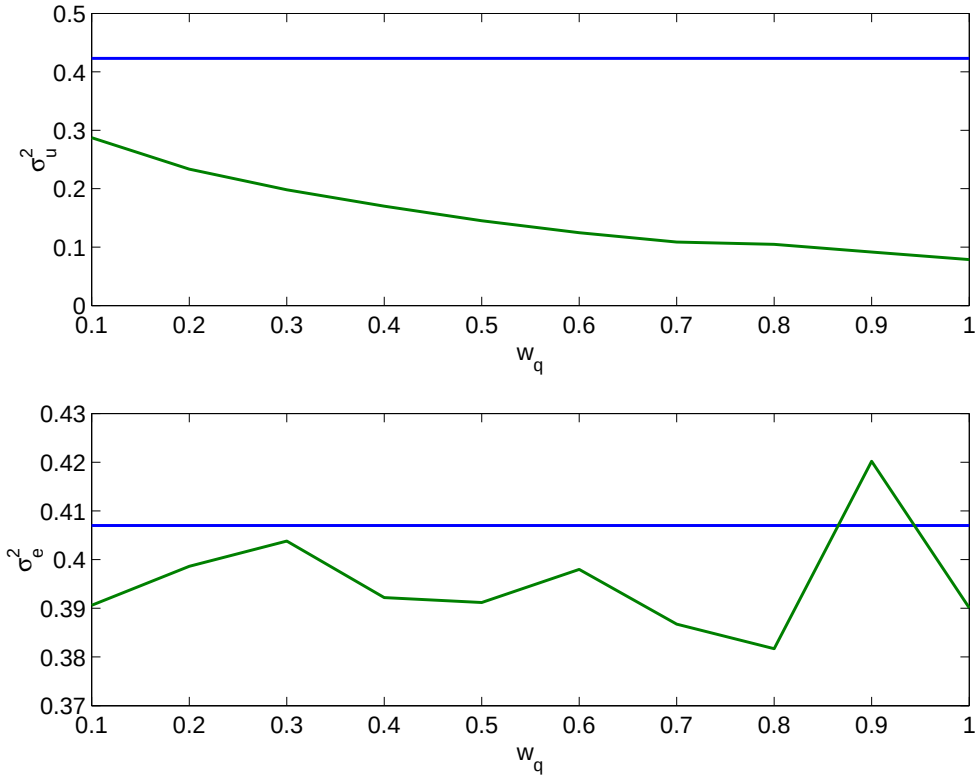

Figure 4.16: Variances of power control command $u(t)$ and power control misadjustment $e(t)$ with varying penalty factor, GMVD-PC. Straight lines are for MVD-PC for comparison.

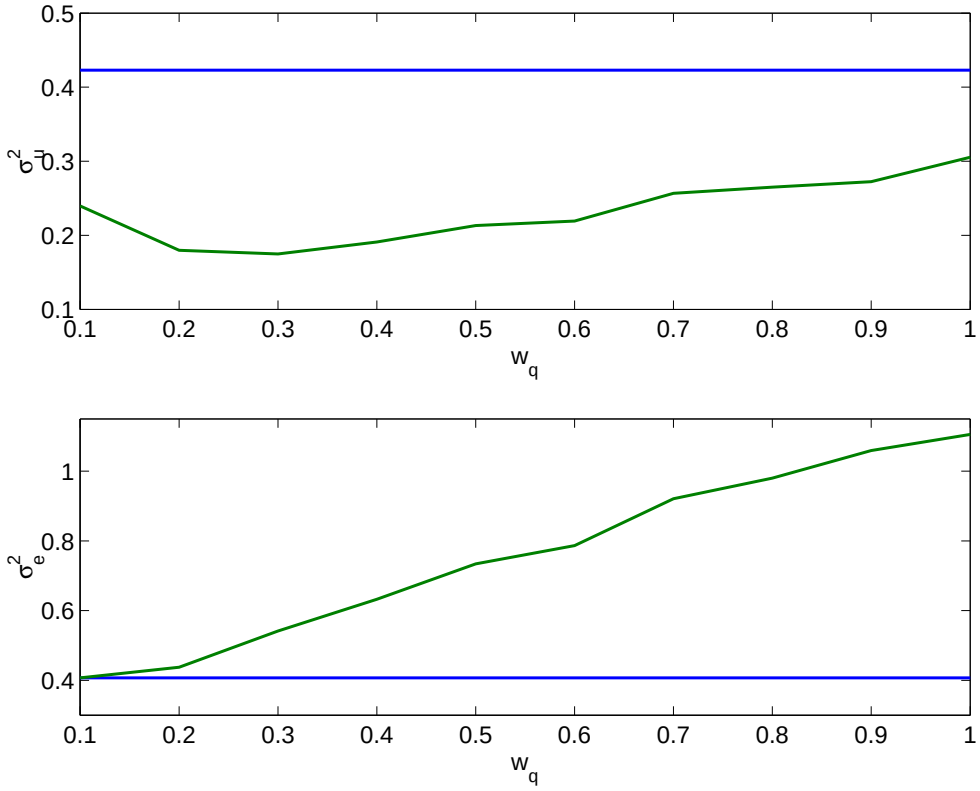

Figure 4.17: Variances of power control command $u(t)$ and power control misadjustment $e(t)$ with varying penalty factor, GMVID-PC. Straight lines are for MVD-PC for comparison.

As discussed in Section 4.2.1, the loop delay is in principle known in cellular communication systems due to the standardized frame structure. However, if the delay is very close to slot boundary, it may happen that due to variations in the processing delays, there are uncertainties in the estimation of the loop delay.

To improve the robustness of the proposed algorithms, the use of the Generalized Predictive Controller is proposed. Generalized predictive control was proposed in [145] to overcome the unknown delay and other robustness problems. It has since then gained popularity both in industry and academia. It has been successfully applied in many industrial processes [146, 144], and has shown good performance and robustness with respect to overparametrization or poorly known delays.

The basic idea of GPC is to calculate a sequence of future control signals in such a way that it minimizes a multistage cost function defined over a prediction horizon. Thus, instead of calculating one k-step ahead prediction and a single control signal as in the MV and GMV methods, a set of future predictions and a sequence of control signals are calculated at each time iteration.

The GPC formulation begins with an ARIMAX or ARIX model of the process, that is, equations (4.11) and (4.12), rewritten here for convenience:

$$\text{ARIMAX}: \qquad Ay(t) = Bu(t-k) + \frac{C}{\Delta}\xi(t) \tag{4.58}$$

$$\text{ARIX}: \qquad Ay(t) = Bu(t-k) + \frac{\xi(t)}{\Delta} \tag{4.59}$$

Since only the ARIX model is used in the simulations, only the formulation based on this assumption is presented here. The colored noise case can be found from [144].

The cost function is

$$\begin{aligned} &J_{\text{GPC}}(N_1, N_2, N_u) = \\ &E\left\{ \sum_{j=N_1}^{N_2} \delta(j) \left[\hat{y}(t+j|\, t) - w(t+j)\right]^2 + \sum_{j=1}^{N_u} \lambda(j) \left[\Delta u(t+j-1)\right]^2 \right\} \end{aligned} \tag{4.60}$$

where $\hat{y}(t+j|\, t)$ is an optimum j-step ahead prediction of the system output based on data up to time t, N_1 and N_2 are the minimum and maximum output (or costing) horizons, N_u is the control horizon, $\delta(j)$ and $\lambda(j)$ are weighting sequences and $w(t+j)$ is the future reference trajectory, which can be calculated as

$$w(t) = y(t); \quad w(t+j) = \alpha w(t+j-1) + (1-\alpha) r(t+j), \quad j = 1 \ldots N \tag{4.61}$$

where $\alpha \in [0, 1]$ is a selectable parameter that controls the smoothness of the approximation from the actual system output towards the known reference, and thus influences the dynamic response

of the system. In the original formulation [145] $\delta(j)$ is considered to be 1 and $\lambda(j)$ is considered to be constant.

As already mentioned, the idea of GPC is to calculate a sequence of future control signals $u(t), u(t+1), \ldots$ in such a way that the future output of the system $y(t+j)$ is driven close to $w(t+j)$. This is accomplished by minimizing $J_{\text{GPC}}(N_1, N_2, N_u)$.

4.9.1 Control law

To minimize the GPC cost function $J_{\text{GPC}}(N_1, N_2, N_u)$, one needs to calculate the optimal predictions of $y(t+j)$ for $N_1 \leq j \leq N_2$. To do this, the following Diophantine equation is employed:

$$1 = E_j A\Delta + q^{-j} F_j \tag{4.62}$$

where E_j and F_j are polynomials with degrees $j-1$ and n_a, respectively. They are uniquely defined given A and the prediction interval j. Multiplying (4.59) by $E_j \Delta q^j$ and substituting for $E_j A\Delta$ from (4.62) one gets

$$y(t+j) = E_j B\Delta u(t+j-k) + F_j y(t) + E_j \xi(t+j) \tag{4.63}$$

As E_j is of degree $j-1$ the noise components are all in the future. Thus the optimal predictor of $y(t+j)$ is

$$\hat{y}(t+j|\, t) = G_j \Delta u(t+j-k) + F_j y(t) \tag{4.64}$$

where $G_j = E_j B$.

The polynomials

$$\begin{aligned} E_j &= e_{j,0} + e_{j,1} q^{-1} + \ldots + e_{j,j-1} q^{-(j-1)} \\ F_j &= f_{j,0} + f_{j,1} q^{-1} + \ldots + f_{j,n_a} q^{-n_a} \end{aligned} \tag{4.65}$$

can be calculated recursively as follows:

$$\begin{aligned} &E_1 = 1 \\ &F_1 = q^j (1 - \Delta A) \\ &E_{j+1} = E_j + f_{j,0}\, q^{-j} \\ &f_{j+1,i} = f_{j,i+1} - f_{j,0} \tilde{a}_{i+1} \quad ; \quad i = 0 \ldots n_a - 1 \end{aligned} \tag{4.66}$$

where $\tilde{a}_i$ denotes the coefficient of the ith term in the polynomial ΔA. From this, the polynomial G_j can be obtained recursively as

$$G_{j+1} = E_{j+1} B = \left(E_j + f_{j,0} q^{-j}\right) B = G_j + f_{j,0} q^{-j} B \tag{4.67}$$

so the first j coefficients of G_{j+1} are identical to those of G_j and the remaining coefficients are given by $g_{j+1,j+i} = g_{j,j+i} + f_{j,0} b_i \quad ; \quad i = 0 \ldots n_b$.

Since the control signal $u(t)$ influences the system output after k sampling periods, the values N_1, N_2 and N_u defining the horizons in $J_{\text{GPC}}(N_1, N_2, N_u)$ can be defined as

$$\begin{aligned} N_1 &= k \\ N_2 &= k + N - 1 \\ N_u &= N \end{aligned} \tag{4.68}$$

where N is the length of the output horizon. Casting equation (4.64) in matrix form, one gets

$$\boldsymbol{y} = \boldsymbol{G}\boldsymbol{u} + \boldsymbol{f} \tag{4.69}$$

where

$$\boldsymbol{y} = \begin{bmatrix} \hat{y}(t+k|\,t) & \hat{y}(t+k+1|\,t) & \dots & \hat{y}(t+k+N-1|\,t) \end{bmatrix}^T \tag{4.70}$$

$$\boldsymbol{u} = \begin{bmatrix} \Delta u(t) & \Delta u(t+1) & \dots & \Delta u(t+N-1) \end{bmatrix}^T \tag{4.71}$$

$$\boldsymbol{G} = \begin{bmatrix} g_0 & 0 & \dots & 0 \\ g_1 & g_0 & \dots & 0 \\ \vdots & \vdots & \ddots & \vdots \\ g_{N-1} & g_{N-2} & \dots & g_0 \end{bmatrix} \tag{4.72}$$

$$\boldsymbol{f} = \begin{bmatrix} F_k y(t) + (G_k - g_0)\, q\Delta u(t-1) \\ F_{k+1} y(t) + (G_{k+1} - g_0 - g_1 q^{-1})\, q^2 \Delta u(t-1) \\ \vdots \\ F_{k+N-1} y(t) + \left(G_{k+N-1} - \sum_{i=0}^{N-1} g_i q^{-i}\right) q^N \Delta u(t-1) \end{bmatrix} \tag{4.73}$$

The control law is designed to minimize $J_{\text{GPC}}(N_1, N_2, N_u)$, which can be written in matrix form as (assuming $\delta(j) = 1$ and $\lambda(j) = \lambda$)

$$J_{\text{GPC}} = (\boldsymbol{G}\boldsymbol{u} + \boldsymbol{f} - \boldsymbol{w})^T (\boldsymbol{G}\boldsymbol{u} + \boldsymbol{f} - \boldsymbol{w}) + \lambda \boldsymbol{u}^T \boldsymbol{u} \tag{4.74}$$

where

$$\boldsymbol{w} = \begin{bmatrix} w(t+k) & w(t+k+1) & \dots & w(t+k+N-1) \end{bmatrix}^T \tag{4.75}$$

The minimization of (4.74) with respect to $\boldsymbol{u}$ yields

$$\boldsymbol{u} = \left(\boldsymbol{G}^T \boldsymbol{G} + \lambda \boldsymbol{I}\right)^{-1} \boldsymbol{G}^T (\boldsymbol{w} - \boldsymbol{f}) \tag{4.76}$$

and from (4.71)

$$\Delta u(t) = \begin{bmatrix} 1 & 0 & \dots & 0 \end{bmatrix} \boldsymbol{u} \tag{4.77}$$

Thus only the first element of the vector $\boldsymbol{u}$ is actually used at each iteration.

To reduce the computational burden involved in the N by N matrix inversion in (4.76), the control horizon N_u can be selected so that $N_u < N$, where it is assumed that the projected control signals are going to be zero after $N_u < N$ samples. In this case $\boldsymbol{G}$ is replaced with a matrix $\tilde{\boldsymbol{G}}$ formed by taking the first N_u columns of $\boldsymbol{G}$. Then $\tilde{\boldsymbol{G}}$ is used instead of $\boldsymbol{G}$ in (4.76), i.e.,

$$\boldsymbol{u} = \left(\tilde{\boldsymbol{G}}^T \tilde{\boldsymbol{G}} + \lambda \boldsymbol{I}\right)^{-1} \tilde{\boldsymbol{G}}^T (\boldsymbol{w} - \boldsymbol{f}) \tag{4.78}$$

Thus the calculation of the control command involves the inversion of only an N_u by N_u matrix.

4.9.2 Properties of the GPC method

The GPC method can deal with unstable and nonminimum-phase processes, and provides weighting of the control increments in the cost function. Also, unlike the GMV method, GPC can be used for nonminimum-phase processes even if the control weighting is not used in the cost function (i.e., $\lambda = 0$).

The coefficients $g_0, \ldots, g_{N-1}$, i.e., the first column of $\boldsymbol{G}$ in (4.72), are equal to the first N samples of the step response of the system, when a unit step is applied to the control input $u(t)$. This can be easily seen from (4.69) assuming that the initial conditions are zero [144]. The step response of the system has been utilized to develop direct form adaptive GPC algorithms, see [154] and the references therein. This is, however, not very useful for the power control problem, since it would require the step response of the power control process to be known or estimated, which would be very difficult due to the rapid changes in the radio propagation channel and interference. Hence an indirect form adaptive algorithm is used in this thesis.

There was originally lack of theoretical results about the properties of predictive control regarding e.g. stability and robustness, and the majority of the stability results are limited to the infinite horizon case. There exist a number of variations of the GPC formulation that allow stability and robustness results to be obtained for small horizons. More information of these can be found from [144].

4.9.2.1 Choice of the output and control horizons

In [145, 144] some instructions for choosing the horizons of the cost function (4.60) are given. As mentioned earlier, since the control signal $u(t)$ influences the output of the system only after k samples, there is no point in selecting N_1 to be less than k. On the other hand, if N_1 is selected to be greater than k, the first points in the reference sequence, being the ones guessed with most certainty, will not be taken into account. Since the GPC controller is here used for the cases when there might be uncertainties in the loop delay, $k = 1$ is the safest choice.

The maximum prediction horizon N_2 should at least exceed $k + n_b$, but in practice it is suggested to use a larger value, corresponding more closely to the rise-time of the system.

The control horizon N_u defines the active time of the control signal. Selecting $N_u = 1$ gives generally acceptable control for simple systems. In this case the matrix inversion in (4.78) reduces to scalar computation. Increasing N_u makes the control signal to be active a longer time, which can be more appropriate for more complex systems.

4.9.3 Generalized predictive control based power control algorithms

The GPC based power control algorithms are now described. Four such algorithms are considered, two with information feedback and two with decision feedback:

- the *generalized predictive power control* (GPC-PC),
- the *generalized predictive decision feedback power control* (GPCD-PC),
- the *generalized predictive incremental power control* (GPCI-PC) and
- the *generalized predictive incremental decision feedback power control* (GPCID-PC)

The latter two are the incremental versions of the first two, as described later. A backup controller is again included as with the minimum variance based algorithms. The algorithms are given in Appendix D. Certain aspects of the algorithms are described in the following.

4.9.3.1 Modifications for feedback signals

The output of the GPC controller is the control increment $\Delta u(t)$, and the actual control signal is then calculated as $u(t) = u(t-1) + \Delta u(t)$, and transmitted as the power control command in the information feedback case. Also another case is considered, where the control *increment* $\Delta u(t)$ is transmitted as the power control command. This is motivated by the fact that the mobile unit, where the command is applied, contains an integrator (see Fig. 3.3). These two feedback methods are summarized in the following.

Information feedback method 1 (IFM1):

Signal $u(t)$ is transmitted as the power control command.

$\diamondsuit$

This method is used in the GPC-PC algorithm described below.

Information feedback method 2 (IFM2):

Signal $\Delta u(t)$ is transmitted as the power control command.

$\diamondsuit$

This method is used in the GPCI-PC algorithm described below.

In [155] the authors proposed a way to modify the GPC method for decision feedback. They utilize the fact that the control horizon N_u is usually quite small in practice (say, 1 to 3), and hence the number of all possible realizations of vector $\boldsymbol{u}$, 2^{N_u}, is small enough so that an exhaustive search for finding the vector $\boldsymbol{u}$ that minimizes (4.74) is feasible. For reference, this method is hereinafter called the *Optimal decision feedback method* (ODFM).

A different method, similar to that in Section 4.7.3.2, is proposed here for modifying the GPC method for decision feedback. It is based on only quantizing the current control output, and feeding relevant signal back to the controller. Thus, the exhaustive search of the method in [155] is avoided. The proposed method is presented for the two considered feedback cases in the following.

Decision feedback method 1 (DFM1):

In the case of decision feedback the control law is modified in such a way that the decisions of the control signal values are fed back to the control equations and parameter estimation. Thus, (4.77) is replaced by the following equations:

$$\Delta\tilde{u}(t) = [1 \quad 0 \quad \dots \quad 0]\,\boldsymbol{u} \tag{4.79}$$

$$u(t) = \text{sign}\,(u(t-1) + \Delta\tilde{u}(t)) \tag{4.80}$$

$$\Delta u(t) = u(t) - u(t-1) \tag{4.81}$$

Signal $u(t)$ is transmitted as the power control command.

$\diamondsuit$

This method is used in the GPCD-PC algorithm. The modification is illustrated in Fig. 4.18.

Decision feedback method 2 (DFM2):

In the case of decision feedback, equation (4.77) is replaced by (4.79) and

$$\Delta u(t) = \text{sign}\,(\Delta\tilde{u}(t)) \tag{4.82}$$

Signal $\Delta u(t)$ is transmitted as the power control command.

$\diamondsuit$

This method is used in the GPCID-PC algorithm.

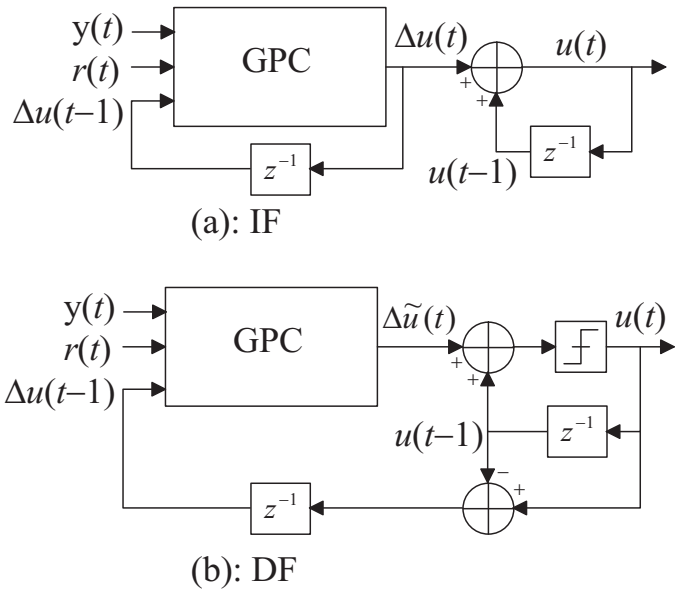

Figure 4.18: (a) Standard GPC control system (information feedback), (b) Modified GPC control system (decision feedback).

Table 4.1: Parameters used for the proposed algorithms in the simulations.

(n_a, n_b, n_c)	(δ_e, δ_u)	λ	(N, N_u)	α
$(2, 2, 0)$	$(3, 3)$	0.1	$(10, 3)$	0.1

4.9.4 Simulation results

Simulation results are again obtained using using the radio network simulator described in Appendix A with $v_{\min} = 0$ km/h, $v_{\max} = 30$ km/h.

Table 4.1 summarizes the parameters used for the algorithms in the simulations.

Fig. 4.19 shows the SIR target tracking performance with various PC algorithms in a simulation where one user – initially connected to the central cell – is randomly selected for observation. The same simulation is repeated with the algorithms in both IFB (first four) and DFB (last four) cases. The velocity of the observed user is set to 5 km/h, which is slow enough for tracking fast fading. The loop delay and SIR target of the observed user were varied as explained in the caption of Fig. 4.19, while the user all the time assumes a loop delay of 1 PC period ($k = 1$). It is seen that the proposed GPCI-PC and GPCDI-PC are able to maintain small variance of the SIR in both IFB and DFB cases. The GPC-PC and GPCD-PC algorithms have significantly more troubles with the changes in the loop delay. The DCPC algorithm is known to be unstable when the loop delay is greater than 1 PC period, which is also shown in the results. The MV-PC and MVD-PC

algorithms operate mainly with the backup controller when the actual loop delay is different from the assumed one. With the FSPC algorithm the variance of the SIR increases significantly when the loop delay increases, as indicated by equation (4.1).

Figures 4.20 and 4.21 show the simulated CDF results in the case that the loop delay equals two PC periods, but the algorithms assume that $k = 1$. It is seen that while the performance of the MV- and GMV-based algorithms is seriously degraded due to the incorrect delay assumption, the GPC-based algorithms still give considerable gain compared to the reference algorithms. The DCPC algorithm is unstable as observed already in the previous section. The gains of the proposed IFB algorithms (GPC-PC and GPCI-PC) compared to the FSPC algorithm at the 2-% probability level are about 1.36 dB and 1.46 dB, respectively, and for the DFB algorithms (GPCD-PC and GPCDI-PC) about 0.83 and 0.75, respectively.

4.9.4.1 About the DFB methods for GPC-based algorithms

Section 4.9.3.1 described an optimal decision feedback method (ODFM) for modifying the GPC-based algorithms for decision feedback. This method is compared to the proposed DFM2 method (GPCID-PC algorithm) in Fig. 4.22 in the cases of no additional loop delay ($n = 0$) and 1-sample additional loop delay ($n = 1$). The GPC-based algorithm employing ODFM is called the GPCIDO-PC algorithm in the Figure. No significant differences are found between these two methods.

4.10 Discussion

The relative E_b/I_o gains of the algorithms at the 2-% probability level are summarized in Tables 4.2 and 4.3.

It can be concluded that, when the loop delay is known exactly, the simplest ones of the proposed algorithms, the MV-PC and MVD-PC, give very attractive performance. The MVI-PC and MVID-PC are based on a modification of the original MV formulation that compromises the minimum variance objective, which shows also in the results. The GMV-based algorithms did not give additional performance gains in the simulation experiments. Of the GPC-based algorithms, the incremental forms, GPCI-PC and GPCID-PC, perform better than the non-incremental forms. The higher-complexity GPC-based algorithms do not seem to bring any gain over the simpler MV-based algorithms in the case when the loop delay is known, however, the GPC-based algorithms were shown to be able to handle also the situation where the loop delay is incorrectly estimated.

A remarkable feature of the decision feedback versions of the algorithms is that the perfor-

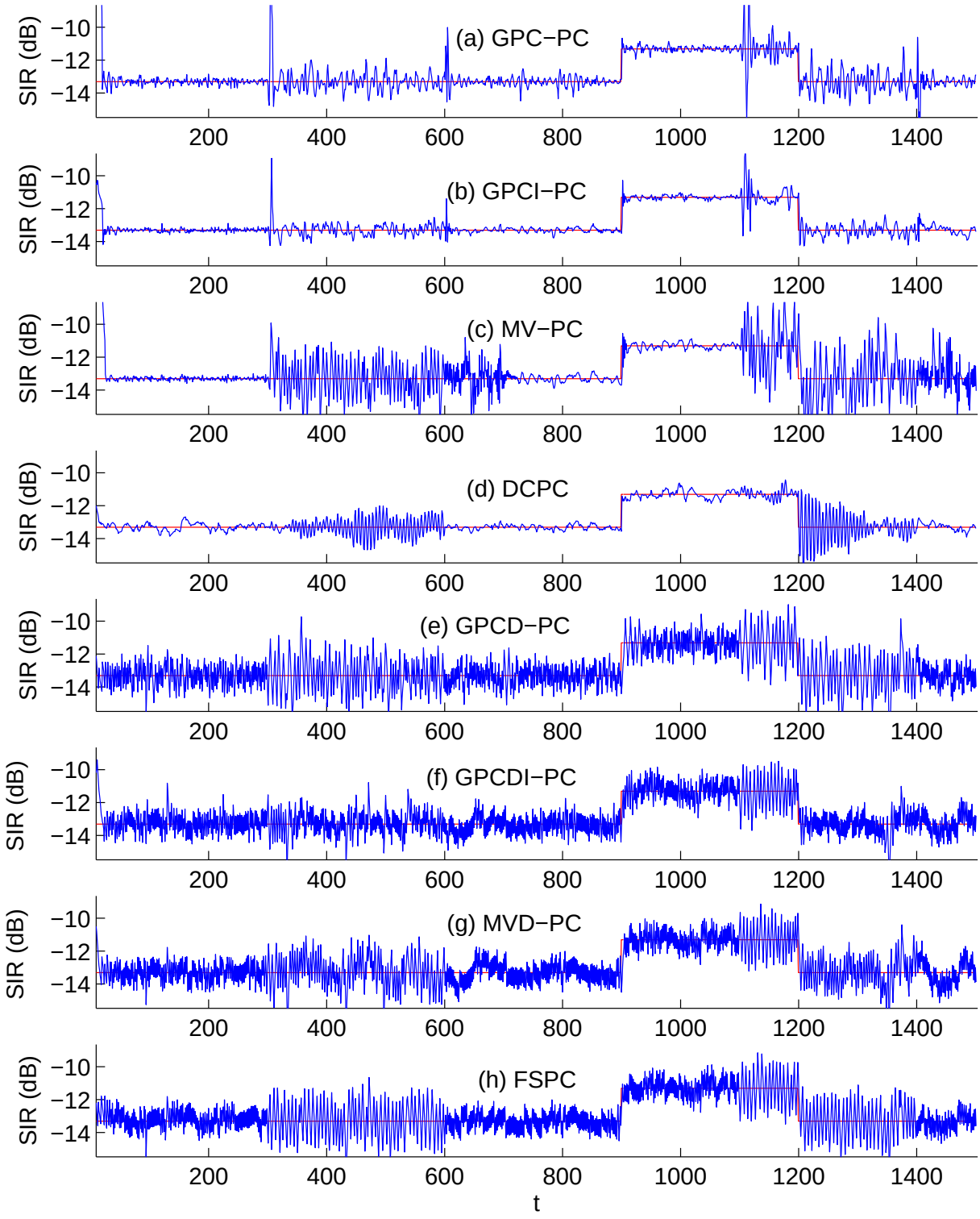

Figure 4.19: Received SIR with various PC algorithms. Loop delay is changed from $k = 1$ to $k = 2$ and back at times $t = 300$ and $t = 600$, respectively, and again at times $t = 1100$ and $t = 1400$. SIR target is raised by 2 dB at time $t = 900$ and lowered by 2 dB at time $t = 1200$.

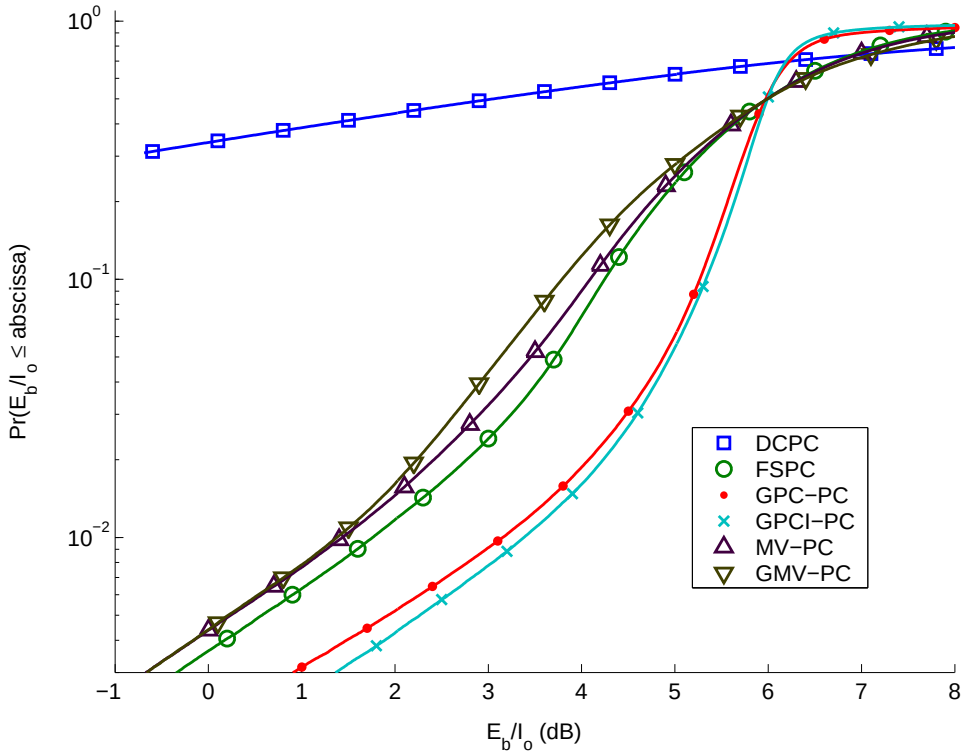

Figure 4.20: Empirical cumulative distribution function (CDF) of E_b/I_o, E_b/I_o target is 6 dB, loop delay 2 T_{PC}, $k = 1$ (wrong delay estimation in the adaptive algorithms), unconstrained PC commands (information feedback).

Table 4.2: E_b/I_o gains of the proposed *information feedback* algorithms at 2-% probability level relative to the reference algorithm (DCPC or FSPC).

PCA	**gain (loop delay $1T_{\text{PC}}$)**	**gain (loop delay $2T_{\text{PC}}$)**
FSPC	−0.76 dB	**0.0 dB**
DCPC	**0.0 dB**	–.–
DCPC with TDC	0.0 dB	0.81 dB
MV-PC	0.53 dB	1.51 dB
MVI-PC	0.17 dB	−0.56 dB
GMV-PC	0.52 dB	1.51 dB
GMVI-PC	0.53 dB	1.53 dB
GPC-PC	0.35 dB	1.33 dB
GPCI-PC	0.26 dB	1.53 dB

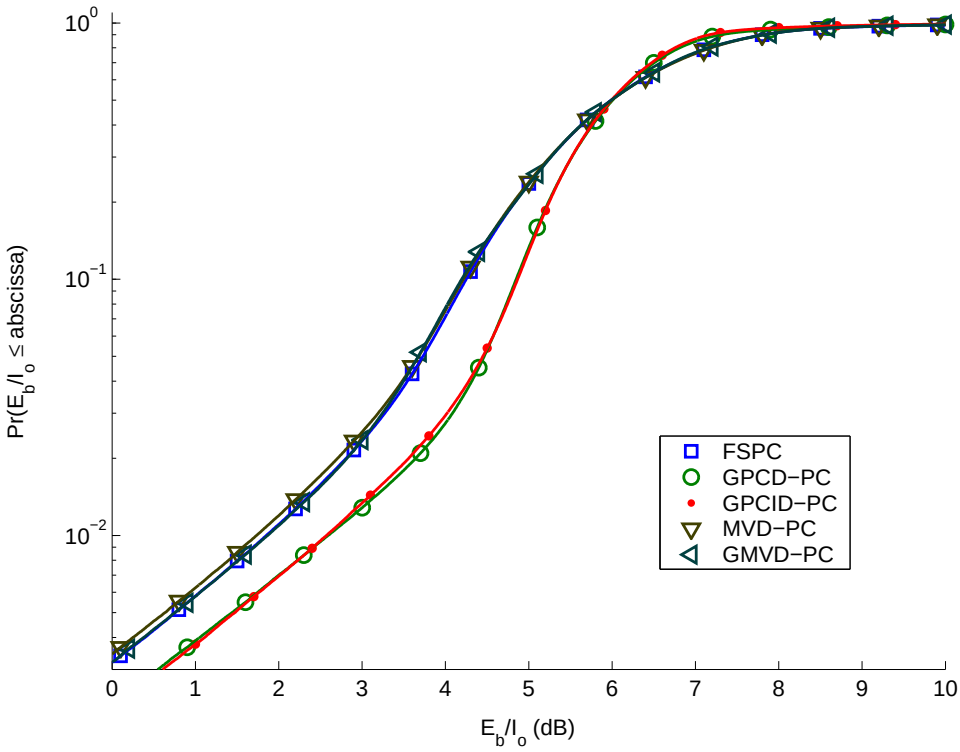

Figure 4.21: Empirical cumulative distribution function (CDF) of E_b/I_o, E_b/I_o target is 6 dB, loop delay 2 T_{PC}, $k = 1$ (wrong delay estimation in the adaptive algorithms), 1-bit PC commands (decision feedback).

Table 4.3: E_b/I_o gains of the proposed *decision feedback* algorithms at 2-% probability level relative to the reference algorithm (FSPC).

PCA	**gain (loop delay 1T_{PC})**	**gain (loop delay 2T_{PC})**
FSPC	**0.0 dB**	**0.0 dB**
FSPC with TDC	0.0 dB	0.31 dB
MVD-PC	0.44 dB	0.80 dB
MVID-PC	0.42 dB	0.38 dB
GMVD-PC	0.43 dB	0.69 dB
GMVID-PC	0.43 dB	0.75 dB
GPCD-PC	0.28 dB	0.85 dB
GPCID-PC	0.40 dB	0.80 dB

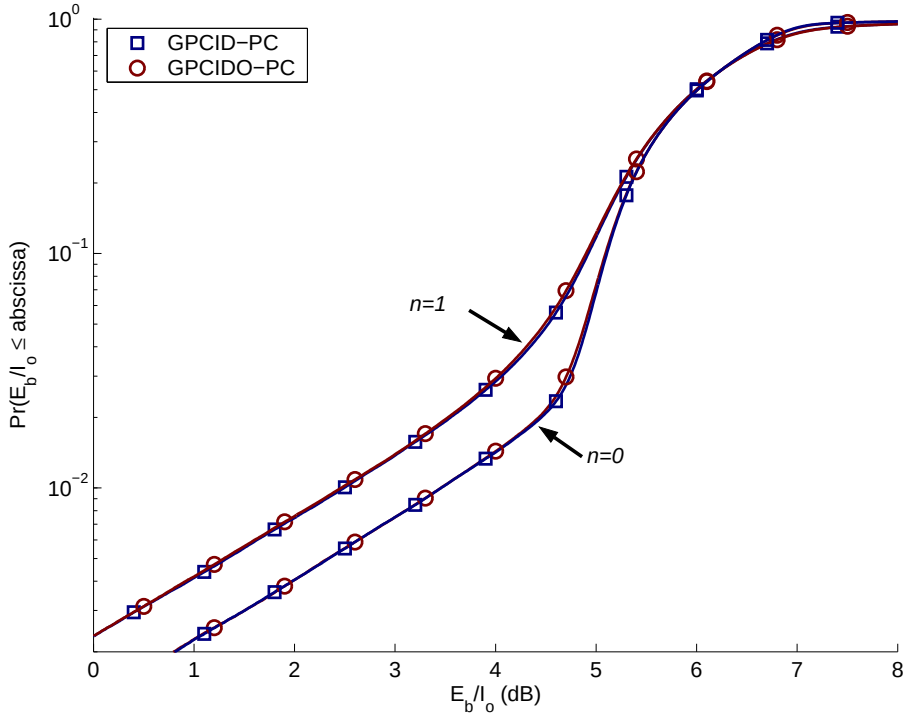

Figure 4.22: Empirical CDF of E_b/I_o, mobile speeds from 0 to 30 km/h.

mance gains can be achieved with zero increase in power control signaling, i.e., only one bit is needed for the power control command that is sent in the feedback channel.

More simulation results are presented in Chapter 7, where the algorithms proposed in this Chapter are combined with the step-size adaptation methods presented in Chapter 6.

Chapter 5

Local loop analysis

5.1 Introduction

The adaptive power control algorithms proposed in this thesis are difficult to analyze due to their highly nonlinear nature. The nonlinearities originate firstly from the complex dependencies between the input and output data of the closed-loop system and the adaptively estimated process/control parameters. Secondly, in the case of decision feedback, the closed-loop system also contains a static nonlinearity, the quantizer (or relay). Linear analysis methods cannot thus be used even if the system/control parameters are assumed to be fixed.

In this chapter the MVD-PC algorithm is analyzed using the *Describing Function* (DF) method. The DF method is well known in the control engineering community. It can be used to analyze certain types of feedback loops that include both linear and nonlinear parts. A thorough treatment of the DF method in continuous time can be found from [156, 157, 158]. The DF analysis has been performed for the conventional Fixed-Step Power Control (FSPC) algorithm in [77].

In order to perform the DF analysis, the MVD-PC algorithm is presented in a simplified form so that the controller parameters are assumed to be fixed, and the inputs to the local loop are assumed to be zero. The results are verified by computer simulations. The results obtained from the analysis match those obtained from simulations, and they give insight in the ways that the MVD-PC algorithm is able to outperform the FSPC algorithm.

5.2 Describing Functions

The describing function (DF) method is now described as in [77]. Consider the system in Fig. 5.1. This feedback system contains a linear transfer function $G(z)$ and a static nonlinearity $f(e)$. The system design objective is to make the output $y(t)$ of the plant $G(z)$ to follow the reference signal

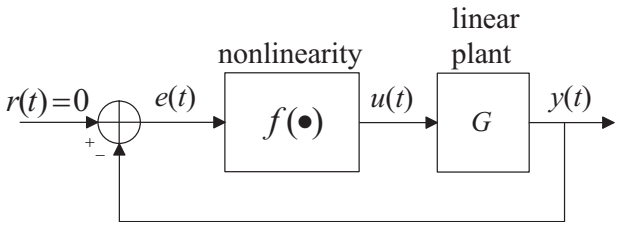

Figure 5.1: A nonlinear system.

$r(t)$.

The development of the describing function starts with the assumption that the input to the nonlinearity is sinusoidal with period N, i.e.

$$e(t) = E\sin(\Omega t) = E\sin\left(\frac{2\pi}{N}t\right), \tag{5.1}$$

where E is the amplitude of the oscillation and $\Omega = 2\pi/N$ is the normalized angular frequency. The signal $u(t) = f(e(t))$ is also periodic with period N, and we may write its Fourier series expansion as

$$\begin{aligned} u(t) = f(E\sin(\Omega t)) = \frac{A_0}{2} + A_1(E,N)\sin(\Omega t + \phi_1(E,N)) + \\ A_2(E,N)\sin(2\Omega t + \phi_2(E,N)) + \dots \end{aligned} \tag{5.2}$$

It is assumed that the constant term is zero, which is the case if the nonlinearity is symmetric with respect to the amplitude of the input.

It is further assumed that the linear system $G(z)$ is sufficiently low-pass with respect to the harmonics in $u(t)$, so that the harmonics in (5.2) can be ignored. With this assumption, we have

$$y(t) \approx A_1(E,N)|G(e^{j\Omega})|\sin(\Omega t + \phi_1(E,N) + \arg(G(e^{j\Omega}))). \tag{5.3}$$

From Fig. 5.1, we also have

$$y(t) = -e(t) = -E\sin(\Omega t) = E\sin(\Omega t + \pi). \tag{5.4}$$

Combining (5.3) and (5.4), an oscillation is predicted if there exists a solution to the following equations

$$A_1(E,N)\left|G\left(e^{j\frac{2\pi}{N}}\right)\right| = E \tag{5.5}$$

$$\phi_1(E,N) + \arg\left(G\left(e^{j\frac{2\pi}{N}}\right)\right) = \pi + 2\pi\nu, \quad \nu \in \mathbf{Z}. \tag{5.6}$$

To find $A_1(E,N)$ and $\phi_1(E,N)$ we can use the complex Fourier series

$$u(t) = \sum_{k=0}^{N-1} C_k(E,N)e^{j\Omega kt}, \tag{5.7}$$

$$C_k^0(E,N) = \frac{1}{N}\sum_{t=0}^{N-1} u(t)e^{-j\Omega kt}. \tag{5.8}$$

By defining the complex number

$$Y_f^0(E,N) = \frac{A_1(E,N)e^{j\phi_1(E,N)}}{E} = \frac{2j}{E}C_1^0(E,N) \tag{5.9}$$

we can combine (5.5) and (5.6) into

$$Y_f^0(E,N)G(e^{j\frac{2\pi}{N}}) = -1. \tag{5.10}$$

The complex number $Y_f^0(E,N)$ is called the *describing function*.

In the above derivation it was assumed that the phase of the input signal to the nonlinearity was zero. Consider the case where the static nonlinearity is a sign-function and the input to it has a small phase shift (less than one sample interval). It can easily be verified that

$$\text{sign}\left(E\sin\left(\Omega(t+a)\right)\right) = \text{sign}\left(E\sin\left(\Omega(t+b)\right)\right) \tag{5.11}$$

for $0 < a \leq b < 1$. Thus, a phase shift of less than one sample interval is a parameter characterizing an oscillation [77]. To take this into account, the describing function is redefined as

$$Y_f(E,N,\delta_e) = \frac{2j}{E}C_1(E,N,\delta_e), \tag{5.12}$$

where

$$\begin{aligned} &C_1(E,N,\delta_e) = \\ &\quad\frac{1}{N}\sum_{t=0}^{N-1} f\left(E\sin\left(\Omega(t+\delta_e)\right)\right)e^{-j(\Omega(t+\delta_e))}, \\ &\qquad\delta_e \in [0,1[. \end{aligned} \tag{5.13}$$

Thus, we look for a solution to

$$Y_f(E,N,\delta_e)G(e^{j\frac{2\pi}{N}}) = -1, \qquad \delta_e \in [0,1[. \tag{5.14}$$

If a solution exists for some (E, N, δ_e) combination, an oscillation is predicted with those parameters.

5.3 DF Analysis of the FSPC algorithm

The DF analysis for the Fixed-Step Power Control (FSPC) algorithm was performed in [77]. The analysis is outlined here to demonstrate the method. In the next subsection the DF analysis is performed for the MVD-PC algorithm.

The FSPC algorithm was introduced in (3.7), and rewritten here for convenience in the same form as in [77]

$$p(t) = p(t-1) + \beta\text{sign}(\gamma^t(t-1) - \gamma(t-1)). \tag{5.15}$$

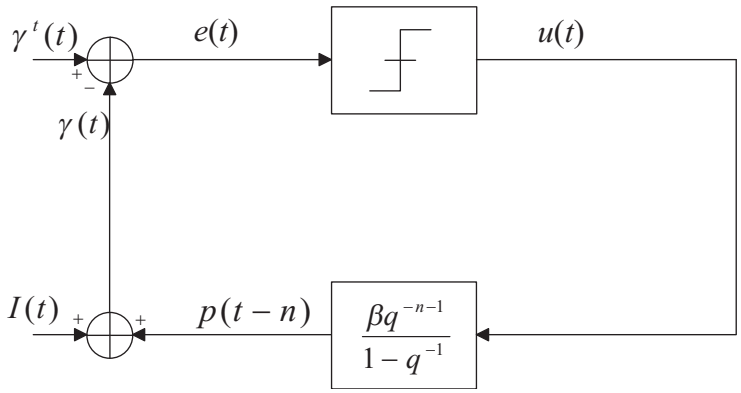

Figure 5.2: The FSPC algorithm.

The block diagram in Fig. 5.2 represents the FSPC algorithm. In Fig. 5.2 n denotes the additional loop delay such that $k = n + 1$. $I(t)$ denotes the difference of channel gain and interference power. The linear part of the block diagram is

$$H(q^{-1}) = \frac{\beta q^{-n-1}}{1 - q^{-1}} \tag{5.16}$$

and, in the frequency domain,

$$H(e^{-j\frac{2\pi}{N}}) = \frac{\beta}{2\sin(\pi/N)} e^{-j(\frac{\pi}{2}+\frac{\pi}{N}+\frac{2\pi}{N}n)} \tag{5.17}$$

The describing function of a relay can be written as [77]

$$Y_f(E, N, \delta_e) = \frac{4}{NE\sin(\frac{\pi}{N})} e^{j\left(\frac{\pi}{N}-\delta_e\frac{2\pi}{N}\right)}. \tag{5.18}$$

Thus, we seek for a solution to

$$Y_f(E, N, \delta_e) H(e^{-j\frac{2\pi}{N}}) = -1, \tag{5.19}$$

which yields

$$E = \frac{2\beta}{N\sin^2(\frac{\pi}{N})}, \tag{5.20}$$

$$\frac{\pi}{2} + \frac{2\pi}{N}(\delta_e + n) = \pi + 2\pi\nu, \quad \nu \in \mathbf{Z}, \quad \delta_e \in [0, 1[. \tag{5.21}$$

Equation (5.21) yields

$$N = \frac{4(\delta_e + n)}{1 + 4\nu}, \quad \nu \in \mathbf{Z}, \quad \delta_e \in [0, 1[\tag{5.22}$$

Since N is a positive integer, $\delta_e \in \{0, 0.25, 0.5, 0.75\}$. Moreover, since an ideal relay together with an integrator cannot have oscillations of odd periods (by Proposition 5.5 in [77]), $\delta_e \in \{0, 0.5\}$.

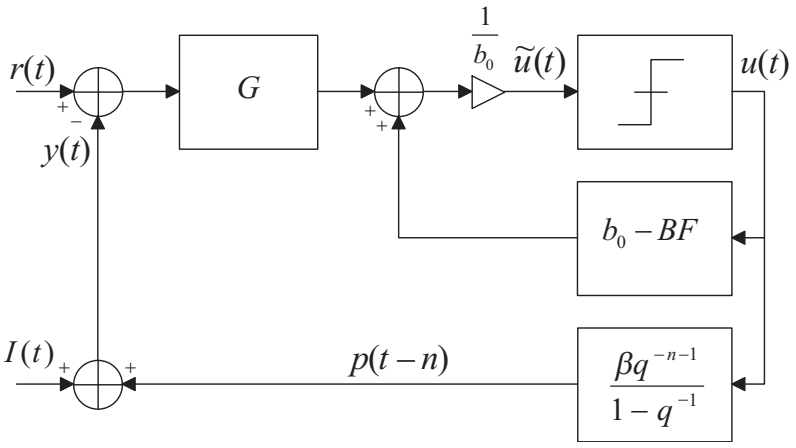

Figure 5.3: The MVD-PC algorithm [140].

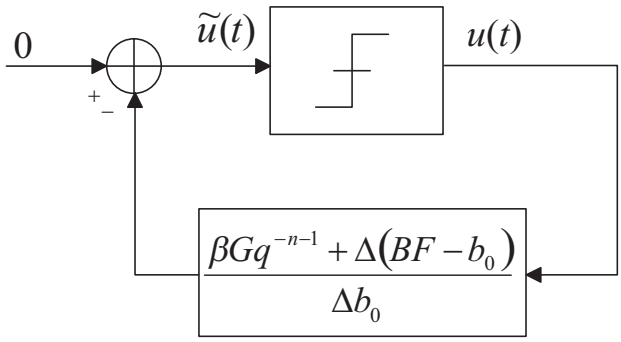

Figure 5.4: The MVD-PC algorithm represented for zero input case.

5.3.1 Example case with $n = 1$

A typical case in WCDMA is $n = 1$ [77, 140]. In this case, (5.22) gives the two possibilities $N = 4$ or $N = 6$. The corresponding amplitudes from (5.20) are β and 1.33β, respectively.

5.4 DF Analysis of the MVD-PC algorithm

The block diagram in Fig. 5.3 represents the MVD-PC algorithm excluding the parameter estimation and backup controller parts. It is assumed in the following that after initial convergence of the controller parameters they remain essentially constant (or change slowly enough). It is considered here that the reference signal $r(t)$ and the external perturbation $I(t)$ (channel gain minus interference power) are zero. This rather unrealistic assumption considerably simplifies the analysis. However, as shown later in the simulations, the results of the analysis are valid for reasonably slowly changing channel and interference conditions. With this assumption and a little block diagram algebra, Fig. 5.3 can be transformed to that shown in Fig.5.4. where

$$H(q^{-1}) = \frac{\beta G q^{-k} + \Delta\left(BF - b_0\right)}{\Delta b_0} \tag{5.23}$$

Fig. 5.4 is now in the form of Fig. 5.1 and is thus suitable for DF analysis.

Let us consider the case $n = 1$ ($k = 2$). This is a typical case in WCDMA as already discussed. The ARX(2,1,2) model is used in the MVD-PC algorithm, as this was found in Chapter 4 to be a reasonable choice for the power control process in WCDMA. From (4.15) we get $F = 1 - a_1 q^{-1}$ and $G = a_1^2 - a_2 + a_1 a_2 q^{-1}$, so

$$H(q^{-1}) = \frac{X q^{-1} + Y q^{-2} + Z q^{-3}}{b_0\left(1 - q^{-1}\right)}, \tag{5.24}$$

where $X = b_1 - b_0 a_1$, $Y = \beta a_1^2 - \beta a_2 - b_1 + b_0 a_1 - b_1 a_1$, and $Z = \beta a_1 a_2 + b_1 a_1$. In frequency domain,

$$H(e^{-j\frac{2\pi}{N}}) = \frac{X e^{-j\frac{2\pi}{N}} + Y e^{-j\frac{4\pi}{N}} + Z e^{-j\frac{6\pi}{N}}}{b_0\left(1 - e^{-j\frac{2\pi}{N}}\right)} = \frac{e^{-j\left(\frac{\pi}{N}+\frac{\pi}{2}\right)}}{2b_0 \sin\left(\frac{\pi}{N}\right)}\left(X + Y e^{-j\frac{2\pi}{N}} + Z e^{-j\frac{4\pi}{N}}\right) \tag{5.25}$$

After some calculations, the polar form is obtained as

$$H(e^{-j\frac{2\pi}{N}}) = \frac{1}{2b_0 \sin\left(\frac{\pi}{N}\right)}\sqrt{f(N)}e^{-j\phi(N)} \tag{5.26}$$

where

$$f(N) = X^2 + Y^2 + Z^2 + 2(XY + YZ)\cos(\tfrac{2\pi}{N}) + 2XZ\cos(\tfrac{4\pi}{N}) \tag{5.27}$$

$$\phi(N) = \frac{\pi}{N} + \frac{\pi}{2} - \arctan\left(g(N)\right) \tag{5.28}$$

$$g(N) = \frac{-Y\sin(\frac{2\pi}{N}) - Z\sin(\frac{4\pi}{N})}{X + Y\cos(\frac{2\pi}{N}) + Z\cos(\frac{4\pi}{N})} \tag{5.29}$$

The describing function of a relay was defined in (5.18). With the condition

$$Y_f(E, N, \delta_e) H(e^{-j\frac{2\pi}{N}}) = -1, \tag{5.30}$$

one gets

$$E = \frac{2}{N b_0 \sin^2\left(\frac{\pi}{N}\right)}\sqrt{f(N)} \tag{5.31}$$

and

$$\frac{\pi}{2} + \delta_e \frac{2\pi}{N} - \arctan\left(g(N)\right) = \pi + 2\pi\nu, \quad \nu \in \mathbf{Z}. \tag{5.32}$$

It is clear that parameter b_0 affects only the amplitude and not the frequency of the predicted oscillations. The frequency is determined by (5.32). Collecting terms from (5.32) and taking

tangent of both sides, one gets

$$g(N) = -\frac{1}{\tan(\delta_e \frac{2\pi}{N})} = -\frac{\cos(\delta_e \frac{2\pi}{N})}{\sin(\delta_e \frac{2\pi}{N})} \tag{5.33}$$

$$\Leftrightarrow [Y \sin(\tfrac{2\pi}{N}) + Z \sin(\tfrac{4\pi}{N})] \sin(\delta_e \tfrac{2\pi}{N}) = [X + Y \cos(\tfrac{2\pi}{N}) + Z \cos(\tfrac{4\pi}{N})] \cos(\delta_e \tfrac{2\pi}{N}) \tag{5.34}$$

$$\begin{aligned} \Leftrightarrow\ & Y \sin(\tfrac{2\pi}{N}) \sin(\delta_e \frac{2\pi}{N}) + Z \sin(\frac{4\pi}{N}) \sin(\delta_e \frac{2\pi}{N}) \\ & = X \cos(\delta_e \tfrac{2\pi}{N}) + Y \cos(\tfrac{2\pi}{N}) \cos(\delta_e \tfrac{2\pi}{N}) + Z \cos(\tfrac{4\pi}{N}) \cos(\delta_e \tfrac{2\pi}{N}) \end{aligned} \tag{5.35}$$

$$\begin{aligned} \Leftrightarrow & \frac{1}{2} Y \left[\cos\left((1-\delta_e)\tfrac{2\pi}{N}\right) - \cos\left((1+\delta_e)\tfrac{2\pi}{N}\right)\right] \\ & + \frac{1}{2} Z \left[\cos\left((1-\tfrac{\delta_e}{2})\tfrac{4\pi}{N}\right) - \cos\left((1+\tfrac{\delta_e}{2})\tfrac{4\pi}{N}\right)\right] \\ & = X \cos(\delta_e \tfrac{2\pi}{N}) + \tfrac{1}{2} Y \left[\cos\left((1-\delta_e)\tfrac{2\pi}{N}\right) + \cos\left((1+\delta_e)\tfrac{2\pi}{N}\right)\right] \\ & + \frac{1}{2} Z \left[\cos\left((1-\tfrac{\delta_e}{2})\tfrac{4\pi}{N}\right) + \cos\left((1+\tfrac{\delta_e}{2})\tfrac{4\pi}{N}\right)\right] \end{aligned} \tag{5.36}$$

$$\Leftrightarrow Y \cos\left((1+\delta_e)\tfrac{2\pi}{N}\right) + Z \cos\left((1+\tfrac{\delta_e}{2})\tfrac{4\pi}{N}\right) + X \cos(\delta_e \tfrac{2\pi}{N}) = 0 \tag{5.37}$$

Now, if $\delta_e = 0.5$, one gets

$$X \cos\left(\tfrac{\pi}{N}\right) + Y \cos\left(\tfrac{3\pi}{N}\right) + Z \cos\left(\tfrac{5\pi}{N}\right) = 0 \tag{5.38}$$

$$\Leftrightarrow (X - 3Y + 5Z) \cos\left(\frac{\pi}{N}\right) + (4Y - 20Z) \cos^3\left(\frac{\pi}{N}\right) + 16Z \cos^5\left(\frac{\pi}{N}\right) = 0 \tag{5.39}$$

It is clear that $\cos(\frac{\pi}{N}) = 0$ gives a solution to (5.39). This is satisfied only with $N = 2$ (since N is an integer). Thus, the DF analysis predicts oscillations with period 2. Other modes of oscillation are also possible from the solutions to (5.39) and with other values of δ_e.

5.5 Simulation results

In this section simulation results are presented for testing the correctness of the analysis in the previous section.

5.5.1 Note on the interpretation of the results

The DF analysis predicts the oscillation period and amplitude of the signal at the input to the relay block. Power control, on the other hand, aims to keep the signal-to-interference ratio (SIR) at the target (or reference) value. Since in the FSPC case the signal at the input to the relay is the power control misadjustment (difference between the SIR target and the SIR), it is desirable that this signal has as small amplitude as possible. In the MVD-PC case the situation is different, since the signal at the input to the relay is the output of the minimum variance controller, which

Table 5.1: Analysis and simulation results for the local loops in Fig. 5.3 and Fig. 5.2.

Algorithm	Oscillation period		Amplitude	
	Analysis	Simulation	Analysis	Simulation
MVD-PC	2 (dominating)	2	3.125	3.125
FSPC	4 or 6	6	1.333	1.15

is a filtered version of the power control misadjustment. If the system is correctly modeled, the algorithm will try to minimize the variance power control misadjustment. Thus in the MVD-PC case it is not necessary to minimize the amplitude of the signal at the input to the relay. However, it is desirable that the amplitude remains low and bounded in order to avoid numerical errors.

The period of the oscillations (N), however, is equally important in both cases. If $N = 2$, this means that the power control misadjustment oscillates around zero, changing sign at every sample, which is the best that can be done with a given fixed step size β. If $N > 2$, this means that consecutive power up or power down commands will be sent to the transmitter, and the power control misadjustment will have larger variation (see [143]).

5.5.2 Simulation of the local loop

The local loop as in Fig. 5.3 was simulated with the following parameters, that are typical for a particular user in a cellular radio system:

- $[a_1, a_2, b_0, b_1] = [-1.5, 0.6, -1.0, 0.7]$
- $\beta = 1$
- $n = 1$ ($k = 2$)
- $p(0) = 0.1$

The above selection of parameters a_1, a_2, b_0, and b_1 is taken from a typical realization using the radio network simulator described in Appendix A. The initial value for $p(0)$ is selected from a practical power range in WCDMA systems [159], and could in practice be the initial power setting after open-loop power control.

All inputs to the loop were set to zero, except that $I(1) = 0.1$ was applied to excite the system. Fig. 5.5 shows the signals entering the relay block for the MVD-PC and the FSPC cases. Table 5.1 shows the amplitudes and periods of these signals predicted by the DF analysis and the simulated ones. As can be seen, the analysis has predicted the oscillations and amplitudes

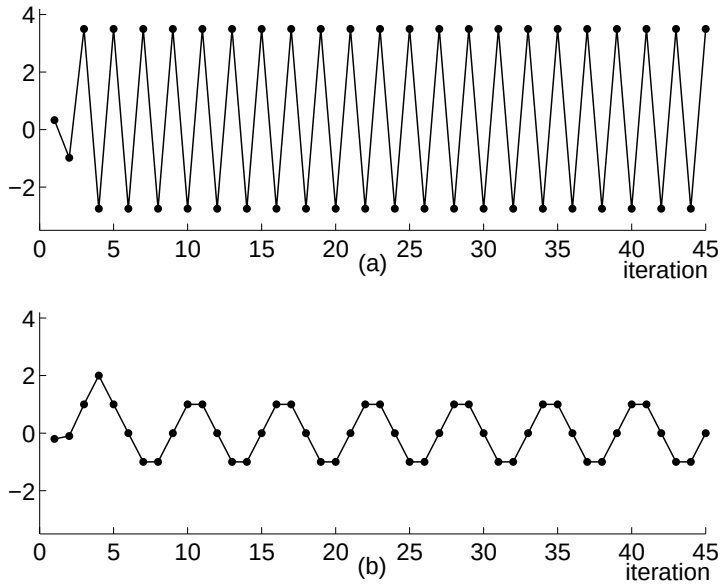

Figure 5.5: Simulation of the signal before the relay in (a) Fig. 5.3 and (b) Fig. 5.2.

well. The results also give some indication of the advantages of MVD-PC over FSPC, since the oscillation period has been reduced from 6 to 2 (see the discussion in section 5.5.1).

5.5.3 Simulation of a WCDMA network

To verify the results in a more realistic environment, the simulation program described in Appendix A was used with ten users, $v_{\min} = 0$ km/h and $v_{\max} = 30$ km/h. One user initially connected to the central cell was selected for observation, and its velocity was set to 2 km/h.

Fig. 5.6 shows the signals entering the relay block for the MVD-PC and the FSPC cases at the middle of the simulation right after the transients have decayed. It is seen that on the average the periods of the oscillations match those predicted by the analysis as well as the local loop simulations. It must be noted that in the analysis all inputs to the loop were set to zero, which is not the case here. For this slowly moving user the simulation gave the same results as the analysis. Figures 5.7, 5.8 and 5.9 show the same results for a user moving at speeds 5, 10 and 15 km/h, respectively. It is seen that as the speed increases, the oscillation becomes increasingly irregular, since the fast fading becomes too rapid for power control to follow it, and the simplifying assumptions made in the analysis are no longer valid. Nevertheless, similar small-scale oscillation is still observable, even with the speed of 15 km/h.

Fig. 5.10 shows the received SIR of the observed user varying around the SIR target (the straight horizontal line), with a speed of 2 km/h. As discussed in section 5.5.1, the variance of the power control misadjustment is generally higher when the oscillation period of the signal at

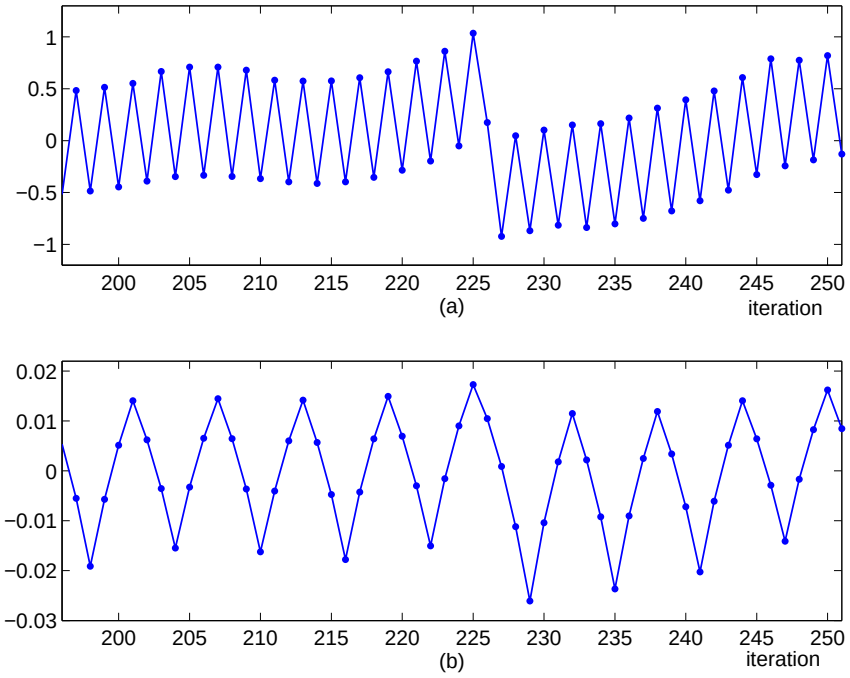

Figure 5.6: The signal before the relay in the WCDMA network simulation, mobile speed 2 km/h, (a) MVD-PC, (b) FSPC.

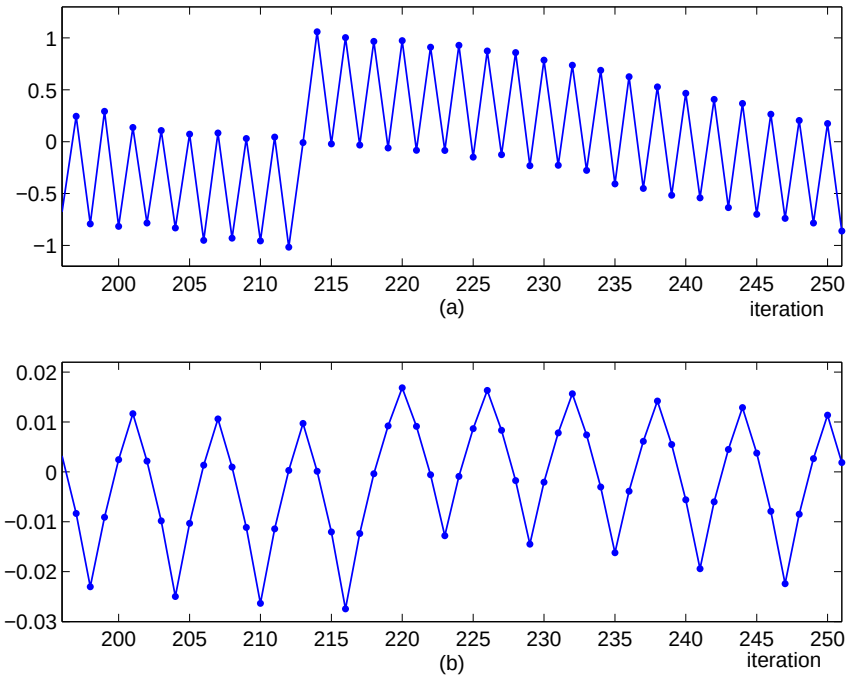

Figure 5.7: The signal before the relay in the WCDMA network simulation, mobile speed 5 km/h, (a) MVD-PC, (b) FSPC.

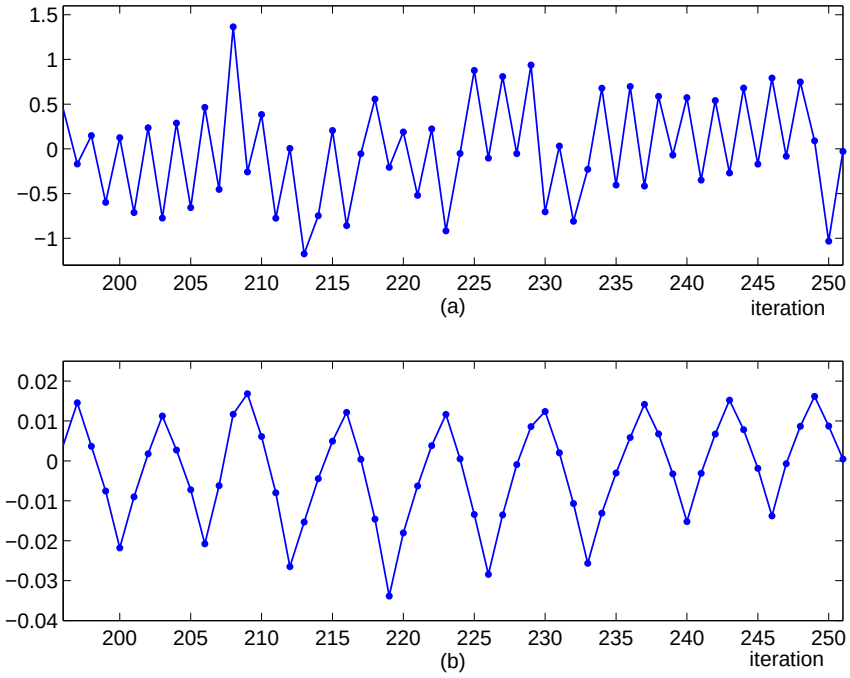

Figure 5.8: The signal before the relay in the WCDMA network simulation, mobile speed 10 km/h, (a) MVD-PC, (b) FSPC.

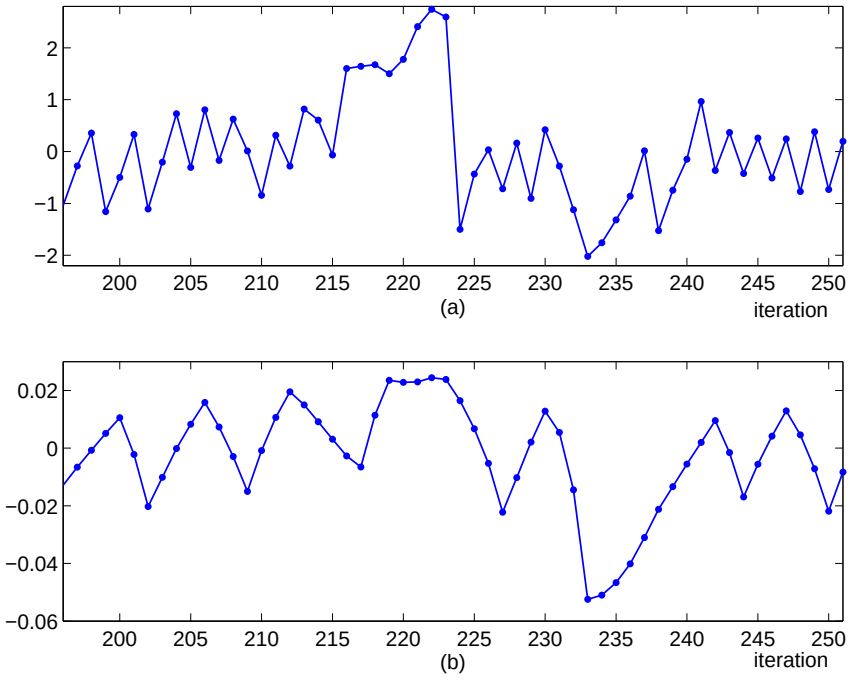

Figure 5.9: The signal before the relay in the WCDMA network simulation, mobile speed 15 km/h, (a) MVD-PC, (b) FSPC.

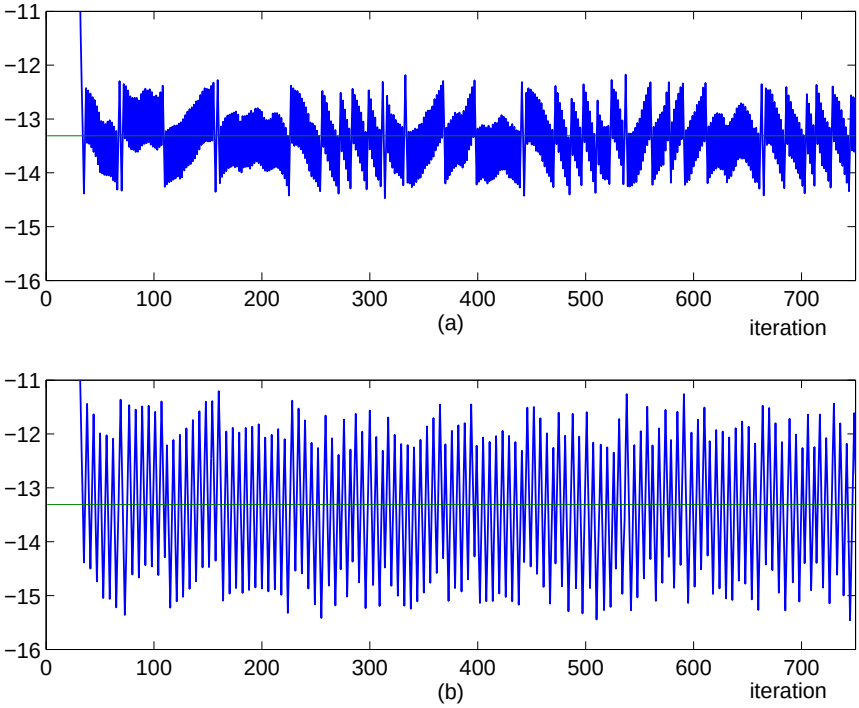

Figure 5.10: The received SIR of the observed user in the WCDMA network simulation, mobile speed 2 km/h, (a) MVD-PC, (b) FSPC.

the input to the relay is longer. This effect is clearly seen in the figure.

5.6 Conclusions of the DF analysis

A describing function analysis was presented for the MVD-PC algorithm. The analysis showed how the MVD-PC algorithm can effectively cancel the power control loop delay, which was assumed to be known. The analysis performed on a simplified closed-loop system employing MVD-PC predicted oscillations with period $N = 2$ and an amplitude dependent on the controller parameters. The results of the analysis were verified by computer simulations, and were shown to be in good agreement with the simulations. The results illustrate the performance advantage that the previously proposed adaptive closed-loop power control algorithms have over the conventional fixed-step power control algorithm in the presence of loop delays.

Chapter 6

Adaptive step-size power control

6.1 Introduction

This chapter introduces a new scheme for adapting the power control step size based on the received ON-OFF power control commands in a decision feedback power control scenario. This scheme can be used in power control for increasing its performance without any increase in the signaling bandwidth used for feeding back the power control commands. The proposed method is called the *adaptive step* (AS) method. The method is combined with the FSPC and DCPC algorithms to construct a new PC algorithm, the *Adaptive Step Power Control* (ASPC) algorithm.

6.1.1 Problem setup

Consider the DCPC and FSPC algorithms. For a particular user, these algorithms are described by (all variables in decibel scale)

$$p(t+1) = \min\left\{p_{\max}, p(t) + \delta e(t)\right\} \tag{6.1}$$

and

$$p(t+1) = \min\left\{p_{\max}, p(t) + \delta \text{sign}\left(e(t)\right)\right\}, \tag{6.2}$$

respectively, where $e(t) = \gamma^t(t) - \gamma(t)$ is the power control misadjustment. It is clear that the DCPC algorithm belongs to the class of *information feedback* (IFB) algorithms and the FSPC algorithm to the class of *decision feedback* (DFB) algorithms. The latter class is used in DS-CDMA systems in practice, since the power update rate is relatively high, and thus the number of bits per power control command must be low so that the power control signaling would not consume too much radio resources. For example, in UMTS the power update rate is 1500 Hz and

only up-down commands are used so that only one bit is needed for the command transmission.[1] Note that if $\delta = 1$, then $e(t)$ in the DCPC case can be regarded as the power update adjustment that would guarantee that $e(t+1) = 0$ if the channel were static and all other users in the system did not update their powers.

The idea of the proposed scheme is to allow the use of an IFB-type algorithm, like the DCPC algorithm, while still employing decision feedback. Thus, the adaptive step size can be thought as a reconstruction of $e(t)$, constructed from the received PC commands $u(t), u(t-1), \ldots$, where $u(t) \in \{-1, 1\}, t = 0, 1, 2, \ldots$.

6.2 Adaptation method

The adaptation method proposed here is referred to as the *Adaptive Step* (AS) method. Let $e(t) = \gamma^t(t) - \gamma(t)$ and $u(t) = \text{sign}(e(t))$. Define

$$a(t, x) = \frac{1}{2}\left[1 + xu(t)u(t-1)\right], \quad x \in \{-1, 1\}. \tag{6.3}$$

Note that

$$a(t, 1) = \begin{cases} 1, & \text{if } u(t) = u(t-1) \\ 0, & \text{if } u(t) \neq u(t-1) \end{cases} \tag{6.4}$$

and

$$a(t, -1) = \begin{cases} 0, & \text{if } u(t) = u(t-1) \\ 1, & \text{if } u(t) \neq u(t-1) \end{cases} \tag{6.5}$$

The AS method can be described by

$$\tilde{e}(t) = a(t, 1)\tilde{e}(t-1) + \delta_e u(t), \tag{6.6}$$

where $\tilde{e}(t)$ is the reconstruction of $e(t)$ and δ_e is a parameter controlling the speed of the update.

While not readily seen from (6.6), the idea of the adaptation method is very intuitive: if the two latest commands have the same sign, the reconstruction of $e(t)$ is updated by δ_e to the direction of the last command $u(t)$ so as to increase the step size of the next power update. If the two latest commands have different signs, a zero crossing must have happened in the signal $e(t)$, and the reconstruction also crosses zero.

[1] The UMTS specifications allow also more than one-bit PC commands, but these are used for reducing the PC command bit errors by repetition, and not for allowing multiple PC command levels [142, 59].

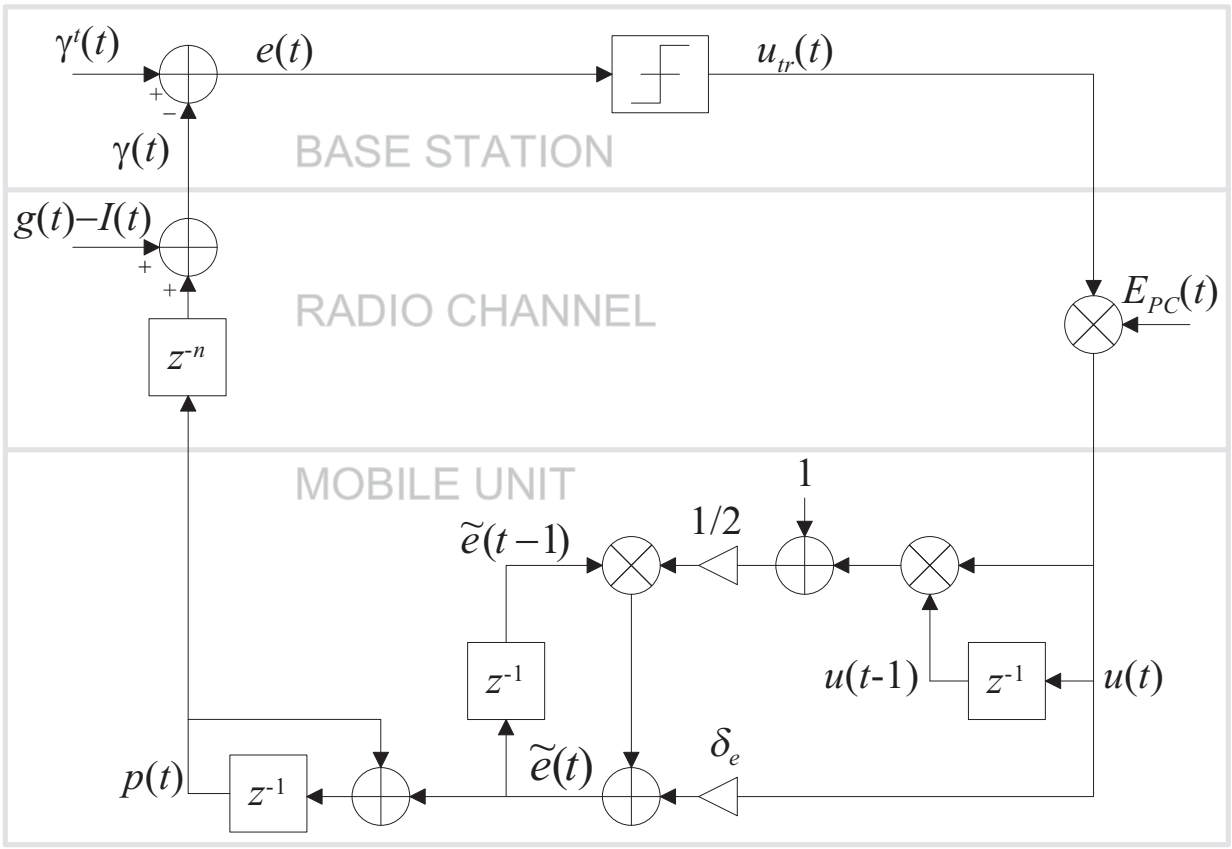

Figure 6.1: Flowchart of the ASPC algorithm.

6.3 The Adaptive Step Power Control (ASPC) algorithm

The ASPC algorithm is simply the combination of the FSPC algorithm, the AS method, and the DCPC algorithm. Considering uplink, the base station generates the commands $u(t) \in \{-1, 1\}$ as in the FSPC algorithm, the commands are transmitted to the mobile station, which applies AS to generate a reconstruction $\tilde{e}(t)$ of the PC misadjustment, and then updates its power as in the DCPC algorithm, but using the reconstructed value instead of the true $e(t)$. This is described by

$$p(t+1) = \min\left\{p_{\max}, p(t) + \delta\tilde{e}(t)\right\}. \tag{6.7}$$

Fig. 6.1 shows a flowchart of the ASPC algorithm (cf. Fig. 3.3).

6.4 Modifications

The performance of the AS method naturally depends on the selection of the parameter δ_e. If too small δ_e is selected, then the reconstruction cannot track the actual misadjustment $e(t)$. This can happen for example during a deep fade in the radio channel. On the other hand, if δ_e is too big,

then the advantage of the "fine-tuning" provided by the adaptation method to the power control algorithm is significantly reduced.

To circumvent these problems, some modifications are proposed to the standard AS method. All these modifications aim to make the parameter δ_e to adapt to various conditions.

6.4.1 AS with asymmetric update step sizes

From closed loop power control point of view, the situation where the SIR is below the target is more serious than vice versa. An intuitive way to allow a more rapid recovery from these situations is to use a larger update parameter when receiving positive commands (increase power) than when receiving negative commands (decrease power). Mathematically this can be put as follows. Let δ_e^{up} and δ_e^{down} be the update parameters in the positive and negative directions, respectively. Define

$$b(t,x) = \frac{1}{4}\left[u(t) + u(t-1) + 2x\right], \quad b \in \{-1, 1\}. \tag{6.8}$$

The *asymmetric AS* (AS-A) is

$$\tilde{e}_{\text{A}}(t) = a(t,1)\left[\tilde{e}_{\text{A}}(t-1) + b(t,1)\delta_e^{\text{up}} + b(t,-1)\delta_e^{\text{down}}\right] + a(t,-1)\delta_e u(t). \tag{6.9}$$

6.4.2 AS with gradually increasing update step size

The convergence of the ASPC algorithm also depends heavily on the selection of δ_e. In a situation where the PC misadjustment is large, it would be better to apply a larger δ_e to speed up the convergence. This can be done by increasing δ_e gradually when receiving consecutive commands that have the same sign. Mathematically, the *Gradual AS* (AS-G) is

$$\tilde{e}_{\text{G}}(t) = a(t,1)\tilde{e}_{\text{G}}(t-1) + \delta_e\left(1 + \sum_{m=1}^{n_s}\delta_m \prod_{k=0}^{m-1} a(t-k,1)\right)u(t), \tag{6.10}$$

where n_s is a parameter that limits the maximum increase of the update parameter, so that after receiving $n_s + 1$ consecutive commands with the same sign, the update parameter is no longer increased. $\delta_m, \quad m = 1, 2, \ldots, n_s$ are weighting factors defining the fraction of δ_e that is to be added to the update parameter when receiving the mth command with the same sign.

A drawback of this method is that it can lead to high overshoot in the reconstructed signal. Therefore, it is be better to set n_s to a relatively low value. In simulation experiments, $n_s = 2$ seemed to be a good compromise between overshoot limitation and tracking speed.

6.4.3 AS with variable update step size

Yet another intuitive method to adapt the update parameter is described here. Consider the FSPC algorithm in (6.2). Since the PC step δ (not to be confused with δ_e) is fixed, the best situation is

achieved when the commands (power updates) generated by the FSPC algorithm are consecutive $+1$'s and -1's, since in this case the PC misadjustment $e(t)$ oscillates between the opposite sides of the origin at consecutive samples. The amplitude of this oscillation depends on the step size δ. Now, consider that we could decrease the step size applied at the transmitter, while maintaining the consecutive up-down command flow. In this case the amplitude of the oscillation of the PC misadjustment would be decreased. If the continuous up-down command flow breaks, the step size could be increased again. This can be done with ASPC and the following modification to the AS method. This modification is called the *Variable Gain AS* (AS-VG). It is described by

$$\tilde{e}_{\text{VG}}(t) = a(t,1)\tilde{e}_{\text{VG}}(t-1) + \delta_e(t)u(t), \tag{6.11}$$

$$\delta_e(t) = \delta_e(t-1) + \delta_{\text{VG}}u(t)u(t-1), \tag{6.12}$$

where δ_{VG} controls the rate of change of the update parameter $\delta(t)$, which is now time-varying. The idea behind this method is that the update parameter is decreased every time the two most recent PC commands have different signs, otherwise it is increased. In this way the algorithm tries to find the smallest update step size that still leads to consecutive up-down PC command flow. A similar method to adjust the power control step sizes is proposed in [112]. To prevent the update step size to grow too large, it should be limited. A limit of 1 dB was used in all the simulations.

6.4.4 Modified ASPC algorithms

The modifications described above can be applied in power control in the same way as the AS method is used in the ASPC algorithm. The modified ASPC algorithms are thus called the ASPC-A, ASPC-G and ASPC-VG algorithms that use the corresponding step size adaptation methods.

6.5 Analysis on the convergence speed

The reason for adapting the step size in the first place is to make the transmission power to change faster if the consecutive TPC commands have the same sign. One can propose the following general adaptive PC algorithm for this purpose as

$$\tilde{e}(t) = c(t)\tilde{e}(t-1) + d(t), \tag{6.13}$$

$$p(t+1) = p(t) + \tilde{e}(t). \tag{6.14}$$

Depending on the choice of $c(t)$ and $d(t)$ one can achieve different speeds of increase of the PC update step size. For instance, exponential increase is obtained with $c(t) > 1$, and polynomial

Table 6.1: General framework for the proposed PC algorithms.

PCA	$c(t)$	$d(t)$
FSPC	0	$\delta u(t)$
ASPC	$a(t,1)$	$\delta_e u(t)$
ASPC-A	$a(t,1)$	$a(t,1)[b(t,1)\delta_e^{\text{up}} + b(t,-1)\delta_e^{\text{down}}] + a(t,-1)\delta_e$
ASPC-G	$a(t,1)$	$\delta_e \left(1 + \sum_{m=1}^{n_s} \delta_m \prod_{k=0}^{m-1} a(t-k,1)\right) u(t)$
ASPC-VG	$a(t,1)$	$\delta_e(0) + \delta_{\text{VG}} \sum_{k=1}^{t} u(k)u(k-1)$

increase is obtained with

$$c(t) = 1, d(t) = O(t^k) \Rightarrow e(t) = O(t^{k+1}) \Rightarrow p(t) = O(t^{k+2}). \tag{6.15}$$

The FSPC algorithm and the proposed algorithms can be fitted in this general framework as shown in Table 6.1.

Consider the case when the TPC command is positive starting from time $t = 0$, i.e., $u(t) = 1, t = 0, 1, \ldots$. Table 6.2 shows the rate of change of $p(t)$ with the different algorithms in this special case.

In the case of FSPC algorithm, the speed of change in the transmission power is linear, while for the proposed algorithms it is either quadratic or cubic. Figure 6.2 shows the power evolution graphically with the following parameters, that were selected using simulation experiments to give reasonable performance:

$$\begin{aligned} &\delta = 1 \\ &\delta_e = 0.1 \\ &\delta_e^{\text{up}} = 0.3 \\ &\delta_m = 1, m = 1, 2, \ldots \\ &\delta_{\text{VG}} = 0.01 \\ &n_s = 2 \end{aligned} \tag{6.16}$$

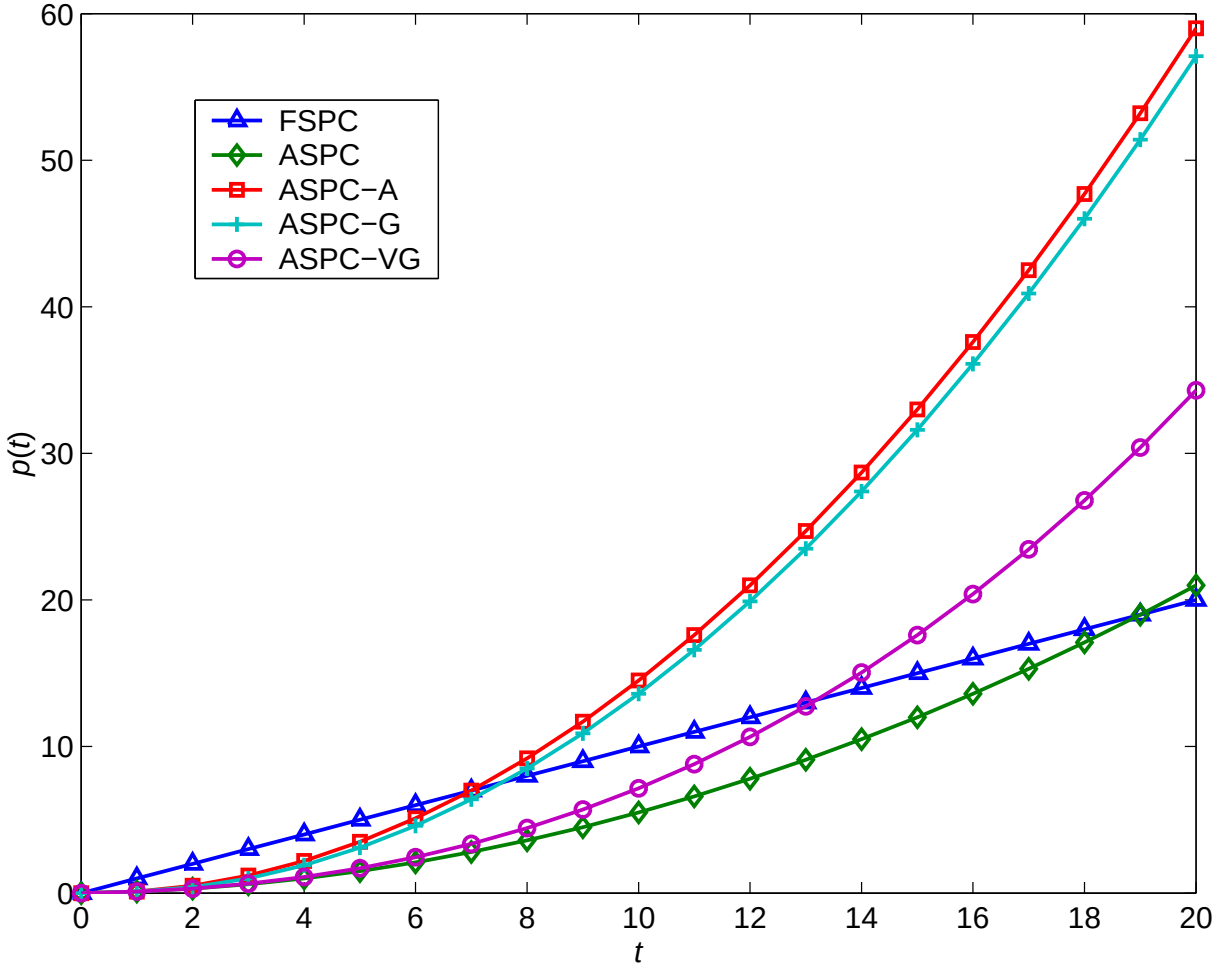

Figure 6.2: Power evolution with various algorithms in the case $p(0) = 0$, $u(t) = 1, \quad t = 0, 1, 2, \ldots$.

Table 6.2: Convergence of power with the proposed PC algorithms.

PCA	$p(t)$	change rate
FSPC	$p(0) + t\delta$	linear
ASPC	$p(0) + \delta_e \frac{t(t+1)}{2}$	quadratic
ASPC-A	$p(0) + \delta_e t + \delta_e^{\text{up}} \frac{t(t-1)}{2}$	quadratic
ASPC-G^2	$p(0) + \delta_e \frac{t(t+1)}{2} + \frac{\delta_e \delta_m}{6}(t^3 - t)$, if $t <= n_s + 1$	cubic
	$p(0) + \frac{\delta_e}{2}(n_s+1)(n_s+2) + \frac{\delta_e \delta_m}{6}((n_s+1)^3 - n_s - 1) + (t - n_s - 1)\left[\delta_e(n_s+1) + \delta_e \delta_m \frac{n_s(n_s+1)}{2}\right] + \frac{(t-n_s)(t-n_s-1)}{2}\delta_e(1 + n_s\delta_m)$, if $t > n_s + 1$	quadratic
ASPC-VG	$p(0) + \frac{\delta_{\text{VG}}}{6}(t^3 - t) + \delta_e\left(\frac{(t+1)(t+2)}{2} - t - 1\right)$	cubic

6.6 Simulation results

Some simulation examples demonstrating the properties and performance of the ASPC algorithms are given here.

6.6.1 Error tracking

Fig. 6.3 shows an example of the PC misadjustment tracking performance of the ASPC, ASPC-A, ASPC-G and ASPC-VG algorithms for a slowly moving (5 km/h) user. This case was simulated

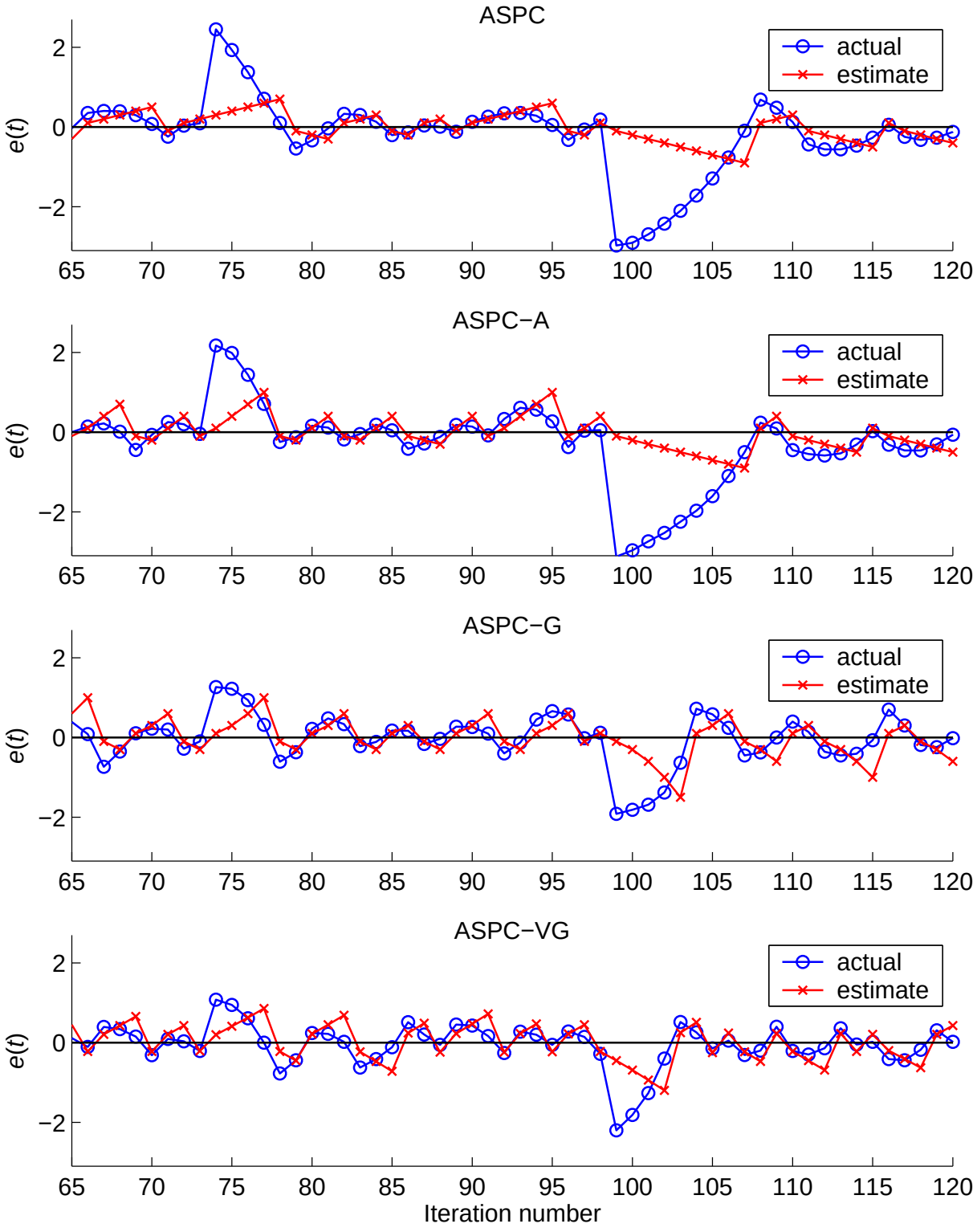

Figure 6.3: Example of the PC misadjustment tracking performance of the ASPC algorithms (mobile speed 5 km/h).

with the simulator described in Appendix A. The parameters were selected as

$$\delta_e = 0.1,$$
$$\delta_e^{\text{up}} = 0.3,$$
$$\delta_e^{\text{down}} = 0.1,$$
$$n_s = 2,$$
$$\delta_1 = \delta_2 = 1,$$
$$\delta_{\text{VG}} = 0.01.$$

These parameters were selected by trial and error to give good results in the simulation experiments. It is seen that the ASPC reconstruction follows the actual misadjustment to some extent, although it is quite coarse. While the actual misadjustment follows somewhat smooth, second-order-type curves, the reconstruction behaves more like a sawtooth wave. If the actual misadjustment stays at one side from zero long times, the reconstruction eventually deviates far from the actual value. Nevertheless, every time a zero-crossing occurs on the actual misadjustment, the reconstruction also immediately crosses zero, thus rapidly decreasing the deviation from the actual value. The parameter δ_e obviously has a great effect on the performance, and it should be selected according to the fading rate. This is a drawback of the ASPC algorithm, and it motivates to investigate the modifications proposed above, where this parameter is adaptive. Considering the modifications, it is seen that the ASPC-A algorithm is able to reduce the amplitude of the $e(t)$ deviation in the positive direction (SIR is below SIR target) around sample number 75. Both the ASPC-G and ASPC-VG algorithms, however, do this more effectively, and also reduce the deviation to the negative direction around sample number 100.

6.6.2 Convergence in two-user case

The power control problem in two-user case was discussed in Section 3.2.2. The two-user case is simulated here to demonstrate some interesting properties of the ASPC algorithms. The simulation was done with the following link gains:

$$\boldsymbol{G} = \begin{pmatrix} g_{11} & g_{12} \\ g_{21} & g_{22} \end{pmatrix} = \begin{pmatrix} 1.0 \cdot 10^{-4} & 4.82253 \cdot 10^{-9} \\ 1.52416 \cdot 10^{-8} & 6.25 \cdot 10^{-6} \end{pmatrix} \tag{6.17}$$

The system load (see Section 3.2) as measured by $\rho(\boldsymbol{H})$ was set to $\rho(\boldsymbol{H}) = 0.95$. The initial powers of the users were $p_1 = 5dBm$ and $p_2 = 12dBm$. These values were selected so that the initial point in the power plane is outside the feasible region. The high load makes the feasible

region very narrow. The parameters were $\delta = 1$ for FSPC, $\delta_e = 0.1$ for ASPC, and $\delta_{\text{VG}} = 0.01$ for ASPC-VG.

Fig. 6.4 shows the convergence of the power vector to the optimal power vector $\boldsymbol{p}^*$ with the DCPC-, FSPC-, ASPC- and ASPC-VG algorithms. The two diagonal curves in the figures are the power requirement limits as in (3.16) (cf. Fig. 3.5). The DCPC algorithm converges to the optimal point as expected. The FSPC algorithm does not converge but oscillates between the two points, since the feasibility region is too narrow for the applied step size (1 dB). Both the ASPC and ASPC-VG algorithms converge to the neighborhood of the optimal point, and start oscillating around it. The oscillation is considerably smaller than with FSPC. Also, the oscillation with ASPC-VG is smaller than with ASPC. Note also that during the convergence, the ASPC algorithms stay very near to the feasible region, while the DCPC algorithm has relatively large oscillations outside the feasible region. The result of this feature is clearly seen in Fig. 6.5, as discussed below.

Fig. 6.5 shows the convergence of SIR to SIR target, measured by $\frac{\gamma_1^t(t)}{\gamma_1(t)}$ and $\frac{\gamma_2^t(t)}{\gamma_2(t)} + 2$ for users 1 and 2, respectively. The offset by 2 for user 2 is for separating the curves in the figures. Here an interesting feature of the ASPC algorithms is clearly visible: the oscillation of SIR around the SIR target during the transient phase is considerably smaller with the ASPC algorithms than with the DCPC algorithm, even though the ASPC algorithms utilize decision feedback and the DCPC algorithm uses information feedback. Also, the ASPC-VG algorithm is able to finally reduce the oscillation much more than the ASPC algorithm, since the adaptive step size is gradually decreasing due to the consecutive up-down commands.

Fig. 6.6 shows the convergence of the power vector towards the optimal power vector, as measured by the norm $||\boldsymbol{p} - \boldsymbol{p}^*||$. Fig. 6.7 shows the same curves on top of each other for easier comparison. It is seen that the ASPC-VG algorithm gets very close to the convergence speed of DCPC. Finally, Fig. 6.8 shows the convergence in a multiuser case with 80 users. Similar behavior is observed as in the two-user case, although the convergence of the DCPC algorithm is in this case much faster than with the ASPC-VG algorithm.

6.6.2.1 A note on the convergence of the ASPC-VG algorithm

For the ASPC-VG algorithm in the static-channel case it sometimes might happen that the parameter updating algorithm (6.12) starts oscillating without converging to a small value. Fig. 6.9 shows an example of this case. The adaptive step-size, PC commands, and deviation of SIR from SIR target are shown for user 1 in the figure. It is seen that the power vector oscillates between four points around the optimal point, causing a continuous $(1, 1, -1, -1)$-pattern for the PC commands. As a result, also (6.12) starts to oscillate between two points and this "deadlock" situation is maintained forever. Thus, some means for detecting this deadlock situation might be

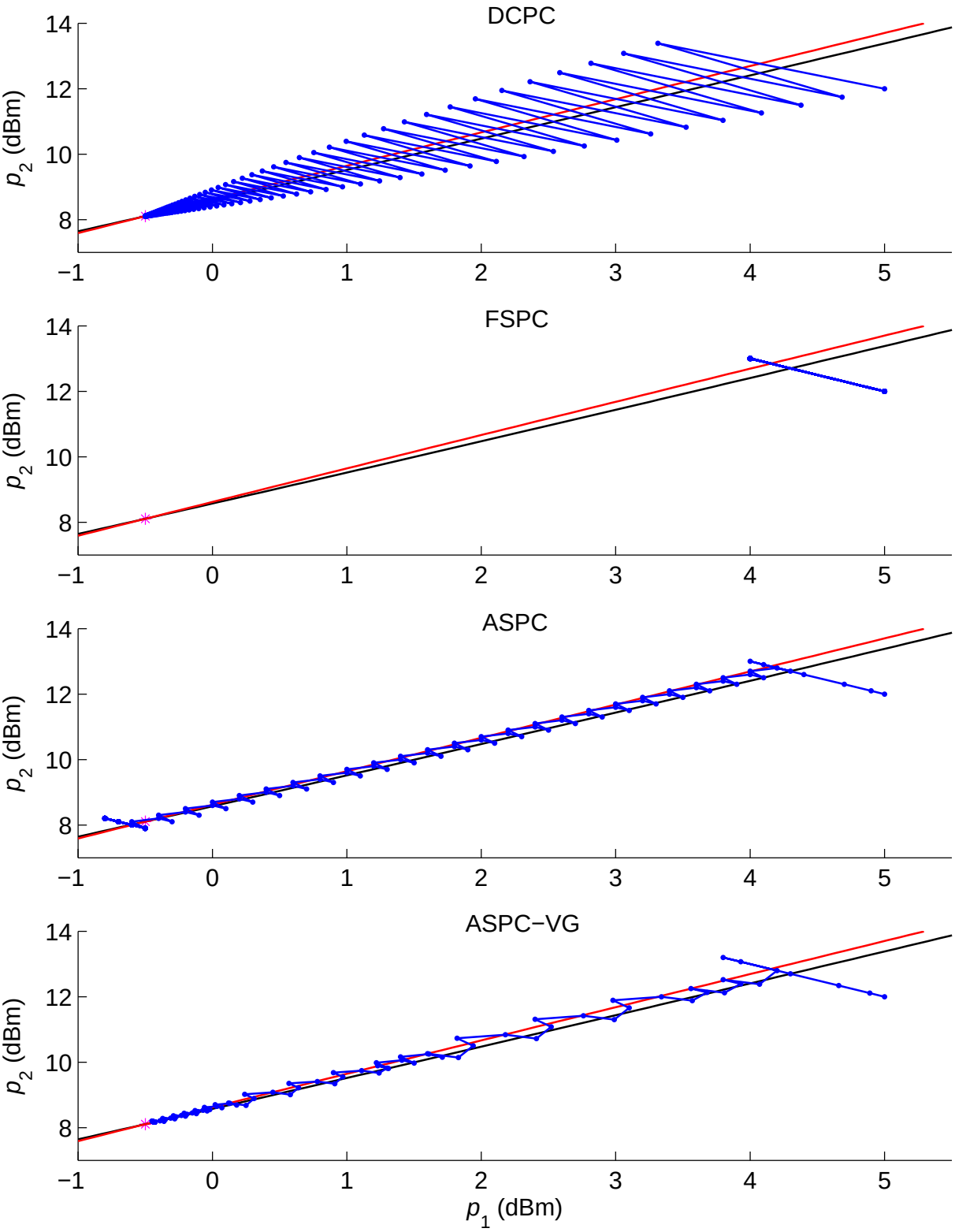

Figure 6.4: Comparison of the convergence of the algorithms for two users and static channel (snapshot simulation).

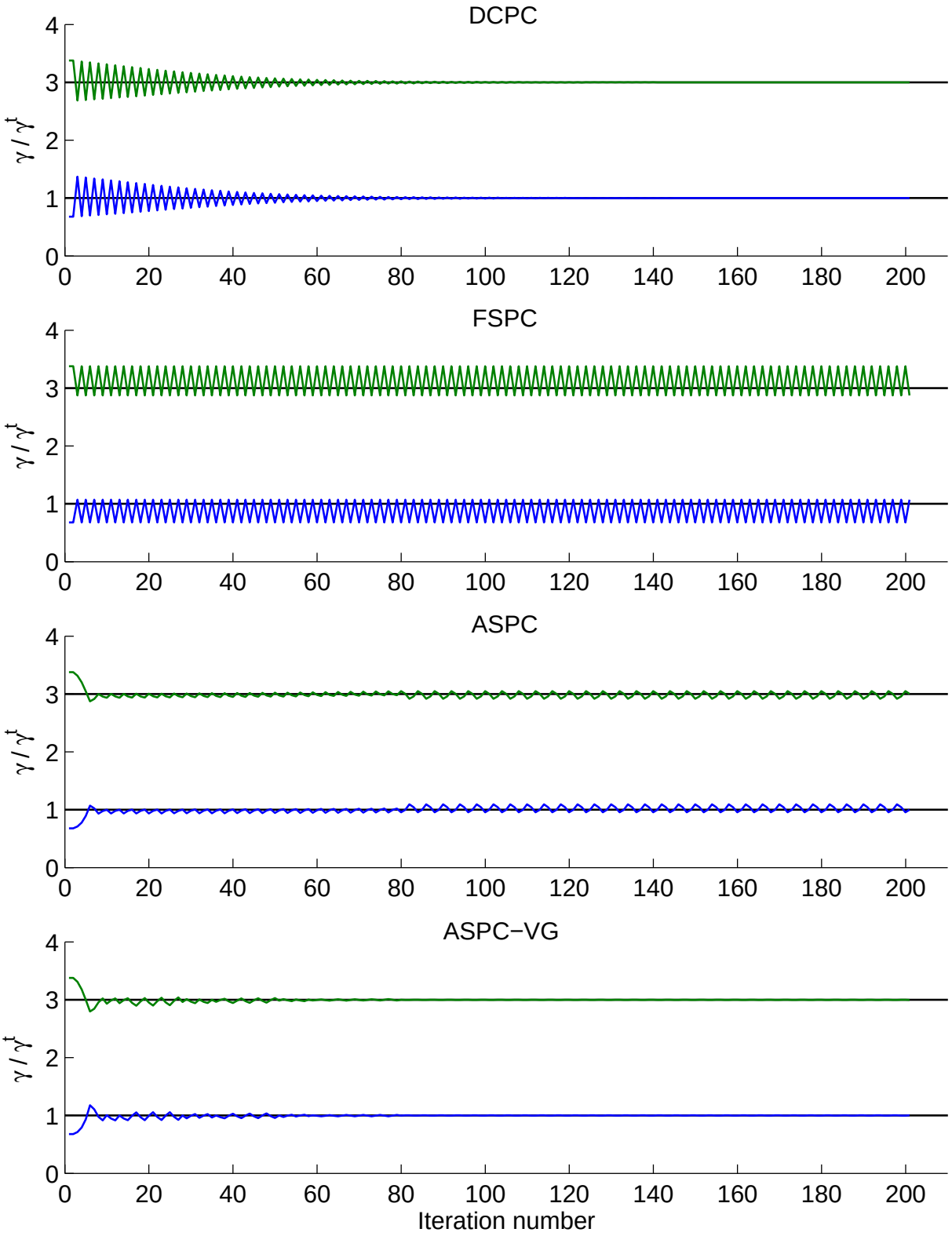

Figure 6.5: Convergence of the SIR to SIR target in two-user snapshot simulation. The graphs of user 2 in the figures is offset vertically by 2 for better illustration.

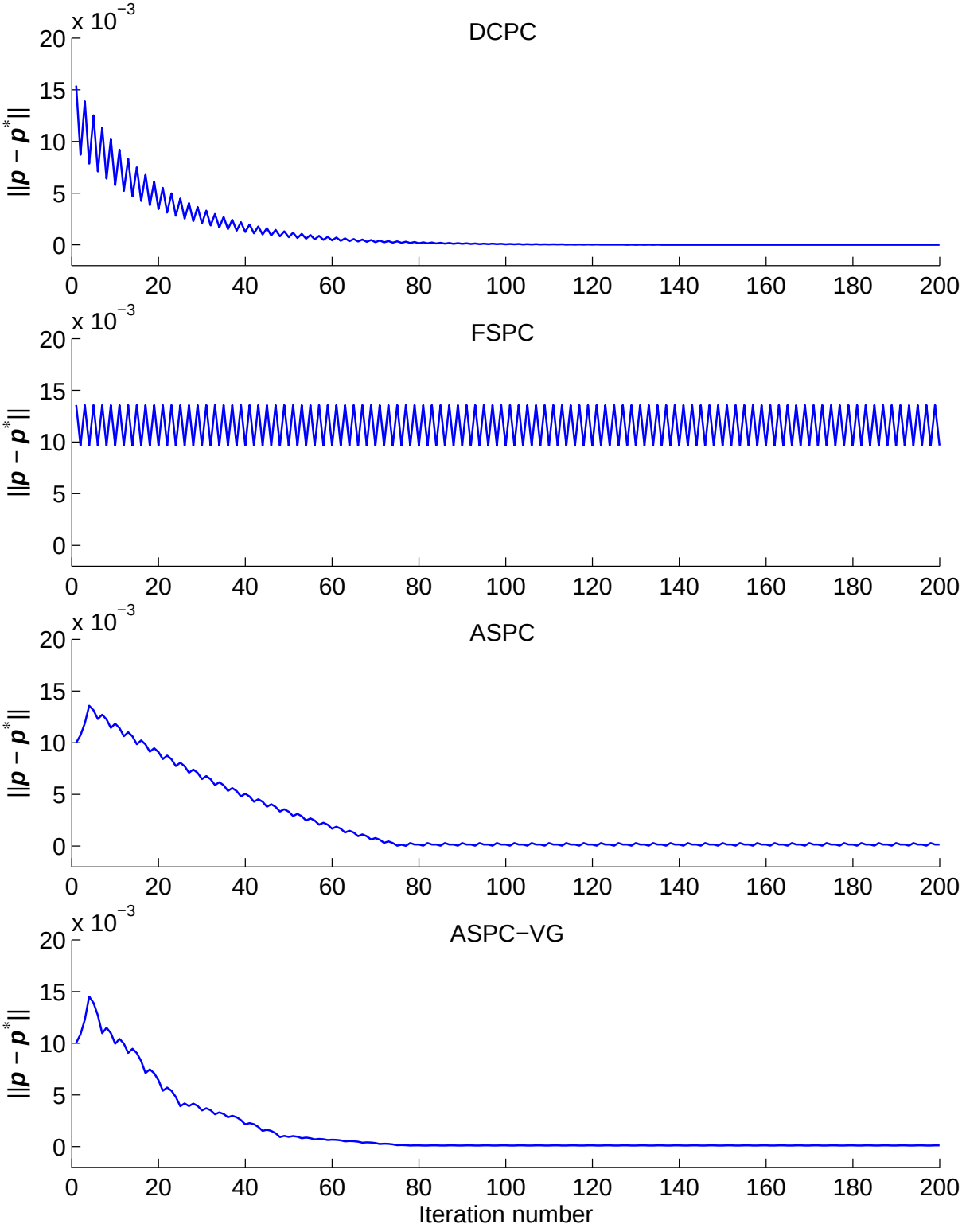

Figure 6.6: Convergence of the norm of the difference between the power vector and the optimal power vector $\boldsymbol{p}^*$ (equation (3.14)) in two-user snapshot simulation.

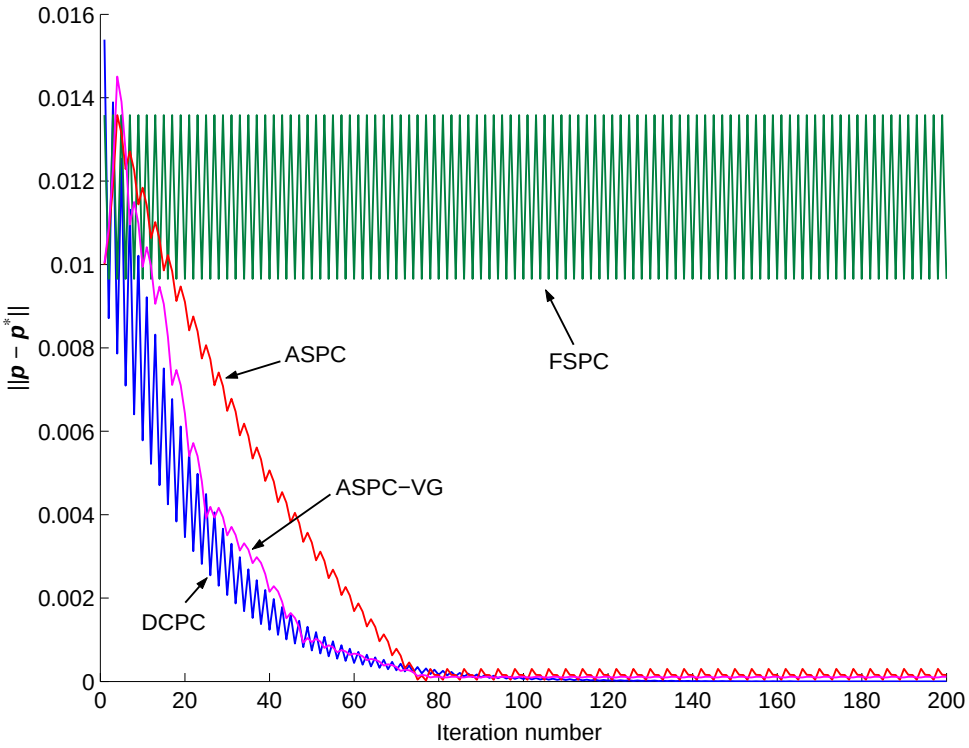

Figure 6.7: Power convergence comparison in two-user snapshot simulation.

needed, e.g., by detecting the $(1, 1, -1, -1)$-pattern from the received PC commands. However, this situation is not very likely to sustain long times in a real dynamic environment with random changes in the channel gains.

6.6.3 Performance of the ASPC algorithms

Figures 6.10, 6.11 and 6.12 show the empirical CDFs of the ASPC algorithm and its modifications ASPC-A, ASPC-G and ASPC-VG, compared to FSPC and DCPC with loop delay of 1 T_{PC}, with $v_{\min} = 0$ km/h and $v_{\max} = 5, 15$ and 30 km/h, respectively. The parameters for the algorithms were the same as in Section 6.6.1. It is seen that the ASPC method is most effective with low mobile speeds in terms of outage probability. The ASPC-A and ASPC-G algorithms are able to reduce the outage probability with a slight degradation in the variance of SIR (or E_b/I_o) around the target. The best compromise seems to be the ASPC-VG algorithm, which has very good performance at wide range of mobile speeds due to its ability to adapt the update parameter according to various conditions.

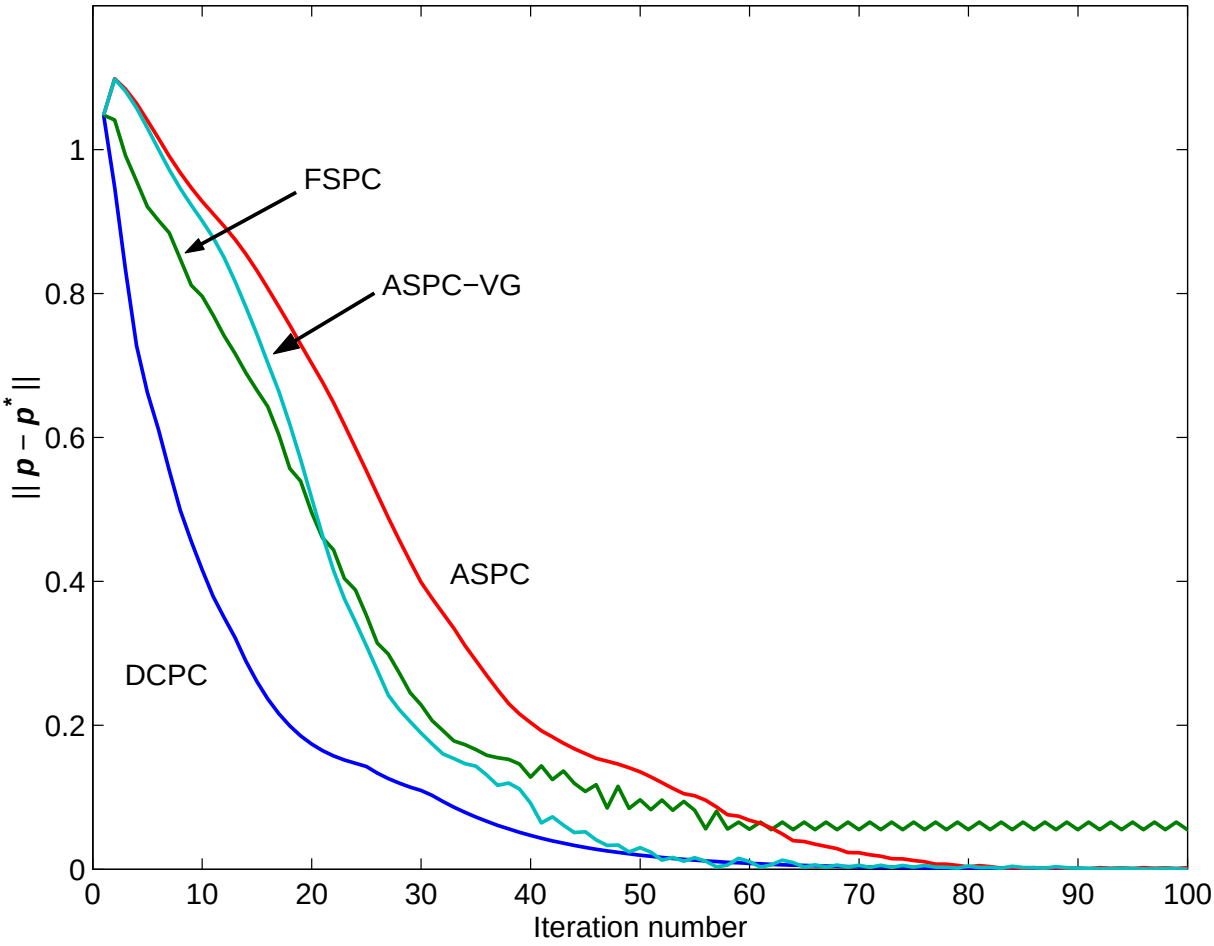

Figure 6.8: Convergence of the norm of the difference between the power vector and the optimal power vector $\boldsymbol{p}^*$ (equation (3.14)) in multiuser snapshot simulation (80 users).

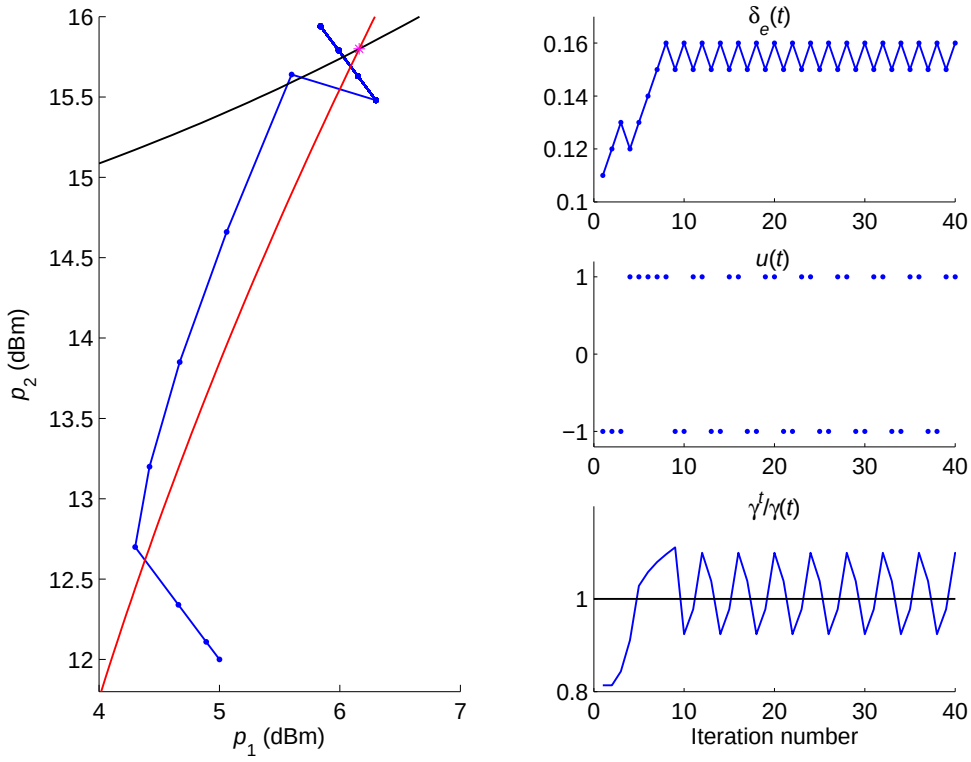

Figure 6.9: Example of a "deadlock" situation with the ASPC-VG algorithm.

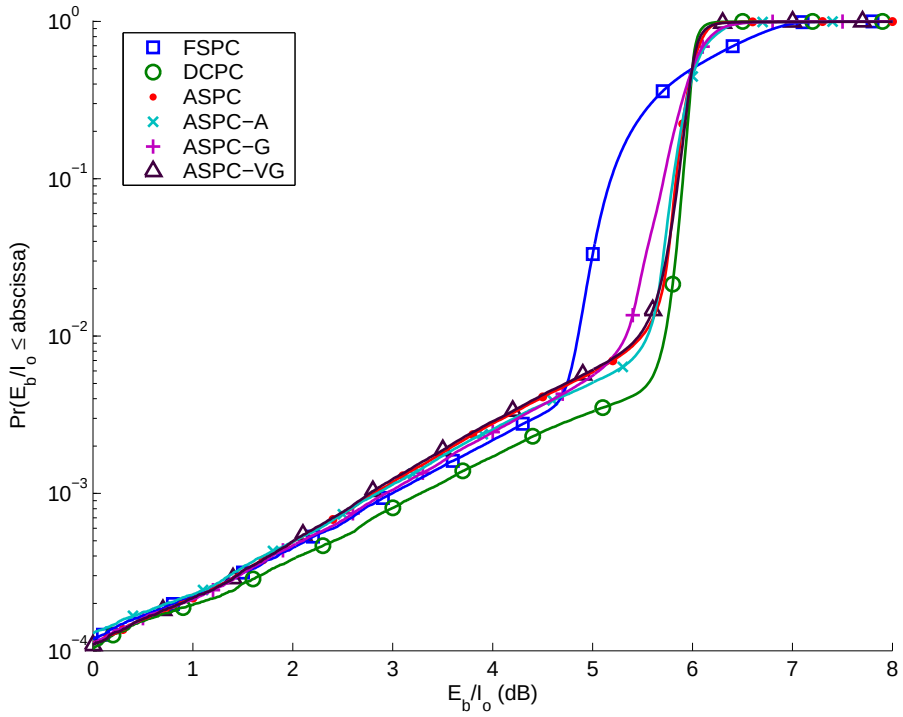

Figure 6.10: Empirical CDF of E_b/I_o, mobile speeds from 0 to 5 km/h.

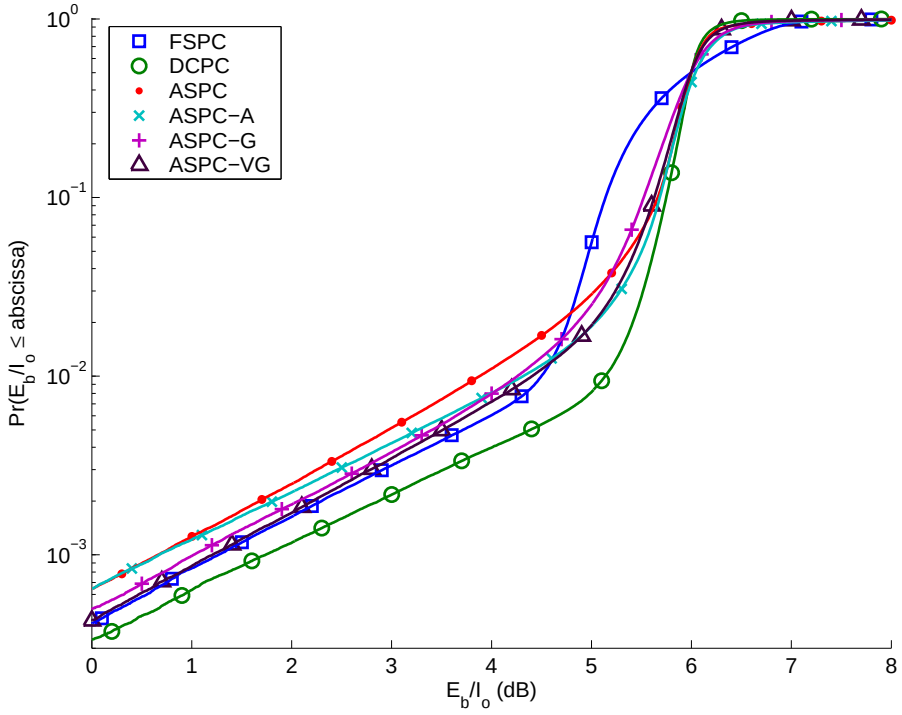

Figure 6.11: Empirical CDF of E_b/I_o, mobile speeds from 0 to 15 km/h.

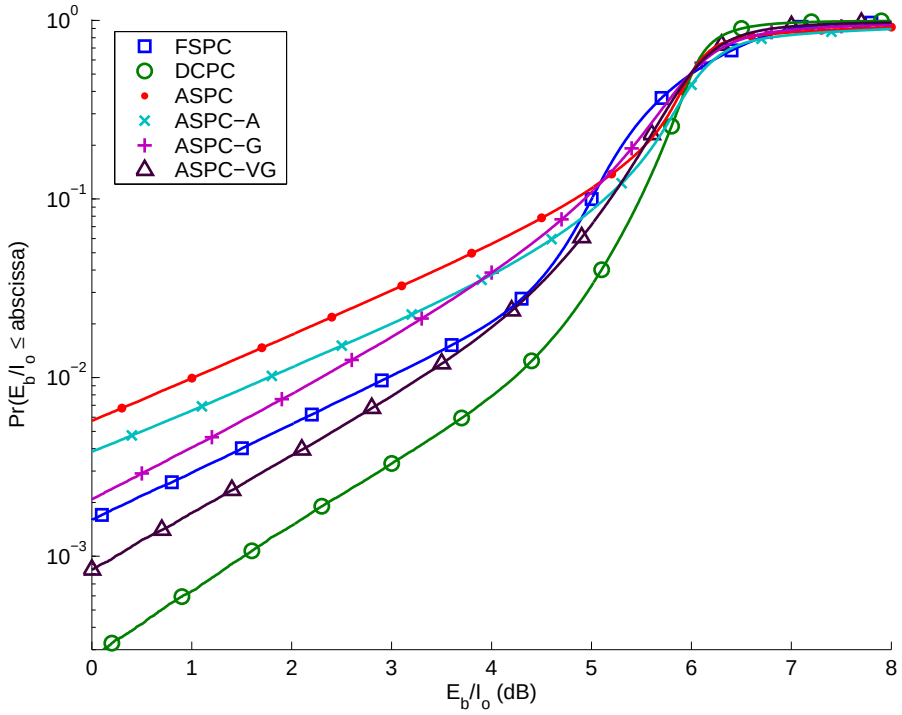

Figure 6.12: Empirical CDF of E_b/I_o, mobile speeds from 0 to 30 km/h.

6.7 Discussion

The ASPC algorithm and its modifications clearly have some interesting properties. Compared to the FSPC algorithm, they are able to significantly decrease the variance of the PC misadjustment without any increase in power control signaling, only one bit is still needed for the PC feedback command. The ASPC-VG algorithm is particularly interesting in its ability to improve the convergence speed of ASPC even close to that of the DCPC algorithm.

As mentioned earlier, the ASPC algorithm and its modifications are combinations of the FSPC and DCPC algorithms with the proposed step-size adaptation methods. These methods could of course be combined with any other algorithms. In Chapter 7 an example of combining the AS method with the MVD-PC algorithm is presented. Moreover, if the information of the SIR target $\gamma^t(t)$ is available to the mobile station (in uplink case), then an reconstruction $\tilde{\gamma}(t)$ of the SIR at the base station can be calculated in the mobile station as $\tilde{\gamma}(t) = \gamma^t(t) - \tilde{e}(t)$. This approach is used in [17] to construct a decision feedback version of the MODPC algorithm called the *Multi-Objective Totally Distributed Power Control (MOTDPC) Algorithm*.

The ASPC algorithm was shown to perform very well at slow mobile speeds, but the performance deteriorates at higher speeds due to the fixed update step size. From the proposed modifications, the ASPC-VG algorithm is most efficient, and works well also with high mobile speeds.

Chapter 7

Combinations and special cases

7.1 Introduction

In this Chapter some special cases with the proposed algorithms are studied. First, the self-tuning control based algorithms proposed in Chapter 4 are combined with the adaptive step size methods of Chapter 6, and with the time delay compensation (TDC) scheme from [106, 107, 77]. It is shown that the combinations can in some cases give further increase in the performance of the basic algorithms. Also the effects of some non-idealities – such as SIR estimation errors and power control command bit errors – to the performance of the algorithms are studied. As a last case, the performance of the algorithms in soft handover is studied.

7.2 Combining the AS method with TDC and other PC algorithms

As discussed in Chapter 6, the AS method and its variations can be combined also with other PC algorithms. Also, the TDC method can be combined with the ASPC algorithm and its modifications. In this Section the performances of various combinations of the AS and TDC methods and the algorithms from Chapter 4 are studied.

Fig. 7.1 shows the empirical CDFs of combinations of the FSPC, MVD-PC and ASPC algorithms with the TDC, AS and AS-VG methods. The simulation was made with $v_{\min} = 0$ km/h, $v_{\max} = 5$ km/h and loop delay of 2 T_{PC}. It is seen that at in this case (with slow mobile speeds), the FSPC with TDC algorithm has similar performance to the MVD-PC algorithm, as well as the MVD-PC with TDC algorithm. The combination of MVD-PC and TDC is made so that TDC is used to compensate the loop delay, and the MVD-PC algorithm is applied as in a system with no additional loop delay, i.e., $n = 0$. The ASPC algorithm without TDC has also quite similar

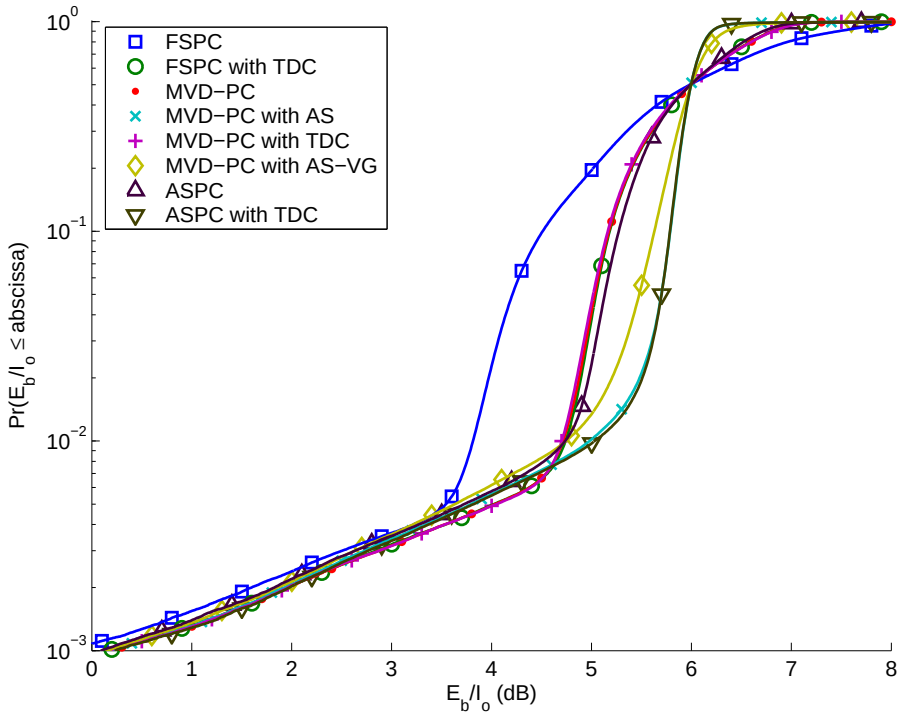

Figure 7.1: Empirical CDF of E_b/I_o, mobile speeds from 0 to 5 km/h.

performance. The combinations of ASPC with TDC and MVD-PC with AS have superior performance. Combining MVD-PC with AS-VG results in some loss of performance, however, as discussed later in this Section, the AS-VG method is a good compromise between slow-speed and high-speed performance. It is also interesting that the combination of MVD-PC algorithm with the AS methods gives good performance at slow speeds, since the MVD-PC algorithm by itself has superior performance at high speeds, as discussed later in this Section.

7.2.1 Effects of estimation errors

In the results presented so far the SIR measurements and PC commands were assumed to be error free. Next, the effects of non-ideal SIR estimation and PC command transmission are in focus. A simple model for the PC command errors (assuming 1-bit commands) is that the received command is in error with probability E_{PC} (cf. Figures 3.3 and 6.1). Also, a simple model for SIR estimation errors is to add lognormal noise to the SIR measurement. This means that the SIR in decibels is corrupted with white Gaussian noise with standard deviation σ_γ.

A simulation was made with the following parameters differing from those given in Appen-

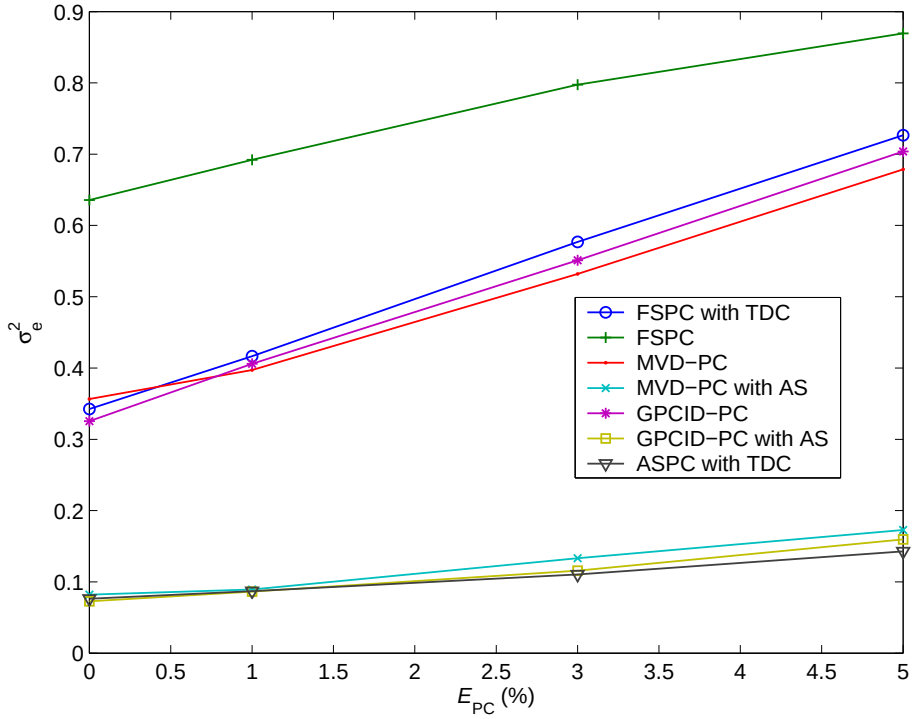

Figure 7.2: Variance of PC misadjustment versus PC command bit error probability.

dix A:

$$N = 100,$$

$$v_{\max} = 4 \text{ km/h},$$

$$v_{\min} = 4 \text{ km/h},$$

$$\text{loop delay} = 2T_{\text{PC}},$$

$$R_b = 15 \text{ kb/s}.$$

The slow speeds of the mobiles allow the PC algorithms to track the fast fading. One user initially connected to the central cell was selected for observation, and SIR data was collected from that user from a period of 6 seconds, giving 9000 SIR samples, with various values of E_{PC} and σ_γ.

Fig. 7.2 shows the variance of the PC misadjustment (σ_e^2) versus E_{PC}. It is seen that PC command errors have significant effect on the variance of the PC misadjustment. However, the effect is much smaller for algorithms employing the AS method.

Fig. 7.3 shows the variance of σ_e^2 versus σ_γ. The additive white Gaussian noise (in decibels) in the SIR measurements naturally increases the variance of the PC misadjustment. The robustness of the GPC-method is clearly visible from this figure, and the combined GPCID-PC and AS method gives the best performance.

It is seen in both figures that the algorithms proposed in the thesis can outperform the FSPC

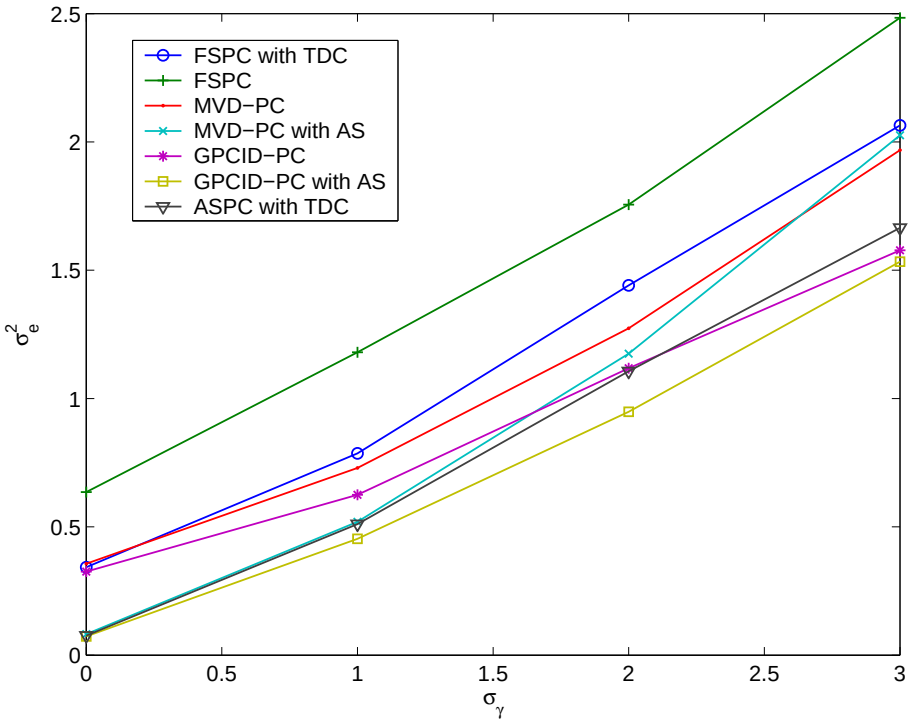

Figure 7.3: Variance of PC misadjustment versus SIR estimation error standard deviation.

algorithm with TPC when nonidealities in SIR estimation and PC command transmission are taken into account.

7.2.2 Effect of mobile speed

Fig. 7.4 shows the variance of σ_e^2 versus mobile speed, which was the same for all the users in the simulation. SIR estimation errors and PC command errors were not taken into account. This Figure clearly shows that the AS methods are most effective with mobile speed range up to about 5 km/h. However, for higher speeds, the update parameter employed in the ASPC algorithm quickly becomes too small to track the fast fading, and the performance deteriorates. The AS-VG method again maintains good performance also with higher mobile speeds while achieving almost the same performance with low speeds as the AS method. However, at higher mobile speeds, the MVD-PC and GPCID-PC algorithms clearly outperform both the FSPC with TDC and ASPC-VG with TDC algorithms.

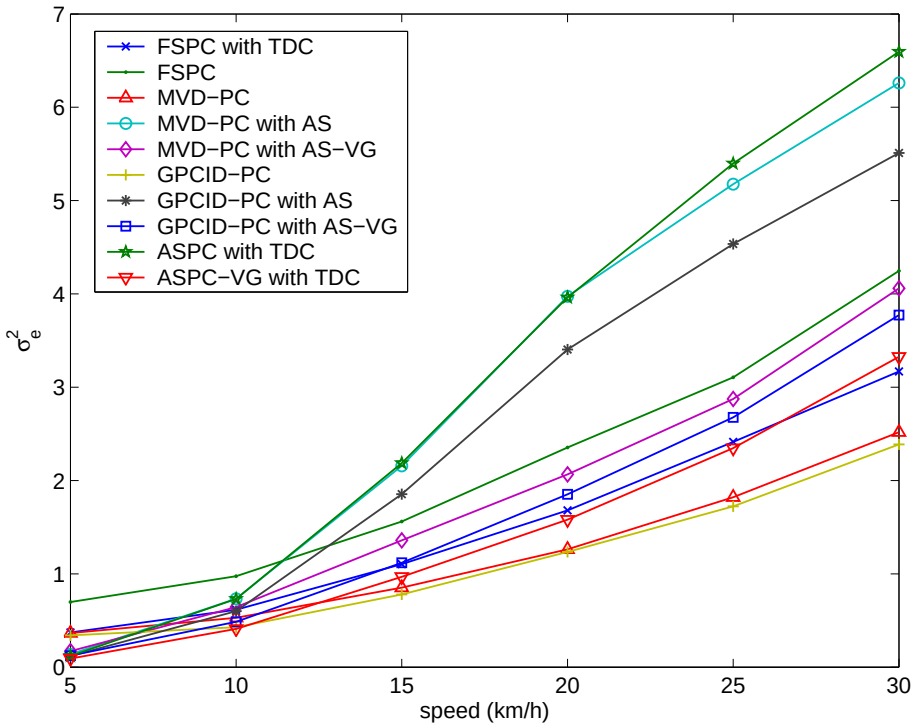

Figure 7.4: Variance of PC misadjustment versus mobile speed.

7.3 Performance in soft handovers

Power control in soft handovers was discussed in Section 3.1.4. From that discussion, it is clear that the operation of the proposed algorithms during soft handovers needs special consideration.

7.3.1 Adaptive self-tuning control based algorithms from Chapter 4

These algorithms (here commonly referred to as *adaptive algorithms*) rely on parameterized system model, and the model parameters are updated at every step during the operation of the algorithms. In the uplink, when a mobile station is engaged in soft handover with another base station, the new base station should start parameter estimation for that mobile station. However, neither of the base stations can be sure that the mobile station followed their command. Thus, the parameter estimation should be disabled during soft handover. For this case, two options are proposed for actions:

Option 1: All base stations in the active set use the FSPC algorithm and start the adaptive algorithm only when soft handover is over.

Option 2: The parameters (and, possibly, the covariance matrix elements) are copied from the old to the new base station, and all base stations in the active set continue using the adaptive

algorithm with the parameter estimation disabled. The parameter estimation is enabled again when soft handover is over.

If the algorithms are employed in the downlink, there are no problems, since the downlink signals transmitted by the base stations in the active set are simply regarded as separate multipath components by the RAKE receiver, and the mobile sends the same command to all the base stations in the active set. Therefore, the parameter estimation can continue normally.

The performance of the proposed algorithms in uplink was evaluated using a radio network simulator capable of simulating soft handovers. The simulator is similar to that presented in Appendix A with the following differences:

- 25 hexagonal cells are simulated
- wrap-around technique[1] is employed to avoid border effects, so data can be collected from all cells
- cell radius is 500 m
- shadowing decorrelation distance is 110 m

The mobile stations choose the base station connections based on the received downlink pilot signal strength on a frame-by-frame basis, where the frame length is 10 ms (15 PC periods). The pilot signals are averaged over the frame. The size of the active set is limited to 2, and the soft handover margin is 3 dB, which means that a secondary base station is included in the active set if its received pilot strength is less than 3 dB below that of the primary base station. For the adaptive algorithms, Option 2 above was employed during soft handovers.

Figure 7.5 shows the empirical CDFs of received E_b/I_o of the FSPC algorithm and the adaptive algorithms. In the simulation, the E_b/I_o targets were set so that the curves cross approximately at a probability level of 2 %. Table 7.1 shows the E_b/I_o targets used in the simulation.

It is seen that the algorithms perform well also with soft handovers.

7.3.2 Adaptive step-size methods of Chapter 6

The AS methods can be used also in soft handover, so that the mobile applies the method for each of the base stations in the active set. The mobile should then choose the power update that results in smallest transmission power.

[1] In wrap-around technique, the left-hand side of the simulation area is adjacent to the right-hand side, and same for the upper and lower sides, so that the two-dimensional simulation area can be viewed as the surface of a doughnut-shape.

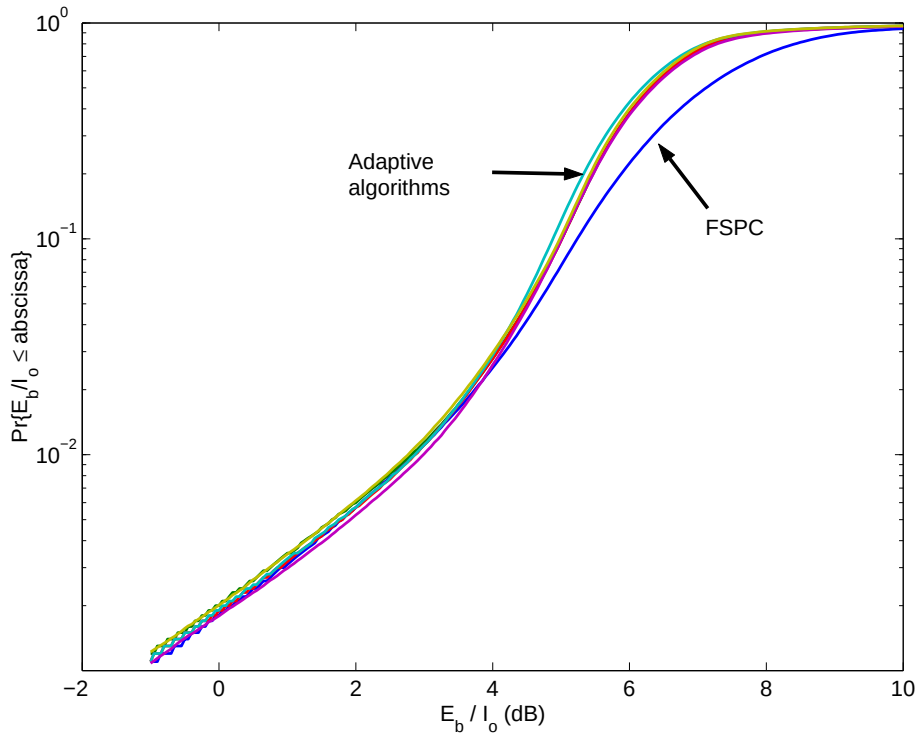

Figure 7.5: Empirical CDF of E_b/I_o, mobile speeds from 0 to 30 km/h, loop delay $2T_{\mathrm{PC}}$. Simulated algorithms are the FSPC and the adaptive algorithms MVD-PC, GMVD-PC, GMVID-PC, GPCD-PC and GPCID-PC. E_b/I_o targets are set so that the curves cross approximately at a probability level of 2 %.

Table 7.1: E_b/I_o targets used in the simulation for the algorithms.

Algorithm	E_b/I_o target
FSPC	7.00 dB
MVD-PC	6.25 dB
GMVD-PC	6.20 dB
GMVID-PC	6.05 dB
GPCD-PC	6.25 dB
GPCID-PC	6.20 dB

Figure 7.6 shows a simulation result with the FSPC, ASPC and ASPC-VG algorithms at slow mobile speeds ($0 \ldots 5$ km/h) and zero additional loop delay. It is seen that the performance of the ASPC-VG algorithm degrades as a result of soft handovers. The ASPC algorithm gives 0.7 dB gain at the 2-% probability level, but the tail of the CDF curve is much heavier than with the FSPC algorithm. It is thus concluded that the AS methods should be used with care, or even disabled, in soft handovers.

7.4 Discussion

The results presented in this thesis indicate that the algorithms proposed in this thesis offer considerable performance gains, and are able to maintain good performance under non-ideal circumstances, such as the presence of loop delays, measurement errors and PC command transmission errors.

It was also shown that the AS methods can be combined with the adaptive self-tuning-control-based algorithms and with the time delay compensation (TDC) method proposed in [106, 107, 77] with very good results.

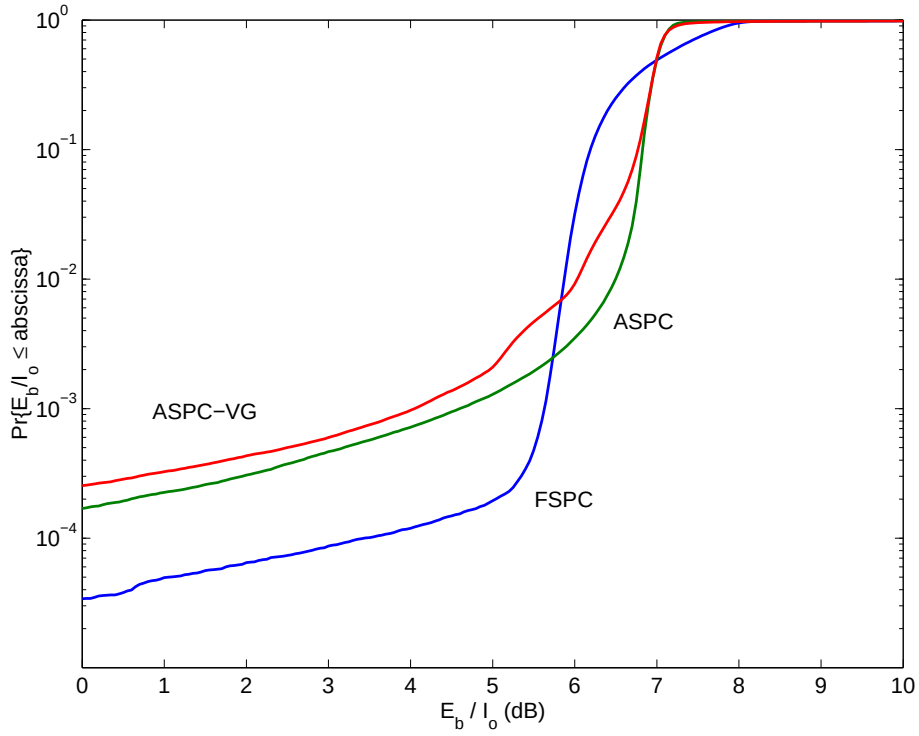

Figure 7.6: Empirical CDF of E_b/I_o, mobile speeds from 0 to 5 km/h, loop delay $1T_{\text{PC}}$, E_b/I_o target is 7 dB.

Chapter 8

Conclusions

Power control is of utmost importance in CDMA cellular communication systems. Such systems are used in the 3rd generation cellular networks, such as UMTS in Europe. These systems are targeted for a large number of subscribers and high-speed wireless multimedia services. The increasing bandwidth demands and the growing number of users call for efficient radio resource management, and thus power control, as an important part of RRM, needs to be carefully considered.

In this thesis new closed-loop power control algorithms have been developed for CDMA cellular communication systems. The algorithms can be divided into two main categories: adaptive algorithms based on self tuning control principles, and adaptive step-size algorithms. Moreover, the proposed adaptive step size methods are independent from the actual power control algorithm, and can also be combined with the other proposed adaptive algorithms.

The proposed adaptive algorithms are based on self-tuning controllers designed for a linear model of the closed-loop power control process. The process parameters are estimated recursively in real time. Three main control approaches were used in the proposed algorithms: the minimum variance (MV), generalized minimum variance (GMV) and generalized predictive controllers (GPC). The MV controller is the simplest one of these, but is not a robust technique. The GMV controller is a modification of the MV controller that aims to overcome the robustness difficulties of the MV controller. The GPC controller is the most complex of these methods, and has been shown in the literature to be highly robust against modeling errors and disturbances. The methods were utilized in various forms, with different approaches to reference tracking and control signal penalization. The algorithms were provided in information feedback (IFB) and decision feedback (DFB) forms, where the former means that the accurate control signal value is communicated to the transmitter, and the latter means that the information of the control signal is quantized to one bit, and only this bit is communicated to the transmitter. In the DFB case, the standard controller structures were also modified to take the information of the command

quantization into the controller structure.

The task of closed-loop power control is to keep the signal-to-interference (SIR) ratios at the receivers at their target values. The target values are set by outer loop power control in order to keep the frame error rates at an acceptable level with minimum possible transmission powers. Since in CDMA all users share simultaneously the same frequency band, they all interfere with one another. Therefore, the minimization of transmission powers leads to increase in capacity. The driving idea of the proposed algorithms is the minimization of the variance of the SIRs at the receivers, while keeping them at the target values. The variance minimization leads to reduction of the required SIR targets, and thus smaller transmission powers. A detailed overview of power control in CDMA cellular systems has been given in the thesis.

As demonstrated in the thesis, the loop delay inherent in the power control process can seriously degrade the performance of the power control algorithms proposed in the literature that do not take the loop delay into account. The main advantage of the proposed algorithms is that the loop delay can be included in the design process, and the histories of the previous SIR measurements and power control commands can be utilized to minimize the effect of the loop delay. The algorithms were shown in the simulations to be able to outperform the previously proposed time delay compensation scheme.

The other class of algorithms proposed in this thesis, the adaptive step-size algorithms are very attractive from implementation viewpoint due to their simplicity and excellent performance with slow-speed mobility. A drawback of the basic ASPC algorithm is that it is only applicable for slowly moving mobiles, and its performance dramatically degrades with increasing speed. Several modifications of the ASPC algorithm were proposed, and shown to be able to enhance the high-mobile-speed performance of the basic ASPC.

The proposed adaptive step (AS) methods can also be combined with the proposed adaptive algorithms in the DFB case, and with the time delay combination (TDC) scheme. Several examples of these combinations were examined in the thesis.

An analytical study of the behaviour of one of the proposed adaptive algorithms in the decision feedback case, namely the MVD-PC algorithm, was given in the thesis using discrete-time describing functions. The outcome of the analysis is a prediction of the oscillation period and amplitude at the input of the nonlinearity, which in the present case is a relay. The analysis was shown with simulations to describe the actual oscillations well.

The performances of the proposed algorithms were investigated through extensive computer simulations. The reference algorithms were the distributed constrained power control (DCPC) algorithm in the IFB case, and the fixed-step power control (FSPC) algorithm in the DFB case, combined with the TDC scheme when appropriate. The simulations indicated that significant performance improvements can be achieved with the proposed algorithms in comparison to the

reference algorithms. In the DFB case, the performance gains come with zero increase in power control signaling, i.e., using only one-bit PC commands as in the FSPC algorithm. This is interesting considering practical implementations of CDMA cellular networks.

Of the adaptive algorithms, the simple MV method (algorithms MV-PC and MVD-PC) was found to be the best choice in the case that the loop delay is correctly known. In the case of incorrect loop delay estimation, the GPC-based algorithms outperform all the other proposed adaptive algorithms and the reference algorithms. The GPC-based algorithms were also shown to be robust against measurement and command transmission errors.

The price of the performance gains of the adaptive algorithms is the increased computational complexity, which might limit the use of these algorithms to uplink only, since the base stations do not suffer from limited mobile battery power.

Of the adaptive step methods, the AS-VG method the related ASPC-VG algorithm seem to be the best compromise, giving acceptable performance at low-speed mobility, and superior performance at high-speed mobility.

8.1 Open problems

Clearly the proposed adaptive algorithms can improve the closed-loop PC performance using only local information. In some cases a part of the link gain matrix may be, at least partially, known. In [99, 160] a method called *block power control* is proposed, which utilizes the partially known link gain matrices. An interesting extension of the adaptive algorithms proposed in this thesis would be to apply similar ideas in block power control using *multivariable* self-tuning controllers, where the user interactions within a block could be taken into account in the system model.

Interesting future studies could include the extension of the proposed adaptive algorithms to jointly control power and data rate, as well as handovers.

The convergence of the AS methods was studied in the thesis by simulations. However, analytical convergence proofs are not yet available, and remain open problems.

Appendix A

Description of the radio network simulation program

In this appendix the radio network simulation program used in various parts of the thesis is described. The standard parameters used in the simulations are given, and they are used unless otherwise noted in the text.

The simulation program is implemented in MATLAB. It has seven cells in a hexagonal pattern (Figure A.1), where the cell radius is 50 m and base station height is 15 m. The users are uniformly distributed over the seven cells. The chip rate is 3.84 Mchip/s as in UMTS, which gives a processing gain of 19.3 dB if channel coding gain is ignored. The target *bit-energy-to-interference-spectral-density ratio* (E_b/I_o) is 6 dB for every user. In the beginning of the simulation, the users are assigned velocities randomly between $v_{\min}$ km/h and $v_{\max}$ km/h and a random direction of movement. These are not changed during simulation. Ideal handovers are assumed in the sense that each user is connected to the base station with the least channel attenuation at all times. The sampling rate of the simulator matches the sampling rate of the power control, which is 1.5 kHz in WCDMA.

The radio link attenuation is modeled as a product of three variables (see Section 2.2.1): the large scale propagation loss that depends on the distance between the transmitter and the receiver, log-normal shadowing with a mean of 0 dB and standard deviation of 8 dB, and motion-induced Rayleigh-distributed multipath fading generated by Jakes' model [18]. It is assumed that the receivers are able to combine two equal-strength paths with independent multipath fading. The log-normal shadowing component is correlated according to the model proposed in [44]. Moreover, the shadowing for each base station consists of two components with equal weights: one is the same for all base stations, and the other is independent from the shadowing of other base stations ([11], Section 6.4.1). The shadowing decorrelation distance is 45 m.

The simulation parameters are summarized in Table A.1. These parameters are used in the

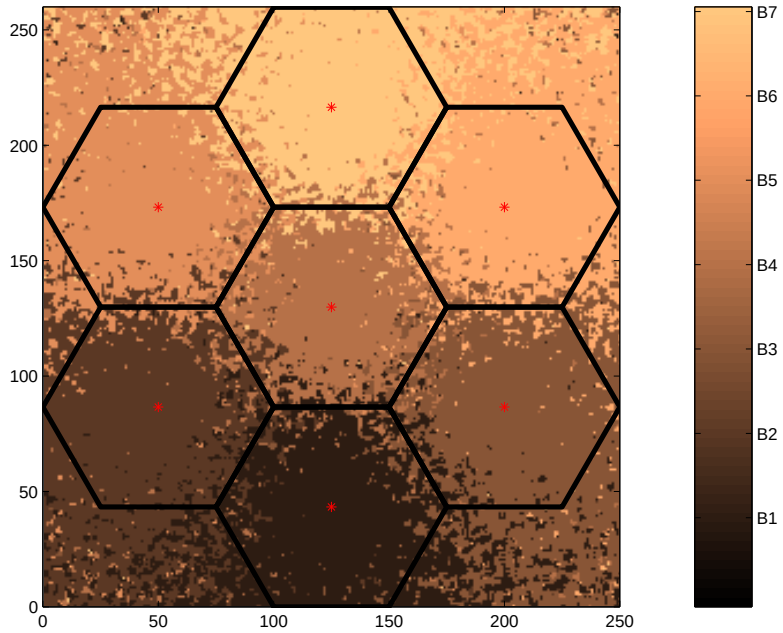

Figure A.1: A seven-cell hexagonal pattern and cell coverage areas in the radio network simulation program.

simulations unless otherwise noted in the text.

Note that with cell radius of 50 m, the assumption of the receiver being able to combine two equal strength paths is not realistic, since the difference of the distances of these two paths should exceed the length that a radio wave propagates within the time of one chip duration. For a chip rate of 3.84 Mchips/s, this length is about 78 m. Also the base station height of 15 m is not realistic. The selection of these parameters was not done by the author, as the channel model was imported from another simulator. However, the simulation scenarios were selected so that the mobile powers stayed within the minimum and maximum power limits and the system was always feasible. Also, for the speed range of the users, the employed PC update rate, and the simulation time in the simulations, the PC algorithms are always able to compensate for the path loss and shadowing. Therefore, increasing the cell size (so that the assumptions would become valid) would not have a significant impact on the simulation results. This statement was verified with the simulator employed in Section 7.3.

Table A.1: Simulation parameters.

parameter	**value**
number of users (N)	80
number of cells (N_{BS})	7
data rate (R_b)	45 kb/s
chip rate (R_c)	3.84 Mchip/s
E_b/I_o target	6 dB
base station height	15 m
path loss exponent (d)	4
shadowing standard deviation (σ_s)	8 dB
shadowing decorrelation distance (D)	45 m
max transmitter power ($p^{\max}$)	21 dBm
min transmitter power ($p^{\min}$)	-50 dBm
thermal noise power (η)	10^{-12} W
power control update rate (f_p)	1500 Hz
carrier frequency (f_c)	1950 MHz
path diversity order	2

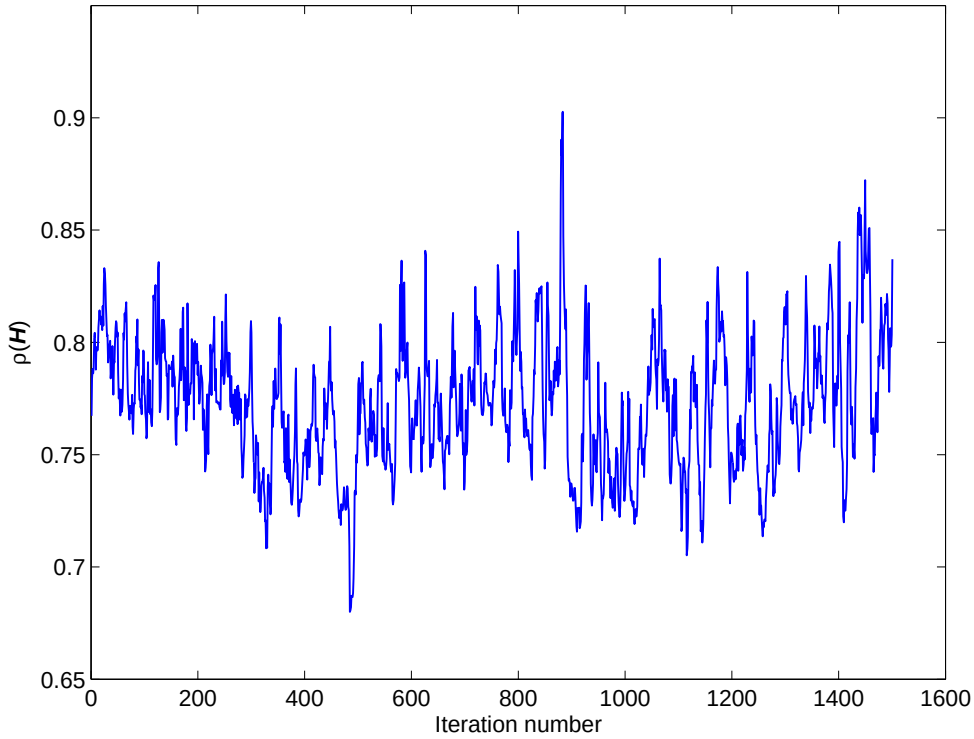

Figure A.2: An example of the evolution of system load during simulation with the default parameters.

A.1 SIR data collection

The SIR data for the simulated cumulative distribution functions (CDFs) are obtained by repeating 150 simulations, where in each simulation the network is run one second (1500 PC periods). The SIR values at all PC periods of those users initially connected to the central cell are stored, excluding the first 200 samples to allow the initial convergence PC algorithms. There are on the average $\frac{80}{7}$ users connected to the central cell. Thus, on the average $\frac{80}{7} \cdot 1300 \cdot 150 = 2\ 228\ 600$ SIR samples are used for a single CDF estimation.

A.2 System load

The parameters in Table A.1 are selected to reflect an example of a relatively highly loaded, but still feasible, system. The average system load, as measured by the spectral radius of $\boldsymbol{H}$ (see Chapter 3), in the simulations with these parameters is around 0.8. Fig. A.2 shows an example of the variation of the system load in a particular simulation.

A.3 Reliability of the simulation results

The probability distribution functions are estimated from simulation results in the following way: Let $P(\gamma \leq a)$ denote the probability of a random variable γ being less or equal to some fixed a, and let

$$F(a) = P(\gamma \leq a) \tag{A.1}$$

be the cumulative distribution function of this random variable. Then

$$\hat{F}_n(a) = \frac{\text{Number of } \gamma_i \leq a}{n} \tag{A.2}$$

is an unbiased estimator of $F(a)$ for a sample size of n [161]. Assume that the samples γ_i are independent, and the number Y of $\gamma_i \leq a$ has the binomial distribution

$$Y : \text{Bin}(p, n) \text{ with } p = F(a) \tag{A.3}$$

The mean and the variance of $\frac{Y}{n}$ are given by

$$E\left\{\frac{Y}{n}\right\} = p \quad \text{and} \quad \text{Var}\left\{\frac{Y}{n}\right\} = \frac{p(1-p)}{n} \tag{A.4}$$

It follows from the central limit theorem that for large sample sizes the error between $\hat{F}_n(a)$ and $F(a)$ has approximately a normal distribution with zero mean and a variance of $\frac{F(a)(1-F(a))}{n}$, which can be further approximated by $\frac{\hat{F}_n(a)\left(1-\hat{F}_n(a)\right)}{n}$. Thus the $100(1-c)\%$ confidence interval for $\hat{F}_n(a)$ is

$$\hat{F}_n(a) \pm z_{c/2}\sqrt{\frac{\hat{F}_n(a)\left(1-\hat{F}_n(a)\right)}{n}} \tag{A.5}$$

where z_u is the uth percentile of the standard distribution, for instance, $z_{0.025} = 1.96$ corresponds to a confidence level of 95 %. If an estimation error less than m % at a given estimated probability is required, then

$$n > \left(\frac{100 z_{c/2}}{m}\right)^2 \left(\frac{1-\hat{p}}{\hat{p}}\right) \tag{A.6}$$

where $\hat{p} = \hat{F}_n(a)$.

In the simulations it was required that at 95 % confidence level there must be less than one percent error at estimated probability level of $\hat{F}_n(a) = 0.02$ when using the assumptions above. Thus, (A.6) gives $n > 1\ 882\ 384$, which is well below the value calculated in Section A.1. Note, that the velocities of the mobiles affect the fading rates, which in turn affect the CDF calculation. However, since the generated environments and fading processes at a single simulation were the same for all the PC algorithms, this will only have a small effect on the exact positions of the CDF curves, but very little effect on the relative positions of the CDF curves between the algorithms.

A.4 Interpretation of the results

Most of the results presented in this thesis are given in the form of empirical CDFs. Some examples are given, where the CDF curves obtained with different PC algorithms are compared at the 2-% probability level, and the gain of a particular algorithm compared to another algorithm is given as the difference of the E_b/I_o values of the respective CDF curves at this level. This definition of the gain is based on the assumptions made in Section 4.2.3, i.e., if the gain is positive, then the SIR target for the same outage probability level can be lowered by the value of the gain. This naturally has a positive effect on capacity, since lower E_b/I_o targets lead to lower transmission powers and, therefore, less interference. A more accurate way of presenting the results would be to seek the required SIR target for each algorithm to achieve the 2-% outage probability with a certain SIR threshold. This is the approach aimed at in the soft handover simulation presented in Section 7.3, although the curves in that simulation do not exactly cross at the 2-% probability level (they are within 0.1 dB of each other). An accurate matching would considerably increase the required simulation times, hence the aforementioned approach is used in all other simulations. Moreover, the simulation presented in Section 7.3 was done by first doing the simulation with a common SIR target, and then doing the same simulation with the SIR targets adjusted by the amount that the probability curves differed at the 2-% probability level. This indicates that the common SIR target approach gives reasonably accurate results.

A simple argument on the amount of capacity enhancement can be made by assuming that the capacity in terms of the maximum possible number of supported users is inversely proportional to the required E_b/I_o targets. This assumption is well supported by the analytical capacity studies in the literature (see, e.g., [12, 11]). Thus, the E_b/I_o gains reported in this Chapter can be directly translated to percentual capacity gains in terms of the possible number of supported users. Formally,

$$\text{Capacity increase} = \left(10^{G_e/10} - 1\right) \cdot 100\ \%, \tag{A.7}$$

where G_e is the E_b/I_o gain in decibels. For example, gains of 0.5 dB, 1 dB and 1.5 dB correspond to capacity enhancements of 12.2 %, 25.9 % and 41.3 %, respectively. These capacity gains should be viewed as upper bounds, as the actual capacity enhancement depends on the ability of the outer loop power control to set the E_b/I_o targets to appropriate levels.

Appendix B

Shift operator calculus

This appendix explains the shift operator calculus employed in this thesis. It is widely used in control theory that is the origin of the methods on which the algorithms proposed in Chapter 4 are built.

The *forward shift operator* is denoted by q. It has the property

$$qx(t) = x(t+1). \tag{B.1}$$

Similarly, the *backward shift operator* is denoted by q^{-1}, and it has the property

$$q^{-1}x(t) = x(t-1). \tag{B.2}$$

With the aid of these operators, the manipulation of difference equations becomes more compact. Consider the difference equation

$$y(t) + a_1 y(t-1) + \cdots + a_{n_a} y(t-n_a) = b_0 u(t-k) + \cdots + b_{n_b} u(t-k-n_b). \tag{B.3}$$

Define the following polynomials in the backward shift operator:

$$\begin{aligned} A(q^{-1}) &= 1 + a_1 q^{-1} + \cdots + a_{n_a} q^{-n_a}, \\ B(q^{-1}) &= b_0 + b_1 q^{-1} + \cdots + b_{n_b} q^{-n_b}. \end{aligned} \tag{B.4}$$

With these polynomial operators, the difference equation (B.3) can be represented as

$$A(q^{-1})y(t) = q^{-k} B(q^{-1}) u(t). \tag{B.5}$$

Operations such as multiplication of a difference equation by an arbitrary polynomial in q^{-1} and addition or subtraction of equations are allowed in this calculus. However, allowing the division by an arbitrary polynomial in q^{-1} requires some care. Specifically, allowing this division implies that all initial conditions for the difference equation are zero. This is the convention used in this thesis. More discussion on the shift operator calculus can be found from [162].

Appendix C

Model identification methods

For ARX models, (4.10) can be cast in the form [151]

$$y(t) = \boldsymbol{x}^T(t)\boldsymbol{\theta} + \xi(t) \tag{C.1}$$

where

$$\boldsymbol{\theta} = [a_1 \dots a_{n_a} \quad b_0 \dots b_{n_b}]^T \tag{C.2}$$

and

$$\boldsymbol{x}(t) = [-y(t-1) \dots -y(t-n_a) \quad u(t-k) \dots u(t-k-n_b)]^T \tag{C.3}$$

For ARIX models, (4.12) can be put in the form

$$\Delta y(t) = \boldsymbol{x}^T(t)\boldsymbol{\theta} + \xi(t) \tag{C.4}$$

where $\boldsymbol{\theta}$ is as before and

$$\boldsymbol{x}(t) = [-\Delta y(t-1) \dots -\Delta y(t-n_a) \quad \Delta u(t-k) \dots \Delta u(t-k-n_b)]^T \tag{C.5}$$

Equations (C.1) and (C.4) are in the familiar linear regression form, which can be used for recursive estimation of the parameter vector $\boldsymbol{\theta}$. The Recursive Least Squares (RLS) algorithm with exponential forgetting is used for the estimation. The RLS equations are

$$\epsilon(t) = y(t) - \boldsymbol{x}^T(t)\hat{\boldsymbol{\theta}}(t-1) \tag{C.6}$$

$$\boldsymbol{P}(t) = \frac{1}{\alpha_f}\boldsymbol{P}(t-1)\left[\boldsymbol{I} - \frac{\boldsymbol{x}(t)\boldsymbol{x}^T(t)\boldsymbol{P}(t-1)}{\alpha_f + \boldsymbol{x}^T(t)\boldsymbol{P}(t-1)\boldsymbol{x}(t)}\right] \tag{C.7}$$

$$\hat{\boldsymbol{\theta}}(t) = \hat{\boldsymbol{\theta}}(t-1) + \boldsymbol{P}(t)\boldsymbol{x}(t)\epsilon(t) \tag{C.8}$$

where $\epsilon(t)$ is the prediction error, $\boldsymbol{P}(t)$ is the inverse of the covariance matrix of the parameter estimates at iteration t, α_f is the forgetting factor and $\hat{\boldsymbol{\theta}}(t)$ is a vector containing the parameter estimates at time t, i.e.,

$$\hat{\boldsymbol{\theta}}(t) = \left[\hat{a}_1(t) \dots \hat{a}_{n_a}(t) \quad \hat{b}_0(t) \dots \hat{b}_{n_b}(t)\right]^T \tag{C.9}$$

For ARMAX and ARIMAX models, $n_c > 0$ and thus information of the previous values of the noise sequence $\{\xi(t)\}$ are needed for estimation of the parameters. However, $\{\xi(t)\}$ cannot be observed (it is a white Gaussian noise sequence). The solution is to replace the previous values of $\{\xi(t)\}$ with previous values of either the prediction error $\epsilon(t) = y(t) - \boldsymbol{x}^T(t)\hat{\boldsymbol{\theta}}(t-1)$ or the *residual* $\phi(t) = y(t) - \boldsymbol{x}^T(t)\hat{\boldsymbol{\theta}}(t)$ (for ARIMAX models, replace $y(t)$ with $\Delta y(t)$). The resulting algorithms are called the *Recursive Extended Least Squares* (RELS) algorithm and the *Approximate Maximum Likelihood* (AML) algorithm, respectively.

The following equations apply for ARMAX models. For ARIMAX models, replace $y(t)$ with $\Delta y(t)$ and $u(t)$ with $\Delta u(t)$.

The RELS algorithm is given as follows. Define

$$\hat{\boldsymbol{\theta}}_{\mathrm{E}}(t) = \begin{bmatrix} \hat{a}_1(t) \dots \hat{a}_{n_a}(t) & \hat{b}_0(t) \dots \hat{b}_{n_b}(t) & \hat{c}_1(t) \dots \hat{c}_{n_c}(t) \end{bmatrix}^T \tag{C.10}$$

$$\begin{aligned} \boldsymbol{\Phi}(t) = \Big[& -y(t-1) \dots -y(t-n_a) \\ & u(t-k) \dots u(t-k-n_b) \quad \epsilon_{\mathrm{E}}(t-1) \dots \epsilon_{\mathrm{E}}(t-n_c) \Big]^T \end{aligned} \tag{C.11}$$

where

$$\epsilon_{\mathrm{E}}(t) = y(t) - \boldsymbol{\Phi}^T(t)\hat{\boldsymbol{\theta}}_{\mathrm{E}}(t-1) \tag{C.12}$$

The RELS equations are

$$\boldsymbol{P}(t) = \frac{1}{\alpha_f}\boldsymbol{P}(t-1)\left[\boldsymbol{I} - \frac{\boldsymbol{\Phi}(t)\boldsymbol{\Phi}^T(t)\boldsymbol{P}(t-1)}{\alpha_f + \boldsymbol{\Phi}^T(t)\boldsymbol{P}(t-1)\boldsymbol{\Phi}(t)}\right] \tag{C.13}$$

$$\hat{\boldsymbol{\theta}}_{\mathrm{E}}(t) = \hat{\boldsymbol{\theta}}_{\mathrm{E}}(t-1) + \boldsymbol{P}(t)\boldsymbol{\Phi}(t)\epsilon_{\mathrm{E}}(t) \tag{C.14}$$

The AML algorithm can be expressed as a modification of the RELS algorithm by replacing the RELS data vector $\boldsymbol{\Phi}(t)$ with

$$\begin{aligned} \boldsymbol{\Psi}(t) = \Big[& -y(t-1) \dots -y(t-n_a) \\ & u(t-k) \dots u(t-k-n_b) \quad \phi_{\mathrm{E}}(t-1) \dots \phi_{\mathrm{E}}(t-n_c) \Big]^T \end{aligned} \tag{C.15}$$

where

$$\phi_{\mathrm{E}}(t) = y(t) - \boldsymbol{\Psi}^T(t)\hat{\boldsymbol{\theta}}_{\mathrm{E}}(t-1) \tag{C.16}$$

and replacing (C.13) and (C.14) with

$$\boldsymbol{P}(t) = \frac{1}{\alpha_f}\boldsymbol{P}(t-1)\left[\boldsymbol{I} - \frac{\boldsymbol{\Psi}(t)\boldsymbol{\Psi}^T(t)\boldsymbol{P}(t-1)}{\alpha_f + \boldsymbol{\Psi}^T(t)\boldsymbol{P}(t-1)\boldsymbol{\Psi}(t)}\right] \tag{C.17}$$

$$\hat{\boldsymbol{\theta}}_{\mathrm{E}}(t) = \hat{\boldsymbol{\theta}}_{\mathrm{E}}(t-1) + \boldsymbol{P}(t)\boldsymbol{\Psi}(t)\epsilon_{\mathrm{E}}(t) \tag{C.18}$$

Appendix D

The adaptive closed-loop power control algorithms proposed in Chapter 4

D.1 Minimum variance based algorithms

D.1.1 MV-PC algorithm

The minimum variance power control (MV-PC) algorithm is:

1. Read the current SIR measurement $\gamma(t)$ and SIR target $\gamma^t(t)$. Assign $y(t) = \gamma(t)$ and $r(t) = \gamma^t(t)$.
2. Estimate the system parameters (coefficients of A, B and C) using one of the identification methods described in Appendix C and the modified process model (4.29).
3. Calculate F and G using (4.15).
4. Calculate $u(t)$ using (4.27).
5. If $|r(t) - y(t)| > \delta_e$ or $|u(t)| > \delta_u$, set $u(t) = \delta \text{sign}\,(r(t) - y(t))$.
6. Adjust the transmission power according to $p(t) = p(t-1) + u(t)$.
7. Set $t = t + 1$ and go back to step 1.

D.1.2 MVI-PC algorithm

The minimum variance incremental power control (MVI-PC) algorithm is:

1. Read the current SIR measurement $\gamma(t)$ and SIR target $\gamma^t(t)$. Assign $y(t) = \gamma(t)$ and $r(t) = \gamma^t(t)$.

2. Estimate the system parameters (coefficients of A, B and C) using one of the identification methods described in Appendix C and the process model (4.9).

3. Calculate F and G using (4.31).

4. Calculate $u(t)$ using (4.30).

5. If $|r(t) - y(t)| > \delta_e$ or $|u(t)| > \delta_u$, set $u(t) = \delta \text{sign}\,(r(t) - y(t))$ and recalculate $\Delta u(t) = u(t) - u(t-1)$.

6. Adjust the transmission power according to $p(t) = p(t-1) + u(t)$.

7. Set $t = t + 1$ and go back to step 1.

D.1.3 MVD-PC algorithm

The minimum variance decision feedback power control (MVD-PC) algorithm is the same as the MV-PC algorithm with the following modifications:

Step 4: Calculate $\tilde{u}(t)$ and $u(t)$ using (4.33) and (4.34).

Step 5: If $|r(t) - y(t)| > \delta_e$ or $|\tilde{u}(t)| > \delta_u$, set $u(t) = \delta \text{sign}\,(r(t) - y(t))$.

D.1.4 MVID-PC algorithm

The minimum variance incremental decision feedback power control (MVID-PC) algorithm is the same as the MVI-PC algorithm with the following modifications:

Step 4: Calculate $\tilde{u}(t)$ and $u(t)$ using (4.36) and (4.37).

Step 5: If $|r(t) - y(t)| > \delta_e$ or $|\tilde{u}(t)| > \delta_u$, set $u(t) = \delta \text{sign}\,(r(t) - y(t))$ and recalculate $\Delta u(t) = u(t) - u(t-1)$.

D.2 Generalized minimum variance based algorithms

D.2.1 GMV1-PC algorithm

The generalized minimum variance power control (GMV-PC) algorithm is the same as the MV-PC algorithm with the following modifications:

Step 3: Calculate F, G and H from (4.44-4.48).

Step 4: Calculate $u(t)$ using (4.46).

D.2.2 GMVD-PC algorithm

The generalized minimum variance decision feedback power control (GMVD-PC) algorithm is the same as the GMV-PC algorithm with the following modifications:

Step 4: Calculate $\tilde{u}(t)$ and $u(t)$ using (4.56) and (4.57).

Step 5: If $|r(t) - y(t)| > \delta_e$ or $|\tilde{u}(t)| > \delta_u$, set $u(t) = \delta \text{sign}\,(r(t) - y(t))$.

D.2.3 GMVI-PC and GMVID-PC algorithms

These algorithms have $(1 - q^{-1})$ as a factor of Q. Otherwise they are the same as their nonincremental counterparts.

D.3 Generalized predictive control based algorithms

D.3.1 GPC-PC algorithm

The generalized predictive power control (GPC-PC) algorithm is:

1. Read the current SIR measurement $\gamma(t)$ and SIR target $\gamma^t(t)$. Assign $y(t) = \gamma(t)$ and $r(t+j) = \gamma^t(t), \quad j = 0 \ldots N$.[1]
2. Calculate $w(t+k), w(t+k+1), \ldots, w(t+k+N-1)$ from (4.61).
3. Estimate the system parameters (coefficients of A, B and C) using one of the identification methods described in Appendix C and the process model (4.59).
4. Calculate $\boldsymbol{f}$, $\boldsymbol{w}$ and $\boldsymbol{G}$ from (4.73), (4.75) and (4.72).
5. Form matrix $\tilde{\boldsymbol{G}}$ by taking into it the first N_u columns of $\boldsymbol{G}$.
6. Calculate $u(t)$ from (4.78) and (4.77).
7. If $|r(t) - y(t)| > \delta_e$ or $|u(t)| > \delta_u$, set $u(t) = \delta \text{sign}\,(r(t) - y(t))$ and recalculate $\Delta u(t) = u(t) - u(t-1)$.
8. Adjust the transmission power according to $p(t) = p(t-1) + u(t)$.

[1] In practical CDMA systems $\gamma^t(t)$ is constant over a frame (e.g. in UMTS the frame length is 15 PC sampling periods). In the case that the prediction interval $t+1, \ldots, t+N$ goes over the frame boundary, an estimated value of $\gamma^t(t+j)$ can be applied for those corresponding values of $r(t+j)$ that go over the frame boundary. If the outer-loop PC algorithm described in section 3.1.3 is used, then a possible estimation for these values would be to assume no frame errors to happen, in which case the γ^t after frame boundary would be equal to γ^t before frame boundary minus Δ_{down}.

9. Set $t = t + 1$ and go back to step 1.

D.3.2 GPCD-PC algorithm

The generalized predictive decision feedback power control (GPCD-PC) algorithm is the same as GPC-PC algorithm with the following modifications:

Step 6: Calculate $\Delta\tilde{u}(t)$, $u(t)$ and $\Delta u(t)$ from (4.79-4.81).

Step 7: If $|r(t) - y(t)| > \delta_e$ or $|\tilde{u}(t)| > \delta_u$, set $u(t) = \delta \text{sign}\,(r(t) - y(t))$ and recalculate $\Delta u(t) = u(t) - u(t-1)$.

D.3.3 GPCI-PC and GPCID-PC algorithms

In these algorithms the control increment $\Delta u(t)$ is used as power update command instead of $u(t)$. Thus, the following modifications are made to GPC-PC:

6) GPCI-PC: Calculate $\Delta u(t)$ from (4.78) and (4.77).
GPCID-PC: Calculate $\Delta\tilde{u}(t)$ and $\Delta u(t)$ from (4.78), (4.79) and (4.82).

7) If $|r(t) - y(t)| > \delta_e$ or $|\Delta u(t)| > \delta_u$ or $|\Delta\tilde{u}(t)| > \delta_u$, set $\Delta u(t) = \delta \text{sign}\,(r(t) - y(t))$.

8) Adjust the transmission power according to $p(t) = p(t-1) + \Delta u(t)$.

Bibliography

[1] *Technical Specification 25.858 V5.0.0. High Speed Downlink Packet Access: Physical Layer Aspects*, The 3rd Generation Partnership Project (3GPP).

[2] T. Ojanperä and R. Prasad, Eds., *Wideband CDMA for Third Generation Mobile Communications*. London: Artech House, 1998.

[3] H. Holma and A. Toskala, Eds., *WCDMA for UMTS*. West Sussex: John Wiley & Sons, 2000.

[4] 3GPP. (2004) The 3rd Generation Partnership Project (3GPP) home page. [Online]. Available: http://www.3gpp.org

[5] S. Moshavi, "Multi-user detection in DS-CDMA communications," *IEEE Commun. Mag.*, vol. 34, no. 10, pp. 124–136, Oct. 1996.

[6] G. Calhoun, Ed., *Digital Cellular Radio*. Norwood, MA: Artech House, 1988.

[7] R. Steele and L. Hanzo, Eds., *Mobile Radio Communications*, 2nd ed. England: John Wiley & Sons, 1999.

[8] P. Jung, P. W. Baier, and A. Steil, "Advantages of CDMA and spread spectrum techniques ofer FDMA and TDMA in cellular mobile radio applications," *IEEE Trans. Veh. Technol.*, vol. 42, no. 3, pp. 357–364, Aug. 1993.

[9] K. S. Gilhousen, I. M. Jacobs, R. Padovani, A. J. Viterbi, L. A. Weaver, Jr., and C. E. Wheatley III, "On the capacity of a cellular CDMA system," *IEEE Trans. Veh. Technol.*, vol. 40, no. 2, pp. 303–312, May 1991.

[10] J. D. Gibson, Ed., *The Mobile Communications Handbook*, 2nd ed. Boca Raton, FL: CRC Press, 1999.

[11] A. J. Viterbi, *CDMA: Principles of Spread Spectrum Communication*. Reading, MA: Addison-Wesley Publishing Company, 1995.

[12] A. M. Viterbi and A. J. Viterbi, "Erlang capacity of a power controlled CDMA system," *IEEE J. Select. Areas Commun.*, vol. 11, no. 6, pp. 892–899, Aug. 1993.

[13] J. G. Proakis, *Digital Communications*, 3rd ed. Singapore: McGraw-Hill, 1995.

[14] L. Milstein, "Wideband code division multiple access," *IEEE J. Select. Areas Commun.*, vol. 18, no. 8, pp. 1344–1354, Aug. 2000.

[15] M. S. Elmusrati, M. Rintamäki, I. Hartimo, and H. Koivo, "Estimated step power control algorithm for wireless communication systems," in *Proc. Finnish Signal Processing Symposium*, Tampere, Finland, May 2003, pp. 32–34.

[16] ——, "Fully distributed power control algorithm with one bit signaling and nonlinear error estimation," in *Proc. IEEE Veh. Tech. Conf. (VTC)*, Orlando, FL, USA, Oct. 2003, pp. 727–731.

[17] M. S. Elmusrati, "Radio resource scheduling and smart antennas in cellular CDMA communication systems," Ph.D. dissertation, Helsinki University of Technology, Espoo, Finland, 2004.

[18] W. C. Jakes, *Microwave Mobile Communications*. New York: John Wiley & Sons, 1974.

[19] J. D. Parsons, *The Mobile Radio Propagation Channel*. London: Pentech Press Publishers, 1992.

[20] M. D. Yacoub, *Foundations of Mobile Radio Engineering*. Boca Raton, FL: CRC Press, 1993.

[21] G. L. Stüber, *Principles of Mobile Communication*, 2nd ed. Boston, MA: Kluwer Academic Publishers, 2000.

[22] ePanorama.net. (2004) Mobile communications page. [Online]. Available: http://www.epanorama.net/links/tele_mobile.html

[23] J. D. Gibson, Ed., *The Communications Handbook*. Boca Raton, FL: CRC Press, 1997.

[24] I. A. Glover and P. M. Grant, *Digital Communications*. Cornwall, UK: Prentice-Hall, 1998.

[25] C. E. Shannon, "A mathematical theory of communication," *Bell Syst. Tech. J.*, vol. 27, pp. 379–423, July 1948.

[26] ——, “A mathematical theory of communication,” *Bell Syst. Tech. J.*, vol. 27, pp. 623–656, Oct. 1948.

[27] ——, “The zero error capacity of a noisy channel,” *IRE Trans. Inform. Theory*, vol. 2, pp. 8–19, Sept. 1956.

[28] T. G. Association. (2004) GSM World – the website of the GSM Association. [Online]. Available: http://www.gsmworld.com

[29] J. Cai and D. J. Goodman, “General packet radio service in GSM,” *IEEE Commun. Mag.*, vol. 35, no. 10, pp. 122–131, Oct. 1997.

[30] R. Dettmer, “Mobilising packet data,” *IEE Review*, vol. 47, no. 4, pp. 9–14, July 2001.

[31] D. Calin and D. Zeghlache, “High speed circuit switched data over gsm: Potential traffic policies,” in *Proc. IEEE Veh. Tech. Conf. (VTC)*, vol. 2, May 1998, pp. 1274–1278.

[32] C. Scholefield, “Evolving GSM data services,” in *Conf. Record IEEE Int. Conf. on Universal Personal Commun.*, vol. 2, Oct. 1997, pp. 888–892.

[33] P. Chaudhury, W. Mohr, and S. Onoe, “The 3GPP proposal for IMT-2000,” *IEEE Commun. Mag.*, vol. 37, no. 12, pp. 72–81, Dec. 1999.

[34] A. K. Salkintzis, “Packet data over cellular networks: the CDPD approach,” *IEEE Commun. Mag.*, vol. 37, no. 6, pp. 152–159, June 1999.

[35] Y.-B. Lin, “Cellular digital packet data,” *IEEE Potentials*, vol. 16, no. 3, pp. 11–13, Aug.-Sept. 1997.

[36] D. N. Knisely, S. Kumar, S. Laha, and S. Nanda, “Evolution of wireless data services: IS-95 to cdma2000,” *IEEE Commun. Mag.*, vol. 36, no. 10, pp. 140–149, Oct. 1998.

[37] A. Furuskär, S. Mazur, F. Müller, and H. Olofsson, “EDGE: Enhanced data rates for GSM and TDMA/136 evolution,” *IEEE Pers. Commun.*, vol. 6, no. 3, pp. 56–66, June 1999.

[38] Ericsson. (2004) This is GSM/EDGE/WCDMA. [Online]. Available: http://www.ericsson.com

[39] 3GPP2, “The 3rd Generation Partnership Project 2 (3GPP2) home page,” 2004. [Online]. Available: http://www.3gpp2.org

[40] UMTSWorld.com, “UMTSWorld home page,” 2005. [Online]. Available: http://www.umtsworld.com

[41] B. Sklar, *Digital Communications, Fundamentals and Applications*, 2nd ed. Upper Saddle River, NJ: Prentice-Hall, 2001.

[42] Y. Okumura, E. Ohmori, T. Kawano, and K. Fukuda, "Field strength and its variability in VHF and UHF land-mobile radio service," *Rev. of the Electrical Commun. Lab.*, vol. 16, no. 9-10, pp. 825–873, Sept.-Oct. 1968.

[43] M. Hata, "Empirical formula for propagation loss in land mobile radio services," *IEEE Trans. Veh. Technol.*, vol. 29, no. 3, pp. 317–325, Aug. 1980.

[44] R. Gudmundson, "Correlation model for shadow fading in mobile radio systems," *Electronics Letters*, vol. 27, no. 23, pp. 2145–2146, Nov. 1991.

[45] W. C. Y. Lee, "Overview of cellular CDMA," *IEEE Trans. Veh. Technol.*, vol. 40, no. 2, pp. 291–302, May 1991.

[46] M. Rintamäki, "Power control in CDMA cellular communication systems," in *Wiley Encyclopedia of Telecommunications*, J. G. Proakis, Ed. John Wiley & Sons, 2002.

[47] W. C. Y. Lee, "Power control in CDMA (cellular radio)," in *Proc. IEEE Veh. Tech. Conf. (VTC)*, St. Louis, Missouri, USA, May 1991, pp. 77–80.

[48] M. K. Simon and M.-S. Alouini, "A unified approach to the performance analysis of digital communication over generalized fading channels," *Proc. IEEE*, vol. 86, no. 9, pp. 1860–1877, Sept. 1998.

[49] A. Baier, U.-C. Fiebig, W. Granzow, W. Koch, P. Teder, and J. Thielecke, "Design study for a CDMA-based third generation mobile radio system," *IEEE J. Select. Areas Commun.*, vol. 12, no. 4, pp. 733–743, May 1994.

[50] W. Tschirks, "Effects of transmission power control on the cochannel interference in cellular radio networks," *Electrotechnik und Informationstechnik*, vol. 106, no. 5, 1989.

[51] T. Fujii and M. Sakamoto, "Reduction of cochannel interference in cellular systems by intra-zone channel reassignment and adaptive transmitter power control," in *Proc. IEEE Veh. Tech. Conf. (VTC)*, Philadelphia, PA, USA, June 1988, pp. 668–672.

[52] T. Nagatsu, T. Tsuruhara, and M. Sakamoto, "Transmitter power control for cellular land mobile radio," in *Proc. IEEE GLOBECOM*, 1983.

[53] J. F. Whitehead, "Signal-level-based dynamic power control for co-channel interference management," in *Proc. IEEE Veh. Tech. Conf. (VTC)*, May 1993, pp. 499–502.

[54] S. Ariyavisitakul and L. F. Chang, "Signal and interference statistics of a CDMA system with feedback power control," *IEEE Trans. Commun.*, vol. 41, no. 11, pp. 1626–1634, Nov. 1993.

[55] S. Ariyavisitakul, "Signal and interference statistics of a CDMA system with feedback power control – part II," *IEEE Trans. Commun.*, vol. 42, no. 2/3/4, pp. 597–605, Feb./Mar./Apr. 1994.

[56] Y.-J. Yang and J.-F. Chang, "A strength-and-SIR-combined adaptive power control for CDMA mobile radio channels," *IEEE Trans. Veh. Technol.*, vol. 48, no. 6, pp. 1996–2004, Nov. 1999.

[57] F. Berggren, S.-L. Kim, R. Jäntti, and J. Zander, "Joint power control and intracell scheduling of DS-CDMA nonreal time data," *IEEE J. Select. Areas Commun.*, vol. 19, no. 10, pp. 1860–1870, Oct. 2001.

[58] TIA/EIA, "Mobile station-base station compatibility standard for dual-mode wideband spread spectrum cellular system," Telecommunications Industry Association," Interim Standard-95, 1993.

[59] *Technical Specification 25.214 V5.3.0. Physical Layer Procedures (FDD)*, The 3rd Generation Partnership Project (3GPP).

[60] S. Naghian, M. Rintamäki, and R. Baghaie, "Dynamic step-size power control in UMTS," in *Proc. IEEE Int. Symp. on Personal, Indoor and Mobile Radio Commun. (PIMRC)*, vol. 4, Sept. 2002, pp. 1606–1610.

[61] S. Naghian, "Location-sensitive interlligent radio resource management and its application in wcdma mobile systems," Ph.D. dissertation, Helsinki University of Technology, Espoo, Finland, 2001.

[62] A. Sampath, P. Kumar, and J. Holtzman, "On setting reverse link target SIR in a CDMA system," in *Proc. IEEE Veh. Tech. Conf. (VTC)*, vol. 2, May 1997, pp. 929–933.

[63] H. Kawai, H. Suda, and F. Adachi, "Outer-loop control of target SIR for fast transmit power control in turbo-coded W-CDMA mobile radio," *Electronics Letters*, vol. 35, no. 9, pp. 699–701, Apr. 1999.

[64] C.-S. Koo, S.-H. Shin, R. A. DiFazio, D. Grieco, and A. Zeira, "Outer loop power control using channel-adaptive processing for 3G WCDMA," in *Proc. IEEE Veh. Tech. Conf. (VTC)*, Apr. 2003, pp. 490–494.

[65] C.-J. Chang, J.-H. Lee, and F.-C. Ren, "Design of power control mechanisms with pcm realization for the uplink of a ds-cdma cellular mobile radio system," *IEEE Trans. Veh. Technol.*, vol. 45, no. 3, pp. 522–530, Aug. 1996.

[66] J.-H. Wen, J.-S. Sheu, J.-Y. Wang, J.-L. Chen, and T.-K. Woo, "A feasible method to implement optimum cir-banalnced power control in cdma cellular mobile systems," *IEEE Trans. Veh. Technol.*, vol. 52, no. 1, pp. 80–95, Jan. 2003.

[67] J.-F. Chamberland and V. V. Veeravalli, "Decentralized dynamic power control for cellular cdma systems," *IEEE Trans. Wireless Commun.*, vol. 2, no. 3, pp. 549–559, May 2003.

[68] S. Ariyavisitakul, "SIR based power control in a CDMA system," in *Proc. IEEE GLOBECOM*, Orlando, Florida, USA, Dec. 1992, pp. 868–873.

[69] J. M. Aein, "Power balancing in systems employing frequency reuse," *COMSAT Technical Review*, vol. 3, no. 2, pp. 277–300, 1973.

[70] H. Alavi and R. W. Nettleton, "Downstream power control for a spread spectrum cellular mobile radio system," in *Proc. IEEE GLOBECOM*, Miami, FL, USA, Nov. 1982, pp. 84–88.

[71] R. W. Nettleton, "Traffic theory and interference management for a spread-spectrum cellular radio system," in *Proc. IEEE Int. Conf. on Commun.*, Seattle, WA, USA, June 1980.

[72] R. W. Nettleton and H. Alavi, "Power control for a spread spectrum cellular mobile radio system," in *Proc. IEEE Veh. Tech. Conf. (VTC)*, Toronto, Canada, May 1983, pp. 242–246.

[73] S. A. Grandhi, R. Vijayan, D. J. Goodman, and Z. J., "Centralized power control in cellular radio systems," *IEEE Trans. Veh. Technol.*, vol. 42, no. 4, pp. 466–468, Nov. 1993.

[74] J. Zander, "Performance of optimum transmitter power control in cellular radio systems," *IEEE Trans. Veh. Technol.*, vol. 41, no. 1, pp. 57–62, Feb. 1992.

[75] R. Prasad and A. Kegel, "Improved assessment of interference limits in cellular radio performance," *IEEE Trans. Veh. Technol.*, vol. 40, no. 2, pp. 412–419, May 1991.

[76] J. Zander, "Transmitter power control for co-channel interference management in cellular radio systems," in *Proc. WINLAB Workshop*, New Brunswick, NF, USA, Oct. 1993.

[77] F. Gunnarsson, "Power control in cellular radio systems: Analysis, design and estimation," Ph.D. dissertation, Linköpings Universitet, Linköping, Sweden, 2000. [Online]. Available: ftp://ftp.control.isy.liu.se/pub/Reports/Ph.D.Thesis/PhD623.pdf

[78] M. Andersin, Z. Rosberg, and J. Zander, "Gradual removals in cellular PCS with constrained power control and noise," *ACM/Baltzer Wireless Networks J.*, vol. 2, pp. 27–43, 1996.

[79] J.-C. Lin, T.-H. Lee, and Y.-T. Su, "Power control algorithm for cellular radio systems," *Electronics Letters*, vol. 30, no. 3, pp. 195–197, Feb. 1994.

[80] T. H. Lee, J. C. Lin, and Y. T. Su, "Downlink power control algorithms for cellular radio systems," *IEEE Trans. Veh. Technol.*, vol. 44, no. 1, pp. 89–94, Feb. 1995.

[81] P. Godlewski and L. Nuaymi, "Auto-interference analysis in cellular systems," in *Proc. IEEE Veh. Tech. Conf. (VTC)*, Houston, TX, USA, May 1999, pp. 1994–1998.

[82] G. H. Golub and C. F. Van Loan, *Matrix Computations*, 2nd ed. London: The Johns Hopkins University Press, 1989.

[83] G. Foschini and Z. Miljanic, "A simple distributed autonomous power control algorithm and its convergence," *IEEE Trans. Veh. Technol.*, vol. 42, no. 4, pp. 641–647, Nov. 1993.

[84] J. Zander, S.-L. Kim, M. Almgren, and O. Queseth, *Radio Resource Management for Wireless Networks*. Norwood, MA: Artech House, 2001.

[85] R. D. Yates, "A framework for uplink power control in cellular radio systems," *IEEE J. Select. Areas Commun.*, vol. 13, no. 7, pp. 1341–1347, Sept. 1995.

[86] C.-Y. Huang and R. Yates, "Rate of converegence for minimum power assignment algorithms in cellular radio systems," *ACM/Baltzer Wireless Networks J.*, vol. 4, no. 3, pp. 223–231, 1998.

[87] C. W. Su and K. K. Leung, "Opportunistic power control for throughput maximization in mobile cellular systems," in *Proc. IEEE Int. Conf. on Commun.*, Paris, France, June 2004, pp. 2954–2958.

[88] ——, "A generalized framework for distributed power control in wireless networks," *IEEE Trans. Inform. Theory*, to appear.

[89] J. Zander, "Distributed cochannel interference control in cellular radio systems," *IEEE Trans. Veh. Technol.*, vol. 41, no. 3, pp. 305–311, Aug. 1992.

[90] S. A. Grandhi, R. Vijayan, and D. J. Goodman, "Distributed power control in cellular radio systems," *IEEE Trans. Commun.*, vol. 42, no. 2/3/4, pp. 226–228, Feb./Mar./Apr. 1994.

[91] T. H. Lee and J. C. Lin, "A fully distributed power control algorithm for cellular mobile systems," *IEEE J. Select. Areas Commun.*, vol. 14, no. 4, pp. 692–697, May 1996.

[92] D. Mitra, "An asynchronous distributed algorithm for power control in cellular radio systems," in *Proc. 4th WINLAB Workshop*, 1993, pp. 249–259.

[93] S. A. Grandhi, J. Zander, and R. Yates, "Constrained power control," *Wireless Personal Communications*, vol. 1, pp. 257–270, 1995.

[94] F. Berggren, R. Jäntti, and S.-L. Kim, "A generalized algorithm for constrained power control with capability of temporary removal," *IEEE Trans. Veh. Technol.*, vol. 50, no. 6, pp. 1604–1612, Nov. 2001.

[95] M. Andersin, Z. Rosberg, and J. Zander, "Distributed discrete power control in cellular pcs," in *Multiaccess, Mobility and Teletraffic for Personal Communications*, B. Jabbari, P. Godlewski, and X. Lagrange, Eds. Boston, MA, USA: Kluwer Academic Publishers, 1996, pp. 1–14.

[96] ——, "Distributed discrete power control in cellular pcs," *Wireless Personal Communications*, vol. 6, no. 3, pp. 211–231, 1998.

[97] C. C. Wu and D. P. Bertsekas, "Distributed power control algorithms for wireless networks," in *Proc. IEEE Conf. Decision and Control*, Phoenix, AZ, USA, Dec. 1999, pp. 3556–3561.

[98] Y. Xi and R. Chandramouli, "Distributed discrete power control for bursty transmissions over wireless data networks," in *Proc. IEEE Int. Conf. on Commun.*, Paris, France, June 2004.

[99] R. Jäntti, "Power control and transmission rate management in cellular radio systems - a snapshot analysis approach," Ph.D. dissertation, Helsinki University of Technology, Espoo, Finland, 2001.

[100] R. Jäntti and S.-L. Kim, "Second-order power control," *IEEE J. Select. Areas Commun.*, vol. 18, no. 3, pp. 447–457, Mar. 2000.

[101] M. S. Elmusrati and H. Koivo, "Multi-objective distributed power control algorithm," in *Proc. IEEE Veh. Tech. Conf. (VTC)*, vol. 2, Sept. 2002, pp. 812–816.

[102] ——, "Multi-objective distributed power and rate control for wireless communications," in *Proc. IEEE Int. Conf. on Commun.*, vol. 3, May 2003, pp. 1838–1842.

[103] P.-R. Chang and B.-C. Wang, "Adaptive fuzzy power control for cdma mobile radio systems," *IEEE Trans. Veh. Technol.*, vol. 45, no. 2, pp. 225–236, May 1996.

[104] ——, "Adaptive fuzzy proportional integral power control for a cellular cdma system with time delay," *IEEE J. Select. Areas Commun.*, vol. 14, no. 9, pp. 1818–1829, Dec. 1996.

[105] S. G. Glisic, *Adaptive WCDMA, Theory and Practice*. West Sussex, England: John Wiley & Sons, 2003.

[106] F. Gunnarsson, F. Gustafsson, and J. Blom, "Dynamical effects of time delays and time delay compensation in power controlled DS-CDMA," *IEEE J. Select. Areas Commun.*, vol. 19, no. 1, pp. 141–151, Jan. 2001.

[107] F. Gunnarsson and F. Gustafsson, "Time delay compensation in power controlled cellular radio systems," *Electronics Letters*, vol. 5, no. 7, pp. 295–297, July 2001.

[108] H.-S. Su and E. Geraniotis, "Adaptive closed-loop power control with quantized feedback and loop filtering," *IEEE Trans. Wireless Commun.*, vol. 1, no. 1, pp. 76–86, Jan. 2002.

[109] J. M. A. Tanskanen, J. Mattila, M. Hall, T. Korhonen, and S. J. Ovaska, "Predictive closed loop power control for mobile CDMA systems," in *Proc. IEEE Veh. Tech. Conf. (VTC)*, Phoenix, AZ, USA, May 1997.

[110] J. M. A. Tanskanen, A. Huang, and I. O. Hartimo, "Predictive power estimators in CDMA closed loop power control," in *Proc. IEEE Veh. Tech. Conf. (VTC)*, Ottawa, Ontario, Canada, May 1998.

[111] J. M. A. Tanskanen, "Polynomial predictive filters: Implementation and applications," Ph.D. dissertation, Helsinki University of Technology, Espoo, Finland, 2000. [Online]. Available: http://lib.hut.fi/Diss/2000/isbn9512256312/

[112] A. A. Mansour and A. H. Sayed, "Adaptive predictive power control for the uplink channel in ds-cdma cellular systems," *IEEE Trans. Veh. Technol.*, vol. 52, no. 6, pp. 1447–1462, Nov. 2003.

[113] M. L. Sim, E. Gunawan, B.-H. Soong, and C.-B. Soh, "Performance study of closed-loop power control algorithms for a cellular cdma system," *IEEE Trans. Veh. Technol.*, vol. 48, no. 3, pp. 911–921, May 1999.

[114] H. S. H. Gombachika, R. Tafazolli, and B. G. Evans, "Predictive power control for s-umts based on least–mean–square algorithm," in *Proc. IEE 3G Mobile Communication Technologies*, London, UK, May 2002, pp. 128–132.

[115] H. S. H. Gombachika, B. G. Evans, and R. Tafazolli, "Filter-shaped lms algorithm-based predictive power control," *Electronics Letters*, vol. 38, no. 21, pp. 1280–1281, Oct. 1902.

[116] G. Yu, H. Wang, and D. Sheng, "Advanced k-step forward prediction algorithm in wireless channel," in *Proc. IEEE Int. Conf. on Commun., Circuits and Systems*, vol. 1, Chengdu, China, June 2004, pp. 277–281.

[117] F. C. M. Lau and W. M. Tam, "Predictive closed-loop power control in cdma mobile systems," *Electronics Letters*, vol. 37, no. 1, pp. 52–54, Jan. 2001.

[118] ——, "Achievable-sir-based predictive closed-loop power control in a cdma mobile system," *IEEE Trans. Veh. Technol.*, vol. 51, no. 4, pp. 720–728, July 2002.

[119] S. Haykin, Ed., *Adaptive Filter Theory*. Englewood Cliffs, NJ: Prentice-Hall, 1986.

[120] P. Diniz, *Adaptive Filtering, Algorithms and Practical Implementation*. Boston, MA: Kluwer Academic Publishers, 1997.

[121] R. Knopp and P. A. Humblet, "Information capacity and power control in single-cell multiuser communications," in *Proc. IEEE Int. Conf. on Commun.*, June 1995, pp. 331–335.

[122] A. J. Goldsmith, "The capacity of downlink fading channels with variable rate and power," *IEEE Trans. Veh. Technol.*, vol. 46, no. 3, pp. 569–580, Aug. 1997.

[123] R. D. Yates and C.-Y. Huang, "Integrated power control and base station assignment," *IEEE Trans. Veh. Technol.*, vol. 44, no. 3, pp. 638–644, Aug. 1995.

[124] N. Bambos, S. C. Chen, and G. J. Pottie, "Channel access algorithms with active link protection for wireless communication networks with power control," *IEEE/ACM Trans. Networking*, vol. 8, no. 5, pp. 583–597, Oct. 2000.

[125] N. Bambos, "Toward power-sensitive network architectures in wireless communications: Concepts, issues, and design aspects," *IEEE Pers. Commun.*, vol. 5, no. 3, pp. 50–59, June 1998.

[126] M. Andersin, Z. Rosberg, and J. Zander, "Soft and safe admission control in cellular networks," *IEEE/ACM Trans. Networking*, vol. 5, no. 2, pp. 255–265, Apr. 1997.

[127] L. Tong and P. Ramanathan, "Adaptive power and rate allocation for service curve assurance in ds-cdma network," *IEEE Trans. Wireless Commun.*, vol. 3, no. 2, pp. 555–564, Mar. 2004.

[128] D. I. Kim, E. Hossain, and V. K. Bhargava, "Downlink joint rate and power allocation in cellular multirate wcdma systems," *IEEE Trans. Wireless Commun.*, vol. 2, no. 1, pp. 69–80, Jan. 2003.

[129] A. Yener, R. D. Yates, and S. Ulukus, "Interference management for CDMA systems through power control, multiuser detection, and beamforming," *IEEE Trans. Commun.*, vol. 49, no. 7, pp. 1227–1239, July 2001.

[130] F. Rashid-Farrokhi, L. Tassiulas, and K. J. R. Liu, "Joint optimal power control and beamforming in wireless networks using antenna arrays," *IEEE Trans. Commun.*, vol. 46, no. 10, pp. 1313–1324, Oct. 1998.

[131] Y.-C. Liang, F. P. S. Chin, and A. C. Kot, "Adaptive beamforming and power control for ds-cdma mobile radio communications," in *Proc. IEEE Int. Conf. on Commun.*, Helsinki, Finland, June 2001, pp. 1441–1445.

[132] J. C. Liberti and T. S. Rappaport, *Smart Antennas for Wireless Communications*. Upper Saddle River: Prentice-Hall, 1999.

[133] D. C. Popescu and C. Rose, "Interference avoidance and power control for uplink cdma systems," in *Proc. IEEE Veh. Tech. Conf. (VTC)*, Orlando, FL, USA, Oct. 2003, pp. 1473–1477.

[134] L. Gao and T. F. Wong, "Power control and spreading sequence allocation in a cdma forward link," *IEEE Trans. Inform. Theory*, vol. 50, no. 1, pp. 105–124, Jan. 2004.

[135] I. Virtej, M. Rintamäki, and H. Koivo, "Enhanced fast power control for WCDMA systems," in *Proc. IEEE Int. Symp. on Personal, Indoor and Mobile Radio Commun. (PIMRC)*, London, UK, Sept. 2000, pp. 1435–1439.

[136] M. Rintamäki, I. Virtej, and H. Koivo, "Two-mode fast power control for WCDMA systems," in *Proc. IEEE Veh. Tech. Conf. (VTC)*, vol. 4, Rhodos, Greece, May 2001, pp. 2893–2897.

[137] M. Rintamäki and H. Koivo, "Adaptive robust power control for WCDMA systems," in *Proc. IEEE Veh. Tech. Conf. (VTC)*, vol. 1, Atlantic City, NJ, USA, Oct. 2001, pp. 62–66.

[138] M. Rintamäki, K. Zenger, and H. Koivo, "Self-tuning adaptive algorithms in the power control of WCDMA systems," in *Proc. Nordic Signal Processing Symp. (NORSIG)*, boat Hurtigruten, Norway, Oct. 2002.

[139] M. Rintamäki, H. Koivo, and I. Hartimo, "Application of the generalized predictive control method in closed-loop power control of CDMA cellular communication systems," in *Proc. Nordic Signal Processing Symp. (NORSIG)*, Espoo, Finland, June 2004.

[140] ——, "Adaptive closed-loop power control algorithms for CDMA cellular communication systems," *IEEE Trans. Veh. Technol.*, vol. 53, no. 6, pp. 1756–1768, Nov. 2004.

[141] ——, "Adaptive closed-loop power control algorithms for CDMA cellular communication systems – part II," *IEEE Trans. Veh. Technol.*, submitted for publication.

[142] *Technical Specification 25.211 V3.5.0. Physical Channels and Mapping of Transport Channels onto Physical Channels (FDD)*, The 3rd Generation Partnership Project (3GPP).

[143] J. D. Herdtner and E. K. P. Chong, "Analysis of a class of distributed asynchronous power control algorithms for cellular wireless systems," *IEEE J. Select. Areas Commun.*, vol. 18, no. 3, pp. 436–446, Mar. 2000.

[144] E. F. Camacho and C. Bordons, *Model Predictive Control in the Process Industry*. London: Springer-Verlag, 1995.

[145] D. W. Clarke, C. Mohtadi, and P. S. Tuffs, "Generalized predictive control – parts I and II," *Automatica*, vol. 23, no. 2, pp. 137–160, Mar. 1987.

[146] D. W. Clarke, "Application of generalized predictive control to industrial processes," *IEEE Control Syst. Mag.*, vol. 8, no. 2, pp. 49–55, Apr. 1988.

[147] B.-K. Lee, B.-S. Chen, and S.-K. Chen, "Adaptive optimal predictive power control of cellular cdma systems," in *Proc. IEEE Int. Conf. on Control Applications*, Taipei, Taiwan, Sept. 2004, pp. 51–56.

[148] P. A. Ioannou and J. Sun, *Robust Adaptive Control*. Upper Saddle River, NJ: Prentice-Hall, 1996.

[149] K. J. Åström and B. Wittenmark, *Adaptive Control*, 2nd ed. New York: Addison-Wesley Publishing Company, 1995.

[150] R. Isermann, K.-H. Lachmann, and D. Matko, *Adaptive Control Systems*. Prentice-Hall, 1992.

[151] P. E. Wellstead and M. B. Zarrop, *Self-tuning Systems, Control and Signal Processing*. West Sussex: John Wiley & Sons, 1991.

[152] H. Koivo, "A multivariable self-tuning controller," *Automatica*, vol. 16, pp. 351–366, 1980.

[153] B. Widrow and S. Stearns, *Adaptive Signal Processing*. Englewood Cliffs, NJ: Prentice-Hall, 1985.

[154] W. Wang, "A direct adaptive generalized predictive control algorithm with guaranteed stability," *Int. J. of Adaptive Control and Signal Processing*, vol. 8, no. 3, pp. 211–222, May/June 1994.

[155] T. T. C. Tsang and D. W. Clarke, "Generalised predictive control with input constraints," *IEE Proc.*, vol. 135, no. 6, pp. 451–460, Nov. 1988.

[156] D. P. Atherton, *Nonlinear Control Engineering*, 2nd ed. London: Van Nostrand, 1982.

[157] J. R. Leigh, "Essentials of nonlinear control theory," in *IEE Topics in Control Series 2*. London: Peter Peregrinus Ltd, 1983.

[158] C. L. Phillips and R. D. Harbor, *Feedback Control Systems*. Englewood Cliffs, NJ: Prentice-Hall, 1988.

[159] *Technical Specification 25.101 V3.5.0. UE Radio Transmission and Reception (FDD)*, The 3rd Generation Partnership Project (3GPP).

[160] R. Jäntti and S.-L. Kim, "Power control with partially known link gain matrix," *IEEE Trans. Veh. Technol.*, vol. 52, no. 5, pp. 1288–1296, Sept. 2003.

[161] E. L. Lehmann, *Elements of Large-Sample Theory*. New York: Springer-Verlag, 1999.

[162] K. J. Åström and B. Wittenmark, *Computer-Controlled Systems : Theory and Design*, 3rd ed. Upper Saddle River, NJ: Prentice-Hall, 1997.